

UNCLASSIFIED



AD NUMBER

AD 372 385

CLASSIFICATION CHANGES

TO UNCLASSIFIED

FROM CONFIDENTIAL

AUTHORITY

OCA; Feb 1, 1978

THIS PAGE IS UNCLASSIFIED

UNCLASSIFIED



AD NUMBER

AD 372 385

NEW LIMITATION CHANGE

TO

DISTRIBUTION STATEMENT - A
Approved for public release;
distribution is unlimited.

LIMITATION CODE: 1

FROM

NO STATEMENT

AUTHORITY

Cmdr, AFRPL; May 7, 1978

THIS PAGE IS UNCLASSIFIED

~~CONFIDENTIAL~~

AFRPL-TR-66-44

372385

(Unclassified Title)

**DEVELOPMENT AND EVALUATION
OF
ADVANCED SOLID PROPELLANTS**

**FINAL TECHNICAL SUMMARY REPORT AFRPL-TR-66-44
(1 January 1965 to 29 December 1965)**

1 February 1966

**AIR FORCE ROCKET PROPULSION LABORATORY
RESEARCH AND TECHNOLOGY DIVISION
EDWARDS AIR FORCE BASE, CALIFORNIA**

In addition to security requirements which must be met, this document is subject to special export controls and each transmittal to foreign governments or foreign nationals may be made only with prior approval of AFRPL (RPPR-STINFO), Edwards, California, 93523.

(Prepared under Contract Nr. AF 04(611)-7554(4) by
The Dow Chemical Company,
Midland, Michigan)

~~CONFIDENTIAL~~



SECURITY

MARKING

The classified or limited status of this report applies to each page, unless otherwise marked.

Separate page printouts MUST be marked accordingly.

THIS DOCUMENT CONTAINS INFORMATION AFFECTING THE NATIONAL DEFENSE OF THE UNITED STATES WITHIN THE MEANING OF THE ESPIONAGE LAWS, TITLE 18, U.S.C., SECTIONS 793 AND 794. THE TRANSMISSION OR THE REVELATION OF ITS CONTENTS IN ANY MANNER TO AN UNAUTHORIZED PERSON IS PROHIBITED BY LAW.

NOTICE: When government or other drawings, specifications or other data are used for any purpose other than in connection with a definitely related government procurement operation, the U. S. Government thereby incurs no responsibility, nor any obligation whatsoever; and the fact that the Government may have formulated, furnished, or in any way supplied the said drawings, specifications, or other data is not to be regarded by implication or otherwise as in any manner licensing the holder or any other person or corporation, or conveying any rights or permission to manufacture, use or sell any patented invention that may in any way be related thereto.

REPRODUCTION QUALITY NOTICE

This document is the best quality available. The copy furnished to DTIC contained pages that may have the following quality problems:

- Pages smaller or larger than normal.
- Pages with background color or light colored printing.
- Pages with small type or poor printing; and or
- Pages with continuous tone material or color photographs.

Due to various output media available these conditions may or may not cause poor legibility in the microfiche or hardcopy output you receive.

☐ If this block is checked, the copy furnished to DTIC contained pages with color printing, that when reproduced in Black and White, may change detail of the original copy.

NOTICE

The information in this report is presented in good faith, but no warranty is made, nor is freedom from any patent to be inferred.

LEGAL NOTICE

When U. S. Government drawings, specifications, or other data are used for any purpose other than a definitely related Government procurement operation, the Government thereby incurs no responsibility nor any obligation whatsoever, and the fact that the Government may have formulated, furnished, or in any way supplied the said drawings, specification, or other data, is not to be regarded by implication or otherwise, or in any manner licensing the holder or any other person or corporation, or conveying any rights or permission to manufacture, use, or sell any patented invention that may in any way be related thereto.

SECURITY NOTICE

This document contains information affecting the National Defense of the United States within the meaning of the Espionage Laws (Title 18, U. S. C., Sections 793 and 794). Transmission or revelation in any manner to an unauthorized person is prohibited by law.

DISTRIBUTION

Four copies of this report have been forwarded to the Directorate of Rocket Propulsion, Edwards Air Force Base, California, and one copy to the Director, Advanced Research Projects Agency, Washington D. C., and one copy to AMRL, Wright-Patterson Air Force Base, Ohio. Further distribution has been made in accordance with the automatic distribution list, plus categories B-1, B-2, and B-3 of the CIA Publication No. 74, Chemical Propulsion Mailing List, March 25, 1965, with subsequent changes.

AFRPL-TR-66-44

Copy Nr. ~~328~~ of 225 Copies.
Series A 328 Pages.

Report Nr. AR-4Q-65
ANNUAL TECHNICAL SUMMARY REPORT (U)
(January - December, 1965)

1 February 1966

Compiled By

R. S. Karpiuk

R. S. Karpiuk

THIS MATERIAL CONTAINS INFORMATION AFFECTING THE
NATIONAL DEFENSE OF THE UNITED STATES WITHIN THE
MEANING OF THE ESPIONAGE LAWS, TITLE 18, U. S. C.,
SECS. 793 AND 794, THE TRANSMISSION OR REVELATION
OF WHICH IN ANY MANNER TO AN UNAUTHORIZED PERSON
IS PROHIBITED BY LAW.

Approved By

W. C. Bauman

W. C. Bauman
Research Director
Chemicals Department

R. P. Ruh
R. P. Ruh
Laboratory Director

AIR FORCE SYSTEMS COMMAND
RESEARCH AND TECHNOLOGY DIVISION
ROCKET PROPULSION LABORATORY
EDWARDS, CALIFORNIA
CONTRACT NR. AF 04(611)-7554(4)

In addition to security requirements which must be met
this document is subject to special export controls and
each transmittal to foreign governments or foreign
nationals may be made only with prior approval of AFRPL
(RPFR-STINFO), Edwards, California, 93523.

SCIENTIFIC PROJECTS LABORATORY
THE DOW CHEMICAL COMPANY
MIDLAND, MICHIGAN

DOWNGRADED AT 3 YEAR
INTERVALS; DECLASSIFIED
AFTER 12 YEARS
DOD DIR 5200.10

~~CONFIDENTIAL~~

FOREWORD

(U) This is the annual technical summary report in partial fulfillment of Contract AF 04(611)-7554(4), describing the work done during the period of January 1 to December 29, 1965.

(C) The primary objective of this program is to characterize and produce investigational quantities of propellant components that can be formulated into practical solid propellant grain compositions which will produce specific impulse values of at least 280 sec. (1000/14.7). The specific goals of the program are concentrated on the stabilization of aluminum hydride, improving the sensitivity of N-F oxidizers, thermochemical studies, and toxicology. A secondary objective of the program is to provide thermodynamic data compilation on a continuing basis in the form of JANAF Thermochemical Tables which are distributed to the Aerospace Industry for use in propellant performance and other high temperature thermodynamic calculations.

(U) The work was administered under the direction of the Rocket Propulsion Laboratory, Edwards Air Force Base, with Mr. J. T. Edwards as Air Force Project Officer.

(U) The work was performed by a number of scientists who are listed at the beginning of each major section. Dr. R. P. Ruhl was the Laboratory Director, with Drs. F. M. Brower, D. A. Rausch, D. R. Stull and H. C. Spencer as principal investigators of the specific sections.

(C) Most of the work described in this report is continuing in 1966 under Air Force sponsorship. The stabilization of aluminum hydride is covered by AF 04(611)-11400, the JANAF Tables by AF 04(611)-11201, the determination of thermodynamic properties and combustion kinetics by AF 04(611)-11202, and the toxicological investigations by AF 33(615)-3842.

(U) This report is Dow Report Nr. AR-4Q-65.

This technical report has been reviewed and is approved.

George F. Babits, Lt. Colonel, USAF
Chief, Propellant Division

~~CONFIDENTIAL~~

CONFIDENTIAL

TABLE OF CONTENTS

I.	(U)	ABSTRACT	1
II.	(U)	SUMMARY	2
III.	(U)	FUELS SYNTHESIS	14
	(C)	FUNDAMENTAL CRYSTALLIZATION STUDIES ON ALUMINUM HYDRIDE	14
	(U)	Solution Stability and Chemistry Studies	14
	(C)	Continuous Crystallization Studies of Aluminum Hydride-1451	45
	(C)	FUNDAMENTAL DECOMPOSITION STUDIES OF ALUMINUM HYDRIDE-1451	90
	(U)	Kinetics and Mechanism of Decomposition	90
	(C)	Magnesium Stabilization of Aluminum Hydride-1451	105
	(C)	Long-Term Surveillance Studies of Aluminum Hydride-1451	115
	(C)	Effect of Doping Aluminum Hydride Crystals with Various Additives	127
	(C)	New Stabilization Agents for Aluminum Hydride-1451	131
	(C)	Effect of Electrical Properties on the Decomposition of Aluminum Hydride-1451	142
	(C)	MISCELLANEOUS STUDIES OF ALUMINUM HYDRIDE-1451	142
	(C)	Effect of Oxygen and Water on the Preparation and Stability of Aluminum Hydride-1451	142
	(C)	Surface Treatment Studies of Aluminum Hydride	149
	(C)	Surface Studies of Aluminum Hydride-1451	157
	(C)	Effect of Magnesium on Unit Cell Dimensions of Aluminum Hydride-1451	159
	(U)	Test Apparatus	161
	(C)	CRYSTAL STRUCTURE STUDIES OF ALUMINUM HYDRIDE	161
	(C)	Comparison of Proposed Aluminum Hydride- 1451 Structures	161
	(U)	X-Ray and Neutron Powder Diffraction Data	165
	(C)	Present State of Refinement of the Aluminum Deuteride-1451 Structure	171
	(C)	Characterization of Aluminum Hydride-1717 and Aluminum Hydride-1563	171
	(C)	EVALUATION OF ALUMINUM HYDRIDE-1451 AS A PROPELLANT INGREDIENT	176

CONFIDENTIAL

TABLE OF CONTENTS (Contd.)

(C)	Compatibility Studies of Aluminum Hydride-1451	177
(C)	Surveillance of Aluminum Hydride-1451 in Propellant Grain	186
(C)	Chemical Analysis of Aluminum Hydride-1451 Double Base Propellant	197
(U)	COMBUSTION AND DECOMPOSITION KINETICS OF HYDRIDE FUELS	202
(U)	General Consideration	202
(U)	Experimental Approach	203
(U)	Experimental Results	207
IV.	(U) OXIDIZER SYNTHESIS	216
(U)	PREPARATION OF NF COMPOUNDS	216
(U)	REACTIONS OF NF COMPOUNDS	219
(U)	Reactions of tris-Compounds	219
(C)	Reactions of PFC	231
(U)	FLUORINATION OF INORGANIC COMPOUNDS	237
(C)	EFFECT OF IMPURITIES ON THE IMPACT SENSITIVITY OF DIFLUOROAMINO COMPOUNDS	237
(U)	Summary	237
(U)	Introduction	239
(C)	Experimental Work with Difluoroamino Compounds	240
(U)	SUMMARY AND CONCLUSIONS	242
V.	(U) PHYSICAL CHEMISTRY	244
(U)	THERMAL MEASUREMENTS	244
(U)	Heats of Formation	244
(U)	High Temperature Enthalpies	251
(U)	THERMODYNAMIC TABULATION	265
(U)	JANAF Heat of Formation of Propellant Ingredients	265
(U)	JANAF Thermochemical Tables	270
VI.	(U) BIOCHEMICAL RESEARCH	277
(U)	SUPPORT FUNCTION TO THE SYNTHESIS LABORATORIES	277
(U)	Environmental Research Support Function	277
(U)	Toxicological Research Support Function	277

CONFIDENTIAL

(This Page is Unclassified)

TABLE OF CONTENTS (Contd.)

(U)	TOXICOLOGICAL RESEARCH ON BERYLLIUM-CONTAINING MATERIALS	278
(U)	Materials	278
(U)	Long-Term Experiments on Rats and Rabbits Using Laboratory Prepared Samples of Beryllium Oxide	288
(U)	Twenty-Four Week Experiments on Rats Using a Laboratory Prepared Sample of Beryllium Oxide Calcined at 1600°C.	293
(U)	Long-Term Serial Study on Rats and Rabbits Using Key Samples of Beryllium Oxide	295
(U)	One-Year Experiments on Rats Using Control Materials	297
(U)	Studies on Exhaust Products from Motor Firings Using Rats	297
(U)	A Pilot Experiment on Selected Beryllium Oxides, Beryllium Hydroxides, and Beryllium Metal Using Rats	298
(U)	BIOCHEMICAL STUDIES	299
(U)	PROJECTED WORK	299
VII.	(U) REFERENCES	301

CONFIDENTIAL

LIST OF ILLUSTRATIONS

- (C) Fig. 1 - Change in Boiling Point Elevation of Lithium Aluminum Hydride and Lithium Aluminum Hydride Containing 0.25 M Aluminum Hydride as a Function of Lithium Aluminum Hydride Molarity 15
- (C) 2 - Degree of Association of Lithium Aluminum Hydride, Aluminum Hydride, and Lithium Aluminum Hydride Containing 0.25 M Aluminum Hydride as a Function of Molarity 16
- (C) 3 - Change in Boiling Point Elevation of Lithium Borohydride and Lithium Borohydride Containing 0.25 M Aluminum Hydride as a Function of Lithium Borohydride Molarity 18
- (C) 4 - Batch Process Solubility Curves of Lithium Aluminum Hydride and Aluminum Hydride at Various Temperatures in the Binary Ether - Benzene System 20
- (C) 5 - Batch Process Solubility Curves of Lithium Borohydride and Aluminum Hydride at Various Temperatures in the Binary Ether - Benzene System 21
- (C) 6 - Batch Process Solubility Curves of Lithium Aluminum Hydride, Aluminum Hydride and Lithium Borohydride in a Mole Ratio of 1:4:1 at Various Temperatures in the Binary Ether - Benzene System 22
- (C) 7 - Batch Process Solubility Curves of Lithium Aluminum Hydride, Aluminum Hydride and Lithium Borohydride in a Mole Ratio of 1:2:1 at Various Temperatures in the Binary Ether - Benzene System 25
- (C) 8 - Batch Process Solubility Curves of Lithium Aluminum Hydride, Aluminum Hydride and Lithium Borohydride in a Mole Ratio of 1:1:1 at Various Temperatures in the Binary Ether - Benzene System 26
- (C) 9 - Batch Process Solubility Curves of Lithium Aluminum Hydride, Aluminum Hydride and Lithium Borohydride in a Mole Ratio of 1:8:1 at Various Temperatures in the Binary Ether - Benzene System 27

CONFIDENTIAL

LIST OF ILLUSTRATIONS (Contd.)

(C)	Fig. 10 - Batch Process Solubility Curves of Lithium Aluminum Hydride, Aluminum Hydride and Lithium Borohydride in a Mole Ratio of 1:16:1 at Various Temperatures in the Binary Ether - Benzene System	28
(C)	11 - Batch Process Solubility Curve of Aluminum Hydride at Various Temperatures in the Binary Ether - Benzene System	29
(C)	12 - Continuous Process Solubility Curves of Lithium Aluminum Hydride, Lithium Borohydride, and Aluminum Hydride at a Constant Temperature of 76°C. in the Binary Ether - Benzene System	31
(C)	13 - Summary of Continuous Process Post-Precipitation Solubility Curves of Lithium Aluminum Hydride, Lithium Borohydride, and Aluminum Hydride at Various Temperatures in the Binary Ether - Benzene System	33
(C)	14 - Continuous Process Solubility Curves of Lithium Borohydride and Aluminum Hydride at a Constant Temperature of 76°C. in the Binary Ether - Benzene System	34
(C)	15 - Continuous Process Solubility Curves of Lithium Aluminum Hydride and Aluminum Hydride at a Constant Temperature of 74°C. in the Binary Ether - Benzene System	36
(C)	16 - Continuous Process Solubility Curves of Lithium Aluminum Hydride and Aluminum Hydride at a Constant Temperature of 77°C. in the Binary Ether - Benzene System	37
(C)	17 - Comparison Between the Continuous Process Solubility Curves of Lithium Aluminum Hydride-Aluminum Hydride and Lithium Aluminum Hydride-Aluminum Hydride-Lithium Borohydride Systems at a Constant Temperature of 77°C. in the Binary Ether - Benzene System	38

CONFIDENTIAL

LIST OF ILLUSTRATIONS (Contd.)

(C)	Fig. 18 - Comparison Between the Continuous Process Solubility Curves of Aluminum Hydride Only and Aluminum Hydride in the Presence of Lithium Aluminum Hydride at a Constant Temperature of 77°C. in the Binary Ether - Benzene System	40
(U)	19 - Chromatograms of Ether Solutions of Aluminum Chloride	42
(C)	20 - Decomposition of Aluminum Hydride on Thermometer Well	46
(C)	21 - Diagram of Photomicrographic Apparatus for Studying Aluminum Hydride Crystallization	49
(C)	22 - Photomicrographs of Changes Occurring with Time During Normal Continuous Crystallization of Aluminum Hydride-1451	51
(C)	23 - Photomicrograph of Changes Occurring with Time During the Preparation of Aluminum Hydride-1563 and Aluminum Hydride-1717 by the Direct Continuous Crystallization Techniques	52
(C)	24 - Infrared Absorption Spectra of Aluminum Hydride-1563 and -1717	65
(U)	25 - Volume Percent Diethyl Ether in n-Hexane	68
(U)	26 - Translation of Volume Percent Diethyl Ether of Various Solvent Systems	70
(C)	27 - Photomicrograph of Typical Aluminum Hydride-1451 Obtained from the DTB Crystallizer	76
(U)	28 - Schematic Diagram of the Draft Tube Baffle Crystallizer	78
(U)	29 - Modified Crystallizer	80
(U)	30 - "Thermal Seeding" Nucleation Methods (Time - Temperature Profiles)	81
(C)	31 - Photograph of Initial Small Particles Present During Beginning Crystallization of Aluminum Hydride-1451	83

CONFIDENTIAL

LIST OF ILLUSTRATION (Contd.)

(U)	Fig. 32 - Schematic Diagram of New Crystallizer	88
(U)	33 - Schematic Diagram of Metallograph Components . . .	92
(C)	34 - Photomicrograph of a Cross-Sectioned Pilot Plant Sample (05134) of Aluminum Hydride Decomposed 47.6%, Magnified 1500 Times	93
(C)	35 - Photomicrograph of a Cross-Sectioned Magnesium Stabilized Sample (5853-128) of Aluminum Hy- dride Decomposed 33.5%, Magnified 1500 Times	94
(C)	36 - Photomicrograph of a Cross-Sectioned Lab- oratory Sample (5853-149) of Aluminum Hydride Decomposed 50.9%, Magnified 1500 Times	95
(U)	37 - Photomicrographs of a Cross-Sectioned Pilot Plant Sample at Various Percent Decom- position, Magnified 500 Times	97
(U)	38 - Photomicrographs of a Cross-Sectioned Lab- oratory Sample at Various Percent Decom- position, Magnified 500 Times	98
(U)	39 - Photomicrographs of a Cross-Sectioned Mag- nesium Stabilized Sample at Various Percent Decomposition, Magnified 500 Times	99
(C)	40 - Type I Symmetrical Pressure-Time Decom- position Curve Exhibited by Aluminum Hydride	103
(C)	41 - Type II Asymmetrical Pressure-Time Decom- position Curve Exhibited by Aluminum Hydride	104
(C)	42 - Infrared Absorption Spectrum of Magnesium- Doped Aluminum Hydride-1451	107
(C)	43 - Effect of Age on the Thermal Stability of a Magnesium-Doped Aluminum Hydride-1451	108
(C)	44 - Decomposition Rate of Aged Magnesium-Doped Aluminum Hydride-1451 at 60°C.	110

CONFIDENTIAL

LIST OF ILLUSTRATIONS (Contd.)

(C)	Fig. 45 - Decomposition Curve of Aluminum Hydride-1451 at 100°C.	112
(C)	46 - Decomposition Curve of Aluminum Hydride-1451 at 130°C. and 150°C.	113
(C)	47 - Arrhenius Plot Obtained for the Acceleration Reaction of Aluminum Hydride-1451	114
(C)	48 - Thermal Stability of a Magnesium-Doped Aluminum Hydride-1451, Sample 5853-143, at 100°C.	116
(C)	49 - Thermal Stability of a Magnesium-Doped Aluminum Hydride-1451, Sample 5853-141, at 100°C.	117
(C)	50 - Effect of Age on the Thermal Stability of Aluminum Hydride-1451, Sample 02044-A, at 60°C.	122
(C)	51 - Change in the Thermal Stability of Aluminum Hydride-1451, Sample 02134A, Measured at 60°C. as a Function of Storage Time	123
(C)	52 - Change in the Thermal Stability of Aluminum Hydride-1451, Sample 03294, Measured at 60°C. as a Function of Storage Time	124
(C)	53 - Change in the Thermal Stability of Aluminum Hydride-1451, Sample 04194, Measured at 60°C. as a Function of Storage Time	125
(C)	54 - Rate of Decomposition of Aluminum Hydride-1451 Alone and with Ethyl Centralite and trans-Stilbene at 100°C.	132
(C)	55 - Effect of Various Weight Percentages of Ethyl Centralite on Decomposition Rate of Aluminum Hydride-1451	134
(C)	56 - Effect of Ethyl Centralite on the Decomposition Rate of Aluminum Hydride at 100°C. and 120°C.	135
(C)	57 - Effect of Various Compounds Containing Phenyl Groups on the Decomposition Rate of Aluminum Hydride-1451	138

CONFIDENTIAL

LIST OF ILLUSTRATIONS (Contd.)

(C)	Fig. 58 - Effect of Diphenylacetylene on the Decomposition Rate of Magnesium-Doped Aluminum Hydride-1451 at 60°C.	140
(C)	59 - Effect of Diphenylacetylene on the Decomposition Rate of Aluminum Hydride at 100°C. . . .	141
(C)	60 - Rate of Decomposition of Aluminum Hydride-1451 Alone and with Lampblack and Electric Potential at 100°C.	143
(U)	61 - Photograph of Oxygen and Water Analyzers	145
(C)	62 - Comparison Between the Original and New Stabilization Obtained under Anhydrous Conditions of Aluminum Hydride-1451 as a Function of Magnesium Concentration at 60°C.	147
(C)	63 - Infrared Absorption Spectrum of Solvated $(AlHO)_x$	150
(C)	64 - Hydrolysis Rate of Various Samples of Aluminum Hydride-1451	151
(C)	65 - Effect of Various Degrees of Surface Oxidation on the Stability of Aluminum Hydride-1451	153
(C)	66 - Effect of Surface Oxidation on the Stability of Aluminum Hydride-1451, Sample 02025A	155
(C)	67 - Effect of Surface Oxidation on the Stability of a Magnesium-Doped Aluminum Hydride-1451 Sample	156
(C)	68 - Unit Cell Dimensions of Aluminum Hydride as a Function of Weight Percent Magnesium Incorporated into Lattice	160
(C)	69 - Aluminum Hydride-1451 Structure Proposed by Duke	163
(C)	70 - Aluminum Hydride-1451 Structure Previously Proposed by Dow	164
(U)	71 - Face-Centered Cubic Structure of Aluminum Metal	166

CONFIDENTIAL

LIST OF ILLUSTRATIONS (Contd.)

(C)	Fig. 72 - Schematic Drawing of the Structure of Aluminum Hydride-1451 in Projection on the (001) Plane Showing the Aluminum Coordination	172
(C)	73 - Schematic Drawing of the (001) Projection of Aluminum Hydride-1451 Structure Showing the Al-H-Al Bridging for One Aluminum	173
(C)	74 - Schematic Drawing of the Structure of Aluminum Hydride-1451 in Projection on the (001) Plane Showing the Bridging of the Three Hydrogens on One Column	174
(U)	75 - Schematic Drawing Illustrating the Relationship Between Duke's and the Newly Proposed Structure as Viewed from the Projection on the (001) Plane	175
(C)	76 - Taliani Data on Aluminum Hydride-1451 (Lot 02055), Typical Composite, and Double Base Propellants at 60°C.	181
(C)	77 - Taliani Data on Polymer Systems With and Without Aluminum Hydride-1451 (Lot 02055)	182
(C)	78 - Taliani Data on Epoxy Systems with Aluminum Hydride-1451 (Lot 02055)	183
(C)	79 - Taliani Data on Aluminum Hydride-1451 (Lot 02055) and Nitro Compounds at 60°C.	185
(C)	80 - Decomposition Rate of Neat Aluminum Hydride	187
(C)	81 - Taliani Data Obtained at 60°C. on the Compatibility and Stability of Magnesium-Doped Aluminum Hydride Alone and in Formulations	188
(U)	82 - Propellant Samples and Aging Bomb	189
(U)	83 - Room Temperature Surveillance Facility	191
(U)	84 - High Temperature Aging Baths	192
(C)	85 - Decomposition of Aluminum Hydride-1451 (Lot 02055) in Double Base Propellant at 25°C.	193
(C)	86 - Decomposition of Aluminum Hydride-1451 (Lot 02055) in Double Base Propellant at 40°C.	194

CONFIDENTIAL

LIST OF ILLUSTRATIONS (Contd.)

- (C) Fig. 87 - Decomposition of Aluminum Hydride-1451
(Magnesium-Doped or Surface Hydrolyzed)
in Double Base Propellant at 25°C. 195
- (C) 88 - Decomposition of Aluminum Hydride-1451
(Surface Hydrolyzed) in Double Base
Propellant at 40°C. 196
- (U) 89 - Block Diagram of Flash Heating Apparatus 204
- (U) 90 - Electronic Circuitry of the Flash Heating
Apparatus 206
- (U) 91 - Flash-Heating Optical Train 208
- (C) 92 - Spectrum of Aluminum Hydride after Flashing 210
- (C) 93 - Infrared Spectrum of $(F_2N)_3C-\overset{\overset{H}{|}}{\underset{\underset{O}{||}}{N}}-\overset{\overset{H}{|}}{\underset{\underset{O}{||}}{C}}-C(NO_2)_3$ or
 $(F_2N)_3C-\overset{\overset{H}{|}}{\underset{\underset{O}{||}}{N}}-\overset{\overset{O}{||}}{C}-O-\overset{\overset{H}{|}}{\underset{\underset{O}{||}}{N}}=C(NO_2)_2$ 220
- (C) 94 - Infrared Spectrum of $NHF-C(NF_2)_2-O-N=C(CH_3)_2$ 223
- (C) 95 - Infrared Spectrum of Product from Nitration
of Adduct of tris-Br and Oxamidoxime 225
- (C) 96 - Infrared Spectrum of tris(Difluoroamino)methyl
Fluorosulfonate 228
- (C) 97 - Infrared Spectrum of Perfluoroformamidine
Fluorosulfonate 232
- (C) 98 - Infrared Spectrum of [tris(Fluorosulfonate)-
methyl] Fluorosulfonatefluoroamine 233
- (C) 99 - Minimum Fire Levels for DPF, Nitro, and
BDBD 240
- (C) 100 - Minimum Fire Levels for Various Difluoro-
amino Compounds 242
- (U) 101 - Deviation of Enthalpy of Titanium Diboride
from Smoothed Curve up to 1800°K. 258
- (U) 102 - Deviation of Enthalpy of Solid Aluminum
from Smoothed Curve up to 1000°K. 261

CONFIDENTIAL

(This Page is Unclassified)

LIST OF ILLUSTRATIONS (Contd.)

(U) Fig. 103 - Heat Capacity of Aluminum	263
104 - Deviation of Enthalpy of Liquid from Smoothed Curve up to 1700°K.	264

CONFIDENTIAL

LIST OF TABLES

(U)	I. Crystallization Variable Study	53
(C)	II. Removal of Chloride from a 0.3 M Aluminum Hydride Solution Containing an Excess of Aluminum Chloride	61
(C)	III. Removal of Chloride from a 0.3 M Aluminum Hydride Solution Containing an Excess of Lithium Aluminum Hydride.	62
(C)	IV. Removal of Chloride from a 1 M Lithium Aluminum Hydride Solution.	63
(C)	V. Analysis of Aluminum Hydride-1563 and Aluminum Hydride-1717 Polymorphs	64
(C)	VI. Lower Boiling Solvent Systems Used in the Preparation of Aluminum Hydride-1451	69
(U)	VII. Summary of DTB Crystallizer Runs	73
(C)	VIII. Summary of Conditions and Results from Series of DTB Crystallizer Runs.	75
(C)	IX. Evaluation of Selected Samples of Aluminum Hydride from DTB Crystallizer.	77
(C)	X. Summary of Dilute Feed Aluminum Hydride Runs	89
(C)	XI. Comparison of Infrared Frequencies of Magnesium-Doped and Standard Aluminum Hydride-1451	106
(C)	XII. Thermal Stability of Magnesium-Doped, Aged Samples of Aluminum Hydride-1451	109
(C)	XIII. Summary of Decomposition Data of Aluminum Hydride-1451 at Various Temperatures Using Prout-Tompkins Equation.	115
(C)	XIV. Long-Term Storage Stability of Aluminum Hydride-1451	118
(C)	XV. Long-Term Storage Stability of Aluminum Hydride-1451 at 40°C.	118
(C)	XVI. Effect of Storing Aluminum Hydride at Ambient Temperature on Thermal Stability.	120

CONFIDENTIAL

LIST OF TABLES (Contd.)

(C)	XVII.	Effect of Storing Aluminum Hydride at -15°C. on Thermal Stability	121
(C)	XVIII.	Effect of Storing Aluminum Hydride at 40°C. on Thermal Stability	121
(C)	XIX.	Ranking of Various Aluminum Hydride- 1451 Stabilizers	137
(U)	XX.	Oxygen Analysis of Dow Pilot Plant Samples	152
(C)	XXI.	Elemental Analysis of Aluminum Hydride- 1451 as a Function of Degree of Surface Hydrolysis	154
(C)	XXII.	Electron Diffraction Studies of the Surface of Long-Term Surveillance Samples of Aluminum Hydride	158
(C)	XXIII.	Unit Cell Dimensions of Aluminum Hydride as a Function of Magnesium Concentration	161
(C)	XXIV.	Comparison of Decomposition Rates of Aluminum Hydride as Measured by the Taliani and Pressure Transducer Apparatus at 60°C.	162
(C)	XXV.	X-Ray Powder Diffraction d-Spacings for Aluminum Hydride-1451 and Aluminum Deuteride-1451	168
(C)	XXVI.	Neutron Powder Diffraction Data for Aluminum Deuteride-1451 Space Group $R\bar{3}c$	169
(C)	XXVII.	Composition of Propellant Formulations	178
(C)	XXVIII.	Composition of Formulations Tested on the Taliani Apparatus at 60°C.	179
(U)	XXIX.	Gas and X-Ray Diffraction Analysis of Components and Residue of 60°C. Taliani Tests after 96 Hours	180
(U)	XXX.	Moisture Analyses of Propellant Ingredients	184
(U)	XXXI.	Surveillance Gas Analysis Data Comparison	198
(U)	XXXII.	Evaluation of Propellant	199
(C)	XXXIII.	Elemental Analysis of Recovered Aluminum Hydride-1451	200

CONFIDENTIAL

LIST OF TABLES (Contd.)

(C)	XXXIV.	Heats of Formation of Aluminum-Hydrogen Compounds	209
(C)	XXXV.	Observed Rotational Band for O-O Transition of BeH in Absorption at $2477 \pm 20^\circ\text{K}$	211
(C)	XXXVI.	Observed Rotational Bands of BeH in the Ultraviolet at $2477 \pm 20^\circ\text{K}$	212
(C)	XXXVII.	Summary of PFG-Adduct Reactions	218
(C)	XXXVIII.	Properties of $(\text{F}_2\text{N})_3\text{C}-\overset{\text{H}}{\underset{\text{O}}{\text{N}}}-\text{C}-\text{C}(\text{NO}_2)_3$ or $(\text{F}_2\text{N})_3\text{C}-\overset{\text{H}}{\underset{\text{O}}{\text{N}}}-\overset{\text{C}}{\underset{\text{O}}{\text{C}}}-\text{O}-\text{N}=\text{C}(\text{NO}_2)_2$	221
(C)	XXXIX.	Properties of tris(Difluoroamino)-methyl Fluorosulfonate	229
(C)	XL.	Properties of Perfluoroformamidine Fluorosulfonate	232
(C)	XLI.	Physical Properties of [tris(Fluoro-sulfonate)methyl] Fluorosulfonate-fluoroamine	233
(U)	XLII.	Summary of Fluorination of Inorganic Compounds	238
(U)	XLIII.	Sensitivity Data on R and PFG	241
(U)	XLIV.	Heat of Explosion of Aluminum Borohydride - Nitrogen Trifluoride Mixtures	245
(U)	XLV.	Nitrogen Trifluoride - Hydrogen Comparison Experiments	246
(U)	XLVI.	The Heat of Combustion of BTU	250
(U)	XLVII.	Heat of Formation of BTU Using Selected Auxiliary Data	250
(U)	XLVIII.	Thermodynamic Functions of α' -Beryllium Chloride	252

CONFIDENTIAL

(This Page is Unclassified)

LIST OF TABLES (Contd.)

(U)	XLIX.	Observed Enthalpy of Titanium Diboride	257
(U)	L.	Smoothed Enthalpy of Titanium Diboride	257
(U)	LI.	Observed Enthalpy of Aluminum	259
(U)	LII.	Smoothed Enthalpy and Heat Capacity of Aluminum	260
(U)	LIII.	Heat of Fusion of Aluminum	265
(U)	LIV.	Series C of Propellant Ingredients	266
(U)	LV.	Series D of Propellant Ingredients	268
(U)	LVI.	JANAF Thermochemical Data Supplement No. 16 . . .	271
(U)	LVII.	JANAF Thermochemical Data Supplement No. 17 . . .	272
(U)	LVIII.	JANAF Thermochemical Data Supplement No. 18 . . .	273
(U)	LIX.	JANAF Thermochemical Data Supplement No. 19 . . .	274
(U)	LX.	JANAF Thermochemical Data Supplement No. 20 . . .	275
(U)	LXI.	Summary of JANAF Tables	276
(U)	LXII.	Properties of Key Samples of Beryllium Oxide Prepared by Calcining Beryllium Hydroxide under Laboratory Conditions	279
(U)	LXIII.	Solubility of Three Key Samples of Beryllium Oxide in Various Media at Room Temperature	280
(U)	LXIV.	Refractive Index Values for Laboratory Preparations of Beryllium Oxides using a Dispersion Staining Technique	281
(U)	LXV.	d-Spacings from Powder Diffraction Data for Beryllium Oxide	283
(U)	LXVI.	Properties of Exhaust Products from Motor Firings	285
(U)	LXVII.	Emission Spectrographic Analyses of Exhaust Products from Motor Firings	236
(U)	LXVIII.	Elemental Analysis of Exhaust Products from Motor Firings	286

CONFIDENTIAL

(This Page is Unclassified)

CONFIDENTIAL

(This Page is Unclassified)

LIST OF TABLES (Contd.)

(U)	LXIX.	X-Ray Powder Diffraction Analysis of Exhaust Products from Motor Firings	287
(U)	LXX.	X-Ray Powder Diffraction Analysis of Components in the Water-Soluble Fraction of Exhaust Products from Motor Firings	288
(U)	LXXI.	Emission Spectrographic Analysis of the Water-Soluble Fraction of Exhaust Products from Motor Firings	289
(U)	LXXII.	Beryllium Concentration in Tissues of Rats Treated Intratracheally with Beryllium Oxide Prepared by Calcining Beryllium Hydroxide for 10 Hrs. at 500°C.	291
(U)	LXXIII.	Beryllium Concentration in Tissues of Rats Treated Intratracheally with Beryllium Oxide Prepared by Calcining Beryllium Hydroxide for 10 Hrs. at 1100°C.	292
(U)	LXXIV.	Beryllium Concentration in Tissues of Rabbits Treated Intratracheally with Beryllium Oxide Prepared by Calcining Beryllium Hydroxide	294
(U)	LXXV.	Beryllium Concentration in Tissues of Rats Treated Intratracheally with Beryllium Oxide Prepared by Calcining Beryllium Hydroxide for 10 Hrs. at 1600°C.	296

CONFIDENTIAL

GLOSSARY OF TERMS

AIBN	Azobisisobutyronitrile
AP	Ammonium perchlorate
BDBD	2,3-bis(Difluoroamino)-1,4-butanediol dinitrate
BDNPA	bis(2,2-dinitropropyl)acetal
BTU	bis[tris(Difluoroamino)methyl]urea
Compound A	Chlorine pentafluoride
Compound Delta	tetrakis(Difluoromethoxy)methane
Compound H	Di(difluoroamino)difluoromethane
Compound R	tris-Fluoride
DEGDN	Diethylene glycol dinitrate
DMF	Dimethylformamide
DPA	Diphenylacetylene
DPF	2,3-bis(Difluoroamino)propyl
EC	Ethyl centralite
Epon 812	Epoxy Resin
FC-43	A fluorocarbon solvent made by Minnesota Mining and Manufacturing Company
HX 735	A polyester made by Minnesota Mining and Manufacturing Company
Hybaline A-4	Aluminum borohydride dimethylamine
INFO-615	tris(Difluoroamino)methoxyammonium perchlorate
INFO-635	2[tris(Difluoroamino)methoxy]ethyl ammonium perchlorate
INFO-635P	2[tris(Difluoroamino)methoxy]ethylamine perchlorate
Kel-F 011	Polychlorotrifluoroethylene
MAPO	tris[1-(2-methyl)aziridinyl]phosphine oxide
NC	Nitrocellulose
2-NDPA	2-Nitrodiphenylamine
NG	Nitroglycerine
NP	Nitronium perchlorate
PFF	Perfluoroformamidine
PFG	Perfluoroguanidine
PGNC	Plastisol grade nitrocellulose

CONFIDENTIAL

GLOSSARY OF TERMS (Contd.)

TAZ	Triaminoguanidinium azide
TEGDN	Triethylene glycol dinitrate
THA	Triaminoguanidinium hydrazinium azide
TMETN	Trimethylolethane trinitrate
tris	(NF ₂) ₃ -
tris-A	tris(Difluoroamino)methylamine
tris-Azide	tris(Difluoroamino)methylazide
tris-Bromide	tris(Difluoroamino)methylbromide
tris-Chloride	tris(Difluoroamino)methylchloride
tris-Fluorosulfonate	tris(Difluoroamino)methylfluorosulfonate
tris-H	tris(Difluoroamino)methane
tris-I	tris(Difluoroamino)methyl isocyanate
tris-Isocyanat	tris(Isocyanato)methane
tris-Iodide	tris(Difluoroamino)methyliodide
tris-NO ₂	tris(Difluoroamino)nitromethane
tris-OF	tris(Difluoroamino)fluoroxymethane
tris-OH	tris(Difluoroamino)methyl alcohol
VCN	Vinyl cyanide (Acrylonitrile)

CONFIDENTIAL

SECTION I

ABSTRACT

(C) In the area of fuels synthesis, the following areas have been investigated. Solubilities for the aluminum hydride system have been measured. Continuous, direct crystallization of aluminum hydride-1451 has been studied and achieved in a draft tube baffle crystallizer (DTB). Four methods of "thermal seeding" the crystallizer have been examined. Solution stability has been a problem. Photomicrographs of the nucleation and growth processes occurring during decomposition of aluminum hydride are presented, and a mechanism is proposed. The crystal structure of AlH_3 -1451 has been elucidated.

(C) Improvements in thermal stability were achieved by aging, diphenylacetylene treatment, and surface hydrolysis. A maximum stability of 1% decomposition in 70 days at 60°C. has been obtained. Surveillance of neat AlH_3 -1451 has indicated less than 1% decomposition at ambient temperature in 1.3 to 1.8 years. Surveillance of AlH_3 -1451 double-base propellant at 25°C. and 40°C. showed a decomposition rate of 0.0012% and 0.003% per day, respectively. A study of the kinetics of decomposition of aluminum and beryllium hydride using flash heating showed the existence of AlH , BeH , and BeH^+ at 2500°K.

(C) A new potential liquid oxidizer, or plasticizer, has been prepared by the reaction of tris-I with nitroform. Exploratory reactions to prepare tris-ionic solids by the displacement of the bromine from tris-bromide indicated a reaction with oximes; however, fluorine was lost, and a PFG adduct was formed. Typical nucleophilic displacement reactions could not be effected on tris-bromide with retention of the tris structure. The effect of impurities on the impact sensitivity of difluoroamino compounds was intensively studied. No appreciable effect was detected for the compounds examined.

(U) The heat of formation of nitrogen trifluoride(g), aluminum borohydride(g), Hybaline A-4(l), hexafluoroethylene radical(g), INFO-635P(c), and BTU(c), and the high temperature enthalpies of allotropic forms of beryllium chloride, and the enthalpies and heat capacities of liquid and solid aluminum were measured and are reported. A summary of Series C and D of the JANAF Tables of Propellant Ingredients and of the four supplements of JANAF Thermochemical Tables issued during 1965 is given.

(U) The toxicological research was concentrated on the beryllium containing materials using controlled samples of the oxide as well as the hydrides, the metal and firing residues. The response in animals of the low-fired oxide is entirely different than the high-fired materials, and evidence of various carcinogenic tumors was detected in lung tissue of the animals exposed to low-fired materials.

CONFIDENTIAL

SECTION II

SUMMARY

A. FUELS SYNTHESIS (U)

(C) The fuels research effort has stressed fundamental stability and crystallization studies oriented toward improving the chemical and physical properties of aluminum hydride.

(C) Molecular weight studies of aluminum hydride have shown that the presence of lithium aluminum hydride in a 0.25 M AlH_3 solution enhances the molecular weight of the species present in diethyl ether solution. There was no indication of a simple complex having a low whole number mole ratio of lithium aluminum hydride to aluminum hydride. Similar studies with aluminum hydride and lithium borohydride showed boiling point elevations that were nearly additive. This indicated only a slight association taking place between aluminum hydride and lithium borohydride in ether solutions.

(C) Solubility curves have been constructed for lithium aluminum hydride, lithium borohydride, aluminum hydride, and combinations thereof in the ether - benzene solvent system used in the batch process for AlH_3 crystallization. It was concluded from various systems containing higher amounts of dissolved hydride per given volume of solvent that the precipitation phenomenon was not solely a function of concentration, since the solute-solvent ratio had little effect upon the precipitation temperature. There does, however, appear to be a temperature-dependent complex which plays a major role in the precipitation phenomenon.

(C) The solubility of aluminum hydride, measured at various temperatures in the ether - benzene solvent system, is not solely a function of ether concentration, but is a function of the binary solvent system.

(C) Solubility curves for the continuous crystallization process have been measured. These curves represent the changes in solubility of lithium borohydride, lithium aluminum hydride, and aluminum hydride in the benzene - ether system as a function of time at constant temperatures of $74^\circ\text{--}78^\circ\text{C}$. The measured solubilities of lithium aluminum hydride, aluminum hydride, and lithium borohydride just prior to precipitation indicate an approximate hydride respective mole ratio of 1:2:1.

(C) Solubility studies of the complete continuous process system at constant temperatures ranging from $74^\circ\text{--}78^\circ\text{C}$. are summarized. The solubilities of lithium aluminum hydride and aluminum hydride in both the pre- and post-precipitation areas decrease with increasing temperature. The solubility of lithium borohydride in the continuous process appears to be unaffected by temperature except at temperatures above 78°C ., at which point the solubility of lithium borohydride also decreases.

CONFIDENTIAL

(C) The solubility curves of lithium aluminum hydride and aluminum hydride together, compared with those obtained in a combination of lithium aluminum hydride, aluminum hydride and lithium borohydride at 74°C. and 77°C., differed only in the increased solubility of lithium aluminum hydride due to the presence of lithium borohydride.

(C) The effect of various concentrations of lithium aluminum hydride on the solubility of aluminum hydride in the continuous process showed only minor variations in solubilities.

(C) In the preparation of aluminum hydride, traces of impurities can adversely affect the stability of the final product. In a study of solvent purity, analysis of high quality benzene from five different sources indicated essentially no differences in impurity content. The amount of water in the benzene appeared to be the most significant factor in its effect on hydride stability.

(C) The analysis of ether solutions of aluminum chloride by gas-liquid chromatography using flame and electron capture detection showed two impurities. No correlation has been made between these impurities and thermal stability of the hydride.

(C) The substitution of aluminum chloride with dimethyldichlorosilane in the reaction with lithium aluminum hydride produced normal AlH_3 -1451, except in some cases in which an improved stable product was obtained.

(C) Preparations of aluminum hydride under anhydrous and oxygen-free conditions continued to indicate a trend toward increased decomposition of the aluminum hydride in very pure systems.

(C) A possible relationship between stray electrical fields and aluminum hydride decomposition was investigated. Heating the conversion flask to 550°C. before using appeared to be beneficial. An investigation of materials of construction showed soft glass and Vycor to produce more decomposition than borosilicate glass. The use of quartz showed no observable decomposition.

(C) A system has been developed for sampling and examining microscopically the solids present during the continuous crystallization process. This apparatus has been found to be very useful in observing the initial precipitation, crystal growth, effect of additives, and phase changes which occur during the preparation of AlH_3 -1451. The sampling system is coupled to a polarizing light microscope with a polaroid camera attachment for permanent recording of these phenomena.

(C) Laboratory crystallization studies have concentrated on developing the conditions necessary to grow continuously single crystals of AlH_3 -1451 directly from solution. These studies have shown that slower feed rates and stirring are important parameters in producing good crystals. Temperature and residence time are

CONFIDENTIAL

CONFIDENTIAL

also contributing factors. Seeding has not been successful and, as a result, a variety of techniques of initiating nucleation has been studied. A study of nucleation has indicated that "thermal seeding" which involves the addition of an ether solution containing lithium aluminum hydride, and aluminum hydride, with or without lithium borohydride, to boiling benzene gives the most rapid and consistent nucleation of AlH_3 -1451.

(C) The role of the crystallization additives, lithium aluminum hydride and lithium borohydride, has been thoroughly investigated. A search for other crystallization additives which would increase the crystallinity of the AlH_3 -1451 has not produced any improvements. The role of the impurities of lithium chloride and water has been shown and methods for their removal developed.

(C) Preliminary work incorporating magnesium into the direct crystallization of aluminum hydride indicated it can be accomplished, but with some difficulty due to residual chlorides and changes in crystal habit.

(C) The continuous direct crystallization of aluminum hydride-1451 has also been studied on a larger scale. A 14-gallon modified Draft Tube Baffle (DTB) crystallizer with a glass elutriation leg for classification of product was used. A description of the process and a summary of runs made in the DTB crystallizer are presented. All preparations were continuous and varied in length from four to eleven hours. Fifty-four percent of the continuous runs resulted in samples containing entirely AlH_3 -1451.

(U) Nucleation of aluminum hydride has been shown to be extremely critical in determining the quality of the final product. Four methods of "thermal seeding" the crystallizer have been used. These methods and the effect of parameters are discussed. Examination of DTB solutions has shown that direct nucleation of AlH_3 -1451 does occur in the DTB crystallizer. Nuclei usually appear as well-formed cubes or hexagons of AlH_3 -1451.

(U) Solution stability has been a problem with random decomposition and deposition on the walls of the crystallizer. Cleaning procedures and control of raw material quality have minimized this problem. Preliminary screening of fundamental parameters indicates that agitation, feed rate, and crystal retention time are the most significant.

(C) During the latter part of the year, a modified crystallizer was designed and fabricated which incorporated several improved features. Data indicate that the mechanical design of the crystallizer is critical. A new concept of aluminum hydride crystallization has also been investigated and is briefly discussed. The method eliminates distillation and the need for high wall temperatures, yet incorporates solvent recovery.

(C) Conversion of AlH_3 -1451 in solvent media other than the benzene - ether system and at lower temperatures has proven to be

CONFIDENTIAL

CONFIDENTIAL

feasible and practical. The following solvent systems have been proven satisfactory as crystallizing media for AlH_3 -1451; n-hexane, b.p., 68°C .; and a benzene - 2,4-dimethylpentane mixture azeotropeing at 75.4°C .; and a benzene - cyclohexane system azeotropeing at 77.4°C . These systems have resulted in the crystallization of AlH_3 -1451 at temperatures of 64° - 66°C ., 71° - 73°C ., and 73° - 75°C ., respectively.

(C) Fundamental decomposition studies of aluminum hydride are interpreted in terms of a three-stage process. The first involves the reaction occurring at the surface of the crystals; the second, the formation of stable aluminum nuclei, and the third; the reaction occurring at the interface between the AlH_3 -1451 and the aluminum metal. Photomicrographs of the nucleation and growth processes which occur during the decomposition of aluminum hydride have been obtained. It is now believed that different mechanisms are operative during the decomposition of AlH_3 -1451. One mechanism involves the formation of additional nuclei by chain branching, while a second involves only the formation of fresh nuclei on the surface. Decomposition may then occur either by a two-dimensional growth which rapidly covers the surface with a layer of aluminum, or it may proceed three-dimensionally without surface growth from the single nucleus site originally formed.

(C) A working hypothesis is proposed to describe the occurrence of the initiation of decomposition in the AlH_3 -1451 lattice. This process is currently thought to involve:

- (1) A diffusion process involving the diffusion of a non-equilibrium concentration of anion vacancies through the hydride by a vacancy transfer mechanism.
- (11) The formation of germ nuclei by capture of electrons by the vacancies at the surfaces or grain boundaries.
- (111) The coalescence of germ nuclei to form active growth nuclei.

(C) This proposed hypothesis explains the observed difference in the decomposition rates of the deuteride vs. the hydride, and suggests explanations for the other aspects of aluminum hydride chemistry such as solution stability, surface treatments, and coloring of the hydride.

(C) The use of various doping agents to increase the stability of AlH_3 -1451 was investigated. Experience demonstrated that the doping agent must be carefully chosen if the element is to be incorporated into the hydride crystal lattice. It appears that the principal criterion is the solubility of the doping agent in the ether-benzene solution. The presence of large amounts of reducing hydrides in the system restricts the additives to metals with a high oxidation potential. Calcium, magnesium, and gallium were incorporated into the hydride lattice in the highest percentages. Phosphorus, germanium, chromium, iron, nickel, titanium,

CONFIDENTIAL

CONFIDENTIAL

strontium, and barium were also examined, but the experiments were unsuccessful in incorporating amounts greater than 0.1%. None of the additives exhibited stabilization of AlH_3 -1451 superior to that observed with magnesium.

(C) It has been discovered that symmetrical diethyldiphenylurea, designated ethyl centralite (a stabilizer for nitrocellulose), stabilizes AlH_3 -1451 at elevated temperatures in a unique manner. The presence of this material during decomposition has been found to essentially stop the decomposition of the hydride at approximately 50%. This stabilization phenomenon appears to be associated in some manner with the phenyl groups present in the molecule. A screening program of various compounds containing phenyl groups which might act as stabilizers for AlH_3 -1451 was initiated. The most effective stabilizer in this class discovered to date is diphenylacetylene (DPA). The length of the induction period was extended sixty-fold at 100°C . The rate of decomposition of a freshly prepared magnesium-doped hydride sample at 60°C . with DPA has exhibited only 0.6% decomposition in 50 days. Preliminary results indicate DPA is a more effective stabilizer for magnesium-doped material than for normal hydride.

(C) A number of macrocrystalline aluminum hydride samples have been under long-term storage surveillance at ambient temperature and at -15°C . from 1.3 to 2.6 years. In addition, six lots are being evaluated at 40°C . The samples are routinely checked by carbon and hydrogen analysis to determine percent decomposition and by the Taliani test at 60°C . to determine changes in thermal stability with age. During this surveillance less than 1% decomposition has been detected at ambient temperature and essentially no decomposition at -15°C . After 97 days' storage at 40°C ., the sample exhibited an average of 2.05% decomposition.

(C) Periodic examination of the samples by the Taliani test at 60°C . has illustrated an aging phenomenon, in which the thermal stability of the hydride does not always decrease but often increases in stability with time. One lot of normal hydride yielded nearly a three-fold improvement in thermal stability during a storage period of sixteen months.

(C) Magnesium-doped hydride samples have also been evaluated by the Taliani test at 60°C . and found to exhibit the same aging phenomenon. Laboratory samples stored at -15°C . for a period of about five months showed a three- to four-fold improvement in stability. One sample reached 70 days before decomposing 1% at 60°C . This aging phenomenon appears to be a characteristic of magnesium-doped material. It has been found that the concentration of magnesium does not correlate with the degree of stability improvement upon storage; however, it has been found that the total amount of gassing during the first day does roughly correlate with the degree of improvement during aging.

(C) The stabilities currently being obtained from magnesium-doped samples at 100°C ., as measured by a pressure transducer, have

CONFIDENTIAL

CONFIDENTIAL

been remarkable, as samples remain at low levels of decomposition for days. In several samples the normal, characteristic, sigmoid-shaped decomposition curve is not present but is preceded by an initial decomposition and induction period before accelerating its rate as normally expected.

(C) The effect of oxygen and water on the preparation and stability of aluminum hydride-1451 was examined. The development of equipment to remove, analyze, and monitor the oxygen and water content has allowed the systematic study of these contaminants. A system was developed so that any dry box or line nitrogen could be simultaneously monitored for oxygen and water concentration in a matter of minutes. Molecular sieves and Dow "Q" Catalyst were found to be most effective for the removal of water and oxygen, respectively.

(C) It was discovered that magnesium-doped materials prepared under water- and oxygen-free conditions were not as stable as originally observed. The stability of the hydride prepared under these conditions again increased as magnesium concentration increased, but the magnitude of improvement was not quite as great as originally observed. The preparation of magnesium-doped AlH_3 -1451 under an anhydrous nitrogen atmosphere containing 10,000 ppm oxygen gave the same stabilities as those obtained under oxygen- and water-free conditions. Experimentation under controlled moisture conditions demonstrated that water, in addition to magnesium, is playing the major role in determining this relationship. The original relationship between magnesium concentration and stability was duplicated under these conditions.

(C) The effect of surface hydrolysis on the stability of AlH_3 -1451 was investigated. An attempt was made to determine the amount of surface oxidation necessary to effectively improve stability. Little additional stability improvement of the hydride was gained by surface hydrolysis in excess of 0.1%. Electron diffraction studies of the surface at this level of oxidation, as well as the samples possessing correspondingly larger amounts of oxygen, showed it to be completely amorphous. Changes in elemental analysis as a function of the degree of hydrolysis showed that a small but definite change in elemental analysis occurs for small degree of surface hydrolysis. A maximum two-fold improvement in thermal stability has been observed after treatment.

(C) The surfaces of the samples currently under long-term surveillance were examined by electron diffraction. Bayerite (aluminum hydroxide), γ - or η -aluminum oxide, and amorphous surfaces were noted. Because of the hydrophilic nature of the surface of aluminum hydride, upon storage it apparently develops a surface of oxides (Al_2O_3), oxy-hydroxides (AlOOH), and hydroxides, $\text{Al}(\text{OH})_3$, varying in degree of molecular order from completely amorphous to crystalline Al_2O_3 .

(C) The reactions of lithium aluminum hydride, lithium borohydride, and aluminum hydride were examined independently with

CONFIDENTIAL

oxygen. Oxygen removes lithium aluminum hydride from solution by precipitation of an amorphous solid. No precipitate formed when oxygen was bubbled through a binary solvent containing lithium borohydride. After the solvent was stripped away, a solid residue was obtained and identified by X-ray analysis as an unknown pattern (1476).

(C) When a limited amount of oxygen was bubbled through an aluminum hydride ether solution, a white precipitate formed. This material was very reactive to water and amorphous to X-ray. Infra-red and elemental analyses have indicated a solvated material with a ratio of Al to H to O of 1:1:1.

(C) A series of samples doped with various amounts of magnesium was evaluated by X-ray on an AEC Guinier type focusing camera with aluminum as the reference to evaluate changes in the unit cell dimensions of the hydride. The lattice constants a and c were found to increase as the magnesium concentration increased. Both the a and c lattice constants showed approximately the same percent expansion, although the c axis changed more than the a axis. The unit cell expansion was found to be nearly a linear function of the percent magnesium incorporated into the lattice.

(C) A measurement of the activation energy for the acceleration period of the decomposition of magnesium-doped hydride samples containing approximately 2% magnesium has yielded activation energies of 35.8 kcal./mole.

(U) The accuracy of the modified Taliani apparatus is currently being examined by comparing the measured decomposition rate with that measured by a pressure transducer apparatus. Some differences in decomposition rates are currently being observed, but, due to the preliminary data, no conclusions can be drawn.

(C) The crystal structure of AlH_3 -1451 has been further elucidated. A rhombohedral lattice proposed by J. R. C. Duke is discussed and compared with Dow's previously proposed hexagonal unit cell. A close relationship was found to exist between Duke's structure of AlH_3 -1451 and that of aluminum metal. The X-ray and neutron powder diffraction patterns are given for both AlH_3 -1451 and AlD_3 -1451. The unit cell dimensions for AlH_3 -1451 and AlD_3 -1451 had been refined using Frevel's method of axial ratios. Results from analysis of the above data show that Duke's structure is correct with respect to the aluminum atoms but is not acceptable with respect to the hydrogen atoms. Data show the unit cell to be twice the value originally reported and of the higher symmetry space group $R\bar{3}c$. Diagrams depicting the unrefined structure of aluminum hydride are shown.

(C) An examination of AlH_3 -1717 by single crystal techniques has suggested that it crystallizes in the orthorhombic system having unit cell dimensions of $a = 8.661 \text{ \AA}$, $b = 9.923 \text{ \AA}$, $c = 12.755 \text{ \AA}$.

CONFIDENTIAL

(C) A study encompassing the stability, compatibility, formulatability, and aging characteristics of double base and composite propellant systems containing AlH_3 -1451, fuel is discussed. Normal hydride, as well as some of the most recently synthesized, improved AlH_3 -1451, was evaluated.

(C) Formulation and compatibility studies have indicated the relative compatibility of AlH_3 -1451 with the different propellant ingredients. Epoxies and BDNPA, bis(2,2-dinitropropyl)acetal, were found to increase the rate of decomposition of the hydride when compared with the neat AlH_3 -1451, but nitrocellulose (which contained ethyl centralite) and other nitro esters (e.g., TMETN) exhibited a stabilizing influence.

(C) Long-term aging studies of double base propellant at 25°C. and 40°C. were also conducted on larger samples, 1/4-lb. motors and 1/5-lb. slabs, stored in surveillance bombs. Periodically, analyses were made of the gas in these bombs to determine the onset of decomposition. Gas analysis showed a slow generation of N_2 and O_2 in addition to hydrogen. Carbon dioxide was also found to be generated in greater amounts from AlH_3 -1451 propellant when compared with the aluminum propellant.

(C) Surveillance studies have provided decomposition rates of AlH_3 -1451 in double base propellant of approximately 0.00112% per day at 25°C. after 125 days, and 0.003% per day at 40°C. after 100 days. If the gassing rate remained constant at these values, the hydride would be expected to exhibit 0.4% decomposition per year of 2% decomposition in five years at 25°C. At 40°C. the hydride should show 1.1% decomposition per year or 5.5% decomposition in five years.

(C) In addition, examination of propellant samples for ballistic and physical property study has given some insight into the aging characteristics of the propellant. A slight hardening and embrittlement of the AlH_3 -1451 double base propellant occurred with age, but voids formed in the propellant by decomposition of the AlH_3 -1451 were not observed.

(C) A procedure has been developed for recovering the AlH_3 -1451 from a cured propellant sample for double base propellant. A solvent is used to remove the other ingredients, leaving the insoluble crystals of AlH_3 -1451. Analytical results from the recovered AlH_3 -1451 indicate that a coating, consisting of oxides of nitrogen, has formed on the surface of the AlH_3 -1451.

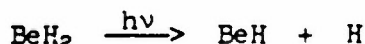
(C) A study of the intermediates and combustion products of aluminum hydride and beryllium hydride using flash heating and spectrographic analysis to determine short-lived atomic and molecular species is presented. Equipment was designed to provide maximum resolution and identification of short-lived species.

(C) The first decomposition kinetic studies of aluminum hydride by flash-heating have been performed. The existence of

CONFIDENTIAL

AlH and hydrogen in the flash decomposition of AlH₃-1451 in a vacuum has been verified. A discussion of proposed thermodynamically favored decomposition reactions is given.

(C) The pyrolytic decomposition of BeH₂ has been studied at 2475°C. The initial step is the removal of a hydrogen atom.



Subsequent reactions are radical-radical induced, and lead to the final products, beryllium metal and hydrogen. The reaction is the same in nitrogen or vacuum.

(C) The BeH molecule at 2500°K. was found to lose an electron forming the charged, seemingly stable, BeH⁺ species. It is suggested that the BeH⁺ species may be responsible for low motor efficiencies when using BeH₂ as a fuel.

(C) The reactions of BeH₂ with O₂, CO, and Cl₂ at 2450°-2500°K. have been examined by flash-heating, and results are discussed.

B. OXIDIZER SYNTHESIS (U)

(C) A new product has been prepared by the reaction of tris-I with nitroform. This product, (F₂N)₃C-NH-C(=O)-C(NO₂)₃ and/or

(F₂N)₃C-NH-C(=O)-N(=O)-C(NO₂)₂, is a viscous liquid with a high boiling point. Its shock sensitivity level indicates that it may be useful as an oxidizer in itself, or as a plasticizer in high energy propellants.

(C) Many reactions have been carried out to obtain tris-ionic solids by displacement of the bromine from tris-bromide. In one of these studies, oximes were found to displace the bromine. However, the concurrent loss of a fluorine from a nitrogen occurred, so that, in effect, a PFG adduct was formed. This reaction sequence was not observed by the infrared studies; however, NMR spectra conclusively proved that the structure of the product with a variety of oximes was (F₂N)₂-C(NHF)-O-N=CR₂.

(C) Typical nucleophilic displacement reactions could not be effected on tris-bromide with retention of the tris structure. However, when tris-Br was treated with peroxydisulfuryl difluoride, (F₂N)₃C-OSO₂F, was formed. The transformation of this product (1) by fluorination into tris-OF or (2) by hydrolysis into tris-OH did not prove successful.

(C) Reactions designed to transform tris-A into tris-NO₂ by oxidation were unsuccessful, as were the transformations of PFG to tris-OH, tris-OF, etc.

(C) The fluorination of inorganic materials was undertaken to prepare oxidizers containing no fuel atom such as carbon.

CONFIDENTIAL

Although a variety of fluorinated materials was obtained, none of the desired products was observed.

(C) The study on the role of impurities in the sensitivity of NF compounds was concluded. The main objective of this work were (1) to determine the degree of shock sensitivity of NF compounds and (2) to ascertain whether impurities or additives increased or decreased the shock sensitivity of NF compounds. The above study revealed that NF₂ compounds are inherently sensitive to impact. This sensitivity increases with an increasing number of NF₂ groups per carbon. The sensitivity was also affected by the impurities. In some cases, impurities increased the sensitivity while, in other cases, they decreased the sensitivity. However, in no case was an impurity or additive effective in decreasing the sensitivity to a level for utilization.

C. PHYSICAL CHEMISTRY (U)

(C) Measured heats of formation are reported for the following compounds:

Compound	ΔH_f ₂₉₈ in kcal./mole
NF ₃ (g)	-31.2
Al(BH ₄) ₃ (g)	-12.4
Hybaline A-4 (l)	-57.9
C ₂ F ₈ (radical) (gas)	-318.2
CF ₃ (radical) (g)	-112.6
INFO-635P (c)	-114.8
BTU (c)	-59.6 ^a
	-66.7 ^b
	-73.7 ^c

- (a) Taking data for HF (aq) from NBS Circular 500,
(b) from NBS Technical Note 270-1, and (c) current
"best value" selected in this report.

(U) High temperature enthalpies were measured for allotropic forms of beryllium chloride from 13°-750°K. Heat of fusion of the α form at 688°K. was found to be 2070 ± 60 cal./mole.

(U) The enthalpy of aluminum has been measured primarily to determine the heat capacity of liquid aluminum which was found to be constant at 7.59 cal./(mole °K.) from 933°-1650°K.

(U) The enthalpy and heat capacity of solid aluminum are believed to be slightly higher near the melting point than previously evaluated data indicated. The heat of fusion was found to be 2560 ± 50 cal./mole.

CONFIDENTIAL

(This Page is Unclassified)

(U) Series C, consisting of 50 substances of the Classified JANAF Tables of Propellant Ingredients, was issued in April, 1965. Series D, consisting of 50 substances, was completed by the end of December, 1965, for comment by the reviewers.

(U) Four supplements to the JANAF Thermochemical Tables (Nos. 16, 17, 18 and 19) were mailed to the users and one additional supplement (No. 20) was prepared for comment. The JANAF Thermochemical Tables, complete through Supplement No. 17, were published for public sale by the Clearinghouse for Federal Scientific and Technical Information.

D. BIOCHEMICAL RESEARCH (U)

(U) The personnel of the Biochemical Research Laboratory continue to be available as consultants in Industrial Hygiene, Toxicology, and Pharmacology to the Scientific Projects Laboratory. A study of the effectiveness of rubber gloves as a barrier to skin contact by TAZ and THA is reported.

(U) The major emphasis of the Biochemical Research Laboratory continues to be the toxicological study of beryllium-containing materials. This research is directed toward obtaining an understanding of the fundamental biological, chemical and physical mechanisms involved in the toxic action of beryllium and its compounds in order to adequately evaluate the relative health hazards presented by beryllium-containing materials, including exhaust products from motor firings.

(U) The chemical and physical studies have been centered upon characterization of several key samples of beryllium oxide. So far as possible, these same procedures and techniques have been used in the characterization of four samples of exhaust products from motor firings received in October from the Aerospace Medical Research Laboratories, Wright-Patterson Air Force Base, Ohio.

(U) The biological investigations have been centered upon the study of animals, treated intratracheally with well-characterized samples of beryllium oxide, in order to determine the nature of the chronic lung disease in animals, including the cellular and biochemical changes that take place during the course of the disease.

(U) Histopathological examinations of the lungs show very clearly a distinct difference in the biological response, depending upon the oxide administered. Thus, lungs from rats treated with beryllium oxide calcined at 500°C. show a widely dispersed focal pneumonitis of granulomatous nature, with the development of tumors after several months. In contrast, lungs from rats treated with the oxide calcined at 1600°C. show minimal pathological effects, similar to those induced by relatively non-harmful "inert" dusts.

CONFIDENTIAL

(This Page is Unclassified)

CONFIDENTIAL

(This Page is Unclassified)

(U) Furthermore, tissues from rats that received the oxide calcined at 500°C. contain considerable beryllium and the concentration of beryllium tends to increase with length of time on the experiment, while in the tissues from the rats that received the oxide calcined at 1600°C., the beryllium concentration is slightly above control values. Studies are continuing to investigate more fully the mode of translocation of beryllium in the body and its mechanism of action.

(U) The long-term studies on rats and rabbits using key samples of beryllium oxide are continuing satisfactorily. Pilot studies also are under way on selected samples of beryllium oxide calcined at temperatures intermediate between 500° and 1600°C. Included in this pilot study are samples of beryllium hydroxide, a sample of "fused beryllium oxide", and beryllium metal. Recently, a limited study was started on the four samples of exhaust products from motor firings received from Wright-Patterson Air Force Base.

(U) All of the laboratory work carried out to date demonstrates a definite gradation in the biological activity of beryllium oxide samples and, further, a striking correlation between their biological activity and their chemical and physical properties. The successful completion of this study should furnish the basic information necessary to more fully evaluate the relative health hazards presented by beryllium-containing materials, including exhaust products from motor firings.

CONFIDENTIAL

(This Page is Unclassified)

CONFIDENTIAL

SECTION III

(U) FUELS SYNTHESIS

Work By: F. M. Brower, R. D. Daniels, N. E. Matzek, R. V. Petrella, J. J. Plomer, P. F. Reigler, C. B. Roberts, J. M. Self, and J. A. Snover.

(C) Research in the fuels area during 1965 has been concentrated on the studies of aluminum hydride. The research effort has stressed fundamental stability and crystallization studies with the goal of obtaining a product having improved properties for storage and use as a solid rocket propellant ingredient.

A. FUNDAMENTAL CRYSTALLIZATION STUDIES ON ALUMINUM HYDRIDE (C)

1. Solution Stability and Chemistry Studies (U)

(C) Solution stability and chemistry studies were performed to determine optimum conditions for the direct crystallization of aluminum hydride as the 1451 polymorphic phase. It was expected that the product obtained in this manner, without undergoing solid state phase transition, would be composed of more nearly perfect crystals and would thus possess greatly improved physical and chemical properties.

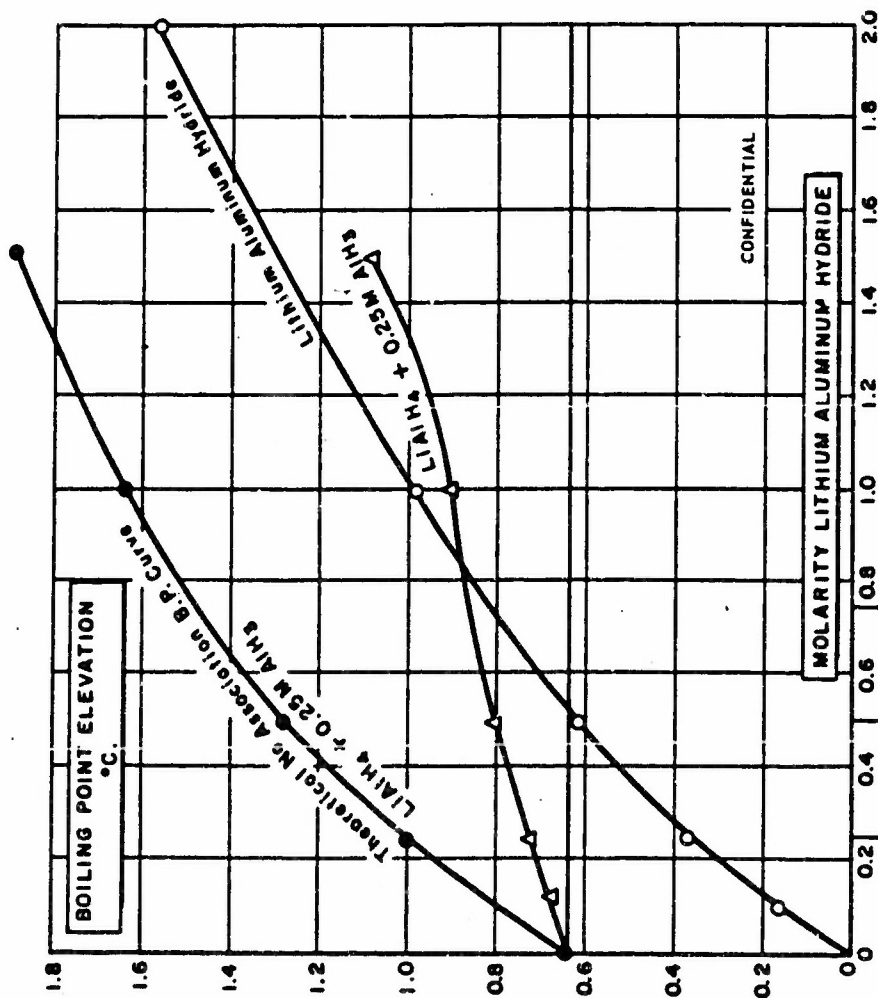
a. Molecular Weight Studies of Soluble Aluminum Hydride, Lithium Aluminum Hydride, and Lithium Borohydride (C)

(C) Aluminum hydride-1451 is generally produced in our laboratory by crystallization from boiling ether-benzene mixtures which contain lithium aluminum hydride and lithium borohydride as additives. The molecular weight studies of the aluminum hydride system and equipment used were a continuation of the data previously reported (1). These studies have indicated an increase in the average molecular weight of aluminum hydride on the addition of lithium aluminum hydride and lithium borohydride to the system. Subsequently, the effect of each constituent on aluminum hydride in solution was studied independently and is reported below.

(1) Molecular Weight Studies of Soluble Aluminum Hydride and Lithium Aluminum Hydride (C)

(C) The degree of association between aluminum hydride and lithium aluminum hydride was determined by ebulliometry, and from these measurements the average molecular weights of mixtures of the two hydrides dissolved in diethyl ether were calculated. The aluminum hydride concentration was maintained at a constant value of 0.25 M and the lithium aluminum hydride concentration was varied from 0 to 1.5 M. The experimental results are summarized in Figures 1 and 2. The data in Figure 1 show that the boiling point of a mixture deviated considerably from the expected

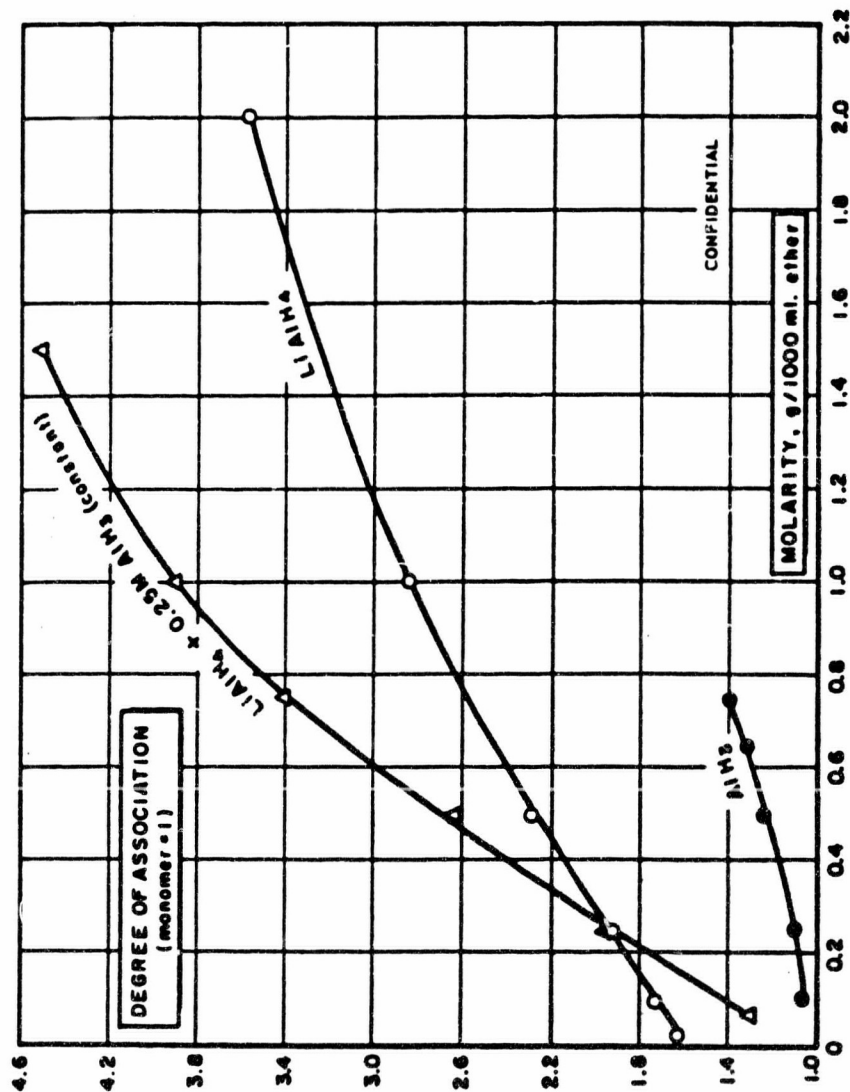
CONFIDENTIAL



(C) Fig. 1 - Change in Boiling Point Elevation of Lithium Aluminum Hydride and Lithium Aluminum Hydride Containing 0.25 M Aluminum Hydride as a Function of Lithium Aluminum Hydride Molarity

CONFIDENTIAL

CONFIDENTIAL



(C) Fig. 2 - Degree of Association of Lithium Aluminum Hydride, Aluminum Hydride, and Lithium Aluminum Hydride Containing 0.25 M Aluminum Hydride as a Function of Molarity

CONFIDENTIAL

CONFIDENTIAL

theoretical curve obtained by assuming no association existed between the two hydrides. There was no sharp break or change in the slope of the experimentally obtained lithium aluminum hydride and aluminum hydride curve, indicating no formation of a simple complex having a low, whole number mole ratio of lithium aluminum hydride to aluminum hydride. The degree of association of lithium aluminum hydride - aluminum hydride solution compared to lithium aluminum hydride and aluminum hydride separately as a function of molarity is shown in Figure 2. It is observed that the presence of lithium aluminum hydride in a 0.25 M AlH_3 solution increases the size of the molecular species present in solution; however, it is not known if the association represents association between lithium aluminum hydride and aluminum hydride or increased association of lithium aluminum hydride, or aluminum hydride due to the presence of the other, or a combination of the two.

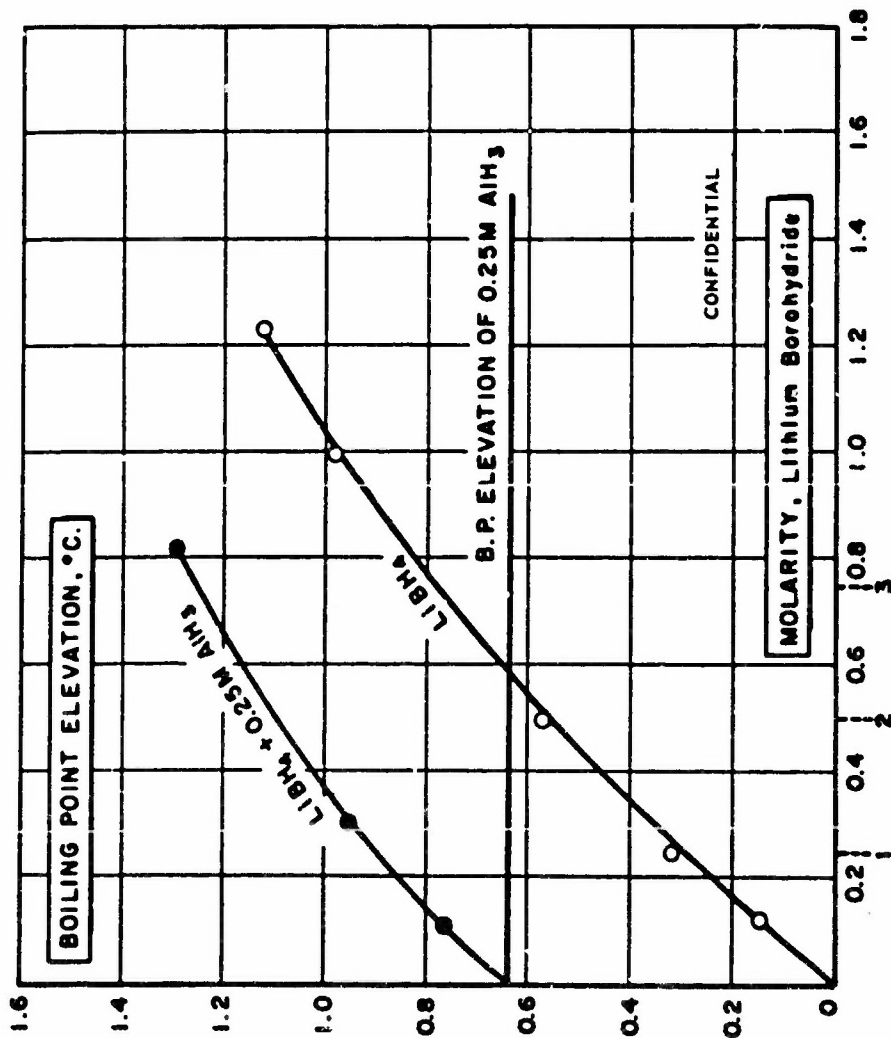
(2) Molecular Weight Studies of Soluble Aluminum Hydride and Lithium Borohydride (C)

(C) A similar study to that described in Section (1) for lithium aluminum hydride was made with lithium borohydride. The aluminum hydride concentration was again maintained at 0.25 M and the lithium borohydride concentration varied from 0 to 0.82 M. In contrast to the aluminum hydride - lithium aluminum hydride system, the boiling point elevation of the two was nearly additive, as shown in Figure 3. Therefore, it is concluded that only a slight association takes place between aluminum hydride and lithium borohydride in ether solution over the concentration range and temperature studied.

b. Solubility Studies of Lithium Aluminum Hydride, Lithium Borohydride, and Aluminum Hydride in Diethyl Ether - Benzene Solvent Systems (C)

(C) Two different processes are used by The Dow Chemical Company for the production of macrocrystalline aluminum hydride-1451. The first is the "batch" process which involves the precipitation, desolvation and conversion of a definite amount of aluminum hydride from a diethyl ether - benzene solution containing a fixed mole ratio of mixed hydrides. The second is the "continuous" process in which a dilute stoichiometric solution of aluminum hydride is continuously added to a diethyl ether - benzene solution containing mixed hydrides. The solubilities of lithium aluminum hydride, lithium borohydride, and aluminum hydride have been measured and described for both systems. In the following work the term "solubility" is used in a broad sense to express the amount of hydride or mixed hydrides in solution, realizing that in some cases equilibrium conditions do not exist. The solubilities of lithium aluminum hydride, lithium borohydride, and aluminum hydride in a hot solution of diethyl ether and benzene were determined according to the following procedure.

CONFIDENTIAL



(c) Fig. 3 - Change in Boiling Point Elevation of Lithium Borohydride and Lithium Borohydride Containing 0.25 M Aluminum Hydride as a Function of Lithium Borohydride Molarity

CONFIDENTIAL

CONFIDENTIAL

(C) A conversion solution composed of the various ingredients was placed in a three-neck, one-liter flask connected to a distillation column. The flask was heated by an oil bath and the contents of the flask stirred mechanically. A filtering stick placed in the flask was then attached to a 250 ml. flask through an appropriate adapter. When necessary, an additional funnel was also connected to the system containing a 0.3 M solution of aluminum hydride in diethyl ether.

(C) The oil bath was heated until the contents of the flask were under a total ether reflux. The diethyl ether was removed by distillation until the desired solution temperature in the range of 75°-78°C. was obtained. After reaching this temperature, the column was returned to total reflux and the conversion solution sampled for soluble lithium aluminum hydride, lithium borohydride, and aluminum hydride as described below.

(U) A hot (115°C.) 250 ml. flask was then attached to the sampling apparatus. After the flask and adapter were isolated from the conversion solution, the sampling system was evacuated and purged with nitrogen. The system was again evacuated and opened to the conversion solution. After collection of approximately 25 ml. of solution, the sample was closed to the conversion solution and again filled with nitrogen. The flask was removed and a 20 ml. aliquot of hot solution was then analyzed for lithium, aluminum and boron. Careful assignment of each constituent in the material balance gave a measure of the solubility of each component. The solubility values were then plotted in mmoles/ml.

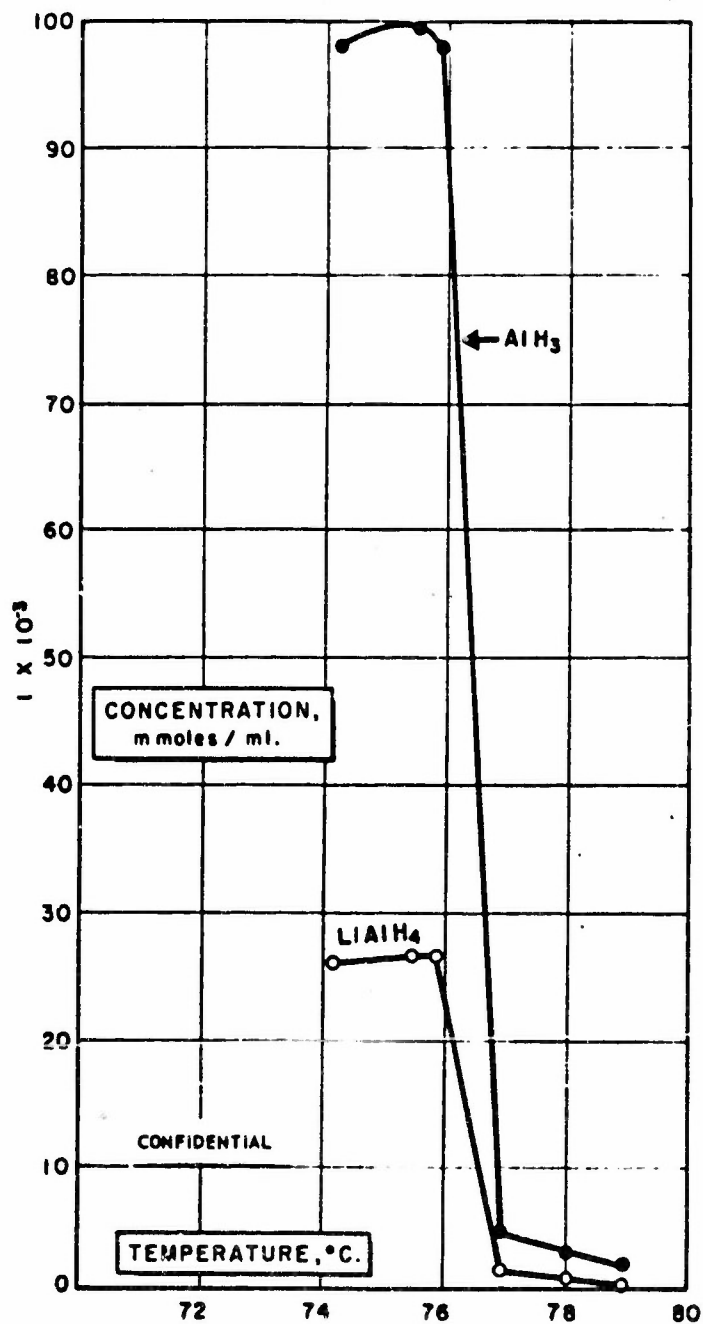
(1) Solubility Studies of Hydrides in the Batch Process (U)

(U) The solubilities of lithium aluminum hydride, lithium borohydride, and mixtures of these compounds in the binary diethyl ether - benzene solvent system were previously reported (1). It was observed that the solubilities of both lithium aluminum hydride and lithium borohydride in the binary solvent system were greatly increased due to the presence of each other in the solution. Such an increase in solubility can be explained by association.

(C) Since lithium aluminum hydride and lithium borohydride associate to some degree in the benzene - diethyl ether solvent system in the temperature range of 74°-79°C., it is necessary to determine whether aluminum hydride also associates with these complex hydrides. The measured solubilities of lithium aluminum hydride, lithium borohydride, and aluminum hydride in the benzene - ether solvent system for the temperature range of 74°-79°C. are shown in Figures 4, 5, and 6. These temperatures represent boiling points, and each temperature represents a different ratio of solvents in the solvent pair. A hydride mole ratio of 1 lithium aluminum hydride: 4 aluminum hydride: 1 lithium borohydride was used during these studies. The volume of benzene and diethyl ether used should have resulted in a theoretical solubility of 26×10^{-3} mmoles/ml. of both lithium aluminum hydride and lithium borohydride

CONFIDENTIAL

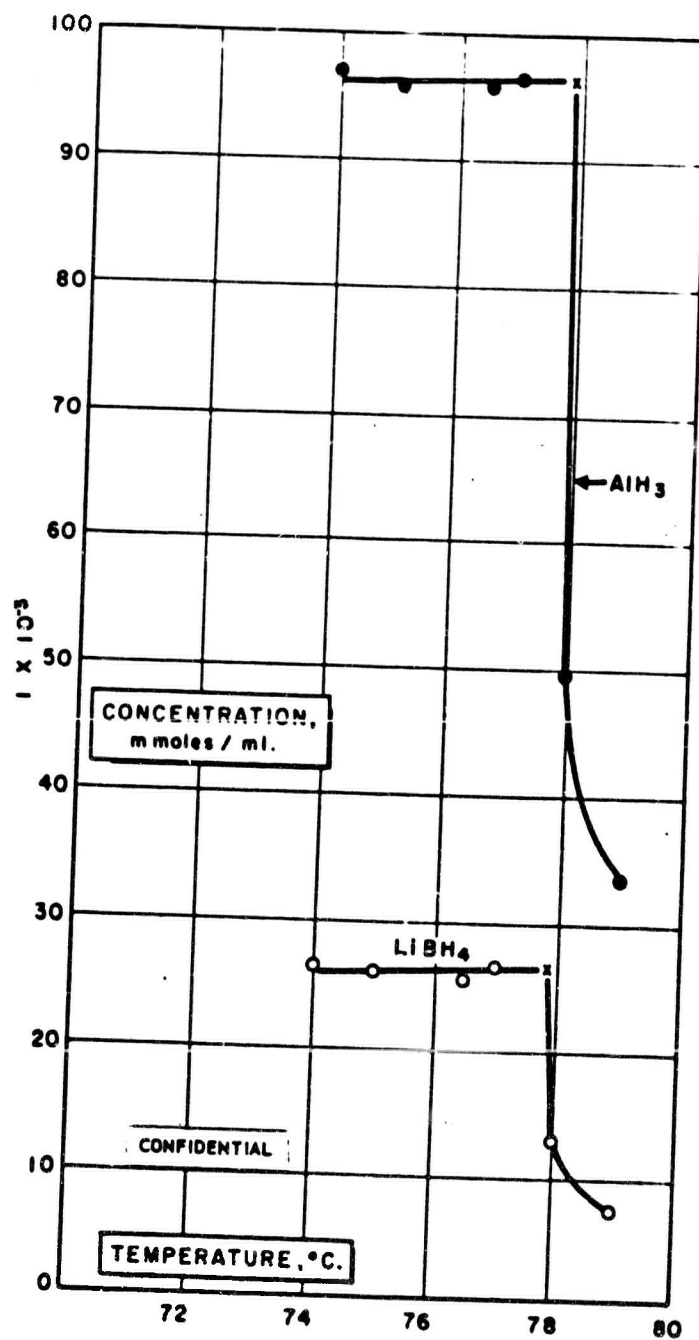
CONFIDENTIAL



(C) Fig. 4 - Batch Process Solubility Curves of Lithium Aluminum Hydride and Aluminum Hydride at Various Temperatures in the Binary Ether - Benzene System

CONFIDENTIAL

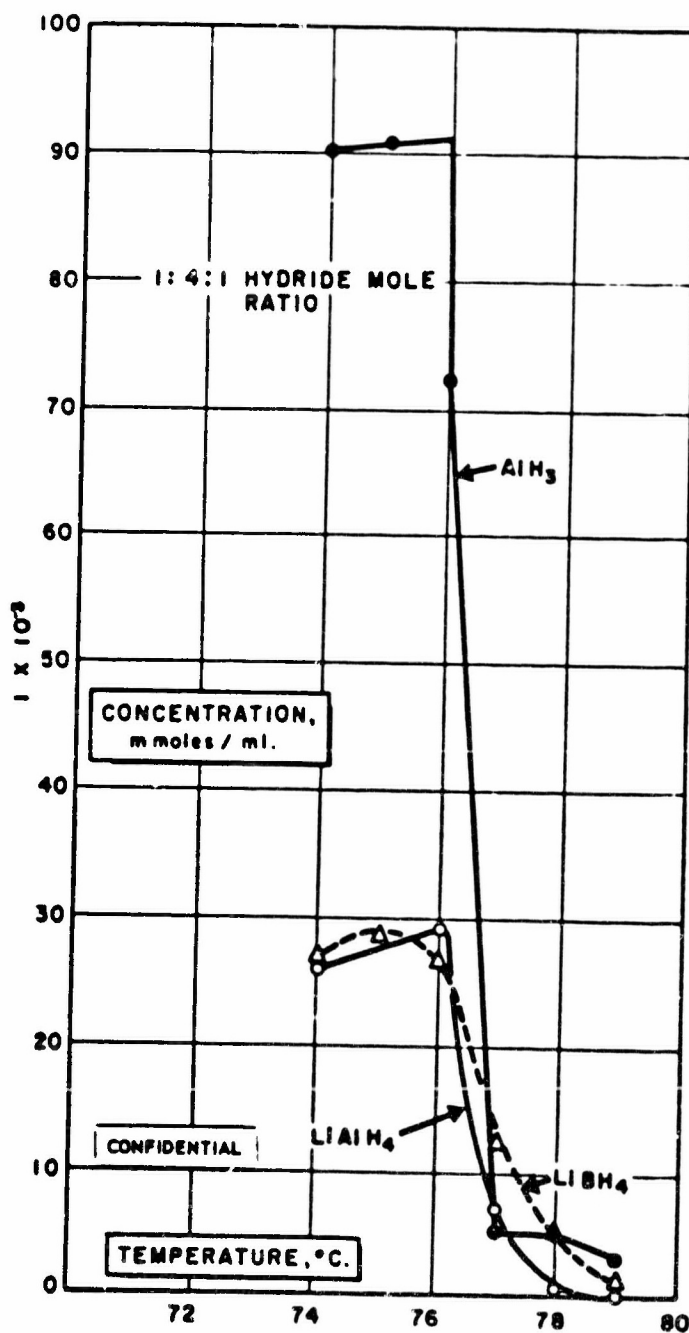
CONFIDENTIAL



(C) Fig. 5 - Batch Process Solubility Curves of Lithium Boro-Hydride and Aluminum Hydride at Various Temperatures in the Binary Ether - Benzene System

CONFIDENTIAL

CONFIDENTIAL



(C) Fig. 6 - Batch Process Solubility Curves of Lithium Aluminum Hydride, Aluminum Hydride and Lithium Borohydride in a Mole Ratio of 1:4:1 at Various Temperatures in the Binary Ether - Benzene System

CONFIDENTIAL

CONFIDENTIAL

and 105×10^{-3} mmoles/ml. of aluminum hydride at the starting temperature of 74°C . Variations from these values in Figures 4, 5, and 6 represent manipulation and recovery errors. The typical solubility curve for aluminum hydride in the presence of lithium aluminum hydride is illustrated in Figure 4. The aluminum hydride also causes an increase in the solubility of lithium aluminum hydride in the temperature range of 74° - 76°C . similar to that observed for lithium aluminum hydride in the presence of lithium borohydride. It should also be noted that when precipitation of aluminum hydride is initiated at 76°C . the effect of time on the slope of the curve is unknown. If maintained at 76°C . and given time to equilibrate, the concentration of aluminum hydride may drop to the same value observed at 77°C . and 78°C .

(C) The solubility of aluminum hydride in the presence of lithium borohydride is shown in Figure 5. The solubilities of both lithium borohydride and aluminum hydride in the higher temperature range (76.5° - 79°C .) are markedly increased, and the temperature of precipitation (77.9°C .) is also higher than observed in any previous system.

(C) Molecular weight studies of soluble aluminum hydride and lithium borohydride in diethyl ether have shown that there is only a slight amount of association between lithium borohydride and aluminum hydride. Therefore, it is concluded that the increased solubility of aluminum hydride and lithium borohydride over a higher temperature range is a result of a secondary solvent effect.

(C) The solubility curve for aluminum hydride in the presence of both lithium aluminum hydride and lithium borohydride is illustrated in Figure 6. The sharp shoulder on the aluminum hydride solubility curve at 76°C . is quite real, since all the aluminum hydride was soluble at that temperature, but precipitated almost immediately after sampling. This abrupt change in solubility at the temperature of precipitation can be attributed to one or both of two factors:

- (i) Dissociation of highly complex associated molecules due to temperature.
- (ii) Precipitation of solids from a super-saturated solution.

(U) The boiling range described in these studies (74° - 79°C .) is a function of the volume percent diethyl ether present in the benzene and, therefore, as the temperature increases the ether concentration decreases. Correspondingly, with respect to diethyl ether, the concentration of solids increases with increasing temperature and lower ether concentrations. Thus, if precipitation is solely dependent on concentration, systems containing higher dissolved solids per given volume of benzene and ether should precipitate prematurely at lower temperatures.

CONFIDENTIAL

CONFIDENTIAL

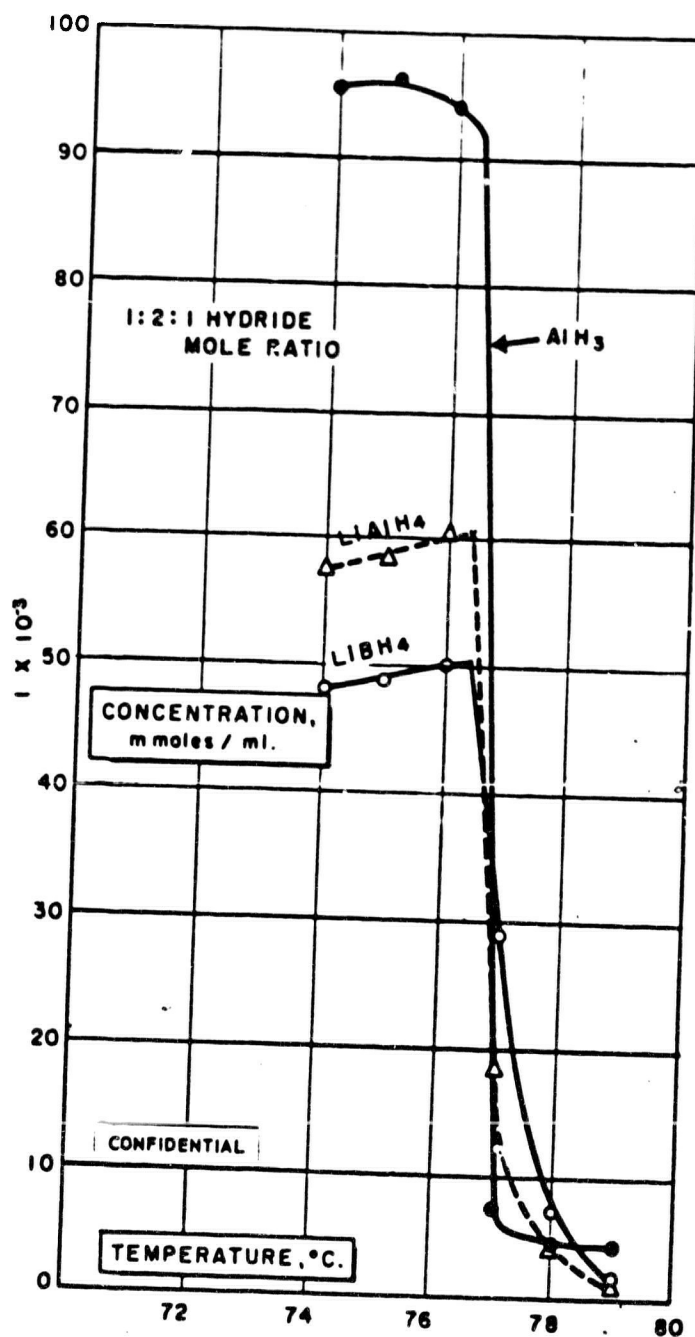
(C) Figures 7 and 8 show the solubility curves for lithium aluminum hydride, aluminum hydride, and lithium borohydride in mole ratios of 1:2:1 and 1:1:1. It can be seen from Figures 7 and 8 that neither system precipitated early. In both cases, precipitation occurred at approximately 76°C. The amount of solids present in the 1:1:1 hydride mole ratio system is twice that in the 1:4:1 mole ratio for any given temperature. Therefore, it must be concluded that the precipitation phenomenon is not solely a function of concentration, but may involve a temperature dependent complex.

(C) To further substantiate the concept of association or complexation, two additional hydride mole ratios were studied. The solubility curves for lithium aluminum hydride, aluminum hydride, and lithium borohydride in mole ratios of 1:8:1 and 1:16:1 are shown in Figures 9 and 10. Aluminum hydride solubility decreased gradually in the temperature range of 76°-77°C., apparently due to the smaller concentrations of complex hydride additives present. This effect was most pronounced in the 1:16:1 mole ratio system. The sharp shoulder predominant in a 1:4:1 hydride mole ratio system, as shown in Figure 6, is no longer present, indicating insufficient associative strength and/or decreased solubility over the temperature range of 74°-77°C. It has been demonstrated that more well-defined crystals are usually obtained using the higher hydride mole ratios. The data, therefore, suggest that a gradual precipitation, desolvation, and conversion may be conducive to crystal growth and perfection in the batch process. The solubility of aluminum hydride in the binary solvent has also been measured and a solubility curve for this hydride at various temperatures, Figure 11, shows that it varies inversely with the temperature.

(C) The boiling temperatures (74°-79°C.) observed in these solubility studies are a function of the volume percent diethyl ether in benzene; thus, it is apparent that aluminum hydride solubility is not solely a function of ether concentration. Considering the ether solvent only, data from the ether-benzene solubility studies show the solubility of aluminum hydride, based on the ether concentration available in the specified temperature range, extends from 1.92 to 2.32 M. Previous investigation of the solubility of aluminum hydride in diethyl ether alone has shown that the concentration of aluminum hydride cannot exceed 0.6 M without relatively rapid precipitation and cannot be conveniently stored at ambient temperatures at concentrations greater than 0.3 M. The solubility under equilibrium conditions appears to be about 0.2 M.

(C) The data thus indicate that the solubility of aluminum hydride in ether-benzene is a function of the binary solvent system and it must be concluded that benzene is more than just a simple diluent. As a result of molecular weight and solubility studies the following conclusions can be made:

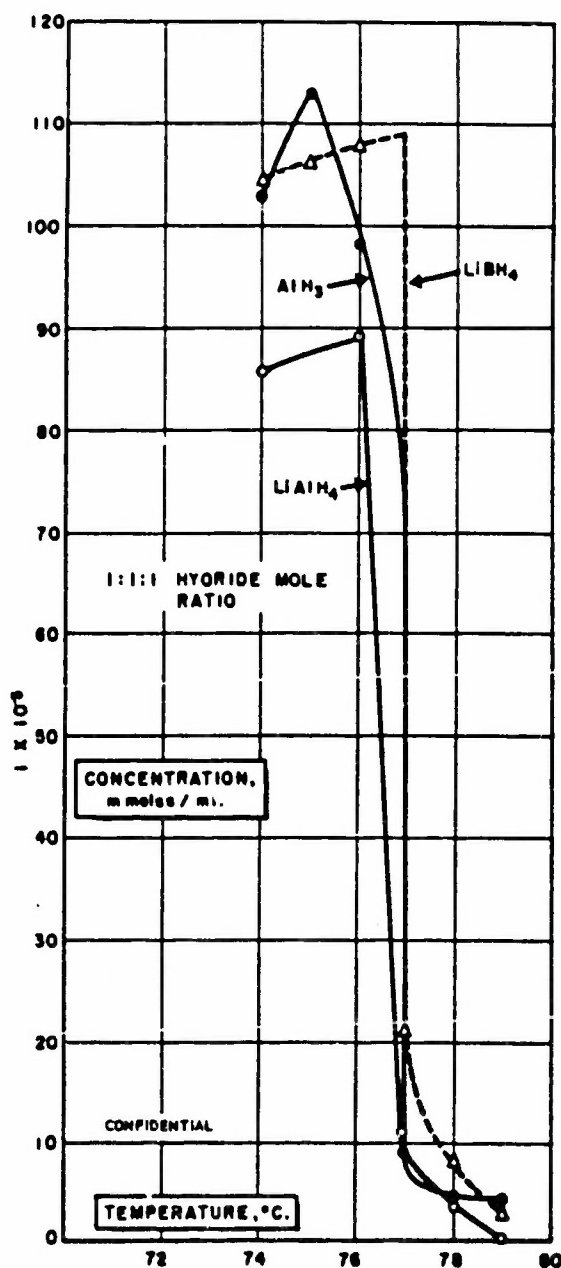
CONFIDENTIAL



(C) Fig. 7 - Batch Process Solubility Curves of Lithium Aluminum Hydride, Aluminum Hydride and Lithium Borohydride in a Mole Ratio of 1:2:1 at Various Temperatures in the Binary Ether - Benzene System

CONFIDENTIAL

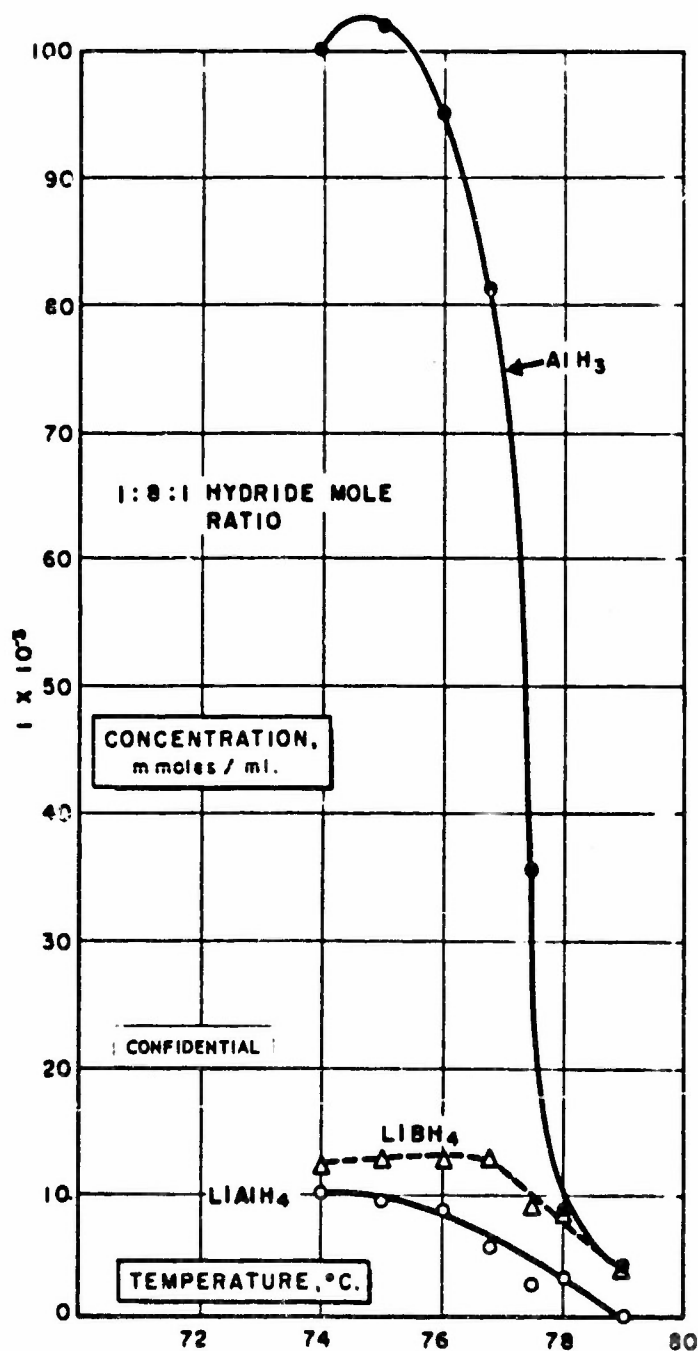
CONFIDENTIAL



(c) Fig. 8 - Batch Process Solubility Curves of Lithium Aluminum Hydride, Aluminum Hydride and Lithium Borohydride in a Mole Ratio of 1:1:1 at Various Temperatures in the Binary Ether - Benzene System

CONFIDENTIAL

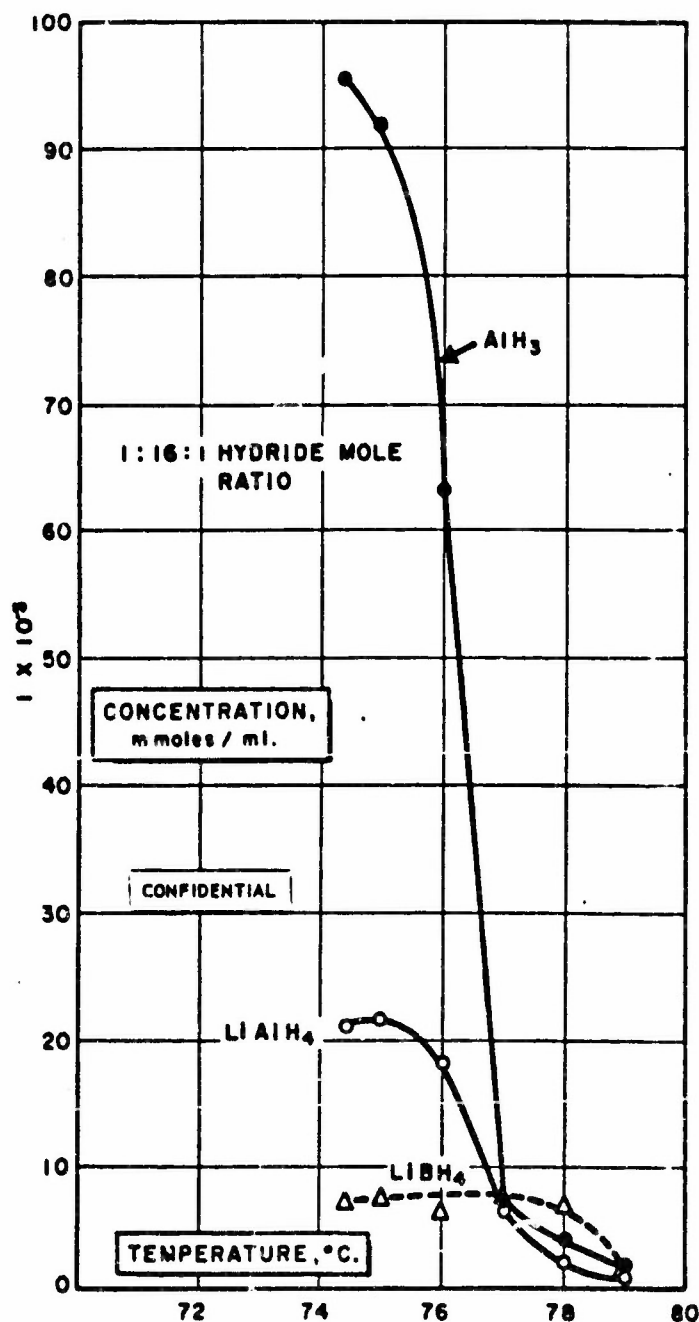
CONFIDENTIAL



(C) Fig. 9 - Batch Process Solubility Curves of Lithium Aluminum Hydride, Aluminum Hydride and Lithium Borohydride in a Mole Ratio of 1:8:1 at Various Temperatures in the Binary Ether - Benzene System

CONFIDENTIAL

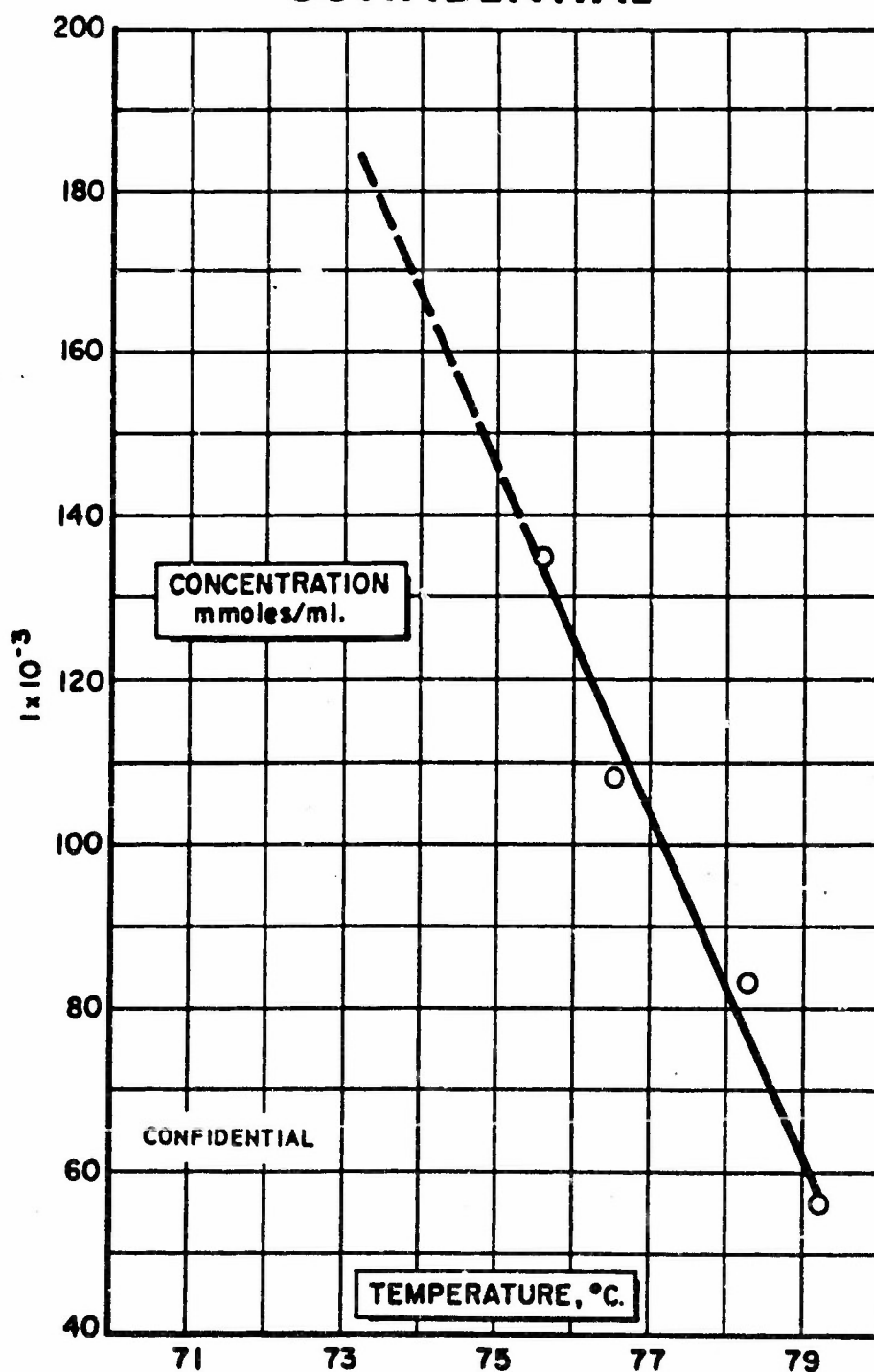
CONFIDENTIAL



(C) Fig. 10 - Batch Process Solubility Curves of Lithium Aluminum Hydride, Aluminum Hydride and Lithium Borohydride in a Mole Ratio of 1:16:1 at Various Temperatures in the Binary Ether - Benzene System

CONFIDENTIAL

CONFIDENTIAL



(C) Fig. 11 - Batch Process Solubility Curve of Aluminum Hydride at Various Temperatures in the Binary Ether - Benzene System

CONFIDENTIAL

CONFIDENTIAL

- (1) Lithium aluminum hydride and lithium borohydride form an associated molecule in ether-benzene solution, thus increasing the solubility of each compound.
- (11) Lithium aluminum hydride and aluminum hydride also form an associated molecule in the binary solvent.
- (111) Formation of these associated molecules in solution are temperature- and, possible, time-dependent.
- (iv) The dissociation of these molecules is not a function of solute-solvent ratios.
- (v) The solubility of aluminum hydride in the ether-benzene solvent is temperature-dependent.
- (vi) Lithium borohydride extends the solubility of aluminum hydride over a higher temperature range. This extended solubility is believed to be the result of a secondary solvent effect rather than association.

(2) Solubility Studies of Hydrides in the Continuous Process (U)

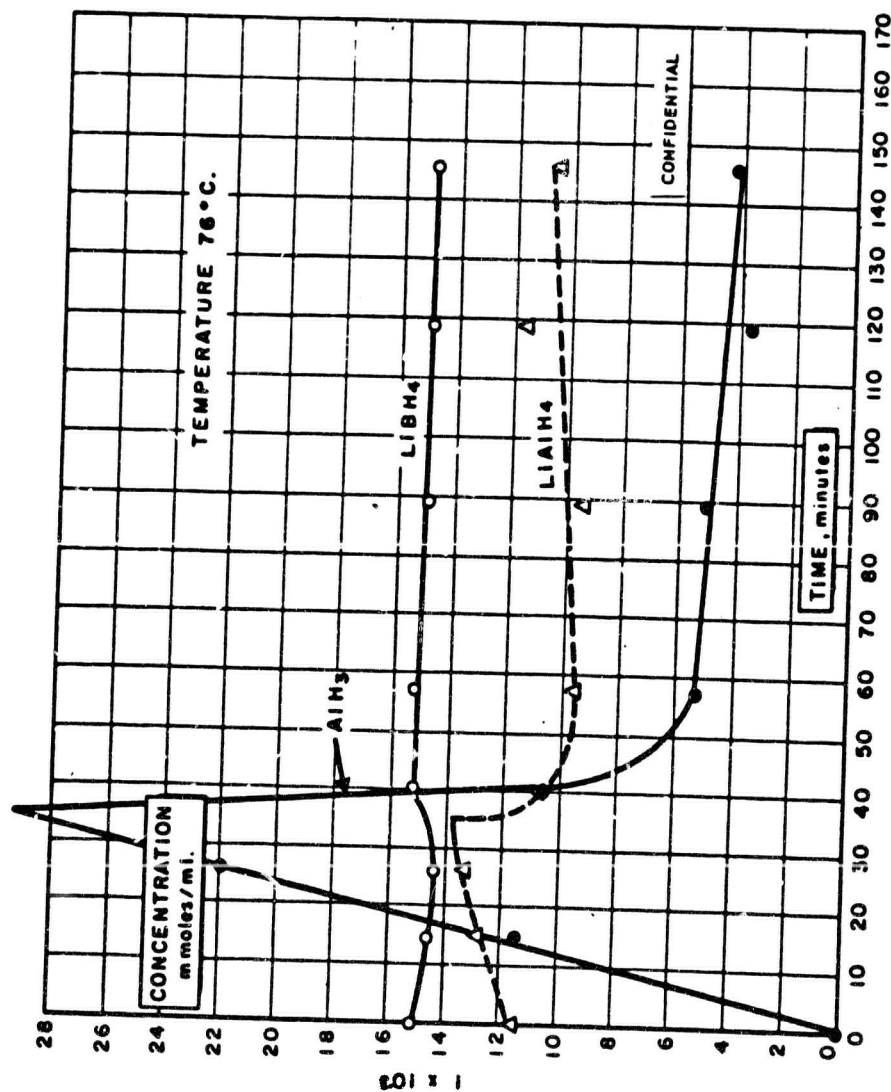
(U) Solubility studies in the continuous crystallization process involve an entirely different situation than that encountered in the solubility studies of the batch process. There is no longer any significance to the particular complex hydride mole ratio used. Based upon present data, there would be no time in the course of addition in the continuous process at which the predetermined mole ratio would be established.

(C) The solubility curve shown in Figure 12 represents the change in solubility of lithium borohydride, lithium aluminum hydride, and aluminum hydride in an ether - benzene system as a function of time at a constant temperature of 76°C. The aluminum hydride is continuously added and ether removed at an approximately constant rate throughout the experiment.

(C) The solubility of aluminum hydride shown in Figure 12 is slightly less than 1/3 of the measured solubility in the batch process illustrated in Figure 8. The solubilities of lithium aluminum hydride, aluminum hydride, and lithium borohydride just prior to precipitation indicate a hydride mole ratio of approximately 1:2:1. The data also show that after precipitation of the aluminum hydride the mole ratio changes to approximately 1:1:1.

(C) The significance of the solubility curve shown in Figure 12 is not in the maximum solubility of aluminum hydride prior to precipitation, but the solubility observed in the post-precipitation region of the curve. It is this solubility that permits crystal growth in the continuous process.

CONFIDENTIAL



(C) Fig. 12 - Continuous Process Solubility Curves of Lithium Aluminum Hydride, Lithium Borohydride, and Aluminum Hydride at a Constant Temperature of 76°C. in the Binary Ether - Benzene System

CONFIDENTIAL

CONFIDENTIAL

(U) The role of lithium aluminum hydride in this process is not fully understood; solubility data indicate that not all of the lithium aluminum hydride added is soluble. The significance of this observation is further discussed in Section A.2.a. (2) (e).

(C) From similar studies at different temperatures it has been shown that the solubilities of lithium aluminum hydride and aluminum hydride in the post-precipitation area decrease with increasing temperature. The solubility of lithium borohydride appears to be unaffected by temperature except at those above 78°C., at which point the solubility of lithium borohydride also decreases, probably as a result of the minimal ether concentration at these high temperatures. The significant factor in the continuous process is the solubility of aluminum hydride in the post-precipitation area because this represents the amount of aluminum hydride actually available for crystal growth. Figure 13 summarizes the solubilities of lithium aluminum hydride, lithium borohydride, and aluminum hydride in ether-benzene in the post-precipitation area.

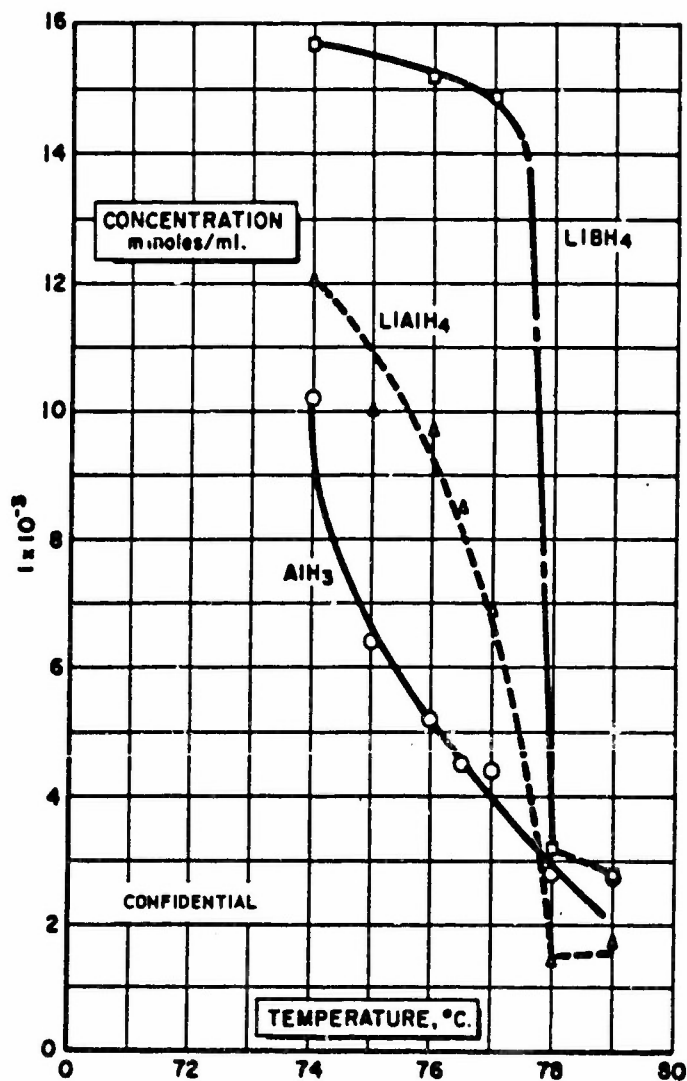
(C) Based on the assumption that soluble lithium aluminum hydride and lithium borohydride are necessary for crystal growth, Figure 13 shows that the effective range of crystallization would lie in the temperature range below 77°C. Above this temperature the solubilities of lithium aluminum hydride and lithium borohydride drop off sharply. The problem of crystal growth, however, is not a matter of simple solubility but also involves proper nucleation, feed rate, and residence time.

(a) Solubility of Lithium Borohydride and Aluminum Hydride in Diethyl Ether-Benzene at Constant Temperature (C)

(C) Molecular weight studies have shown that there appears to be little, if any, association between lithium borohydride and aluminum hydride in an ether solution. To determine whether this condition exists in the ether-benzene binary mixture and to clarify, if possible, the role of lithium borohydride in the continuous process, the solubilities of lithium borohydride and aluminum hydride in the binary solvent were measured at several temperatures. The results obtained at 76°C. are shown in Figure 14.

(C) The initial lithium borohydride concentration at ambient temperature was approximately 13×10^{-3} mmoles/ml. of solution. The same amount of aluminum hydride (80 mmoles) was added to this solution. If all the aluminum hydride remained soluble, a maximum solubility of 110×10^{-3} mmoles/ml. would be obtained. Comparison of this curve with other solubility curves in the continuous process reveals that this curve is unique. In none of the other solubility curves except Curve A₁, shown in Figure 18, did the aluminum hydride solubility approach the calculated maximum (110×10^{-3} mmoles/ml.). The similarity of the above aluminum hydride solution obtained in the absence of lithium aluminum hydride and lithium borohydride compared to the one obtained in the presence of lithium borohydride alone suggests little, if any, association between these two species in the ether-benzene binary solvent.

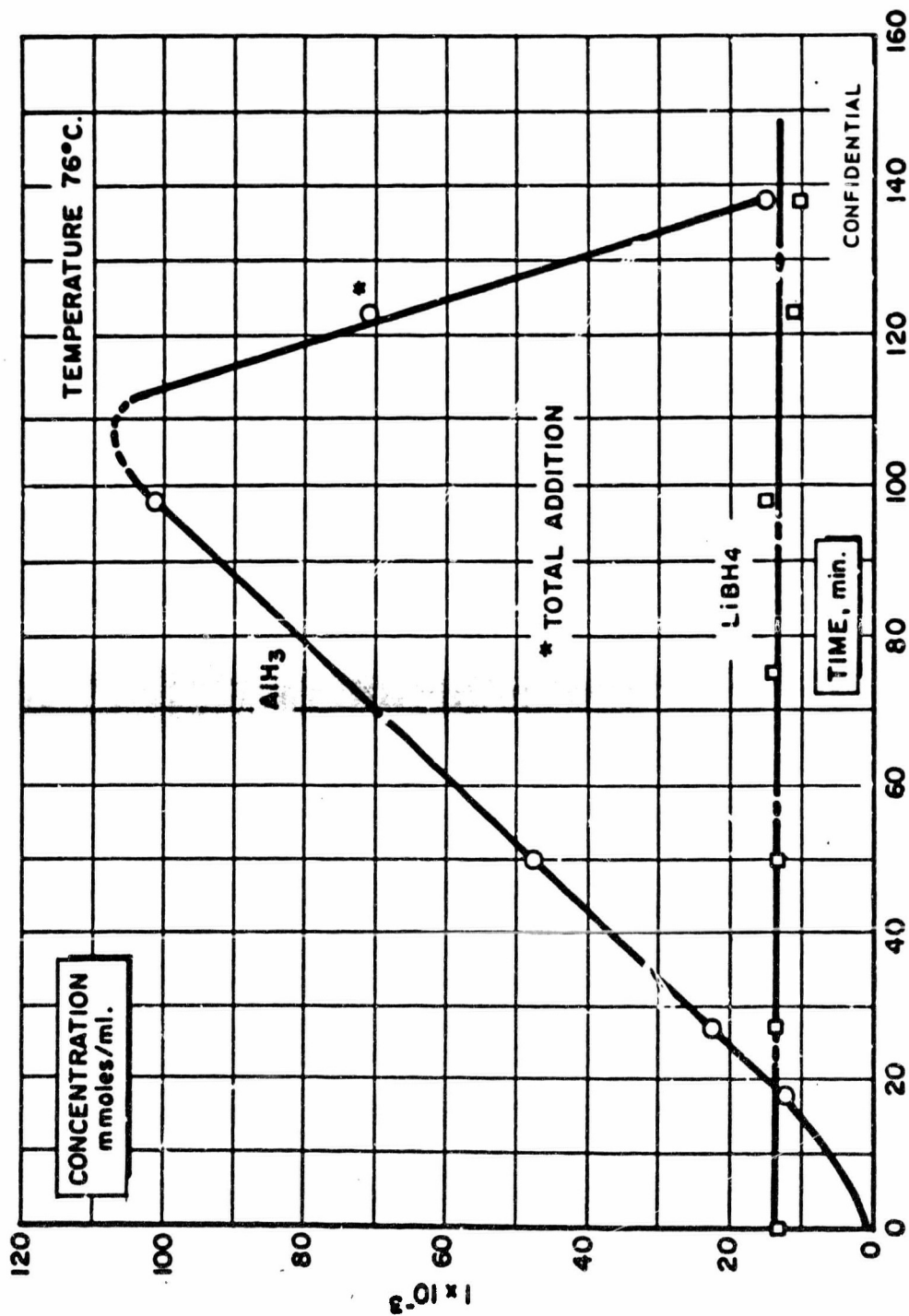
CONFIDENTIAL



(C) Fig. 13 - Summary of Continuous Process Post-Precipitation Solubility Curves of Lithium Aluminum Hydride, Lithium Borohydride, and Aluminum Hydride at Various Temperatures in the Binary Ether - Benzene System

CONFIDENTIAL

CONFIDENTIAL



(c) Fig. 14 - Continuous Process Solubility Curves of Lithium Borohydride and Aluminum Hydride at a Constant Temperature of 76°C. in the Binary Ether - Benzene System

CONFIDENTIAL

CONFIDENTIAL

(b) Solubility of Lithium Aluminum Hydride and Aluminum Hydride in Diethyl Ether-Benzene at Constant Temperature (C)

(C) The exact role of lithium aluminum hydride in the preparation of aluminum hydride-1991, other than the knowledge that a small amount is necessary for desolvation, is also not clearly understood.

(C) Solubility studies in the batch and continuous processes have shown that not all the lithium aluminum hydride added remains soluble. A certain small fraction is generally insoluble in the solvent over most of the temperature range studied. The insolubility varies directly with the temperature. In order to further elucidate the role of lithium aluminum hydride in the continuous process, the solubilities of lithium aluminum hydride and aluminum hydride in the binary solvent were measured at 74°C. and 77°C. These two temperatures were chosen to evaluate conditions on either side of the normal conversion temperature (76.5°C.), and should be indicative of a family of solubility curves in this temperature range. The results are shown graphically in Figures 15 and 16.

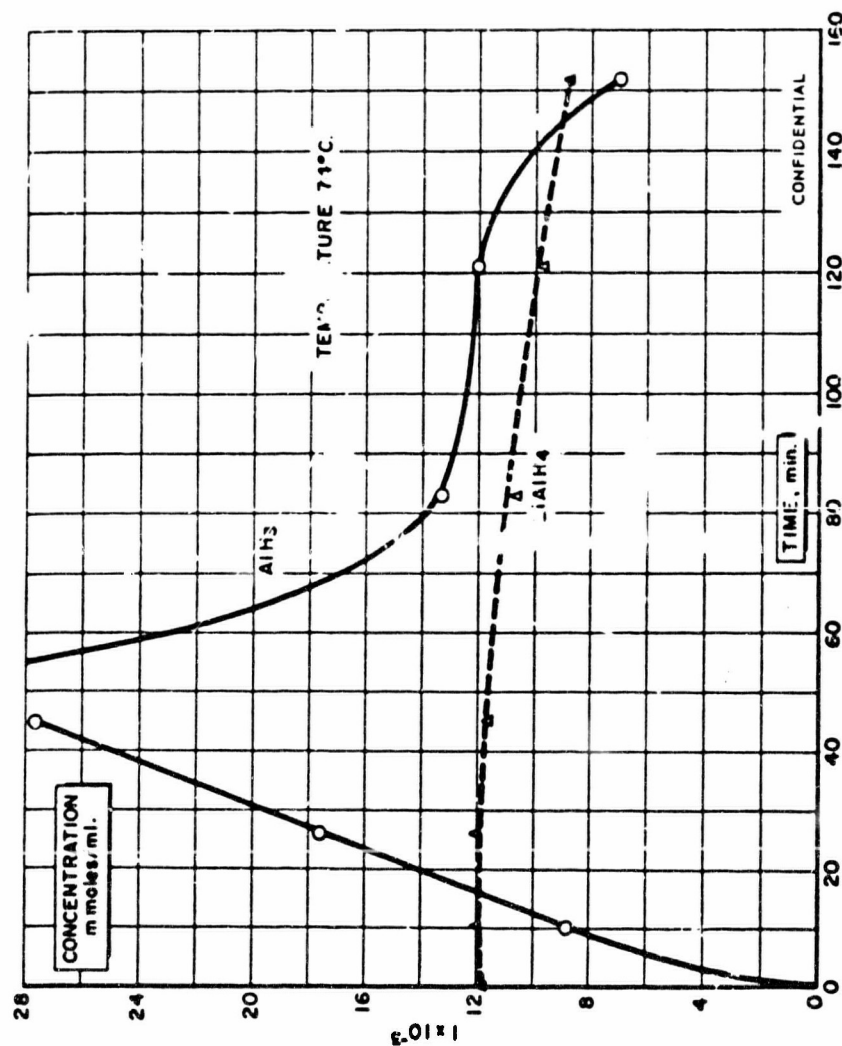
(C) The initial soluble lithium aluminum hydride concentration at ambient temperature in the ether-benzene solution was held constant at 13×10^{-3} mmoles/ml. To this solution, at the prescribed temperature, was added 80 mmoles of aluminum hydride. The figures show that the solubilities of both lithium aluminum hydride and aluminum hydride decrease with increasing temperature. It is also noted in Figure 16 that the solubility of lithium aluminum hydride decreased at the point of precipitation. This could be interpreted as the dissociation of a complex $\text{LiAlH}_4 \cdot \text{AlH}_3$ molecule with temperature.

(C) Figure 17 compares the solubility curves of lithium aluminum hydride and aluminum hydride together with that obtained in the combination of lithium aluminum hydride, aluminum hydride, and lithium borohydride at 77°C.

(C) Curves A₁ (AlH_3) and B₁ (LiAlH_4) represent solubility curves of the binary combination, whereas Curves A (AlH_3), B (LiAlH_4) and C (LiBH_4) are those observed in the ternary combination. The only discernible difference between these curves is the markedly increased solubility of lithium aluminum hydride due to the presence of lithium borohydride, especially at higher temperatures. Molecular weight and solubility studies in the batch process indicated that lithium aluminum hydride and lithium borohydride form an associated or complex molecule in solution. This is further substantiated by the increase in solubility of the lithium aluminum hydride in the continuous process due to the presence of lithium borohydride.

(C) Molecular weight studies in diethyl ether, as well as solubility studies in the batch process, have indicated that some degree of association exists between lithium aluminum hydride

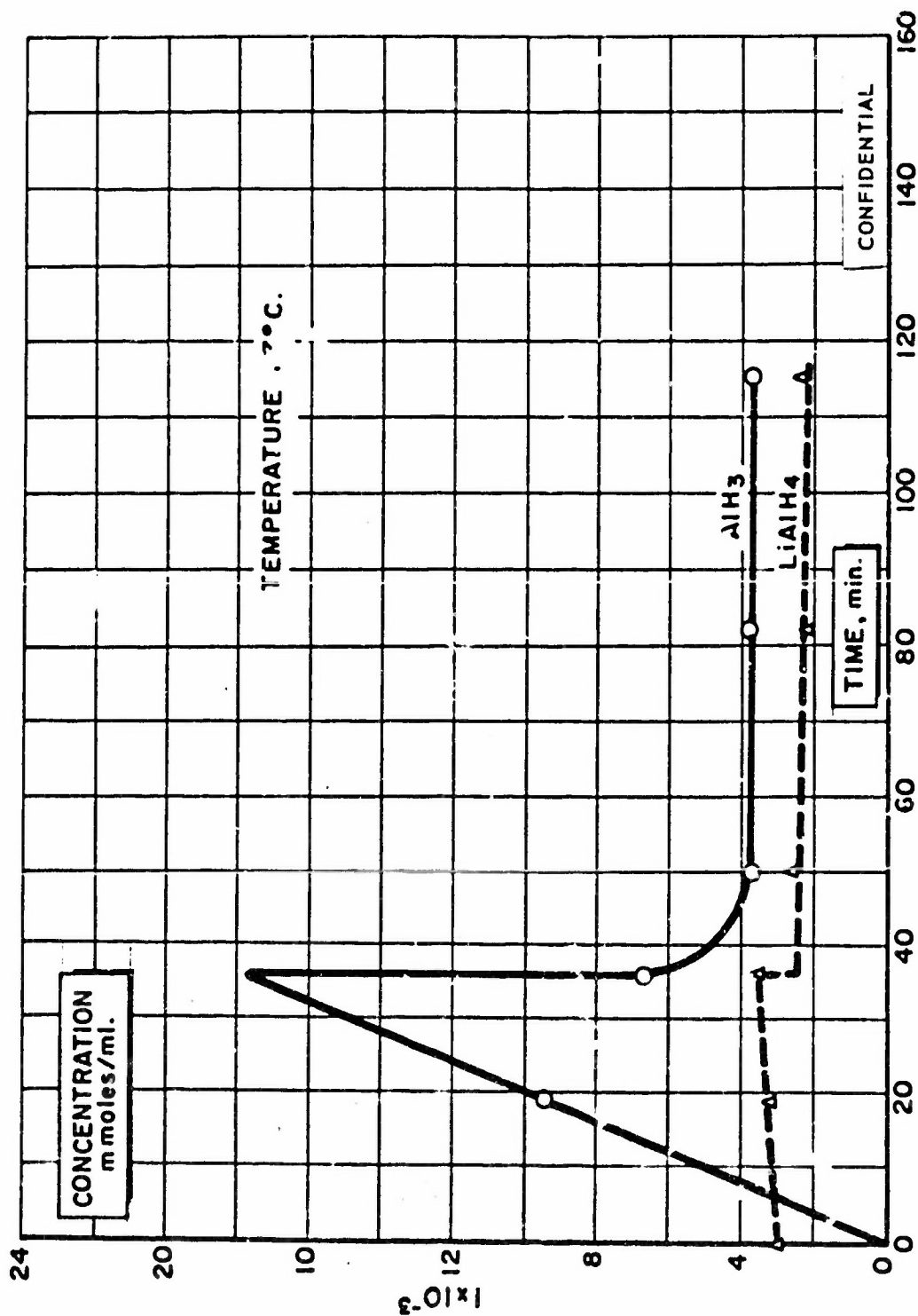
CONFIDENTIAL



(C) FIG. 15 - Continuous Process Solubility Curves of Lithium Aluminum Hydride and Aluminum Hydride at a Constant Temperature of 74°C. in the Binary Ether Benzene System

CONFIDENTIAL

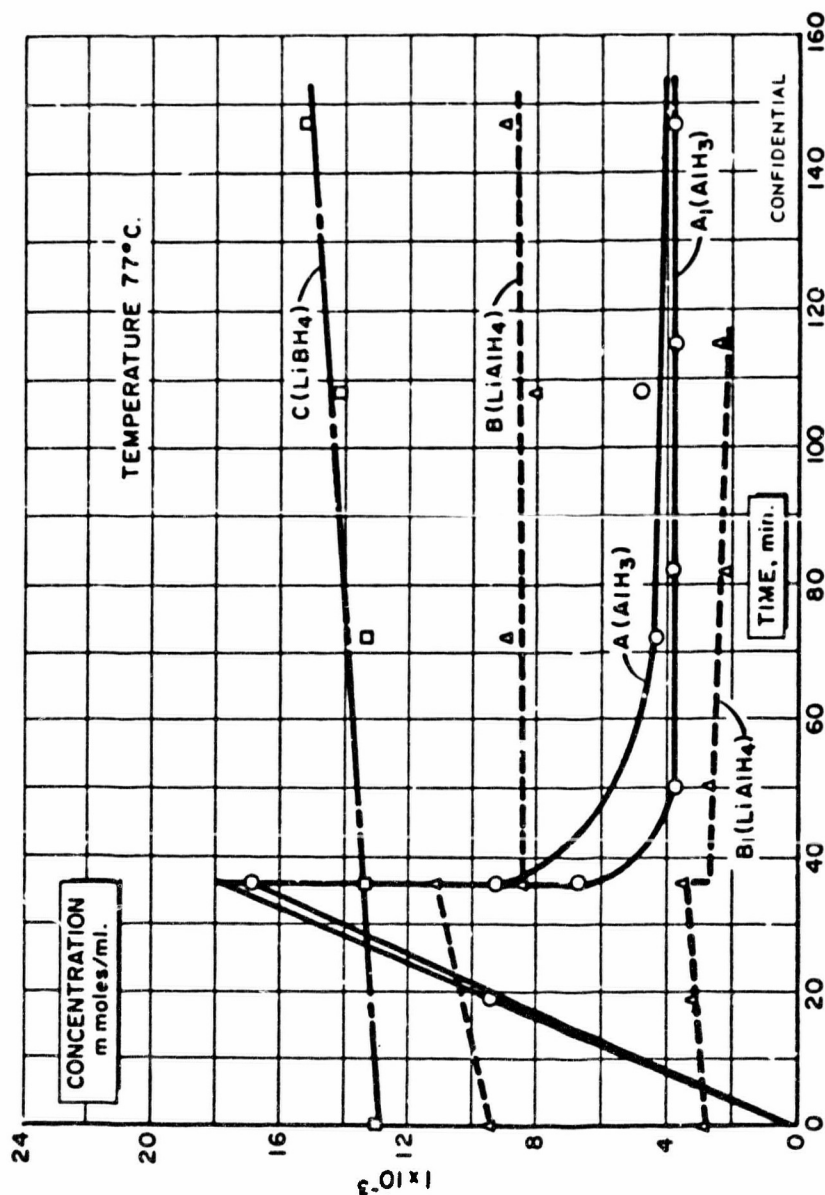
CONFIDENTIAL



(C) Fig. 16 - Continuous Process Solubility Curves of Lithium Aluminum Hydride and Aluminum Hydride at a Constant Temperature of 7°C. in the Binary Ether - Benzene System.

CONFIDENTIAL

CONFIDENTIAL



(C) Fig. 17 - Comparison Between the Continuous Process Solubility Curves of Lithium Aluminum Hydride-Aluminum Hydride and Lithium Aluminum Hydride-Aluminum Hydride-Lithium Borohydride Systems at a Constant Temperature of 77°C. in the Binary Ether - Benzene System

CONFIDENTIAL

CONFIDENTIAL

and aluminum hydride. The extent of this complexing and the effect of varying concentrations of lithium aluminum hydride on the solubility of aluminum hydride in the binary ether-benzene solvent were previously unknown. For this reason, it was decided to examine the effect of various concentrations of lithium aluminum hydride on the solubility of aluminum hydride.

(C) Figure 18 shows the solubility curves for aluminum hydride in ether-benzene at a temperature of 77°C. Curve A₁ (AlH₃) represents the measured solubility of only aluminum hydride in ether-benzene. Curves A (AlH₃) and B (LiAlH₄) represent the solubilities of these compounds in ether-benzene in the presence of each other. The initial soluble concentration of lithium aluminum hydride at ambient temperature was 13×10^{-3} mmoles/ml. The large suppression of the solubility of aluminum hydride due to the presence of lithium aluminum hydride can be explained at this time.

(C) In order to study further the effect of lithium aluminum hydride on the solubility of aluminum hydride, a series of experiments was designed in which the temperature (76.5°C.), the quantity of aluminum hydride and lithium borohydride added, and the volume of solvent were held constant. The initial concentration of lithium aluminum hydride at ambient temperature was varied from ~ 3 to 17×10^{-3} mmoles/ml. of solution. However, only minor variations in solubilities were observed.

c. Purity of Raw Materials (U)

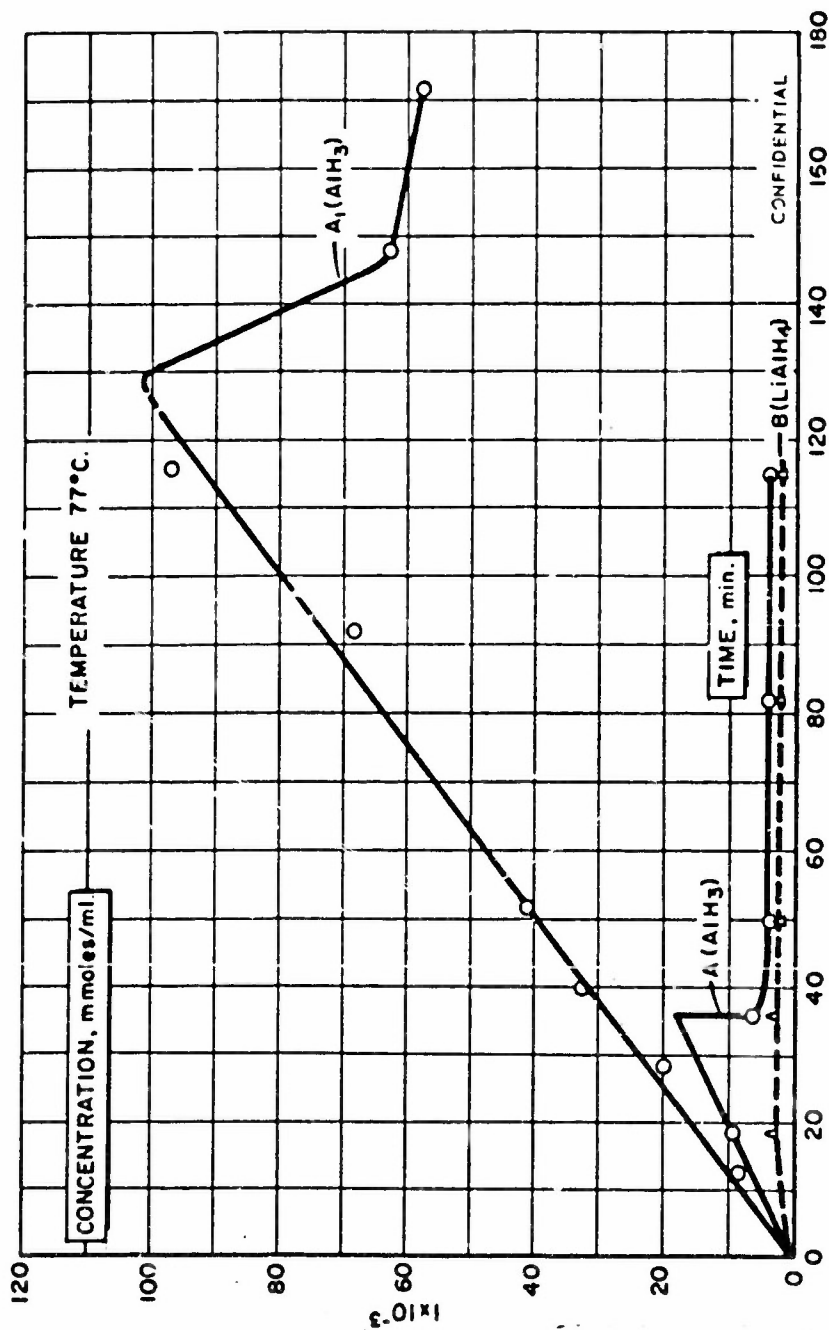
(1) Benzene (U)

(C) It was observed that the amount of decomposition during crystallization of aluminum hydride-1451 from ether-benzene solvent varied as benzene from different sources was used. Analyses of benzene from five different sources showed it to be low in unsaturation (less than 5 ppm. in >C=C<) and to produce no color with concentrated sulfuric acid. The chloride and sulfur content in all cases was found to be below 1 ppm. Gas-liquid chromatographic analysis showed the presence of low amounts of aliphatic and cyclic hydrocarbons in addition to small amounts of toluene. No correlation was obtained from any of the above tests or impurities with the resulting stability of the aluminum hydride prepared with various grades of benzene from the five sources. The only other common impurity in the hydrocarbon, water, was found to vary in concentrations between 50 and 120 ppm. When the water was removed by drying the various grades of benzene over lithium aluminum hydride, very little difference in product quality was observed. However, using the benzene without drying produced a marked change.

(C) Three different methods have been employed for water removal from benzene:

(1) Drying overnight with lithium aluminum hydride.

CONFIDENTIAL



(C) Fig. 18 - Comparison between the Continuous Process Solubility Curves of Aluminum Hydride Only and Aluminum Hydride in the presence of Lithium Aluminum Hydride at a Constant Temperature of 77°C. in the Binary Ether - Benzene System

CONFIDENTIAL

CONFIDENTIAL

(11) Drying overnight over Linde 5-A, 1/8", molecular sieves.

(111) Passing the benzene through an ion exchange column.

(U) In all three cases the water content is lowered to between 10 and 20 ppm., as determined by the modified Gilbarco hygrometer described in Section C.1.a. The manner in which the benzene is dried apparently does not affect the results, since in nearly all cases some decomposition occurred during the conversion step using the batch process. A significant reduction in the amount of decomposition, although not entirely eliminated, was noted when each grade of benzene was used without drying.

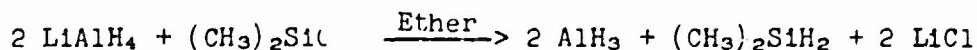
(C) The oxygen content of the aluminum hydride-1451 produced was also found to increase when wet benzene was used. Observations of the effect of water on the continuous crystallization process will be discussed in Section A.2.a.(4). It does appear, however, that water is an important variable which needs to be controlled if reproducible results are to be obtained.

(2) Differences in Ether Solutions of Aluminum Chloride (U)

(C) In order to further elucidate the effects of trace impurities on aluminum hydride stability, a study of the purity of the starting material, aluminum chloride, was undertaken. Several ether solutions of aluminum chloride were analyzed by gas-liquid chromatography using flame ionization and electron capture detection devices simultaneously. No significant differences were observed using electron capture; however, flame ionization detection revealed the presence of two impurities. One impurity peak precedes the ether peak, while the other follows the ether peak as shown in Figure 19. The amounts of these impurities were found to vary in concentration for the different aluminum chloride solutions evaluated, although no correlation has been obtained between the stability of aluminum hydride and the amount of these impurities present in the initial aluminum chloride solution.

(3) Comparison of Aluminum Chloride and Dimethyldichlorosilane as Initial Starting Materials (U)

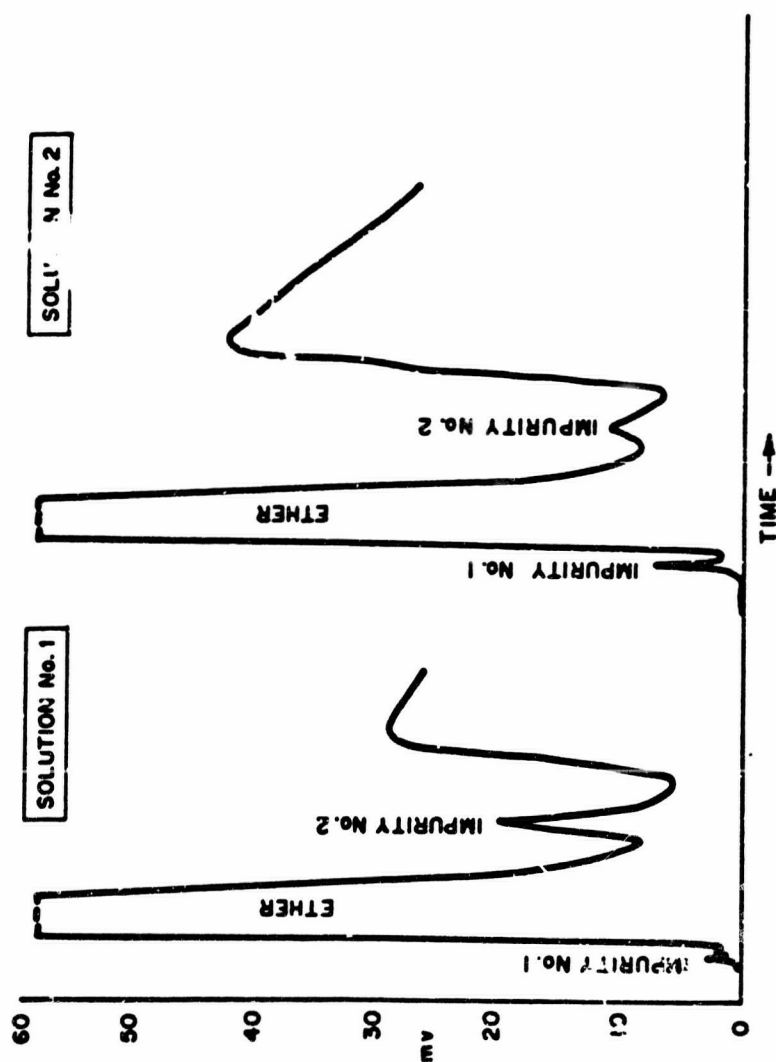
(C) Due to the possibility of impurities originally present in aluminum chloride solutions causing hydride decomposition during preparation, it was decided to circumvent this problem by replacing the aluminum chloride with dimethyldichlorosilane as a starting raw material. The preparation reaction is as follows:



(C) Several batch runs have been made successfully using the dimethylchlorosilane as the starting material. The aluminum hydride product from these preparations appeared comparable to that

CONFIDENTIAL

(This page is Unclassified)



(U) Fig. 19 - Chromatograms of Ether Solutions of Aluminum Chloride

CONFIDENTIAL

CONFIDENTIAL

produced from aluminum chloride, although, in a few cases, the stability was improved. Chemical analysis indicated essentially no incorporation of silicon (0.03%). Two continuous crystallization runs using dimethyldichlorosilane showed good stability during preparation, but no improvement in crystal formation.

(4) Ultra-pure Starting Reagents (U)

(C) An attempt was made to improve the stability of aluminum hydride-1451 by preparing it from high purity starting raw materials in a dry box atmosphere free from contaminants. A dry box was carefully cleaned and contained nitrogen with no known contaminants except for approximately 1 ppm. of oxygen and 17 ppm. of water. Carefully resublimed aluminum chloride and recrystallized lithium aluminum hydride and lithium borohydride were used as starting materials. The diethyl ether and benzene both contained less than 1 ppm. of oxygen and less than 15 ppm. of water.

(C) Extensive decomposition on the sides of the flask was apparent during the preparation of aluminum hydride under these conditions. While these results may indicate that an anhydrous, high-purity system tends to favor decomposition, it has been observed since these experiments that other factors such as active decomposition sites on the surface of glass and electrical field effects may be the actual determining factors in causing decomposition during crystallization. When these other factors are eliminated, high-purity materials may be found to produce a better quality of aluminum hydride-1451.

d. The Effect of an Electrical Field on the Decomposition of Aluminum Hydride During Preparation (C)

(C) One of the most serious problems encountered in the manufacture of aluminum hydride-1451 is the random decomposition of the compound during crystallization. Generally, the degree of decomposition observed during normal batch operation is not serious, although it probably contributes to the variability observed in product stability. However, the problem of solution stability is magnified by long continued operation. In some preparations in laboratory equipment, decomposition, as manifested by a gray or metallic color, will not be observed, while in others it will appear on the thermometer well, but not on the sides of the flask, or it may appear on both. The result is a product that varies from white to light gray, depending upon the extent of the decomposition. As expected, Taliani tests at 60°C. show a direct correlation between the amount of decomposition observed during the preparation and stability.

(U) The nature of this random decomposition suggests that it may be due to electrical effects such as the uneven distribution of electrical charges on the surface of the glassware, resulting in an electrical field which varies in strength, especially at the

CONFIDENTIAL

glass surface. Such a possibility seems likely, considering that all the materials involved are poor conductors of electricity. The streaks on the thermometer well could result from the concentration of electrical charges on striations formed during fabrication, while the decomposition observed on the side of the flask which generally appears near the oil bath stirrer may result from electrical fields set up by the friction of the stirrer with the silicone oil and/or rapid circulation of the oil against the exterior of the flask.

(C) Several experiments were performed to determine the effect of an electrical potential across an aluminum hydride solution. Two bands of aluminum foil, each approximately 1/2" wide, were wrapped around the outside of the conversion flask and a potential of 45 to 180 volts applied. In two runs, the flask which has the potential across the bands showed the most decomposition when compared to runs made from the same solution but without applied potential. However, the difference, while significant, was not large and the higher applied voltages did not augment the effect.

(C) In another experiment of this type, 45 volts were applied across a platinum foil immersed in the conversion flask and an aluminum foil surrounding the flask. No appreciable difference was noticed in either the amount of product adhering to the sides of the flask or the degree of decomposition. Likewise, when 45 volts were applied across two platinum electrodes immersed in a 0.3 M ether solution of aluminum hydride for two days, no decomposition was observed.

(C) Attempts to measure an electrical potential due to a static charge in the solution have been unsuccessful, probably due to the small quantity of electricity involved. The best approach appears to be to remove any possible electrical charge which might build up either in the solution or on the surface of the conversion vessel. Grounding of both the solution by means of a platinum electrode and the outside of the conversion flask by means of aluminum foil seems to reduce the amount of adhesion, but from visual observation there appeared to be no reduction in decomposition. Taliani tests, however, showed a marked difference in product stability. A sample of material made in a grounded flask required 12 days to reach 1% decomposition, while material made from the same aluminum hydride solution, but converted in an ungrounded flask, required only 5 days to reach 1% decomposition. Several additional experiments, using the same solutions, but grounding only one of the two conversion flasks, are being carried out to determine if the results obtained for the pair of samples are reproducible.

(U) Heating the crystallization flask to 550°C. in an annealing oven prior to use has resulted in less decomposition on the sides of the flask. The reason for this is not clear, but a possible explanation is that any static charge on the glass surface is bled off at this high temperature.

CONFIDENTIAL

CONFIDENTIAL

e. Materials of Construction (U)

(C) The decomposition of aluminum hydride-1451, when borosilicate glass was used during phase conversion, suggested that this type of glass may influence the decomposition, with the random nature of the decomposition being dependent upon both the manner of fabrication of the glass and the clean-up procedure.

(C) This is illustrated by the decomposition often found on the thermometer well as shown in Figure 20. The decomposition pattern follows the striations in the glass which are formed when it is drawn. The reason for this decomposition pattern is not presently known. However, it is known that it is not caused simply by a rough surface, since a thermometer well with its surface roughened by sand blasting did not exhibit any decomposition. It may be concluded that catalytic effects which promote decomposition of aluminum hydride may be inherent in the borosilicate glass and that the proper treatment of the glass surface to entirely eliminate these effects has not been found.

(U) Soft glass, such as that used for thermometers, and Vycor produce more decomposition than borosilicate glass. Several runs made in a Vycor flask with a thermometer well of the same material resulted in a smooth aluminum mirror on the flask and thermometer well.

(U) Four runs made with a removable quartz thermometer well resulted in no decomposition, even though the striations were more pronounced than in borosilicate glass.

(C) The noticeable differences in the amount of decomposition observed with the four different materials demonstrate the importance of materials of construction. Quartz is approximately 99.9% SiO_2 , Vycor contains 96% SiO_2 , and borosilicate glass 80.5% SiO_2 . If the amount of silica were the only determining factor, Vycor would be much better than borosilicate glass. This, however, is not the case, indicating the difference must be in other components of the glass or in the processes involved in manufacturing the material. A quartz flask is being fabricated to evaluate its effectiveness in reducing aluminum hydride-1451 decomposition during conversion.

2. Continuous Crystallization Studies of Aluminum Hydride-1451 (C)

a. Laboratory Crystallization Variable Studies (U)

(C) Past experience with aluminum hydride has indicated that, as with other crystalline materials, crystals which are more nearly perfect are more thermally stable. Considerable effort has, therefore, been expended toward developing a process which will reliably produce single crystals.

CONFIDENTIAL

(This page is Unclassified)



(U) Fig. 20 - Decomposition of Aluminum Hydride
on Thermometer Well

-46-

CONFIDENTIAL

(This Page is Unclassified)

CONFIDENTIAL

(C) The most promising approach to making single crystals involves the nucleation of the aluminum hydride-1451 phase, after which the crystals are grown to the desired size by continuous feeding of an aluminum hydride solution. In our work, additive hydrides (lithium aluminum hydride and lithium borohydride) are generally incorporated in the crystallization media. After nucleation of aluminum hydride, ether solution is fed to the crystallizer while the same amount of ether is removed by distillation. The discoveries and improvements resulting from the laboratory investigations will be incorporated into the 10-gallon continuous DTB crystallizer to produce a material with improved thermal stability and formulatability properties.

(1) Physical Factors Affecting the Crystallization of Aluminum Hydride-1451 (C)

(U) Several physical and mechanical factors of the continuous crystallization process have been examined in an attempt to produce a more crystalline product.

(a) Stirring (U)

(U) Most laboratory work has been done with the use of a magnetic stirrer. It was felt that the use of a direct-drive mechanical stirrer would not only give better control of the amount of agitation, but would also decrease the amount of attrition between the stirrer and the walls of the flask.

(C) A glass propeller-type stirrer of about 1 inch in diameter was tried, but was found to be ineffective in stirring the rapidly boiling ether-benzene solution unless operated at high speeds. At these high speeds, it was observed that decomposition occurred on the stirrer blades and left gray deposits of aluminum and aluminum hydride.

(U) A large Teflon, paddle-blade stirrer operating at slow speeds and at a distance of 5-10 mm. from the walls of the flask was found to be much more effective. It provides better control, complete mixing, and more uniform heat transfer, which minimizes the amount of solids deposited on the walls of the flask.

(C) The use of this stirrer has markedly improved the particle size of the aluminum hydride-1451 produced in the continuous process. Particles of 50-100 μ are easily obtained, and, in some instances, particles >200 μ have been obtained in the laboratory. No significant increase in the perfection of the aluminum hydride-1451 crystals, however, was observed as a result of changing the type of agitation.

(b) Method of Addition (U)

(C) In the continuous crystallization process the ether solution of aluminum hydride is added directly to the boiling ether-benzene mixture at 76°-77°C. It was thought that addition

CONFIDENTIAL

CONFIDENTIAL

of this approximately 0.3 M ether solution to the benzene containing only 5-6% ether might cause a large concentration gradient, which in turn would result in rapid precipitation of the aluminum hydride in a finely divided or unstable etherated phase.

(C) An adapter tube was constructed so that the aluminum hydride solution was diluted by the liquid refluxing from the bottom of the fractionation column. The dilution factor for the 0.3 M hydride solution was approximately 10. This technique, as well as the blade stirrer, has led to a general improvement in the laboratory production of aluminum hydride-1451 in the continuous process.

(c) Temperature Control (U)

(C) The control of temperature by the rate of addition of ether solution and the rate of ether removal from the fractionation column is extremely difficult on the laboratory scale. Even when the rates of addition and removal are balanced, change in solution when the aluminum hydride desolvates rapidly can upset this balance and affect the temperature. It is fully realized that this is probably one of the most important factors controlling the crystallization of aluminum hydride-1451 and one of the main reasons for scaling up this area of work. (See Section A.2.b.)

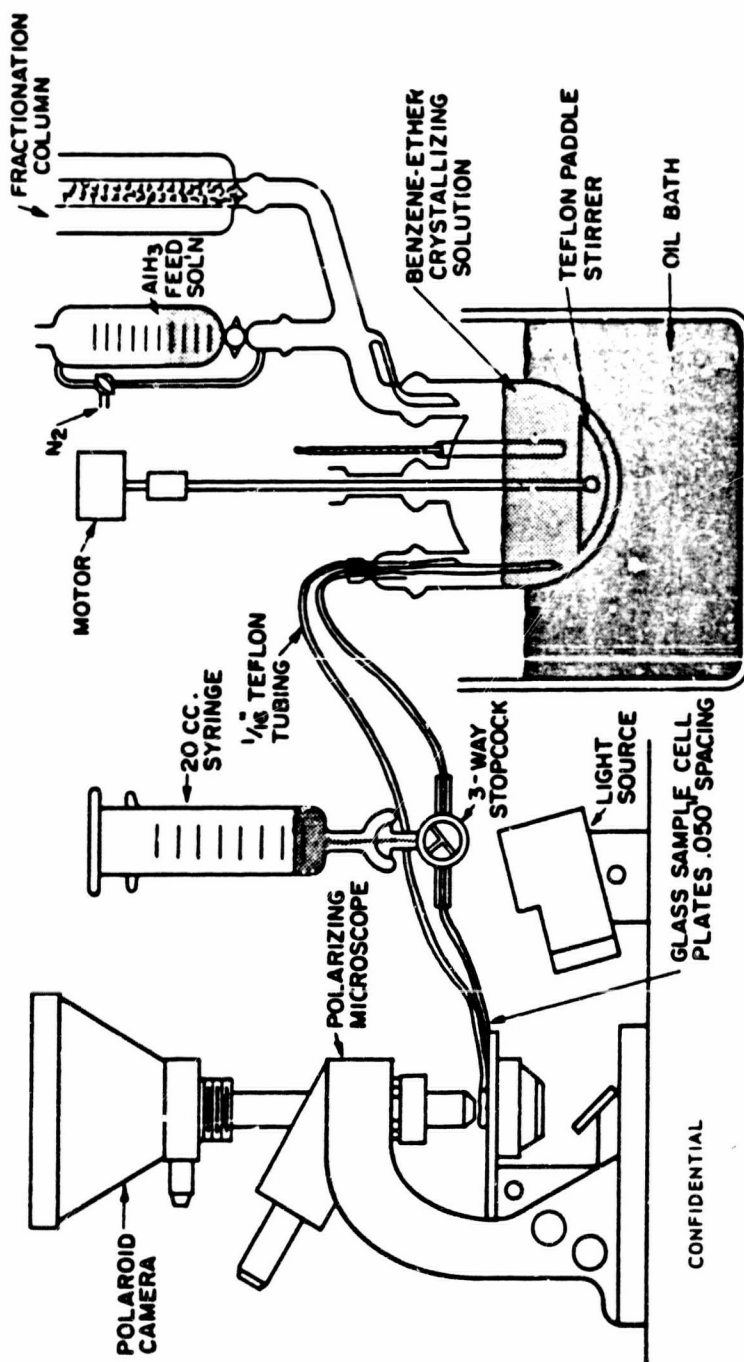
(U) A laboratory system has been developed and evaluated which employs a thermocap regulator with an actuated solenoid valve to control the feed solution by the conversion flask temperature. This system maintains the crystallization temperature to within $\pm 0.1^{\circ}\text{C}$. In addition to the very precise control of temperature, this new technique also allows accurate control of the feed rate relative to the take-off rate of diethyl ether from the still head.

(d) Photomicrographic Apparatus (U)

(C) A technique for sampling and examining microscopically the solids present during the continuous crystallization process was developed to study this dynamic crystallization system. This approach has been found to be very useful in observing the initial precipitation, crystal growth, effect of additives, and phase changes which occur during the preparation of aluminum hydride-1451. The sampling system has been coupled to a polarizing light microscope with a polaroid camera attachment for recording the observations. Figure 21 shows schematically a diagram of the apparatus.

(C) Samples of the solution are withdrawn from the crystallizing flask through a three-way stopcock into the syringe. The stopcock is then rotated 180° and the sample is flushed through the glass cell on the microscope and returned into the flask. The stopcock is turned to stop flow while the particles suspended in solution are observed and photographed. By slowly moving the syringe plunger with the stopcock open, the solid particles can be moved and

CONFIDENTIAL



(C) Fig. 21 - Diagram of Photomicrographic Apparatus for Studying Aluminum Hydride Crystallization

CONFIDENTIAL

CONFIDENTIAL

rolled over for better observation and characterization. Figures 22 and 23 are examples of observations recorded by this apparatus.

(2) Study of Nucleation and Growth Parameters (U)

(a) Feed Rate, Stirring Rate and Crystallization Temperature (U)

(C) A series of experiments was performed to evaluate the effects of feed rate, stirring, and temperature on the crystallinity of aluminum hydride-1451. The normal conditions employed in the laboratory continuous process are summarized as follows:

- (i) A feed rate of 2-3 ml./min. of 0.3 M aluminum hydride-ether solution.
- (ii) Stirring rate of approximately 150 rpm.
- (iii) Crystallization temperature, after nucleation, of 76.0°-76.5°C.

The normal conditions were varied in a series of eight runs and the results are summarized in Table I. The relative ratings shown in Table I were judged on the basis of microscopic examination of the products and also on the amounts of polymorphic aluminum hydride-1444 and aluminum hydride-1433 present as determined by X-ray analysis. The higher the value of the relative rating, the better the crystallinity. The relative ratings represent runs of one variable, i.e., all slow feed or all fast feed, etc.

(C) Although these results are qualitative in nature, the trends are clearly discernible. Feed rate has been shown to be an important and controlling factor in the crystallization of aluminum hydride-1451. The data suggested that slower feed rates were most beneficial. Slower stirring rates also appeared to be beneficial in the laboratory scale runs, but did not appear to be directly translatable to the DTB continuous crystallizer. The effect of temperature on crystal growth appeared to be less important in the process, and the optimum probably lies between the two temperatures studied in this series.

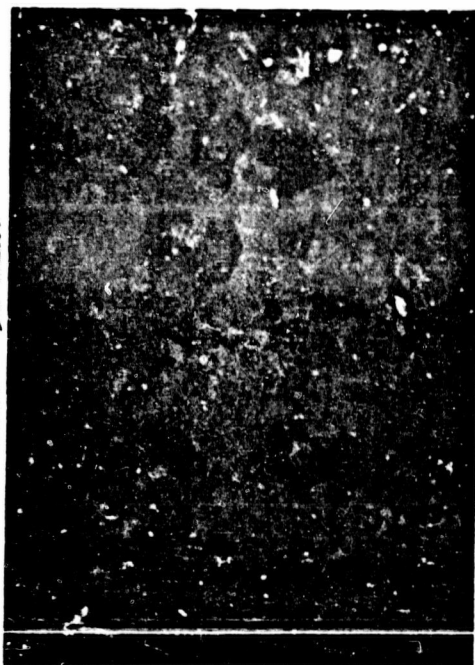
(b) Residence Time

(C) The photomicrographic examination of the aluminum hydride produced in the continuous crystallization process has strongly suggested that the residence time of the aluminum hydride-1451 crystals in solution is a very important factor. Generally it has been observed that the first aluminum hydride-1451 crystals formed are quite clear and regular in shape. As additional aluminum hydride feed solution is added, the aluminum hydride-1451 crystals begin to become polycrystalline and opaque after approximately one hour. Frequently agglomeration and/or fusing of particles appears to occur after this time. Unfortunately, in the laboratory it is not possible to remove the crystals when they are of the

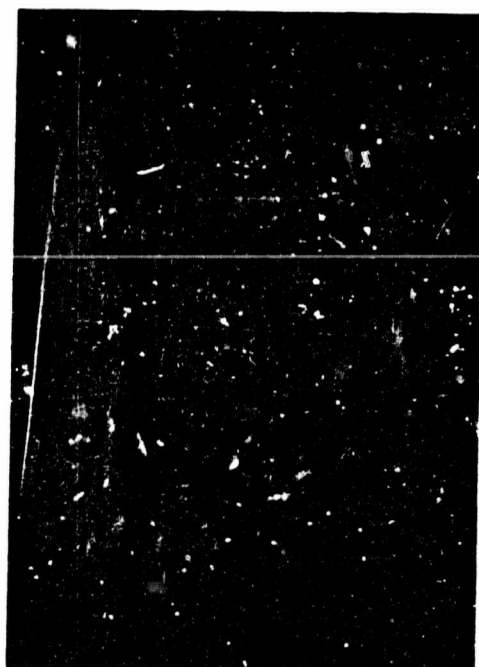
CONFIDENTIAL



Time - 30 min.



Time - 90 min.



Time - 18 min.



Time - 60 min.

(c) Fig. 22 - Photomicrographs of Changes Occurring with Time During Normal Continuous Crystallization of Aluminum Hydride-1451

CONFIDENTIAL

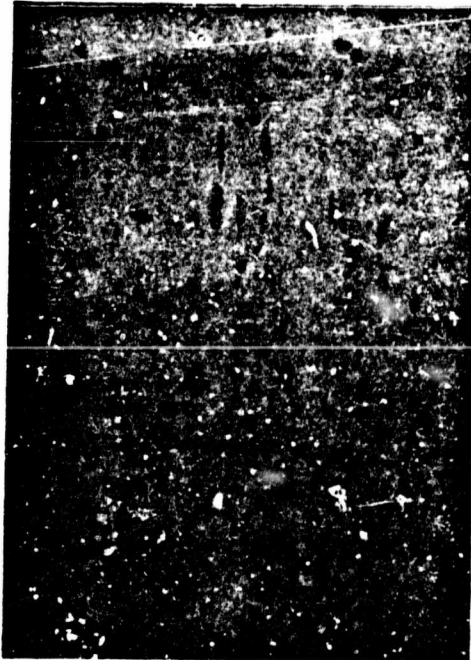
CONFIDENTIAL



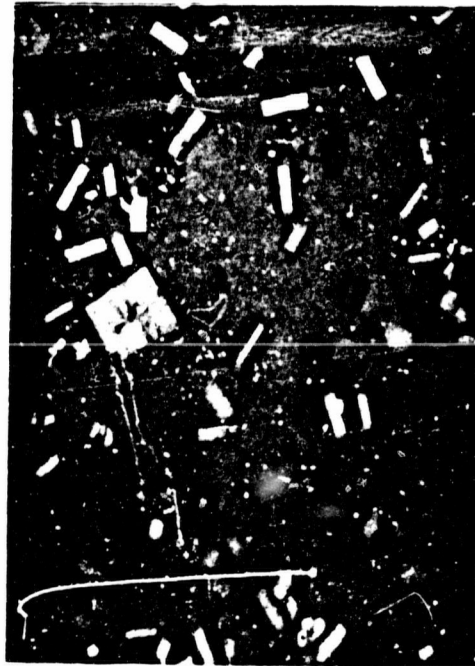
Time - 7 min.



Time - 60 min.



Time - 1 min.



Time - 20 min.

(C) FIG. 23 - Photomicrograph of Changes Occurring with Time
During the Preparation of Aluminum Hydride-1563 and
Aluminum Hydride-1717 by the Direct Continuous
Crystallization Technique

CONFIDENTIAL

CONFIDENTIAL

correct size and continue the crystallization. However, this is possible in the DTB crystallizer as described in Section A.2.b. It is hoped that a set of working conditions can be established, including residence time, which will continuously yield single crystals of aluminum hydride-1451.

Table I

(U) Crystallization Variable Study

<u>Run No.</u>	<u>Feed Rate mmoles/min.</u>	<u>Stirring rpm</u>	<u>Temperature, °C.</u>	<u>Relative Rating (0-10)</u>
1	0.2 ^a	100 ^c	75.0 ^c	9
2	0.2	100	77.5 ^f	7
3	0.2	200 ^d	75.0	3
4	0.2	200	77.5	8
5	1.0 ^b	200	75.0	2
6	1.0	200	77.5	1
7	1.0	100	75.0	4
8	1.0	100	77.5	6

^aSum of Relative Rating; slow = 27.

^bSum of Relative Rating; fast = 13.

^cSum of Relative Rating; slow = 26.

^dSum of Relative Rating; fast = 14.

^eSum of Relative Rating; low = 18.

^fSum of Relative Rating; high = 22.

(c) Seeding (U)

(C) In normal crystallizations where several different crystalline phases are possible, seeding with the desired phase usually induces crystallization of this phase. However, seeding the ether-benzene solution with samples, which were shown by X-ray analysis to be all aluminum hydride-1451, did not give rise to larger crystals of aluminum hydride-1451. Although the product from these runs was all converted to aluminum hydride-1451, microscopic examinations showed the particles were polycrystalline and not single crystals.

(C) It is currently believed that the ineffectiveness of aluminum hydride-1451 seed to induce proper crystal growth is due to the surface imperfection of the seeds. This occurs even if the seeds

CONFIDENTIAL

are freshly ground under a solvent. It is known that fracturing of the aluminum hydride-1451 crystals generates a measurable quantity of hydrogen. This loss of hydrogen causes some rearrangement of the aluminum hydride-1451 surface structure, thereby making the seed ineffective.

(d) Methods of Nucleation (U)

(C) Various methods which have been evaluated as techniques for controlling the initial nucleation of aluminum hydride are listed below, along with a discussion of the results.

(C) Method No. 1 - The ether-benzene solution containing lithium aluminum hydride and lithium borohydride is heated to the operating temperature (76.5°C.) and a feed solution of aluminum hydride in diethyl ether added until nucleation occurs, followed by continued feeding at that temperature.

(C) This method is the original technique for producing aluminum hydride-1451 by the continuous process. However, it has been found to be quite variable, depending on impurities, time, temperature, and feed solution profiles. Observations of this procedure with the photomicrographic sampling device showed that there was apparently an initial formation of a few large particles of aluminum hydride-1433 crystals during the initial feeding, followed by gross precipitation of smaller aluminum hydride-1433, and then subsequent conversion to aluminum hydride-1451. This method of nucleation appears to be too variable for consistent preparation of aluminum hydride-1451 possessing good crystallinity.

(C) Method No. 2 - The ether-benzene solution containing lithium aluminum hydride and lithium borohydride is heated to some high temperature (>77.5°C.) and the aluminum hydride feed solution added until nucleation occurs. The temperature is then allowed to drop to the optimum temperature range of 76.0°-76.5°C. for the remainder of the run.

(C) This appears to be a more consistent method of producing good nucleation, except that usually lithium aluminum hydride and lithium borohydride precipitate above 76.5°C., redissolving slightly as aluminum hydride feed solution is added. The amount of aluminum hydride present when nucleation occurs, however, tends to be variable and has been observed to affect the course of crystallization, yielding some inconsistent results.

(C) Method No. 3 - The ether-benzene solution containing a ratio ranging from 1 LiAlH₄:1 AlH₃:1 LiBH₄ to 1 LiAlH₄:4 AlH₃:1 LiBH₄ is heated until nucleation occurs at >77.5°C., after which the temperature is reduced as the aluminum hydride feed solution is added until the optimum temperature range of 76.0°-76.5°C. is obtained.

(C) This "thermal seeding" appears to be the most consistent method evaluated to date. The concentrations in mole ratios of lithium aluminum hydride, aluminum hydride, and lithium borohydride

CONFIDENTIAL

have been varied to some degree; however, the optimum combination has not yet been established. In the laboratory this nucleation technique usually involves the formation of aluminum hydride-1433 and/or aluminum hydride-1451, followed by conversion to clear cubes of aluminum hydride-1451. After approximately one hour of feeding, these clear cubes become polycrystalline and occasionally exhibit some agglomeration. The aluminum hydride-1433 usually disappears at approximately this time, and the cubes formed continue to grow, becoming larger and less clear. It should be noted, however, that in the continuous DTB crystallizer this technique does not show any significant amount of aluminum hydride-1433 formation during or following nucleation, but consistently nucleates directly from solution as aluminum hydride-1451.

(C) Method No. 4 - The benzene solution is heated to its boiling point of 80.0°C. and an initial feed solution containing a mole ratio of 1 LiAlH₄:1 AlH₃:1 LiBH₄ is either rapidly or slowly added until nucleation occurs and the temperature has been reduced to the optimum temperature range, followed by the addition of an aluminum hydride feed solution.

(C) This method was investigated in an effort to shorten the initial heat-up time, which in the laboratory does not appear to be significant, but could be in the operation of the DTB crystallizer. In the DTB crystallizer, it usually takes approximately 2 hours to achieve nucleation after the initial feed solution of lithium aluminum hydride, aluminum hydride, and lithium borohydride is added to cold benzene.

(U) In two laboratory runs in which this initial feed solution was rapidly added to the boiling benzene, the solution failed to nucleate and had to be reheated. If the feed solution is added slowly, however, the solution readily nucleates and has yielded a slightly improved crystalline product.

(C) Method No. 5 - The benzene is heated to 80°C. and a feed solution containing a mole ratio greater than 1 LiAlH₄:4 AlH₃ (with or without 1 LiBH₄) is added, during which time nucleation occurs. The temperature is then reduced to the optimum operating temperature as the addition of the feed solution is continued.

(C) This method is more simple in operation, since it is not necessary to prepare different feed solutions, and the problem of making a stoichiometric solution of aluminum hydride is circumvented. This nucleation step has been found to produce essentially the same type of product as the other methods, although the nucleation involves the formation of less aluminum hydride-1433 and some agglomeration of the small aluminum hydride-1451 nuclei.

(C) Recent work has shown that nucleation Methods 4 or 5 and slow feed rates (0.1 mmole/min.) can give aluminum hydride-1451 in the laboratory without the formation of any aluminum hydride-1433 or aluminum hydride-1444 phases. The combination, along

CONFIDENTIAL

with the other improvements in the continuous process, allows the preparation of larger, clearer, more crystalline aluminum hydride-1451. With proper control of the process variables of feed rate, stirring, temperature, residence time and impurities, the crystal growth of aluminum hydride can be controlled.

(C) However, the nucleation step is still variable and very sensitive to unknown parameters. Photomicrographic observations of a large number of nucleations of aluminum hydride-1451 suggest that there is an insufficient number of nuclei formed initially in this process. The first nuclei formed appear to grow very rapidly and become imperfect, polycrystalline and sometimes agglomerated. As a result, they deplete the solution of aluminum hydride concentration and decrease the rate of new nuclei formation. However, if the feed rate is increased to compensate for this, then phase problems occur usually as aluminum hydride-1433 or aluminum hydride-1444. Therefore, to insure slow growth of each crystal it would appear necessary to have a large number of crystals continuously present in the solution. Based on this hypothesis, it now appears very advantageous to develop a nucleation process which will produce a sufficient number of small nuclei.

(U) An attempt to increase the number of nuclei and improved crystallinity by simply increasing the volume of crystallizing solution relative to the same feed rate has not been found to produce any detectable improvement.

(U) Methods of producing nuclei in a hot zone (79°-80°C.) and then removing them to the crystallizing medium at 76°C. for crystal growth are being evaluated. This would separate the nucleation and growth stages and, hopefully, would yield better control of each. If such an external nucleation system can be developed, it could easily be adapted to the DTB continuous crystallizer to help control nucleation, feed rate, and product quality.

(u) Complex Hydride Additives (C)

(C) Varying ratios of lithium aluminum hydride and lithium borohydride have been investigated in this process and have been found necessary for the desolvation and conversion of aluminum hydride to the stable 1451 polymorph. A large excess of both lithium aluminum hydride and lithium borohydride was tried separately. In both cases, the product was an agglomerated aluminum hydride-1451. When the concentrations of additives was decreased to approximately 0.01 M in the ether-benzene mixture, the amount of agglomeration decreased, but this did not produce good single crystals, but generally a polycrystalline, grainy, aggregate particle.

(C) The photomicrographic apparatus was used to study the effect of changing concentrations of lithium aluminum hydride and lithium borohydride on the crystallization of aluminum hydride. Varying the concentration of both lithium aluminum hydride and lithium borohydride simultaneously from 13×10^{-3} to 0.7×10^{-3} M

CONFIDENTIAL

in seven runs did not show any significant improvement in crystallinity or decrease the amount of agglomeration in the crystalline aluminum hydride-1451 product. Hence, it appears that only a trace amount of lithium aluminum hydride is necessary for the formation of aluminum hydride-1451.

(C) Photomicrographic observations of recent runs in which only aluminum hydride-1451 was produced have led to the conclusion that the presence of solid lithium aluminum hydride in the crystallizing solution does not seriously affect the crystals. However, it has been observed that if the lithium aluminum hydride crystallizes, as a result of saturation during the growth of aluminum hydride-1451, the crystals tend to become more opaque and polycrystalline. This can be rationalized as being a result of the lithium aluminum hydride growing from the aluminum hydride-1451 crystal surfaces as it precipitates, thereby interfering with the normal growth of the crystal. However, if solid lithium aluminum hydride is present, the precipitation apparently results in growth of the already existing crystals of lithium aluminum hydride and does not appear to interfere with the aluminum hydride-1451 crystal growth. The only effect of lithium borohydride on the crystallizing system which has been demonstrated is an enhancement of the solubility of lithium aluminum hydride.

(3) New Crystallization Additives (U)

(C) An attempt was made to find other additives which would be more effective in promoting the crystallization of aluminum hydride-1451. One problem in this area is that the reactive chemicals in this system will often not remain in the form added. Thus, the effects may result from some reaction product rather than the compound originally added.

(a) Aluminum Borohydride (C)

(C) Aluminum borohydride (produced by the reaction of lithium borohydride and aluminum chloride in an ether-benzene solution, and separated from the coproduct, lithium chloride, by filtration) was used as a crystallization additive in an otherwise normal run. The aluminum borohydride was found to have considerable effect on the precipitation of the aluminum hydride. It delayed the initial precipitation of aluminum hydride until 240 ml. of the 300 ml. of 0.3 M solution had been added, compared with 50-100 ml. without aluminum borohydride. The product was agglomerated spheres, some of which were crystalline on their outer edges. The product was identified by X-ray analysis as solvated aluminum hydride-1443 and aluminum hydride-1535.

(b) Lithium Bromide (U)

(C) Lithium bromide has been reported to hold aluminum hydride in ether solution and prevent precipitation. A preparation

CONFIDENTIAL

CONFIDENTIAL

was made using lithium bromide in place of lithium borohydride in a continuous process to evaluate its effect. The lithium bromide, although soluble in ether, was precipitated to a large extent when mixed with the benzene. The product contained only 20% aluminum hydride-1451, while the remaining portion was unidentified by X-ray analysis.

(c) Kel-F Oil (U)

(C) This oil was evaluated to determine if it would prevent adhesion of the product to the walls of the reaction vessel. The additive was attacked by lithium aluminum hydride, producing large amounts of lithium chloride in the run, along with the undesirable phases of aluminum hydride, 1443, 1535, and 1444.

(d) Dow Corning 200 Silicone Oil (U)

(C) This additive was also evaluated to determine if it would prevent adhesion and/or promote increased crystallinity of the aluminum hydride-1451. However, it caused excessive foaming, and, although it did not appreciably degrade the product, it failed to show any improvement.

(e) Diisobutyl Aluminum Hydride (C)

(C) Diisobutyl aluminum hydride was added to the crystallizing solution to determine if it would increase the solubility and crystallinity of aluminum hydride-1451. However, serious decomposition was observed during the run, resulting in a dark gray product.

(f) Butyl Lithium (U)

(C) An attempt was made to examine the use of bases other than lithium aluminum hydride and lithium borohydride in the crystallization of aluminum hydride. The use of butyl lithium resulted initially in the formation of some irregular, colored crystals, but as the run progressed decomposition was observed and a gray agglomerated product was recovered.

(g) Pyridine (U)

(C) Pyridine reacts with LiAlH_4 to form $\text{LiAl}(\text{pyr-H})_4$. This compound was also examined as a potentially different base for the hydride system. The initial yellow-orange color of the crystallizing medium faded as aluminum hydride solution was added. No significant change in crystallinity of the product recovered from the system was observed.

(h) Aromatics (U)

(C) Aromatic compounds, such as trans-stilbene, tetraphenylethylene, and 4-phenylazodiphenylamine, were examined but showed no improvement or decrease in the crystallinity of the

CONFIDENTIAL

aluminum hydride-1451. Their effect on thermal stability of aluminum hydride-1451 is being evaluated.

(i) Boric Acid (U)

(C) This compound was investigated as an additive based upon information obtained in the study of the effect of water in the preparation of aluminum hydride-1451. It was found that water reacted with lithium aluminum hydride and lithium borohydride in wet benzene to form a mixture of lithium aluminate, LiAlO_2 , and lithium monohydroxyborohydride, LiB(OH)H_3 . Solubility considerations of the two compounds in ether-benzene favored the latter. Hence, boric acid was examined as an analog of lithium monohydroxyborohydride because of its slight solubility in diethyl ether and availability.

(C) The addition of boric acid to the system gave some indication of favoring the formation of single hexagonal crystals during nucleation. The product was aluminum hydride-1451, but agglomeration during crystal growth was still observed.

(j) Aluminum Hydride-1444 (C)

(C) It has been observed that the hexagonal crystal habit of aluminum hydride-1451 has generally been associated with the undesirable polymorph, aluminum hydride-1444. Therefore, it was decided to determine if there was something unique about the aluminum hydride-1444 phase which caused the nucleation and propagation of the hexagonal aluminum hydride-1451 crystal.

(C) A small portion of aluminum hydride-1444, containing 10-20% of aluminum hydride-1451, was added to the conversion solution. Microscopic examination of the crystals during the progression of a few runs indicated a predominance of the hexagonal shaped aluminum hydride-1451.

(C) Therefore, it is concluded that aluminum hydride-1444 can alter the crystal habit of aluminum hydride-1451 from the cubic form to that of the hexagonal. However, current crystallization conditions which favor the nucleation of single crystal, hexagonal-shaped aluminum hydride-1451 also favor the nucleation of aluminum hydride-1444.

(k) Magnesium Chloride (U)

(C) Current technology on the incorporation of magnesium into the aluminum hydride-1451 crystal lattice as a stabilizer has, in the past, been based on preparation by the "batch process." Very little work has been done to determine the most advantageous stage for the introduction and incorporation of magnesium into the "continuous process." Preliminary work has been initiated to study the effect of magnesium addition.

CONFIDENTIAL

(C) Magnesium as magnesium chloride can be conveniently introduced into the "continuous process" by incorporation in either the aluminum hydride feed solution and/or the conversion solution. The aluminum hydride feed solution in the "continuous process" is made at stoichiometry. The addition of magnesium chloride either necessitates an excess of lithium aluminum hydride over stoichiometry in the aluminum hydride feed solution, or a prior reaction of the lithium aluminum hydride and magnesium chloride, followed by subsequent addition of this solution to the feed. Both approaches were found to incorporate magnesium as shown by the X-ray diffraction analysis of the expanded aluminum hydride-1451 crystal lattice. Chemical analysis has shown a maximum concentration of 0.72% magnesium incorporated by this technique. However, extraneous crystalline phases were also detected. These probably resulted from the presence of residual chloride and/or water in the system. It is possible that some water of hydration of the magnesium chloride was present. It was also noted that the aluminum hydride-1451 crystals were small and agglomerated. This latter problem is now being extensively investigated to find a method which will incorporate magnesium into the aluminum hydride-1451 crystal lattice and at the same time retain the crystallinity of the product.

(C) Several attempts have been made using the continuous crystallization technique to incorporate magnesium via the conversion solution. The conversion solution is composed of benzene, ether, and excess lithium aluminum hydride and sometimes lithium borohydride. The following summarizes the preliminary results obtained:

- (1) Reaction of Magnesium Chloride with Lithium Aluminum Hydride without Lithium Borohydride - Normal cubic aluminum hydride-1451 crystals were obtained from the use of this conversion solution. However, no expansion of the hydride lattice was observed by X-ray diffraction.
- (11) Reaction of Magnesium Chloride with Lithium Borohydride and Lithium Aluminum Hydride - The crystals obtained from this solution were normal in physical appearance, but no lattice expansion was detected.
- (111) Reaction of Magnesium Chloride with Lithium Aluminum Hydride, Followed by Lithium Borohydride Addition - Using this conversion solution, only in random samples was some expansion detected, indicating the presence of magnesium.
- (iv) Reaction of Magnesium Chloride with Lithium Borohydride, Followed by Lithium Aluminum Hydride Addition - When this conversion solution was used, preliminary results indicated that magnesium was incorporated into the hydride lattice.

In almost all of the above situations, the final product was contaminated with residual chlorides, and in some cases extraneous

CONFIDENTIAL

crystalline phases. Preliminary work indicates that the incorporation of magnesium into the continuous process can be achieved, but not without difficulties.

(4) Crystallization Contaminants (U)

(a) Chloride (U)

(C) In the crystallization of aluminum hydride-1451 the effect of residual chloride, presumably lithium chloride, and its removal have been a source of concern for some time. In the past, the chloride content in the batch process was removed or reduced by a sodium borohydride treatment. However, a more critical examination of chloride removal was deemed necessary, since it was observed from direct crystallization studies of aluminum hydride-1451 that residual lithium chloride may be capable of causing the crystallization of extraneous and undesired phases. An effort was therefore made to determine the best method of technique for removing residual chloride from the aluminum hydride feed solution and from the complex hydrides, lithium aluminum hydride and lithium borohydride.

(C) In actual practice it is difficult to prepare a stoichiometric solution of aluminum hydride. Tables II and III show the results of the treatment of two aluminum hydride solutions with sodium aluminum hydride, sodium borohydride, and a mixture of the two. Table II shows the results obtained in the treatment of a hydride solution containing an excess of aluminum chloride. Sodium aluminum hydride appears to be more beneficial in removing residual chloride than either sodium borohydride or a combination of the two.

Table II

(C) Removal of Chloride from a 0.3 M Aluminum Hydride Solution Containing an Excess of Aluminum Chloride

Compound	Concentration, g./l.			
	Untreated	Treated for 15 Minutes		
		NaAlH ₄ ^a	NaBH ₄ ^b	NaAlH ₄ -NaBH ₄ ^c
LiCl	0.37	Nil	0.12	0.02
AlCl ₃	0.21	Nil	Nil	Nil
LiAlH ₄	--	0.16	--	0.11
LiBH ₄	--	--	0.04	0.11
NaAlH ₄	--	Nil	--	Nil
NaBH ₄	--	--	Nil	Nil

^a0.1 g. of NaAlH₄ in 50 ml. of above solution.

^b0.1 g. of NaBH₄ in 50 ml. of above solution.

^c0.2 g. of NaAlH₄-NaBH₄ in 50 ml. of above solution.

CONFIDENTIAL

(C) Table III shows the results obtained in the treatment of a hydride solution containing an excess of lithium aluminum hydride. These results suggest that sodium aluminum hydride, sodium borohydride and a mixture of sodium aluminum hydride - sodium borohydride are equally effective in the removal of chloride. Treatment of the aluminum hydride solution with sodium aluminum hydride seems to be preferable because the final solution will contain only one extraneous compound, namely lithium aluminum hydride. Treatment with sodium borohydride introduces lithium borohydride into the final solution. Due to the presence of excess lithium aluminum hydride in this solution, some solubility of sodium aluminum hydride and sodium borohydride is noted. This is undoubtedly due to a secondary solvent effect, and the solubility of the treatment compounds will increase with the increasingly larger amounts of excess lithium aluminum hydride. In general, sodium aluminum hydride treatment of the aluminum hydride solution is more desirable because of completeness of the reaction when excess aluminum chloride is present and the simplicity of the reaction product.

Table III

(C) Removal of Chloride from a 0.3 M Aluminum Hydride Solution Containing an Excess of Lithium Aluminum Hydride

Compound	Concentration, g./l.			
	Untreated	Treated for 15 Minutes		
		NaAlH ₄ ^a	NaBH ₄ ^b	NaAlH ₄ -NaBH ₄ ^c
LiCl	0.05	N11	N11	N11
LiAlH ₄	1.60	1.76	1.71	1.81
LiBH ₄	--	--	0.02	--
NaAlH ₄	--	0.14	--	0.21
NaBH ₄	--	--	0.08	--

^a0.1 g. of NaAlH₄ in 50 ml. of above solution.

^b0.1 g. of NaBH₄ in 50 ml. of above solution.

^c0.2 g. of NaAlH₄-NaBH₄ in 50 ml. of above solution.

(C) A 1 M lithium aluminum hydride solution in diethyl ether was also found to contain a residual chloride value of 0.45 g. LiCl/l. This is not unexpected due to the method of preparation of the lithium aluminum hydride. Treatment of 50 ml. of a 1 M LiAlH₄ solution with various hydrides such as MgH₂, Mg(AlH₄)₂, NaH, and KAlH₄ for the removal of residual chloride showed only sodium aluminum hydride and sodium borohydride were effective in reducing the chloride content. Table IV shows that the chloride content of a lithium aluminum hydride solution can be significantly reduced; however, a definite solubility of sodium aluminum hydride

CONFIDENTIAL

and sodium borohydride is observed. In some cases, the high solubilities of these materials have been known to cause phase problems in the crystallization process of aluminum hydride-1451.

(C) The net result of this treatment is that all residual aluminum and lithium chlorides are consumed and lithium aluminum hydride, aluminum hydride and ether-insoluble sodium chloride are generated. There appears to be no solubility of sodium aluminum hydride as a result of this treatment. The treatment with sodium borohydride does not appear to be as effective, since the reaction of sodium borohydride does not go to completion.

Table IV

(C) Removal of Chloride from a 1 M
Lithium Aluminum Hydride Solution

<u>Compound</u>	<u>Concentration, g./l.</u>		
	<u>Untreated</u>	<u>Treated for 15 Minutes^a</u>	
		<u>NaAlH₄</u>	<u>NaBH₄</u>
LiCl	0.57	0.07	0.08
LiBH ₄	--	--	1.23
NaAlH ₄	--	1.49	--
NaBH ₄	--	--	1.20

^a0.1 g. of the hydride slurried in 25 ml. of the 1 M LiAlH₄ solution.

(C) An attempt was made to reduce or remove the chloride present in lithium borohydride solutions. However, to date, no treatment has been successful. Both sodium aluminum hydride and sodium borohydride were found to be ineffective in the reduction of chloride. Considerable solubility of these compounds in the borohydride solution was noted.

(C) Treatment of the aluminum hydride feed solutions in the continuous crystallization process with sodium aluminum hydride was found to be effective. However, treatment of the lithium aluminum hydride and lithium borohydride solutions used in the process, which were also found to contain traces of lithium chloride, resulted in phase problems during crystallization. Long rod-shaped particles of aluminum hydride-1433 were obtained, especially when sodium aluminum hydride was used in the pre-treatment of the lithium aluminum hydride and lithium borohydride solutions. These long rods of aluminum hydride-1433 usually failed to convert completely in the normal time to aluminum hydride-1451. In addition, small amounts of other phases such as aluminum hydride-1444 and aluminum hydride-1717 were also present.

CONFIDENTIAL

(C) Treatment of only the aluminum hydride feed solutions with sodium aluminum hydride yields aluminum hydride-1451 with no lithium chloride detectable by X-ray analysis. In general, if the feed solution is not pre-treated, lithium chloride is detected.

(b) Formation of Non-Solvated Aluminum Hydride-1563 and Aluminum Hydride-1717 (C)

(C) Two laboratory runs during the year produced some remarkably large, clear, single crystals of non-solvated aluminum hydride. The concentration of single crystals and degree of perfection of the crystals obtained from these runs had never been previously observed in our laboratories.

(C) Figure 23 shows the two different types of single crystals observed, along with a small amount of polycrystalline aluminum hydride-1451. The rectangularly shaped crystals, with the dark edges (due to the diamond-shaped cross-section) were highly colored under polarized light and identified by X-ray analysis as aluminum hydride-1563. The flat, square-shaped plates, possessing slightly beveled edges, were identified as aluminum hydride-1717. Elemental and X-ray analyses of the two phases which were separated by screening are shown in Table V. The elemental analysis indicates that both phases are non-solvated polymorphs of aluminum hydride. The material balance for both samples is low, indicating a high concentration of oxygen. A density of 1.30-1.34 g./cc. was measured for both phases by the density gradient method using orthodichloro- and bromobenzene. The infrared spectra of the two phases are shown in Figure 24. The thermal stability obtained from the two fractions at 100°C. was approximately equal to normal aluminum hydride-1451; however, at 60°C., the sample containing predominantly aluminum hydride-1563 reached 1% decomposition in two days.

Table V

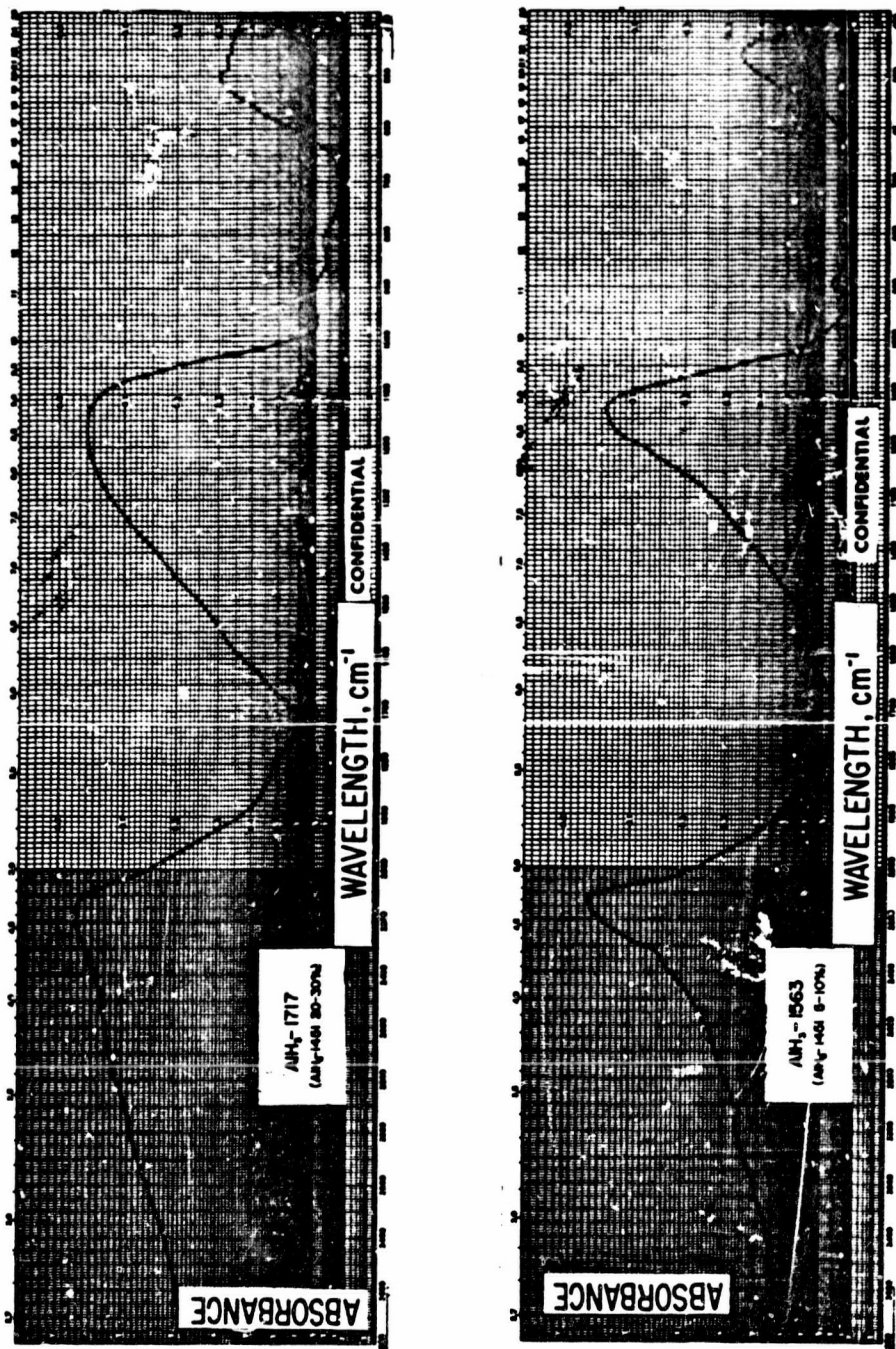
(C) Analysis of Aluminum Hydride-1563 and Aluminum Hydride-1717 Polymorphs

<u>Sample No.</u>	<u>Elemental Analysis, %</u>					<u>X-Ray Analysis</u>	<u>Density g./cc.</u>
	<u>C</u>	<u>H</u>	<u>Al</u>	<u>Cl</u>	<u>Li</u>		
8281-57A-S	0.2	9.7	86.8	<0.05	0.31	1563 c.c. 1451 5-10% Trace 1717	1.30-1.34
8281-57A-P	0.2	9.8	87.9	<0.05	0.25	1717 c.c. 1451 20-30%	1.30-1.34

(c) Effect of Water on the Preparation of Aluminum Hydride-1563 and Aluminum Hydride-1717 (C)

(U) Because of the size and perfection of these crystals, an effort was made to determine the mechanism or conditions which

CONFIDENTIAL



(c) Fig. 24 - Infrared Absorption Spectra of Aluminum Hydride-1563 and -1717

CONFIDENTIAL

CONFIDENTIAL

initiated and propagated the growth of these crystals. Experimentation with process variables, reagents, and equipment ultimately led to the conclusion that the phenomenon observed was the result of water and/or some soluble or colloidal product thereof.

(C) To investigate the role of water in the formation of the two new polymorphs of aluminum hydride, particular attention was paid to the anhydrous conditions of both the starting reagents and the dry box atmosphere.

(C) The addition of lithium aluminum hydride and lithium borohydride solutions to a benzene solution containing 75-220 ppm. water usually resulted in the formation of an ether-benzene insoluble precipitate. The inclusion of this insoluble material in the preparation of aluminum hydride-1451 by the continuous process resulted in the final product being contaminated with the extraneous crystalline phases, aluminum hydride-1563 and aluminum hydride-1717. Removal of this insoluble matter by filtration generally yielded good crystalline aluminum hydride-1451, free from contamination with these phases. Experimental results have proven that filtration is satisfactory for the removal of this insoluble material from a benzene mixture containing 75-220 ppm. of water. However, if the benzene contains a concentration of water in excess of 220 ppm., a single filtration does not appear to be adequate. Apparently at high concentrations of water, either a soluble or colloidal portion is not removed by filtration and ultimately leads to the generation of aluminum hydride-1563 and aluminum hydride-1717.

(C) In an attempt to identify the insoluble material, a portion was purged dry with nitrogen and submitted for X-ray diffraction analysis. The results showed a novel crystalline pattern, designated unknown pattern 1747, and having its strongest lines at 10.7 Å and 6.5 Å. This is believed to be a composite phase. The infrared spectrum of a similar material showed it to be a hydrated material which did not contain any Al-H stretching frequencies. This spectrum also suggested the presence of lithium borohydride and, possibly, γ-aluminum oxide. Chemical analysis of the residue coupled with the above data strongly suggested the formation of lithium aluminate, LiAlO_2 , and lithium monohydroxyborohydride, LiB(OH)H_3 .

(C) Experiments were also performed in an attempt to selectively show which reagent in the conversion solution was producing the water reaction product. A benzene solution containing 140 ppm. of water was first treated with a solution of lithium aluminum hydride, filtered, and then treated with lithium borohydride. In a hydride preparation using the resulting solution, a product containing equal amounts of aluminum hydride-1451 and aluminum hydride-1717, along with 5% aluminum hydride-1563, was generated. X-Ray diffraction analysis of the water reaction product indicated the material to be mainly amorphous with approximately 5% lithium aluminum hydride. Similarly, benzene containing 140 ppm. of water was treated with lithium borohydride, filtered, and then treated

CONFIDENTIAL

CONFIDENTIAL

with lithium aluminum hydride. This solution produced 10% to 15% of aluminum hydride-1717 and aluminum hydride-1563 in addition to aluminum hydride-1451. X-Ray diffraction analysis of the water reaction product indicated a material designated as UP-1476, which has previously been identified as either a hydrolysis or decomposition product of lithium borohydride. Therefore, without further knowledge it is difficult to determine from the data which of the initial reagents is responsible for the formation of aluminum hydride-1563 and aluminum hydride-1717.

(5) Crystallization of Aluminum Hydride-1451 at Reduced Temperatures (C)

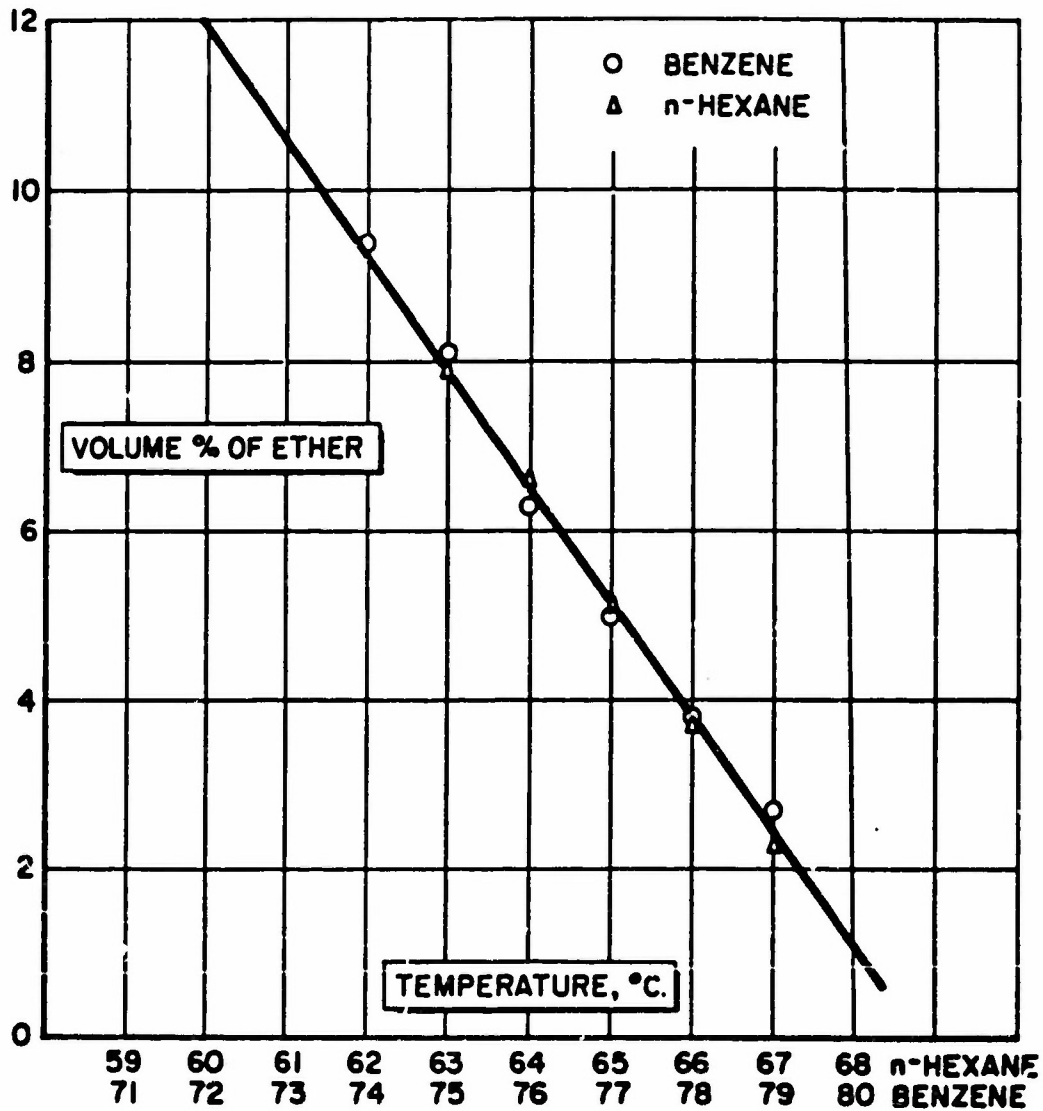
(C) All the parameters of preparation are inherently coupled to the ultimate stability of aluminum hydride-1451, especially the temperature of crystallization. It is postulated that higher crystallization temperatures, or even prolonged heating of aluminum hydride-1451 at the normal crystallization temperature of 76°C., is detrimental to the long-term thermal stability of the final product. Thus, the preparation of hydride at a lower temperature which is adaptable to the production and growth of aluminum hydride-1451 crystals should increase the thermal stability of the final product. Ideally, it was hoped to find a solvent system which would provide a crystallization temperature not much above that of diethyl ether, b.p. = 34.6°C.

(U) The list of solvents considered and investigated during the past year is shown in Table VI.

(C) The use of the n-hexane aliphatic solvent system produced a range of boiling point temperatures between 62°-68°C., due to the non-azeotropic property of the diethyl ether - n-hexane system. The curve of volume percent diethyl ether in n-hexane in the above temperature range was found to be identical to the curve for the volume percent diethyl ether in benzene in the temperature range of 74°C. to 80°C., as shown in Figure 25. The ether - n-hexane system was used in the preparation of aluminum hydride-1451 on the assumption that the knowledge of solubility, conversion temperature, etc. obtained in the study of the ether - benzene system, would apply to this lower boiling system. On that assumption, a conversion temperature of 64°C. to 66°C. was chosen. Unfortunately, nucleation by the continuous process did not originally occur in the proper manner. The entire aluminum hydride solution added initially remained soluble, but later precipitated, yielding solvated aluminum hydride-1443. The etherate was then transformed into a non-solvated aluminum hydride-1433, followed by conversion to aluminum hydride-1451, similar to the original fine powder process. Additional work, however, has shown that proper nucleation from solution can be achieved by careful control of solubility and addition rate, resulting in a satisfactory product.

CONFIDENTIAL

(This Page is Unclassified)



(U) Fig. 25 - Volume Percent Diethyl Ether in n-Hexane

CONFIDENTIAL
(This Page is Unclassified)

CONFIDENTIAL

Table VI

(C) Lower Boiling Solvent Systems Used
in the Preparation of Aluminum Hydride-1451

Solvent Systems	Temperature, °C.					
Benzene	80	79	78	77	76	75
Benzene - cyclohexane ^a	77	76	75	74	73	72
Benzene - 2,4-dimethylpentane ^a	75	74	73	72	71	70
Benzene - n-hexane ^b	72	71	70	69	68	67
n-Hexane	68	67	66	65	64	63
Benzene - 3-methylpentane ^c	67	66	65	64	63	62
Benzene - 2,3-dimethylbutane ^c	64	63	62	61	60	59
3-Methylpentane	63	62	61	60	59	58
Benzene - 2,2-dimethylbutane	60	59	58	57	56	55
2,3-Dimethylbutane	58	57	56	55	54	53
2,2-Dimethylbutane	50	49	48	47	46	45
Volume Percent Diethyl Ether at Indicated Temperatures	1.2	2.4	3.8	5.2	6.5 ^d	7.8

^aAzeotrope

^b1:1 Mixture

^c1:1.5 Mixture

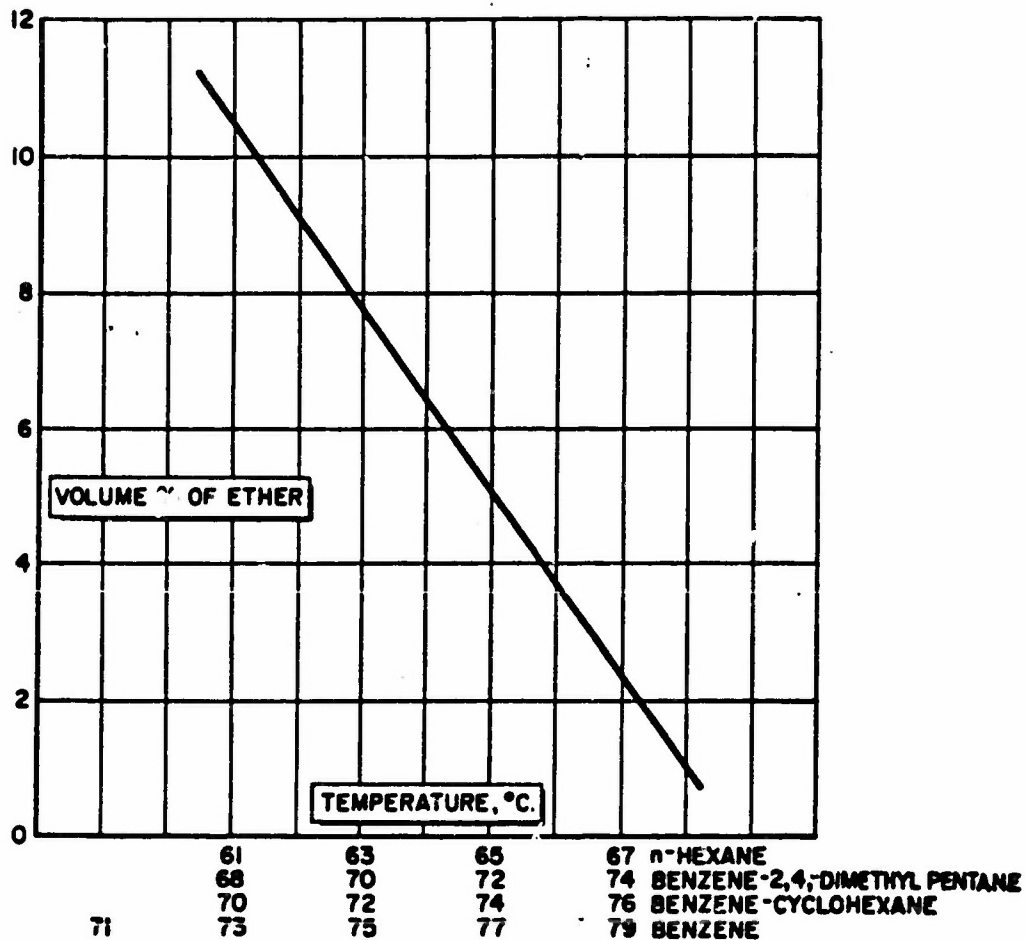
^dPercent diethyl ether present during crystallization.

(U) The benzene - 2,4-dimethylpentane system azeotropered at 75.4°C., with the distillate being 48.3% benzene by weight. The benzene - cyclohexane mixture azeotropered at 77.4°C., with the distillate being 49.7% benzene by weight.

(U) A range of boiling temperatures for each of the solvent systems was obtained by varying the volume percent diethyl ether, since the ether did not azeotrope with any of the individual or combined components. The volume percent diethyl ether curves obtained for these azeotropes again proved to be the same as in the ether - benzene system. Thus, for the same volume percent diethyl ether in a varying co-solvent, an extended series of boiling temperatures was obtained, as illustrated in Figure 26.

CONFIDENTIAL

(This Page is Unclassified)



(U) Fig. 26 - Translation of Volume Percent Diethyl Ether of Various Solvent Systems

CONFIDENTIAL

(This Page is Unclassified)

CONFIDENTIAL

(C) Both of these azeotropes were used in the preparation of aluminum hydride-1451. The range of nucleation and conversion temperatures was 71°-73°C. for the benzene - 2,4-dimethylpentane azeotrope and 73°-75°C. for the benzene - cyclohexane system. Though some difficulty was observed in initiating proper nucleation, both systems yielded good aluminum hydride-1451 crystals in a reasonable length of time. A slower addition rate, however, was found to be necessary as a result of the lower temperatures of conversion.

(C) Little success was achieved using 3-methylpentane (b.p. = 63.3°C.), 2,3-dimethylbutane (b.p. = 57.5°-58.5°C.), and 2,2-dimethylbutane (b.p. = 49.7°C.) as solvents in the preparation of aluminum hydride-1451. It was observed that the solubilities of lithium aluminum hydride, lithium borohydride, and aluminum hydride in these aliphatic solvents were too low to produce proper crystal nucleation. In attempts to increase the solubility of the complex hydrides, benzene was added to the aliphatic solvents; the results were unsuccessful.

(C) Proper nucleation appeared to be the key to the successful utilization of any of these lower boiling solvents. In general, the parameters affecting nucleation of aluminum hydride-1451 as determined in the benzene system have been translated to these other solvent systems. One of the most critical parameters appeared to be the solubility of lithium aluminum hydride, lithium borohydride and aluminum hydride in the various solvent systems. Low solubilities were observed particularly with the aliphatic solvents.

(C) In general, the solvent systems 1 through 4, as shown in Table VI, were successfully used in the preparation of aluminum hydride-1451, whereas solvent systems 5 through 10 did not produce the desired results. In most of the latter cases, nucleation was either very difficult or impossible.

(C) It is concluded that a temperature threshold probably exists, below which sufficient energy is not present to desolvate and nucleate the aluminum hydride-1451.

b. Development of a Continuous Crystallizer (U)

(C) A program was initiated in January, 1965, to improve the physical and chemical properties of aluminum hydride by means of controlled direct crystallization of aluminum hydride-1451 from solution. The goal of this work was to develop a continuous crystallizer which would produce uniform, single crystals of aluminum hydride-1451. The experimental approach consisted of three phases:

Phase I - Design and installation of equipment.

Phase II - Initial crystallization studies.

Phase III - Fundamental crystallization parameter studies.

CONFIDENTIAL

CONFIDENTIAL

(C) Phase I, the design and installation of the Draft-Tube Baffle (DTB) crystallizer, was completed during the first quarter. Phase II involved a performance evaluation of the DTB crystallizer, establishment of the standard operating procedures, and definition of operating conditions for the continuous production of aluminum hydride-1451. These initial studies were completed during the second quarter. Products consisting entirely of aluminum hydride-1451 usually resulted, but problems with both nucleation and solution stability were encountered in these initial studies and delayed the study of Phase III (fundamental crystallization parameters).

(C) Considerable progress has been made during the past year in understanding and controlling the conditions required for reproducibly obtaining acceptable aluminum hydride-1451 nuclei. Similar progress has been made in the reduction of aluminum hydride decomposition during crystallization. Each of these areas will be discussed in detail later.

(1) Process Description (U)

(U) A detailed description of the operating conditions and procedures established during the year is outlined below.

(a) Reaction (U)

(C) Ether solutions of lithium aluminum hydride and aluminum chloride are added to additional ether, distilled from lithium aluminum hydride and dried with molecular sieves, in a batch reactor at ambient temperature. A slight excess (3-5 volume percent) of lithium aluminum hydride is normally used to assure complete reaction of the aluminum chloride. Rapid reaction, followed by filtration, yields a 0.3 molar solution of aluminum hydride in ether. This solution is treated with sodium borohydride, filtered, and added to the crystallizer feed tank which is at ambient temperature. Premature precipitation of the aluminum hydride in the feed tank has not been a problem. However, the excess lithium aluminum hydride currently used does create some problems in the crystallization step and this will be discussed later.

(b) Crystallization (U)

(C) Benzene, distilled from lithium aluminum hydride and dried with molecular sieves, is charged to the DTB crystallizer and heated to 80°C. Ether solutions of the additive hydride(s), lithium aluminum hydride, or lithium aluminum hydride and lithium borohydride, and a small amount of aluminum hydride are added to the hot benzene. This solution is heated and agitated until nucleation occurs. Aluminum hydride feed solution in ether or diluted with benzene and make-up benzene is added to the bottom of the draft-tube continuously. The upward draft of the propeller agitator gently moves the feed solution to the surface. This internal circulation reduces flashing and results in uniform boiling action over the entire exposed surface. Internal classification

CONFIDENTIAL

CONFIDENTIAL

of the aluminum hydride crystals is obtained by circulating an elutriation stream drawn off the top of the settling annulus and introduced into the bottom of the elutriation leg. The volume and temperature of the circulating magma are maintained at the desired operating conditions by controlling the rate of distillate removal. The crystals formed are continuously removed from the classifying leg of the DTB crystallizer by gravitational settling into a cold benzene reservoir.

(c) Evaluation (U)

(C) The aluminum hydride-1451 recovered from the crystallizer is evaluated by a series of physical and chemical tests. All samples are observed under a microscope to qualitatively evaluate particle configuration and crystallinity. Sample color is noted. Photographs of most samples are made to give a permanent record of particle appearance. The aluminum hydride phase is established by X-ray diffraction. Bulk density, screen, and elemental analyses are obtained on selected samples. Thermal stability is evaluated by the modified Taliani apparatus at 60°C. Finally, a few samples are formulated in the DJA 5020 system to evaluate castability and compatibility.

(2) Results (U)

(C) Seventy-two runs, summarized in Table VII, were made this year, with 39 producing entirely aluminum hydride-1451. Most runs were continuous and varied in length from 4-14 hours, the shorter runs being those in which the aluminum hydride did not properly nucleate or where excessive decomposition occurred. Product from the remaining runs was contaminated with other aluminum hydride phases 1433 and 1444, and the decomposition product, aluminum. Most of the runs failing to yield all aluminum hydride-1451 can be related to either poor nucleation, decomposition and/or excess chlorides in the crystallizer.

Table VII

(U) Summary of DTB Crystallizer Runs

<u>Phases</u>	<u>No.</u>	<u>%</u>
1451	39	54
1451 + 1444	19	26
1451 + 1433	2	3
Decomposition	8	11
Excess Cl ⁻	4	6
	<u>72</u>	

CONFIDENTIAL

(C) A summary of the conditions and results for many of these runs is given in Table VIII. Recovery has been generally low, averaging approximately 5%, due to decomposition and product adherence to the vessel walls. Maximum recovery has been approximately 80%, with material balance calculations accounting for better than 95% of the aluminum hydride fed.

(C) Selected samples of product from runs producing aluminum hydride-1451 were evaluated using the methods outlined. Hexagonal or cubic shaped, single crystals of aluminum hydride-1451 have been observed in many of the runs. Other particles are polycrystalline granules similar to batch material. A typical recovered sample of aluminum hydride-1451 from the DTB crystallizer is shown in Figure 27. The color of most samples is an off-white to light gray. The recovered product does tend to darken as the run progresses, indicating long crystal retention times in the crystallizer. Typical bulk density, screen, elemental analysis and thermal stability data are described in Table IX.

(3) Discussion (U)

(C) During the past year continuous direct crystallization of aluminum hydride-1451 has definitely been demonstrated. However, several problems were encountered in the development program and have delayed many of the fundamental studies. Progress which has been made in delineating and solving these problems along with the experimental effort is discussed below.

(a) Mechanical Design (U)

(C) The Draft-Tube Baffle crystallizer, shown schematically in Figure 28, was originally selected for the aluminum hydride crystallization work. An experimental unit having a capacity of 14 gallons was designed and fabricated of heresite-coated mild steel. A problem with pinholes in the heresite developed, and eventually led to the deterioration of the coating as a result of acid leaching of the base metal during clean-up acidizing. This deterioration occurred primarily in weld areas and where sharp, square edges existed. Modifications in the design of the draft-tube and draft-tube supports improved the durability of the heresite coating, but some problems were still experienced, particularly in the weld between the cylindrical section and the cone-shaped bottom. No problems with the heresite have been noted on smooth, flat surfaces.

(U) The crystallizer liquid level and temperature are used to control the flow rates of feed solution and make-up benzene, respectively. The control loop for the feed solution includes a Dynatrol[®] liquid level sensing device, a millivolt converter, and a recorder-controller to convert the electrical signal to a pneumatic signal. A similar control loop, based on temperature of the circulating fluid, regulates the flow of make-up benzene. The control ranges for these two loops are $\pm 2\%$ of full scale for the level

CONFIDENTIAL

Table VIII

(C) Summary of Conditions and Results from Series of DTE Crystallizer Runs

Run No.	Time Hrs.	Feed Rate mol./hr.	Temperature			Nucleation Method	Results				Remarks
			CoHe °C.	Nucleation °C.	Range °C.		1433 %	1433 %	1444 %	AT %	
31	6.5	0.475	--	78.1	78.1-76.2	--	100	--	--	--	
32	5.0	0.95	--	--	77.9-75.5	--	--	--	--	--	Cl ⁻ in feed.
33	5.5	0.500	--	78.3	78.3-76.9	--	--	--	100	--	
34	5.9	0.595	--	78.0	78.0-76.5	--	100	--	--	--	
35	6.0	0.570	--	78.0	78.0-76.6	--	95+	<5	--	--	1433 nucleated
36	7.0	0.517	--	76.8	76.8-76.6	--	100	--	--	--	Excess decomposition.
37	10.5	0.642	--	77.5	77.5-76.5	--	tr	amorphous	--	--	Cl ⁻ in feed.
38	5.5	0.543	--	77.5	77.5-76.0	--	100	--	--	--	
39	3.5	0.560	--	--	75.7-77.5	--	--	--	--	--	Cl ⁻ in feed.
40	4.2	--	--	77.1	77.1-75.0	--	90	--	--	10	
41	5.3	0.740	--	77.4	77.4-75.8	--	100	--	--	--	
42	6.5	--	--	77.9	77.9-74.8	--	100	--	--	--	Feed valve stuck; nucleation at 5 hrs.
43	2.5	--	--	--	75.0-72.5	--	5	--	95	--	Feed valve stuck.
44	7.0	0.495	--	78.7	78.7-76.5	--	100	--	--	--	
45	5.3	2.64	--	77.6	77.6-75.8	--	100	--	--	--	
46	6.5	0.495	--	78.4	78.4-77.7	--	100	--	--	--	
47	7.0	--	--	78.2	78.2-76.8	--	50	35	15	--	Excess decomposition.
48	4.7	0.77	--	78.2	78.2-77.5	--	95+	--	tr	--	
49	7.5	0.42	--	77.5	77.5-75.9	--	50	--	50	tr	
50	6.5	0.745	--	77.8	77.8-75.2	--	100	--	--	--	
51	4.3	0.567	--	78.1	78.1-77.4	--	100	--	--	--	
52	6.0	--	--	78.2	78.2-76.0	--	100	--	--	--	
53	5.0	0.334	AMB	77.7	77.7-76.8	1	100	--	--	--	LLC shorted.
54	5.5	0.344	AMB	77.5	77.5-76.8	1	100	--	--	--	Manual feed.
55	5.0	0.445	AMB	78.5	78.5-77.0	1	25	--	70	<5	Manual feed.
56	3.5	1.250	AMB	78.2	78.2-76.5	1	100	--	--	--	
57	5.0	0.295	68.0	77.6	77.6-77.0	2	--	--	--	--	Solution decomposition.
58	2.5	0.760	76.5	78.5	78.5-77.8	2	100	--	--	--	Product sticking.
65	5.0	0.422	75.5	77.9	77.9-77.5	2	100	--	--	--	
66	5.0	0.278	79.4	77.2	77.2-76.5	3	50	--	50	--	
67	--	--	--	--	--	--	--	--	--	--	Solution decomposition.
68	3.0	--	76.0	77.2	77.2-76.5	2	100	--	--	--	
69	4.0	1.20	69.0	77.2	77.2-76.2	2	100	--	--	--	
70	4.0	0.625	79.4	79.0	79.0-78.0	4	75	--	25	--	
71	--	--	79.4	78.4	--	4	100 ^b	--	--	--	Leaks in feed system.
72	8.0	0.428	79.1	78.0	78.0-75.5	4	100	--	--	--	
73	2.5	--	79.5	--	--	4	--	--	--	--	Excess Cl ⁻ .
74	8.0	0.360	78.7	78.0	78.0-77.2	4	100	--	--	--	
75	3.0	0.72	80.0	78.3	78.3-76.0	4	100	--	--	--	
76	--	--	--	--	--	--	--	--	--	--	Excess Cl ⁻ .
77	4.5	0.530	79.6	78.9	78.9-77.0	4	100	--	--	--	
78	6.0	--	79.9	79.0	79.0-75.0	4	100	--	--	--	

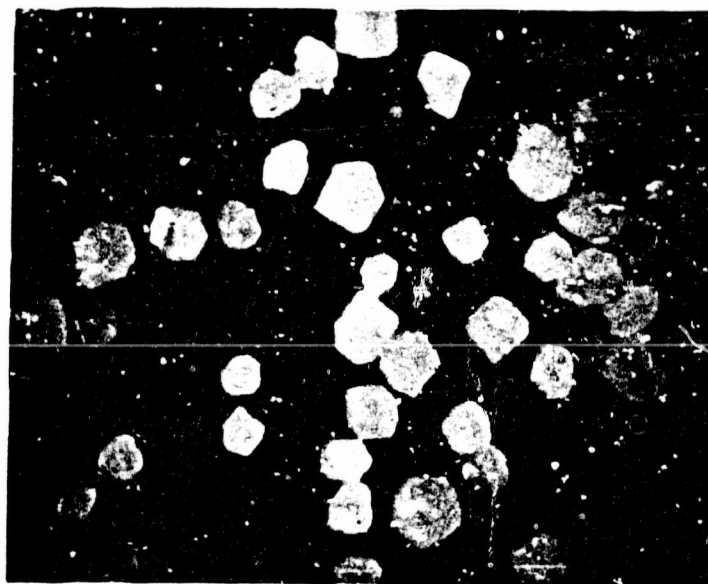
^aTemperature range after nucleation.

^bVisual observation of nuclei.

CONFIDENTIAL



Transmitted Light



Reflected Light

(C) Fig. 27 - Photomicrograph of Typical
Aluminum Hydride-1451 Obtained
from the DTB Crystallizer

CONFIDENTIAL

CONFIDENTIAL

Table II
(C) Evaluation of Selected Samples of Aluminum Hydride from DTB Crystallizer^a

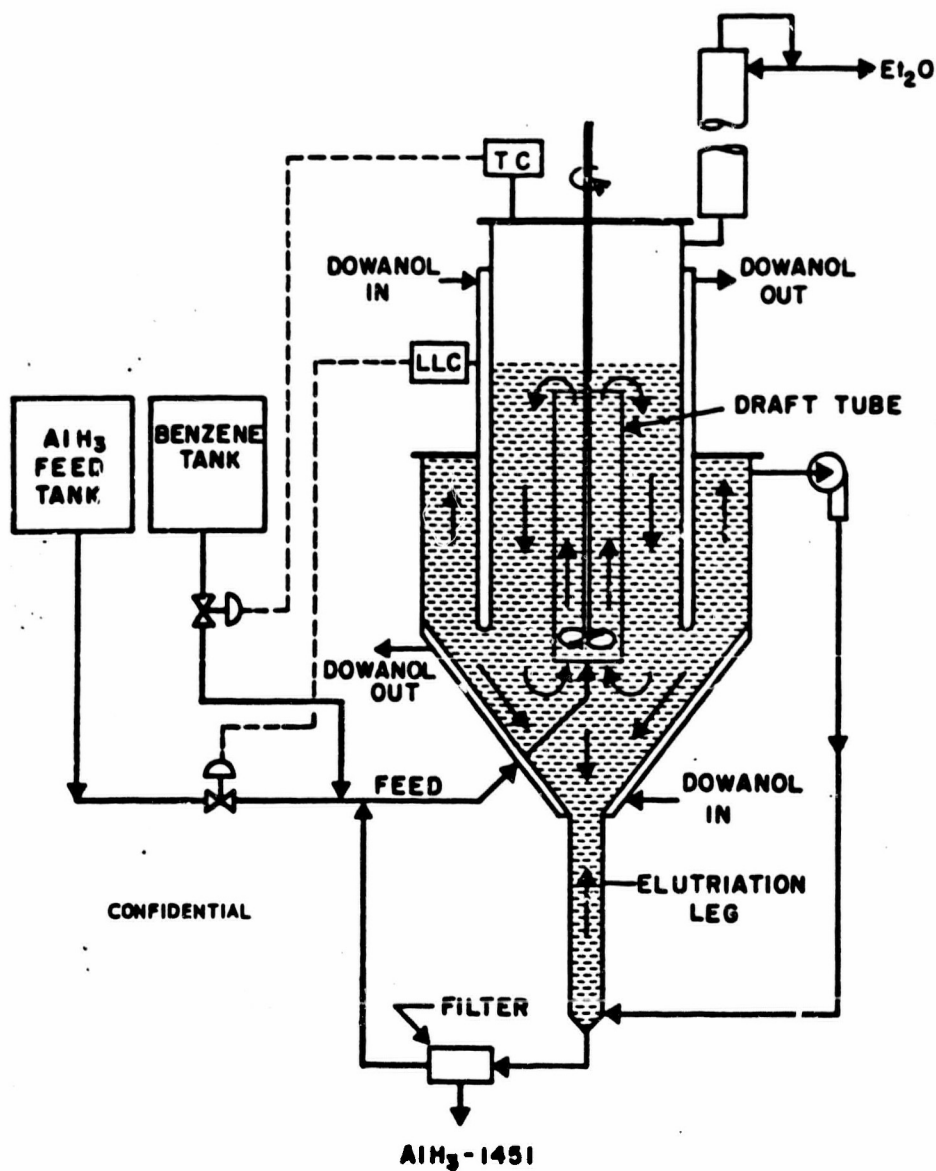
Sample No.	Particle Shape	Color	Bulk Density g./cc.	Stability % Decomposed 60°C., Days				Elemental Analysis, %				
				2	4	6	8	Al	H	C	Li	Cl
5A	Cube	Light gray	0.65	0.20	0.35	0.66	1.35	--	--	--	--	--
6C	Cube	Light gray	0.73	0.11	0.31	0.81	2.60	89.0	9.94	0.75	0.29	0.09
7B	Cube	Light gray	--	0.16	0.50	1.20	2.80	--	--	--	--	--
25C	Rock	Off white	--	0.09	0.28	0.85	--	--	--	--	--	--
26Gb	Rock	Light gray	0.88	0.17	0.67	2.60	--	87.2	--	0.20	0.35	<0.05
29F	Cube	Light gray	0.90	--	--	--	--	--	--	--	--	--

^aX-Ray analysis indicated 100% 1451 phase in all runs.

^bPercent retained on 100, 150, and 200 and 270 mesh screens were 1.1, 15.2, 60.0, and 19.5, respectively.

CONFIDENTIAL

CONFIDENTIAL



(U) Fig. 28 - Schematic Diagram of the Draft Tube Baffle Crystallizer

CONFIDENTIAL

CONFIDENTIAL

controller and $\pm 0.2^{\circ}\text{C}$. for temperature. Other instruments such as a pressure indicator, temperature recorders, flow meters, etc. were installed and calibrated. In addition, water and oxygen analyzers were installed to monitor the concentrations in ppm. of these impurities in the solvents, gaseous nitrogen system, and the dry box atmosphere.

(C) Mechanical design of the aluminum hydride crystallizer is believed to be extremely critical. It is known that impurities, including oxygen and water, affect both the crystallization step and the quality of the final product. Since the original DTB crystallizer is relatively complex, making it more difficult to effectively clean, dry, and purge the unit, a modified crystallizer was designed. The revised unit, shown schematically in Figure 29, is based on the same operating principles as the DTB and is designed to integrate with all existing auxiliary equipment. Features of the new unit include (i) the elimination of the settling annulus which is a "hidden surface"; (ii) an increased L/D ratio; (iii) an increased cone angle from 60 to 75 degrees; (iv) a reduced surface to volume ratio; and (v) a radius of curvature on all welds where the slope changes. Fabrication and heresite coating of the modified unit have been completed. The new unit will be installed during the first week in January, 1966.

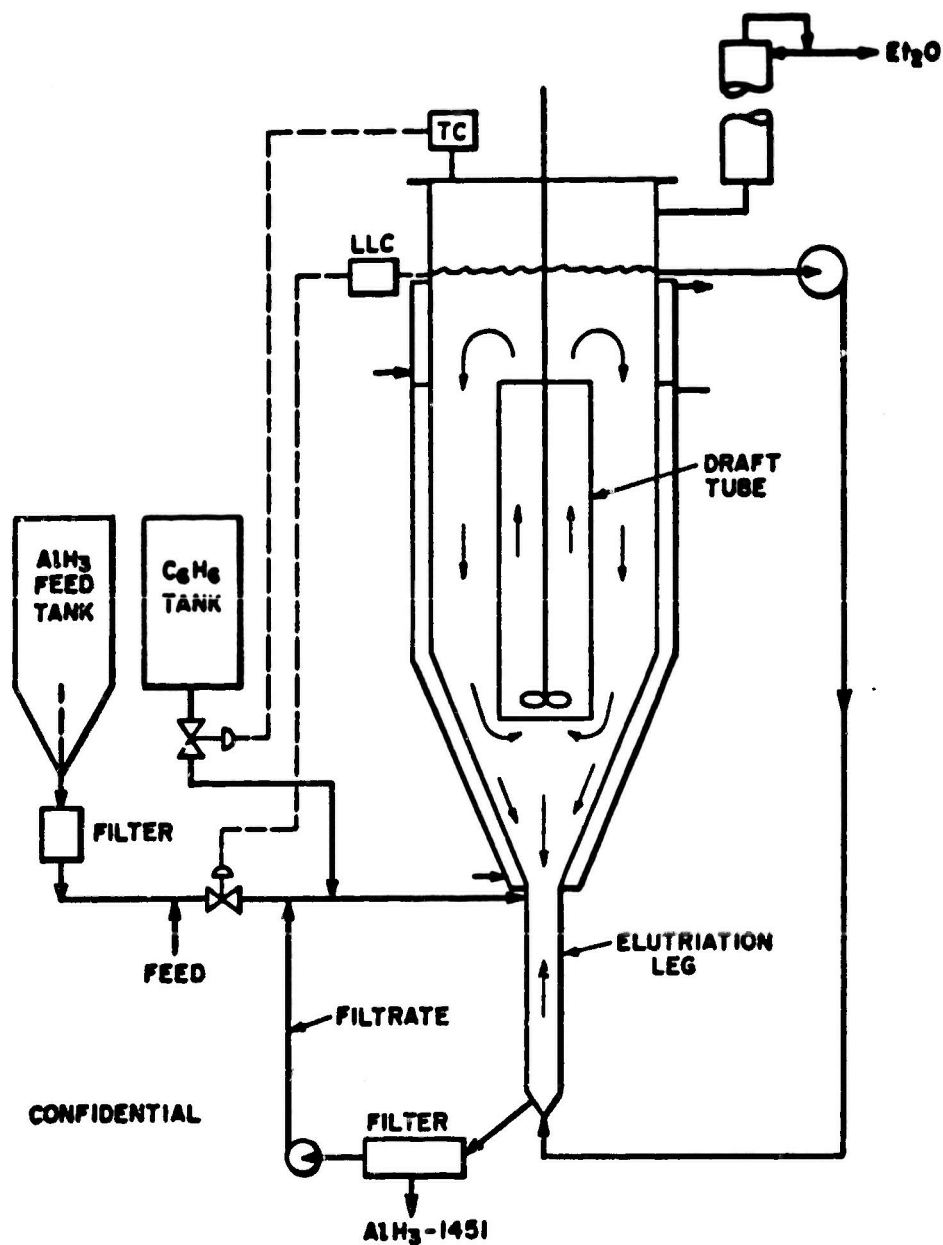
(b) Nucleation (C)

(C) The conditions and mechanism of nucleation of the aluminum hydride are extremely critical in determining the quality of the final product. Investigation of the nucleation process has been a major part of this year's effort. The purpose of these studies was to elucidate the nucleation process and to determine and optimize those parameters which control the formation of nuclei.

(C)(1) Methods - All runs have been nucleated by a "thermal seeding" technique developed in the laboratory. Four methods, shown in Figure 30, have been evaluated. The first method consisted of adding an ether mixture of aluminum hydride, lithium aluminum hydride, and lithium borohydride to ambient temperature benzene and heating until nucleation occurred. The long heating time resulting in excessive decomposition in the solution. The second method was adapted to reduce this heat treatment time. In this method the hydride mixture was added to preheated benzene. The third method consisted of charging batch-wise the same mixture to boiling benzene. This method resulted in a temperature drop without nucleation occurring. By reheating the solution to a higher temperature, nucleation could be obtained. The fourth method is a variation of the third with the initial feed introduced over a period of time (20-30 minutes), maintaining a high temperature, thus a low ether concentration. The final method has given the most reproducible nucleation results and will be used in most future work.

CONFIDENTIAL

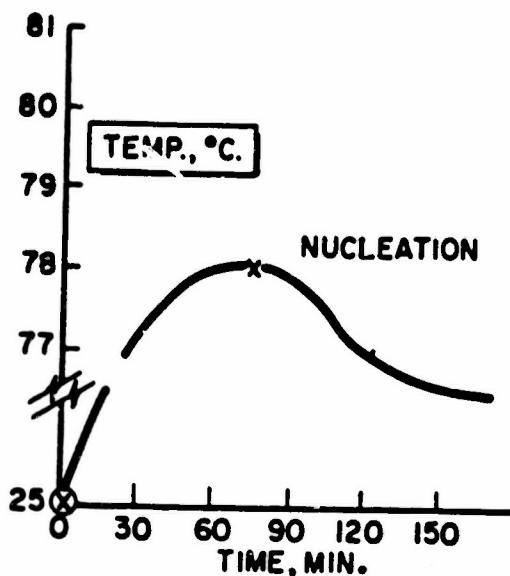
CONFIDENTIAL



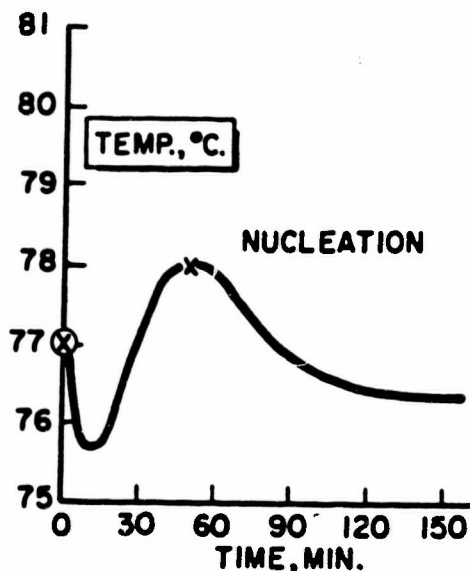
(U) Fig. 29 - Modified Crystallizer

CONFIDENTIAL

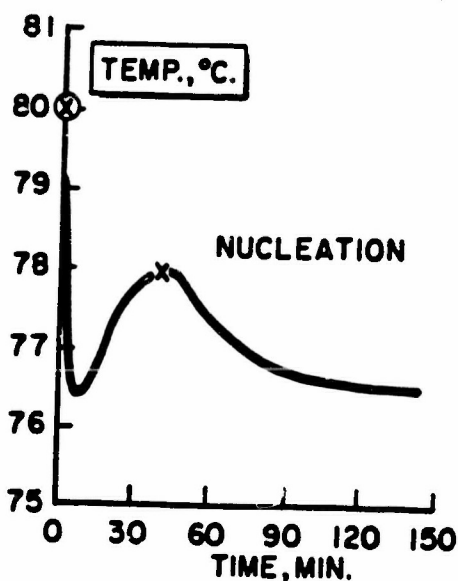
CONFIDENTIAL



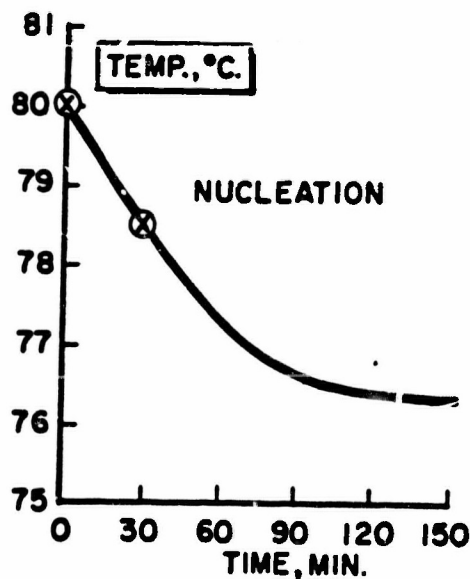
Method 1



Method 2



Method 3



Method 4

⊗ NUCLEATION FEED SOLUTION ADDED TO CRYSTALLIZER

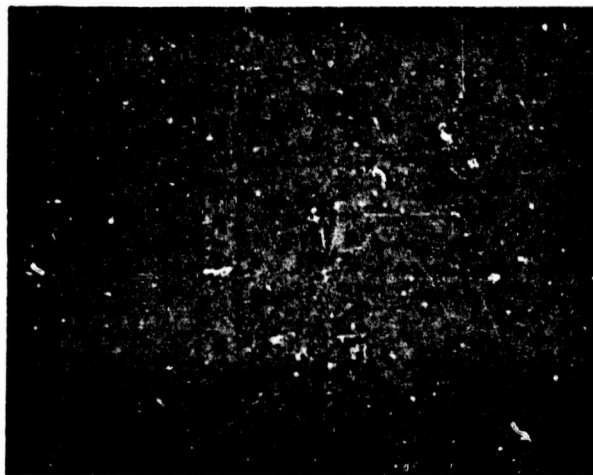
(U) Fig. 30 - "Thermal Seeding" Nucleation Methods (Time - Temperature Profiles)

CONFIDENTIAL

- (C) (11) Parameters - The parameters which apparently control the nucleation process are aluminum hydride concentration, additive concentration, solution feed rate, and temperature. The hydride parameters were studied in both the laboratory and the DTB crystallizer. The optimum conditions for nucleation and the functional relationship between the controlling parameters have not been completely established. Further studies are planned in the near future, as reproducible nucleation is mandatory for other parameter studies.
- (C) The aluminum hydride concentration at nucleation has varied between 0.003 and 0.015 M. At higher concentrations, nucleation of undesirable phases, particularly aluminum hydride-1444, is obtained. It is known that direct nucleation can occur at concentrations as low as 0.003 M, if the conditions are ideal. The lithium aluminum hydride concentration has varied from 0.001 to 0.010 M based on the excess lithium aluminum hydride added. This concentration is not exact, but it is related to the reaction stoichiometry and will be discussed later. The nucleation temperature depends upon feed rates and concentrations. It is believed that the nucleation temperature should be 78.5°C. to 79.0°C. for best results. Rapid addition of aluminum hydride usually results in the formation of undesirable phases, particularly aluminum hydride-1433, which subsequently affects crystallinity.
- (C) (111) Mechanism - In all the batch and many of the early continuous crystallization laboratory runs most of the aluminum hydride nucleated as aluminum hydride-1433 and changed rapidly to the desired aluminum hydride-1451 phase. This mechanism has predominated in most of the aluminum hydride process work. It is postulated that direct crystallization of aluminum hydride-1451 from solution was possible in a continuous crystallizer and should lead to improved crystallinity. Experimentation has shown that direct nucleation of aluminum hydride-1451 does occur in the DTB crystallizer. In fact, only a few runs have nucleated as aluminum hydride-1433.
- (C) Nuclei usually appear as either well formed cubes or hexagons of aluminum hydride-1451. The crystal growth rate is generally very rapid, resulting in imperfections. Additional problems of agglomeration are noted in some runs. An extremely small (<5 μ) foreign material precipitates prior to the aluminum hydride nucleation, as shown in Figure 31. The effect of this material on nucleation is not fully understood. It is believed that this material is lithium chloride which enters the

CONFIDENTIAL

CONFIDENTIAL



(C) Fig. 31 - Photograph of Initial Small Particles Present during Beginning Crystallization of Aluminum Hydride-1451

crystallizer in solution and/or as very small particles ($<3 \mu$). Laboratory data have shown that the solubilities of the various hydrides and reaction products are complex and interrelated. These unknown particles do not appear to change after initial precipitation. Attempts to isolate and identify these particles have not been successful.

(C) (iv) Conclusions - The following conclusions can be drawn from the nucleation work:

- Direct nucleation of aluminum hydride-1451 is both feasible and practical and under controlled conditions can occur rapidly.
- The presence of Cl^- either as AlClH_2 , AlCl_3 , or possibly LiCl inhibits the nucleation of AlH_3 .
- High concentrations of aluminum hydride result in the formation of some undesirable phases.
- Temperature must be high or, more specifically, ether content low, to obtain acceptable nuclei.

CONFIDENTIAL

(c) Solution Stability (U)

(C) Random decomposition of aluminum hydride on the inner walls of the crystallizer and elutriation system has continually been a major crystallization problem, and thus it has delayed the fundamental parameter studies. This problem is related primarily to the presence of impurities in the crystallizer media. Impurities may be generated in the reactor train (Cl^-); or they may be introduced from starting materials, the atmosphere (water and oxygen), the residue from the previous run, etc. Considerable effort has been expended to eliminate these impurities in order to control the decomposition problem.

(U) Originally the impurities were believed to be introduced by the reactants and solvents and/or related to the effectiveness of the cleaning procedure. Hence, raw material quality was evaluated in the laboratory and found to yield comparable product. The cleaning procedure was also extensively evaluated and standardized. The procedure is detailed, but consists primarily of acidizing, rinsing with distilled water, drying, rinsing with ether and/or benzene, and purging with dry nitrogen. The random and severe decomposition originally observed has been nearly eliminated by high temperature treatment. The exact effect of the heat treatment is not clearly known; however, it appears to be very necessary. Although these steps have significantly reduced decomposition, they have not completely eliminated it. Therefore, additional work is necessary to delineate the other factors responsible.

(C) Impurities are also generated during reaction. The by-product, lithium chloride, is essentially insoluble in the ether solvent system, although it has been shown to have some slight solubility when hydrides are present. It is believed that this lithium chloride may initiate and/or accelerate the observed decomposition. Therefore, several steps have been taken to reduce or eliminate the lithium chloride. A treatment with sodium borohydride at 30°C . to chemically react with the lithium chloride is included. Dilution of the feed solution with benzene also precipitates some lithium chloride. Therefore, a standpipe was installed in the feed tank to give a settling chamber for particles precipitated during dilution. In addition, a final $3\ \mu$ filter has been installed between the feed tank and crystallizer. Analysis of the feed solution will be made to compare with previous data.

(C) Several other possible causes of solution decomposition are being evaluated. Included are electrical effects, residue in the distillation column, materials of construction, i.e., heresite and glass, etc. However, no definite causative relationships have been established as yet in any of these areas.

(C) It is also believed that mechanical design is a contributing factor in the decomposition problem, due to "hidden surfaces," flanges, or unused nozzles and other fittings which hold product and/or are difficult to clean. The modified crystallizer design discussed earlier should minimize many of these problems.

CONFIDENTIAL

(d) Reaction Stoichiometry (U)

(C) It is known that the presence of soluble chlorides in the crystallizing media significantly increases the solubility of aluminum hydride. In several runs in the DTB crystallizer, large quantities of aluminum hydride were added without nucleation occurring. Elemental analysis of both the feed solution and crystallizer filtrate confirmed the presence of chlorides.

(C) Stoichiometric quantities of lithium aluminum hydride and aluminum chloride are reacted in a batch reactor. Since the quantity of reactants charged is based on concentrations of ether solutions, small errors in concentrations and measurements lead to errors in stoichiometry and, consequently, to excess chloride in the feed solution, resulting in a problem not encountered in the batch process. At present, no rapid chemical or physical method of determining the end-point of this reaction exists. Work has been initiated to develop a reliable method. However, until such a method is operational, a small excess of lithium aluminum hydride is added to assure complete reaction. The presence of the excess lithium aluminum hydride is not advantageous, as the solubility of lithium aluminum hydride at operating conditions is small, resulting in the precipitation and presence of lithium aluminum hydride crystals in the crystallizer at all times. The effect of these crystals on the nucleation and growth of aluminum hydride is not fully understood, but some data indicated a deleterious effect on crystallinity and product adhesion.

(e) Crystallization Parameters (U)

(C) The detailed fundamental parameter studies were delayed until the solution decomposition and nucleation problems were solved. Information, however, has been collected which indicates the effect of the major parameters. Based on these observations, agitation, feed rate, and crystal retention time are the most significant.

(C)(1) Agitation - It has been shown in the laboratory that agitation does affect both the particle size and shape. Variation in agitation has been studied in the DTB crystallizer, including the use of various flow patterns. The speed of the propeller type agitator has been varied from 50 to 250 rpm. Variations in results have been observed; however, no definite conclusion can be drawn from the preliminary data. Extensive investigation of this parameter is planned in the future. The agitator type, speed, and flow pattern will all be studied.

(C)(11) Feed Rate - The normal feed rate of a 0.3 molar aluminum hydride feed solution to the DTB crystallizer is approximately 0.5 moles/hr. No attempts have been made to vary the feed concentration, as premature

CONFIDENTIAL

precipitation of the aluminum hydride becomes a problem at higher concentrations. The addition rate has been varied from about 0.3 to 0.75 moles/hr. However, no conclusions could be drawn from the preliminary data, although it has been shown in the laboratory that feed rates do affect both the nucleation and growth processes.

- (C) (iii) Crystal Retention - Accurate data on the average retention time of crystals in the crystallizer have not been obtained. In general, however, the present residence time appears to be too long, as both particle agglomeration and crystal imperfections increase as the run time increases. Therefore, it appears mandatory that methods be adopted which will reduce the crystal retention time if product quality is to be improved.

It is anticipated that continuous removal of crystals by filtration instead of settling will significantly reduce the retention time and improve the crystallinity of the product. An all-Teflon diaphragm, which should be compatible with the system, will be evaluated early in 1966. Total recycle rates of 30-60 minutes for crystallizer contents through the filter are projected.

- (C) (iv) Additives - Concentrations of lithium aluminum hydride and lithium borohydride have varied from 0.002 to 0.02 moles/l. with respect to the total solution in the crystallizer. These concentrations are not exact, as they depend on the stoichiometry of the reaction mixture as discussed earlier. Feed solution containing a slight excess of lithium aluminum hydride causes the concentration in the crystallizer to be constantly changing. Hence, excess lithium aluminum hydride and lithium borohydride are sometimes observed to precipitate in the crystallizer along with the aluminum hydride. It is believed that crystals of either additive hydride affect the crystallinity and growth of the aluminum hydride-1451. Several runs were made omitting the initial addition of lithium borohydride to the crystallizer. However, some is added due to the sodium borohydride treatment. These runs resulted in aluminum hydride-1451 with similar nucleation and growth. The product did, however, contain a higher percentage of hexagonal, single crystals in some of the runs. Therefore, the presence of lithium borohydride may affect the crystal habit of aluminum hydride-1451. Additional work is being done to optimize the concentrations of the additive hydrides and to determine the effect of each on nucleation and growth.

CONFIDENTIAL

CONFIDENTIAL

(C) (v) Additional Parameters - There are several other parameters of the system which require investigation, such as temperature, elutriation recycle rates, nucleation and growth additives, stabilizing additives, etc. The effect of temperature was discussed earlier and is not believed to have a significant effect on the growth rate; however, it is critical during nucleation, as discussed earlier.

(f) Crystallization Concept (U)

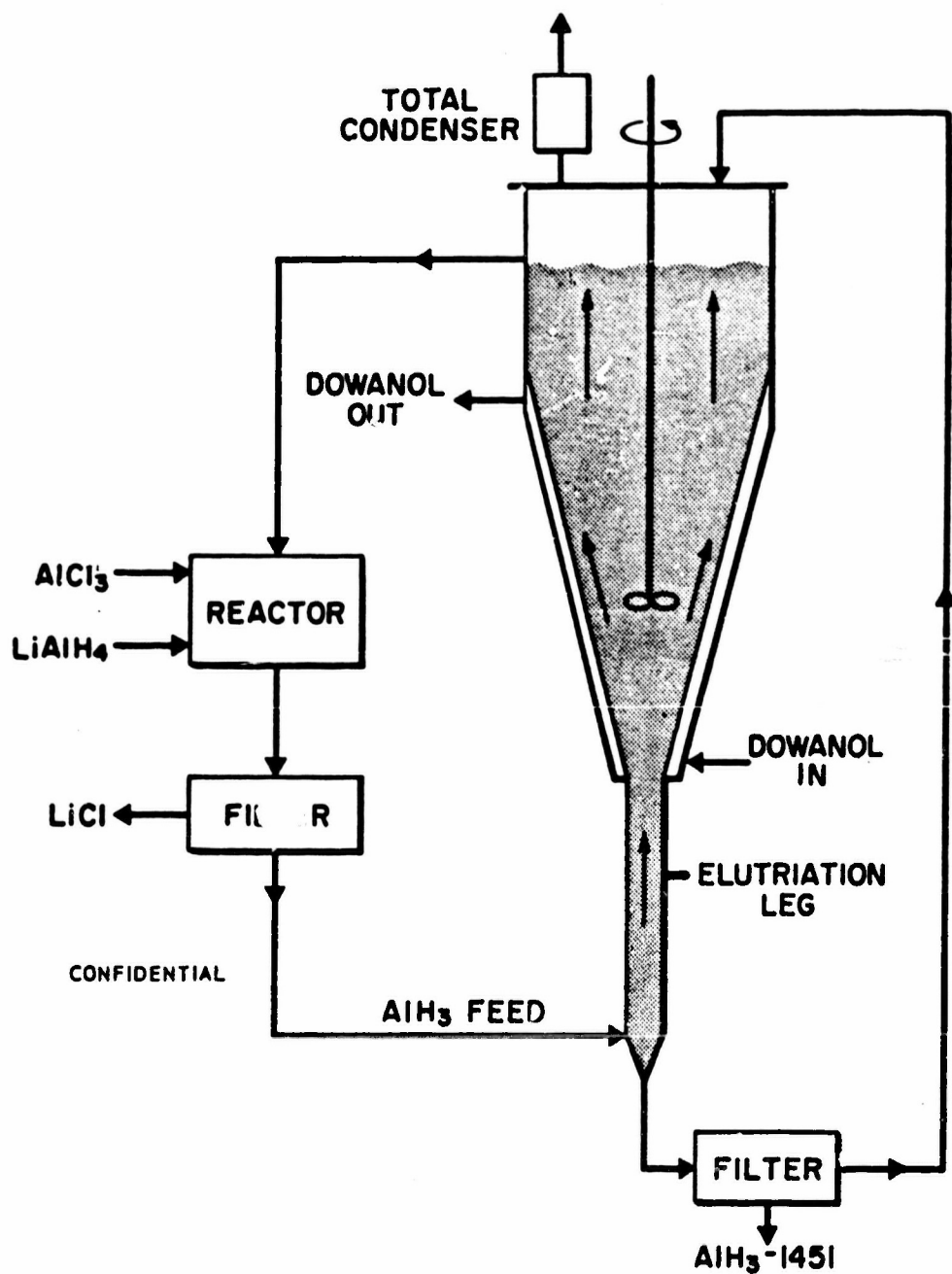
(C) A new concept of aluminum hydride crystallization has been briefly investigated during the last quarter of the year. The concept involves a dilute feed which eliminates distillation from the aluminum hydride process, yet incorporates solvent recycle. The main advantage of this process is the elimination of the need for high heat transfer rates, and, consequently, high wall temperatures which accelerate product decomposition. Secondary advantages include simplification of the crystallization process, and economic savings in both direct and indirect costs.

(C) A schematic diagram of the process is presented in Figure 32. The system consists of a reactor, filter, and crystallizer employing a single solvent system. Feed solution is prepared by recycling the overflow from the crystallizer through a reactor where solid lithium aluminum hydride and an ether-benzene solution of aluminum chloride are added continuously. The reactor effluent is filtered to remove insoluble lithium chloride and charged to the crystallizer at the bottom of an elutriation leg where classification of the crystalline product occurs. The flow rate is adjusted to yield the desired particle size. The aluminum hydride crystallizes, reducing the concentration in the overflow stream to the equilibrium value. The "single solvent" is a constant boiling ether-benzene mixture. It consists of 6 volume percent ether and 94 volume percent benzene at an operating temperature of 76°C. The unit is equipped with a total condenser to maintain the desired operating temperature. The concentration and flow rate of the reactor effluent stream establish the crystallization rate.

(C) Experimental work has demonstrated the feasibility of the crystallization step. Dilute feed solutions of aluminum hydride were prepared in an ether-benzene system in the batch reactor train and transferred to a hold tank. Continuous addition of this dilute feed to the crystallizer resulted in samples containing entirely aluminum hydride-1451. Results of fourteen runs made in the unit are summarized in Table X. The major problem appears to be reproducibly obtaining acceptable nuclei of aluminum hydride-1451. No significant problems were experienced with decomposition.

CONFIDENTIAL

CONFIDENTIAL



(U) Fig. 32 - Schematic Diagram of New Crystallizer

CONFIDENTIAL

CONFIDENTIAL

Table X

(c) Summary of Dilute Feed Aluminum Hydride Runs

Run No.	Feed Rate ml./min.	Solution Concentration			Temp. °C.	Product			Remarks
		Et ₂ O %	C ₆ H ₆ %	AlH ₃ M		1451 %	1444 %	Al %	
C-1	--	0.5	95	0.05	77.6	--	--	--	No nuclei.
C-2	45	5	95	0.05	78.5-75.2	25	75	--	
C-3	33	5.7	94.3	0.05	79.5-76.0	Not sampled			Some decomposition.
C-4	23	5	95	0.05	77.8-76.7	75	25	--	
C-5	20	4	96	0.043	78.2-77.0	100	--	--	
C-6	20	4	96	0.04	77.6-77.0	--	100	--	
C-7	41	4	96	0.04	78.2-77.0	80	20	--	
C-8	19	4	96	0.038	79.8-77.2	100	--	--	1433 present.
C-9	19	4	96	0.038	78.4-76.7	Not sampled			Some decomposition
C-10	--	4	96	0.04	78.2-76.3	--	--	--	
C-11	28	4	96	0.06	79.2-77.2	25	75	--	No nuclei.
C-12		Terminated during heat-up							
C-13	21	4	96	0.06	78.3-76.8	100	--	--	
C-14	--	4	96	0.06	78.2-77.4	--	--	--	No nuclei.

CONFIDENTIAL

CONFIDENTIAL

(C) The data obtained are preliminary and inconclusive. It is, however, apparent that the concept is feasible, and that with additional development work a practical aluminum hydride-1451 process can be developed.

B. FUNDAMENTAL DECOMPOSITION STUDIES OF ALUMINUM HYDRIDE-1451 (C)

(C) It is believed that the development of a sound theoretical explanation of all the observed facts of aluminum hydride decomposition will greatly assist in devising methods to improve the stability of aluminum hydride. A discussion of current results and their interpretation in terms of modern solid state decomposition theory are presented.

1. Kinetics and Mechanism of Decomposition (U)

(C) The decomposition of aluminum hydride invariably produces a sigmoid-shaped curve when the percent decomposition, or change in pressure over the hydride, is plotted as a function of time. This type of curve, characteristic of many other solid state decompositions, indicates the possibility of an autocatalytic reaction. However, from the theory of solid state reactions, a general hypothesis has been made that explains the apparent autocatalytic nature of the reaction in terms of the formation of nuclei at certain localized spots in the reactant, followed by the relatively rapid growth of these nuclei.

(C) Supporting evidence of the AlH_3 -1451 general decomposition theory should be interpreted in terms of the formation and growth of aluminum nuclei. In the past this has originated from a study of the aluminum metal formed after total decomposition of the hydride, surface area changes, and application of mathematical equations successfully applied to the decomposition of other solids. From the previous studies it was suggested that the decomposition of the hydride should be interpreted in terms of a three stage process:

- (i) The initial reaction occurring at the surface of the crystals.



- (ii) The formation of stable aluminum nuclei.
- (iii) The reaction occurring at the interface between the AlH_3 -1451 and the aluminum metal.

It has been pointed out that the last two processes, nucleation and nuclei growth, are independent and will vary with time. Initially, the nucleation process will dominate, while later it will progressively lose some of its importance.

CONFIDENTIAL

CONFIDENTIAL

(C) During the past year, a new technique applied to the study of the decomposition of aluminum hydride resulted in a more fundamental understanding of the nucleation and growth process occurring during decomposition of the hydride. The use of a metallograph¹, depicted in Figure 33, for the first time, allowed direct observation of the sites where aluminum nuclei originate in the AlH₃-1451 lattice and, indirectly, the growth of these nuclei as the decomposition of the hydride progresses. It should be pointed out that nuclei can only be observed microscopically after they have already been growing for some time. From these photomicrographs, it was very surprising to find that there existed a significant difference between various lots of hydride in the formation of aluminum metal in the aluminum hydride particles. The most surprising discovery was the existence of aluminum nuclei throughout the interior of the particle, a condition characteristic of some lots of hydride, as illustrated by a sample of pilot plant material (05134) in Figure 34. This is in marked contrast to other lots of hydride, such as the magnesium stabilized laboratory sample and another laboratory sample in Figures 35 and 36, respectively, representing materials decomposed to approximately the same degree.

(C) The white areas in the photomicrographs represent aluminum metal, whereas the gray material represents the hydride. These differences in the formation of aluminum in an aluminum hydride particle suggest that different decomposition mechanisms may be operative.

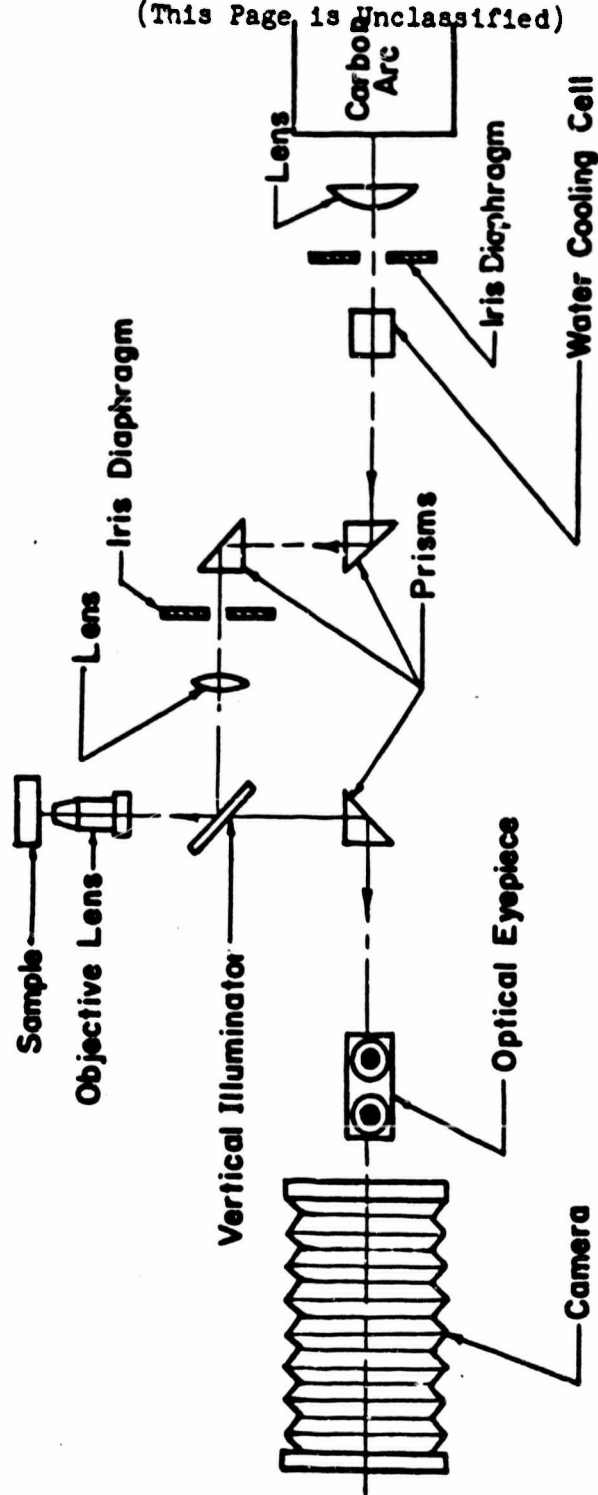
(C) In an effort to determine the quantity of dislocations, grain boundaries, etc. present in aluminum hydride particles, the mounted cross-sectioned samples were etched with a 2% HF solution for five seconds. The results obtained from the examination of three different types of hydride demonstrated that the pilot plant material had a much larger concentration of cracks, grain boundaries, dislocation lines, etc. than does the laboratory or single crystal samples. It is thought that many of the etched lines in the laboratory and pilot plant samples represent grain boundaries present in the agglomerate; however, the differentiation between grain boundaries, cracks, etc. would require additional study.

(C) It was also found that decomposition caused a marked increase in the concentration of etched lines. A sample decomposed 7.1% at 100°C. under vacuum, prior to mounting and etching, demonstrated an observed increase in concentration of etched lines, compared to the control sample. This is believed to be due to an increased cracking of the aluminum hydride particle due to strain

¹We wish to acknowledge the assistance of H. Diehl and D. Baker of the Metallurgical Laboratory of The Dow Chemical Company for their contributions to this section.

CONFIDENTIAL

(This Page is Unclassified)



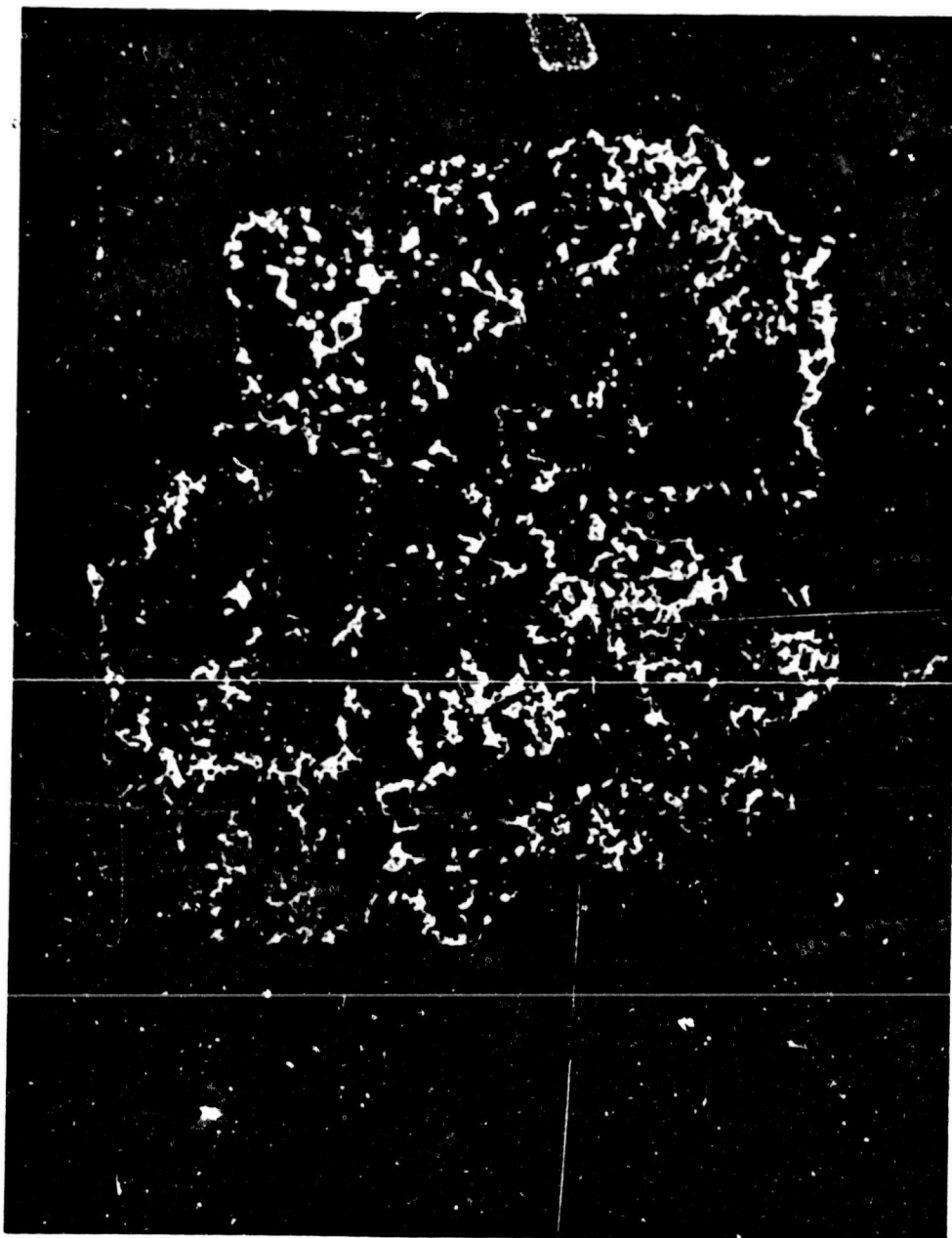
(U) Fig. 33 - Schematic Diagram of Metallograph Components

CONFIDENTIAL

(This Page is Unclassified)

CONFIDENTIAL

(This Page is Unclassified)



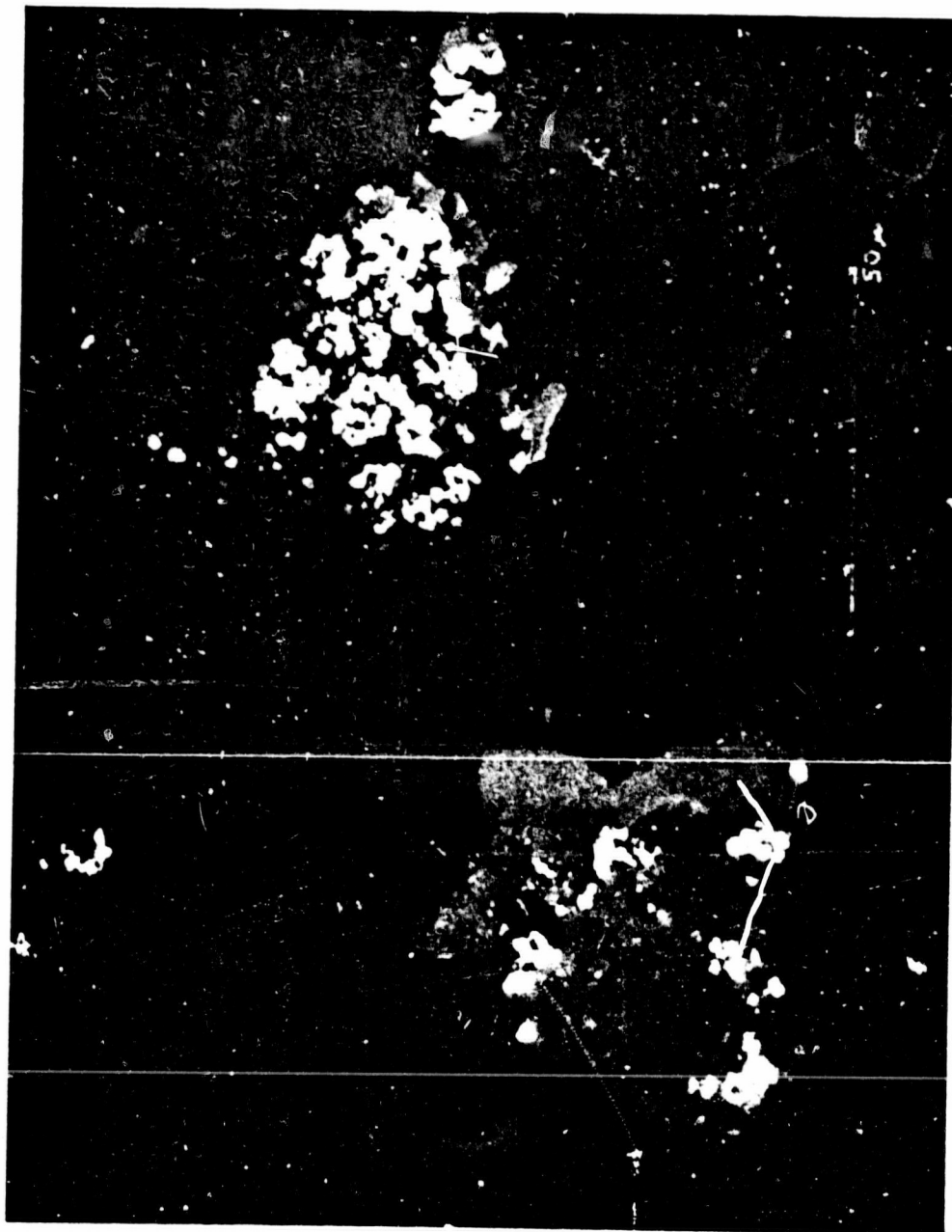
(C) Fig. 34 - Photomicrograph of a Cross-Sectioned
Pilot Plant Sample (05134) of Aluminum Hydride
Decomposed 47.6% Magnified 1500 Times

-93-

CONFIDENTIAL

(This Page is Unclassified)

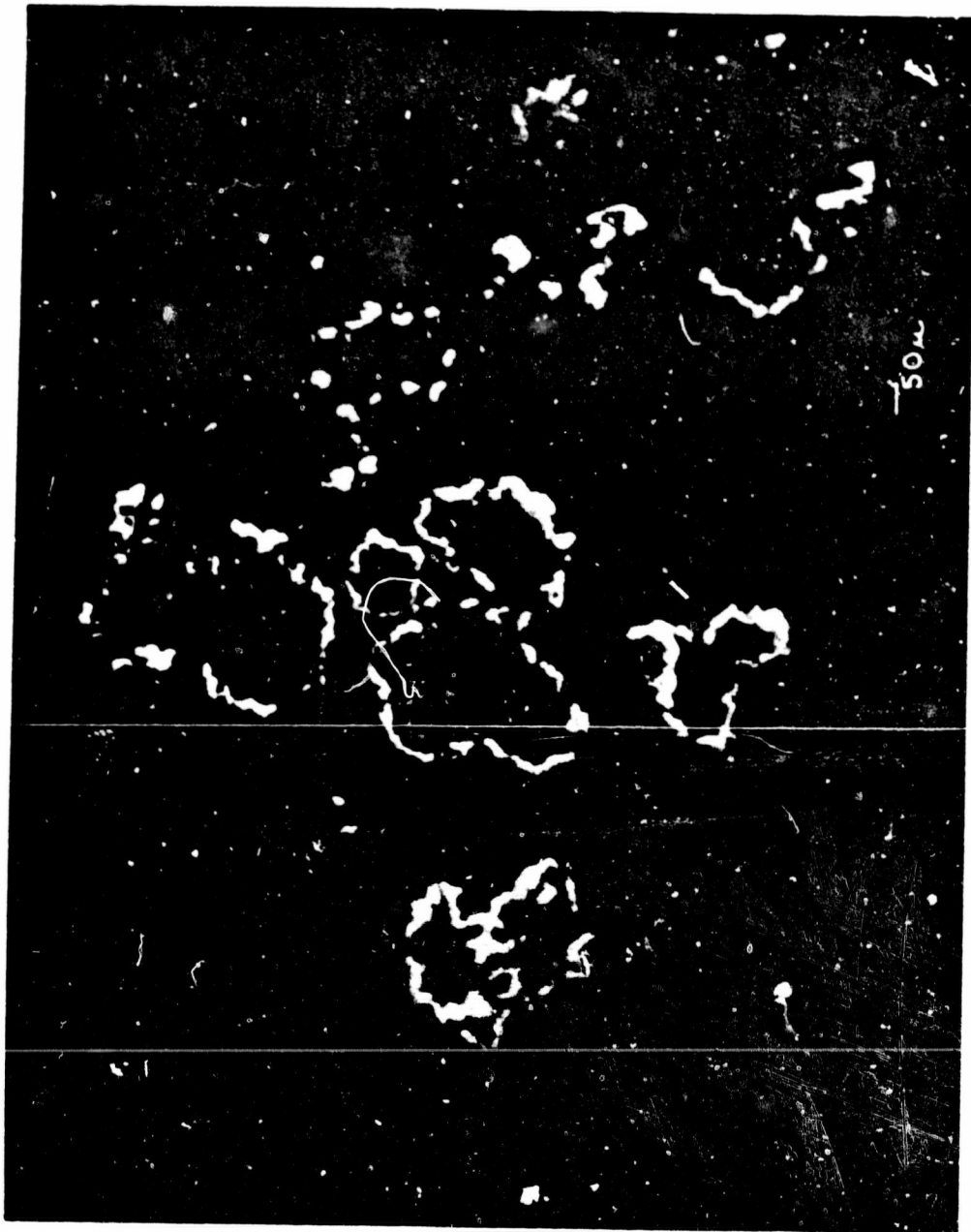
CONFIDENTIAL



(c) Fig. 35 - Photomicrograph of a Cross-Sectioned Magnesium Stabilized Sample (5853-128) of Aluminum Hydride Decomposed 33.5%, Magnified 1500 Times

CONFIDENTIAL

CONFIDENTIAL



(C) Fig. 36 - Photomicrograph of a Cross-Sectioned Laboratory Sample (5853-149) of Aluminum Hydride Decomposed 50.9%, Magnified 1500 Times

CONFIDENTIAL

CONFIDENTIAL

caused by aluminum formation, and strongly implies that the hypothesis suggested by Prout and Tompkins (2) as a general explanation of the propagation of their chain-branching mechanism is correct.

(C) Additional information about the decomposition of aluminum hydride was obtained by partially decomposing a given lot of material to various percentages at 100°C. under vacuum prior to cross-sectioning. Three different lots having different preparation histories are shown in Figures 37, 38, and 39. In addition to illustrating the differences in nucleation and growth during the decomposition of aluminum hydride, as discussed earlier, it is also shown that the hydride particles do not appreciably change their external size or shape during decomposition. Thus, the hydride is transformed during decomposition into very porous aluminum metal particles as shown in the above figures. The absence of crumbling or disintegration during decomposition had also previously been noted from decomposition studies performed on a hot stage under a microscope.

(U) It has also been observed that not all particles appear to decompose at the same rate. However, it is possible that this is a consequence of the particular region cross-sectioned, and, for that reason, it cannot be said with certainty that this is the case. It would, however, not be surprising, since differences in particle perfection, purity, size, etc., must exist and these are known to influence the rate at which decomposition is initiated.

a. Nucleation Process (U)

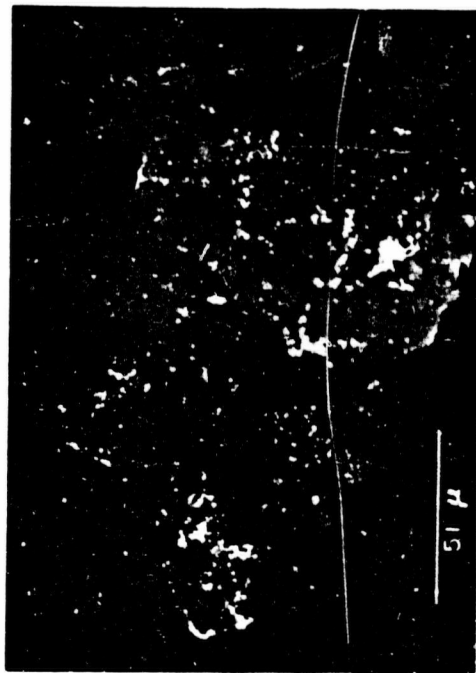
(C) During the past year consideration of the origin of initiation of decomposition in the lattice has led to a proposed working hypothesis on an atomic scale. It should be emphasized that this proposed hypothesis is based on current thoughts regarding the decomposition of aluminum hydride, and will be modified, changed, and expanded as new data dictate.

(C) The proposed nucleation mechanism of aluminum hydride decomposition originates from the interpretation of the decomposition of other solids presented in the open literature (3, 4, 5).

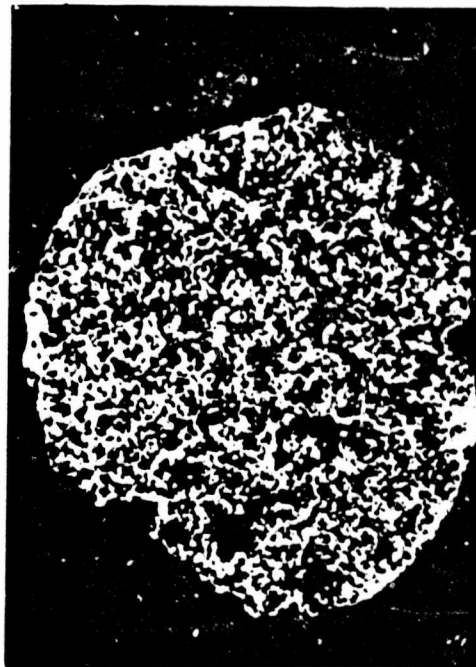
(C) The nucleation of aluminum nuclei in the AlH_3 -1451 lattice is thought to involve a three-step process:

- (i) A process involving the diffusion of an nonequilibrium concentration of anion vacancies through the hydride by a vacancy transfer mechanism.
- (ii) The formation of "germ nuclei" by capture of electrons by the vacancies at the surface or grain boundaries.
- (iii) The coalescence of "germ nuclei" to form active growth nuclei.

UNCLASSIFIED



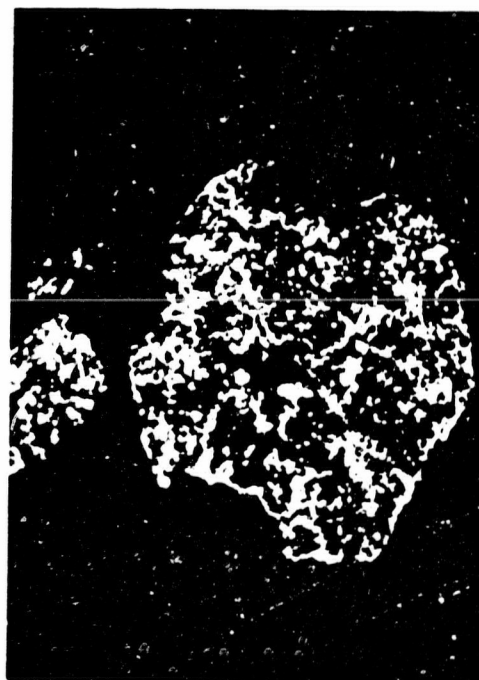
4.8% Decomposition



100% Decomposition



Control

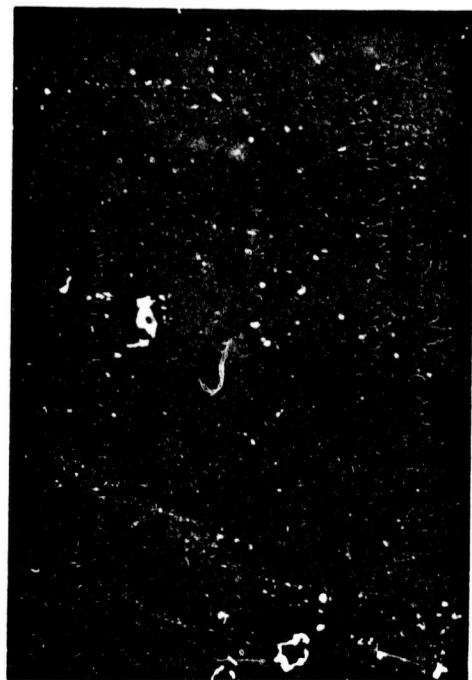


50.5% Decomposition

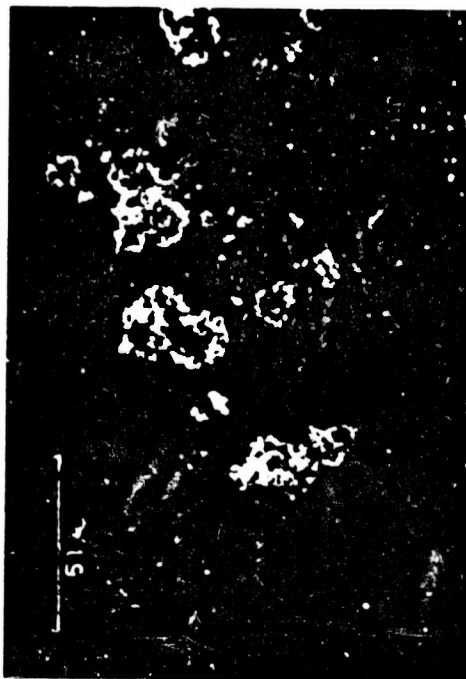
(U) Fig. 37 - Photomicrographs of a Cross-Sectioned Pilot Plant Sample at Various Percents of Decomposition, Magnified 500 Times

UNCLASSIFIED

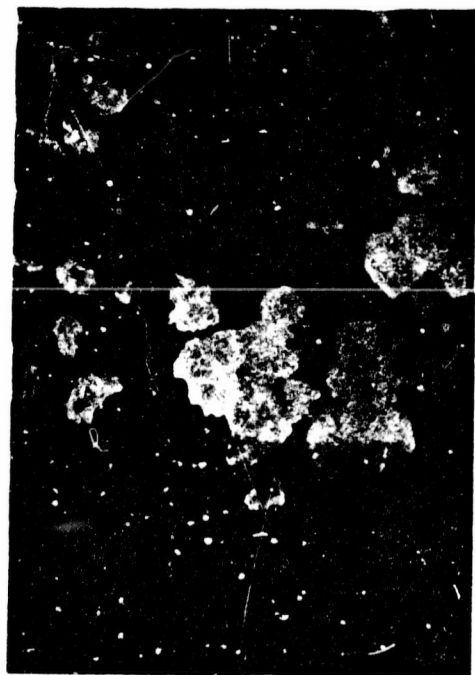
UNCLASSIFIED



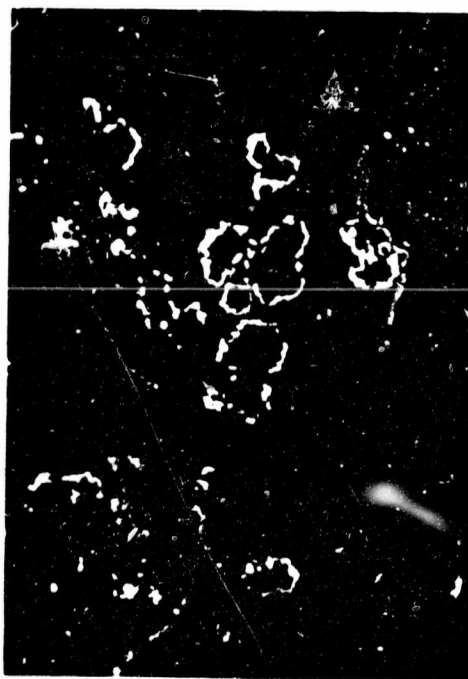
6.4% Decomposition



100% Decomposition



Control



50.9% Decomposition

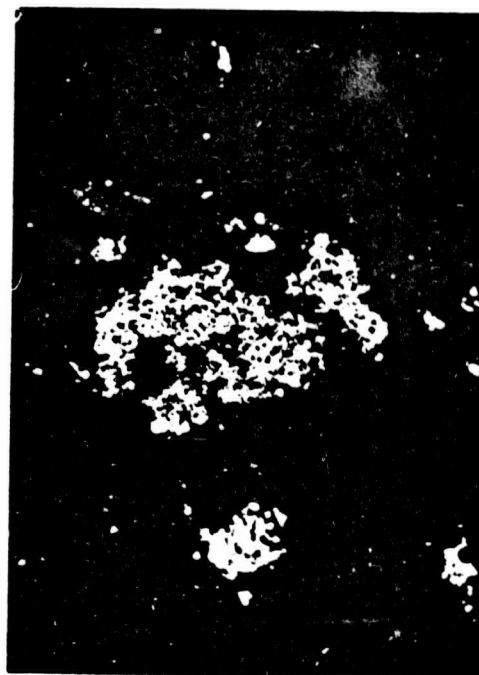
(U) Fig. 38 - Photomicrographs of a Cross-Sectioned Laboratory Sample at Various Percents of Decomposition, Magnified 500 Times

UNCLASSIFIED

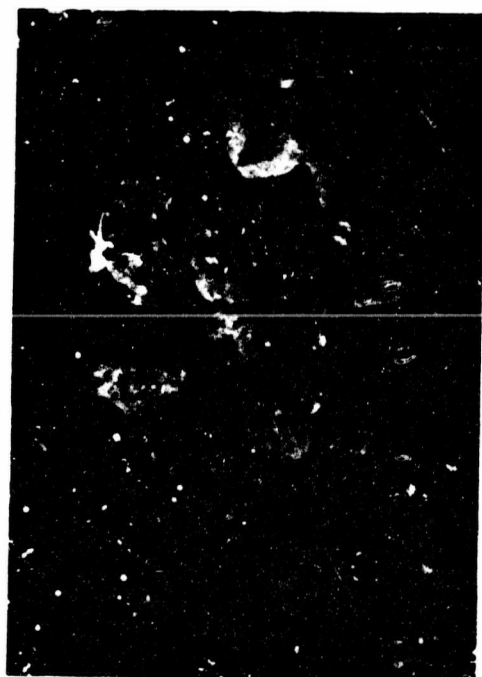
CONFIDENTIAL
(This Page is Unclassified)



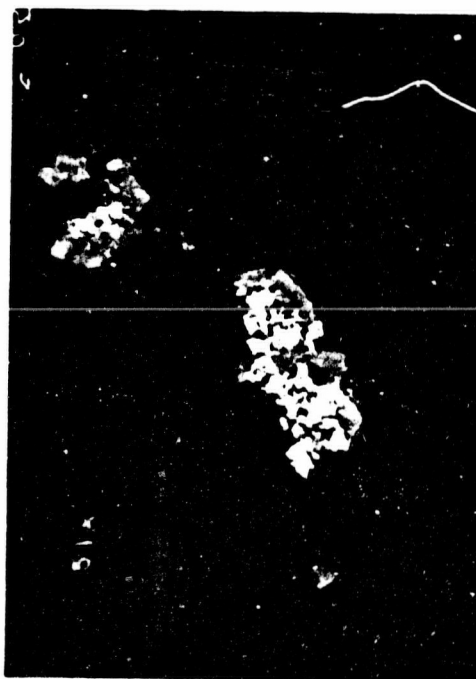
4.5% Decomposition



87% Decomposition



Control



50.5% Decomposition

(U) Fig. 39 - Photomicrographs of a Cross-Sectioned Magnesium Stabilized Sample at Various Percentages of Decomposition, Magnified 500 Times

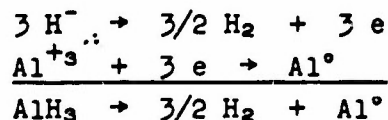
CONFIDENTIAL
(This Page is Unclassified)

CONFIDENTIAL

(C) Structure considerations strongly suggest that anion vacancies could easily be produced in excess of the equilibrium concentration during preparation of AlH_3 -1451.

(C) If the AlH_3 -1433 structure, as suggested by Duke (6) and supported by infrared data, contains one terminal hydrogen, and if the AlH_3 -1451 lattice is a completely three-dimensional hydrogen bridged structure, then it is proposed that, during the phase transition of AlH_3 -1433 to AlH_3 -1451, not all of the terminal hydrogens in the AlH_3 -1433 structure become bridged in the AlH_3 -1451 lattice. When this occurs during transition, it is postulated that hydrogen gas is evolved, leaving a defective AlH_3 -1451 lattice possessing a non-equilibrium concentration of anion vacancies. It is recognized that loss of hydrogen is not necessary to produce anion vacancies, but loss of hydrogen during this transition has been observed. It should also be pointed out that loss of hydrogen from the surface of the hydride will likewise contribute to the formation of a non-equilibrium concentration of anion vacancies.

(C) If this hypothesis is correct, the direct crystallization of AlH_3 -1451, without going through the AlH_3 -1433 phase, should certainly yield a more perfect crystal. This hypothesis also suggests that perhaps some of the difficulty observed with the decomposition during the preparation of aluminum hydride is a result of the following equation:



(C) In the above equations, if the hydride ions combine to form hydrogen, electrons must be given up. Electrons trapped in crystal lattices generally impart color to the crystals. Because solid AlH_3 -1451 is normally white, it would appear that the electrons are not trapped in the solid. Hence, it is presumed that the electrons reduced either Al^{+3} or some other more easily available or reducible species. Therefore, a small electrolytic cell may have been built into the system, causing decomposition.

(C) The proposed rate-determining step for the initiation of decomposition (nucleation) is the rate of diffusion of anion vacancies through the lattice by a vacancy transfer mechanism. Eventually these vacancies are presumed to arrive at a surface or grain boundary where they form active aluminum nuclei. The diffusion coefficient for this process is obtained from the following equation:

$$D = A e^{-Q/RT}$$

where D is the diffusion coefficient, A the frequency factor, Q the activation energy, T the temperature, and R the gas constant. The diffusion mechanism of anion vacancies through the lattice of

CONFIDENTIAL

CONFIDENTIAL

AlH₃-1451 would also explain the increased stability of aluminum deuteride compared to aluminum hydride, as the diffusion coefficient, D, will be much lower for the deuteride than for the hydride.

(C) Non-solvated AlH₃-1451, as originally prepared, was light brown; however, later samples were found to be snow white. Since then it has been demonstrated that UV irradiation, electron bombardment, and gamma radiation of the hydride result in a similar light brown color. Doping of the hydride with transition metal impurities such as nickel and iron also produces a light brown hydride.

(C) Therefore, the color of aluminum hydride can originate either from:

- (i) Transition metal ions incorporated into the hydride lattice, or
- (ii) Excitation of electrons in the solid, followed by trapping at anion vacancies forming color centers.

(C) Since the formation of "germ nuclei" results from the ability of anion vacancies to capture electrons generated by the excitation of a hydride ion, surface treatments will:

- (i) Reduce the mobility of anion vacancies and electrons at surfaces, thus slowing down the rate of initiation of decomposition, and
- (ii) Reduce the mobility of "germ nuclei" which must coalesce to form aluminum nuclei of a critical diameter before they become active growth nuclei.

(C) It has always been assumed that the decomposition of the hydride originated predominantly at the external and internal surfaces of the hydride. The original metallographic observation of aluminum formation throughout the interior of the particle, as shown in Figure 34, was therefore unexpected. The Prout-Tompkins (2) chain-branching mechanism does, however, readily account for this observation. The decomposition employing this model is still thought to originate at the external and internal surfaces but propagates by crack formation, etc., resulting in the formation of new surfaces for nuclei formation.

(C) The formation of additional nuclei by the chain-branching mechanism is apparently a much more important process than the formation of fresh nuclei for certain hydride lots. The reason for this difference is not exactly known, but is believed to be related possibly to the degree of perfection of the hydride particles.

CONFIDENTIAL

CONFIDENTIAL

(C) Different techniques used in the preparation of aluminum hydride are believed to be capable of affecting the degree of crystal perfection. The Prout-Tompkins (2) equation is derived theoretically on the basis of a branching mechanism for the reaction which arises because of mechanical strains set up by the layer of product on the surface. The branching mechanism is considered to be due to crack formation in the crystals, which leads ultimately to mechanical disruption. Our recent studies appear to support this hypothesis as an explanation of the branching mechanism. The rapid propagation of the branching chain through the crystal, as shown in Figure 34, tends to separate the aluminum hydride particle into a number of mosaic blocks.

(C) The range of decomposition over which the equation fits varies, depending upon the shape of the pressure-time curve. Examples of the extreme degrees of symmetry observed for the P-T decomposition curves for aluminum hydride are shown in Figures 40 and 41. It has been found that the Prout-Tompkins (2) equation frequently holds for the P-T curves of Type I over the range of 5-90% decomposition. However, the fit is not nearly as good for hydrides exhibiting a Type II P-T curve.

b. Growth Processes (U)

(C) Metallographic studies of the formation and growth of aluminum nuclei of various lots of hydride have shown that apparently two different growth models for decomposition sites in aluminum hydride can exist following nucleation. Once nucleation commences, either rapid, two-dimensional growth at the surface occurs, as shown in Figure 36, so that the surface or edges of the particle are rapidly covered with a layer of aluminum, or the reaction may spread out three-dimensionally from a single nucleus, as shown in Figure 35.

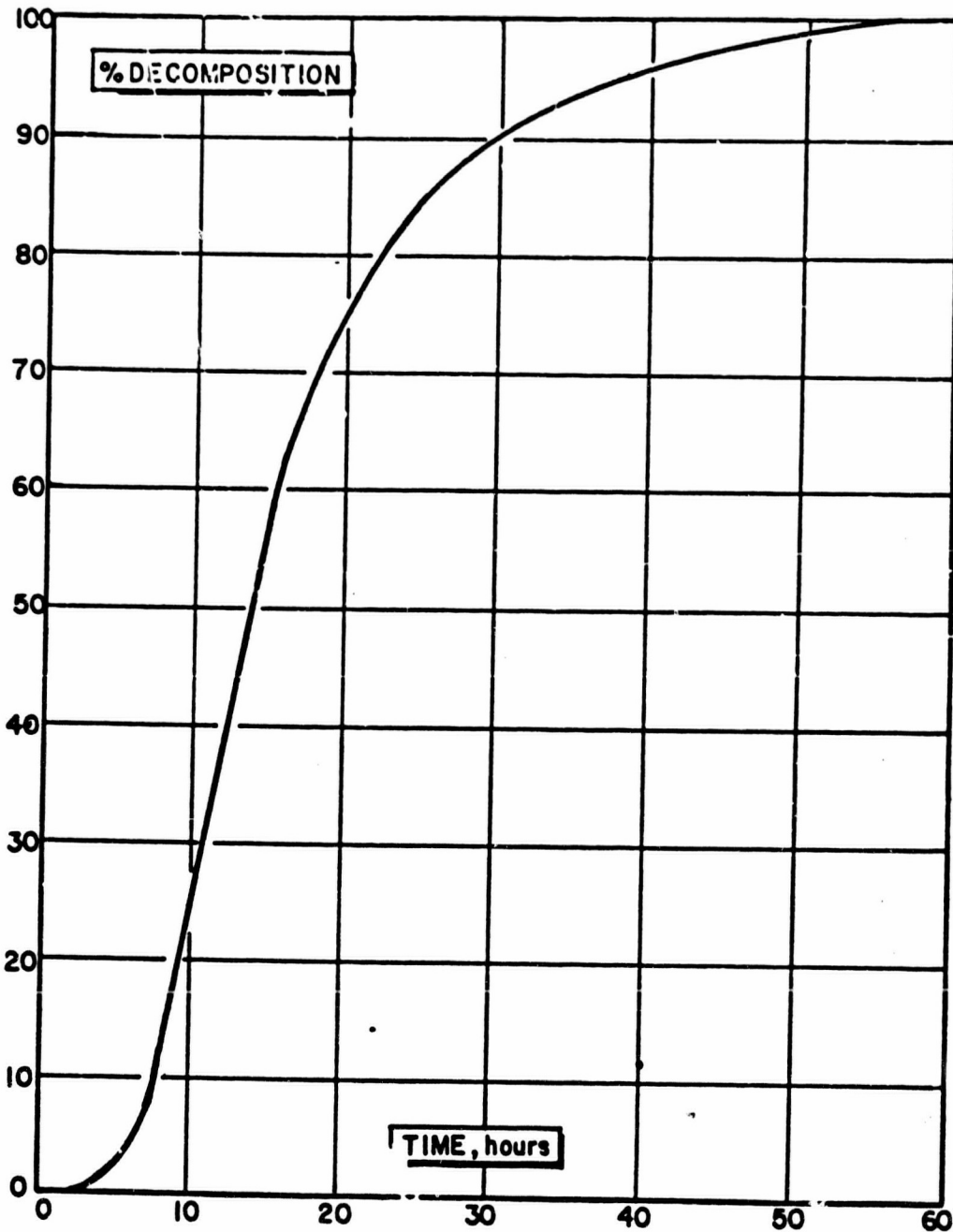
(C) The mathematical equations theoretically derived for these and other solid state decomposition models have been summarized by Garner (7). However, the observation that different nucleation (normal vs. chain-branching) and growth processes (two dimensional vs. three-dimensional) are involved in the thermal decomposition of aluminum hydride has added to the complexity of this process. It is now obvious that the surface area of the interface at which decomposition is occurring not only changes as decomposition proceeds, but the original interface surface area also differs, depending upon the type of growth.

c. Interface Decomposition Reaction (U)

(C) To have a comprehensive understanding of the complete decomposition of aluminum hydride, it is also necessary to understand the reaction occurring at the interface between the AlH_3 -1451 lattice and the aluminum nuclei as the decomposition proceeds at the interface.

CONFIDENTIAL

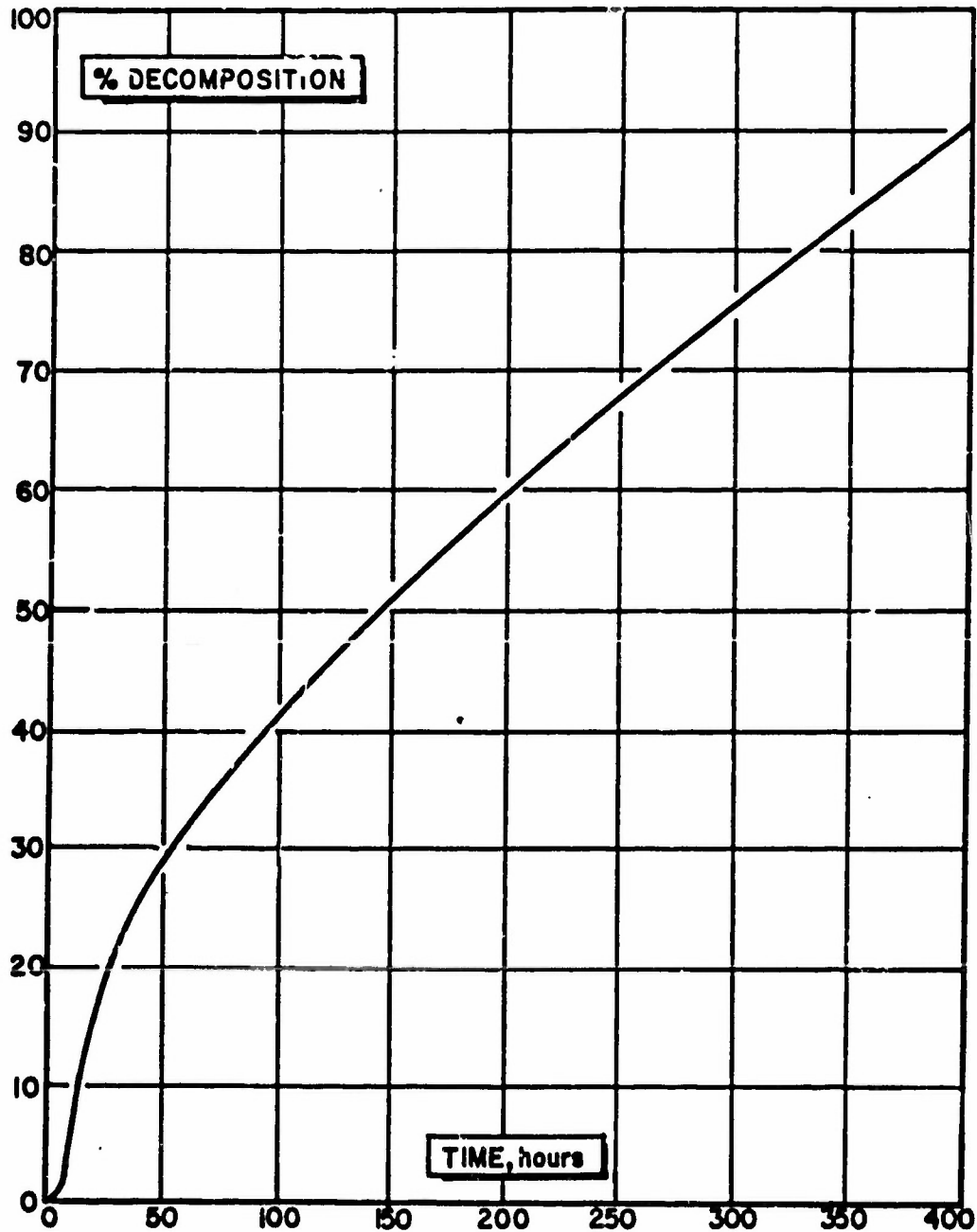
CONFIDENTIAL



(C) Fig. 40 - Type I Symmetrical Pressure-Time Decomposition Curve Exhibited by Aluminum Hydride

CONFIDENTIAL

CONFIDENTIAL



(C) Fig. 4. - Type II Asymmetrical Pressure-Time Decomposition Curve Exhibited by Aluminum Hydride

CONFIDENTIAL

CONFIDENTIAL

(C) In writing the overall reaction for the decomposition of aluminum hydride to aluminum and hydrogen, it is assumed that several transient species such as $H\cdot$, AlH_2 , and AlH actually exist for finite periods of time. In addition, it is expected that free aluminum atoms momentarily exist in other spatial arrangements before the formation of the aluminum metal structure. Information generated from mass spectrographic (8), electron spin resonance, and flash heating studies of the decomposition of aluminum hydride² has indicated the existence of several intermediate species depending upon experimental conditions. Further work, however, will be required to identify the exact chemical nature of all the species formed during decomposition.

2. Magnesium Stabilization of Aluminum Hydride-1451 (C)

a. Presence of Magnesium in the Aluminum Hydride-1451 Lattice (C)

(C) It has been noted that magnesium-doped aluminum hydride samples appear to be much more light-sensitive than normal hydride, and will turn light brown very quickly upon exposure to UV irradiation. This sensitivity of magnesium-doped hydride to discolor suggests that magnesium stabilizes aluminum hydride by controlling the rate at which anionic vacancies and/or electronic imperfections diffuse through the solid to crystal imperfections, probably grain boundaries, and to the surface where they form aluminum nuclei.

(C) The known stabilization of aluminum hydride by incorporation of magnesium into the crystal lattice can now be explained in terms of the ability of magnesium to create an energy barrier for the diffusion of anion vacancies through the lattice to the surface or grain boundaries where clustering and electron capture produce active aluminum nuclei, and, hence, the initiation of decomposition. The exact location of magnesium in the lattice of aluminum hydride and the mechanism by which it creates this energy barrier are not clearly known. Magnesium is, however, known to be randomly incorporated into the crystal structure because the lattice of magnesium-doped material is expanded. A knowledge of the exact location of the magnesium in the hydride lattice and its immediate environment should give further insight into the stabilization of the hydride.

(C) Recent studies have produced additional information towards resolving and elucidating these questions. The actual chemical species incorporated into the AlH_3 -1451 lattice during magnesium doping is thought to be magnesium aluminum hydride. This is based on the following information:

- (1) There is good evidence that the doping agent is soluble magnesium aluminum hydride.

²These will be discussed later in this report.

CONFIDENTIAL

- (11) Magnesium-doped AlH_3 -1451 samples display a small absorption shoulder at 2000 cm^{-1} in the infrared; this is in the same absorption frequency region of an aluminum-hydrogen stretching mode in magnesium aluminum hydride.

(111) Changes occur with age.

(C) A careful analysis of the infrared spectrum obtained from magnesium-doped hydride, as shown in Figure 42 and Table XI, indicates two additional small absorptions normally not observed in AlH_3 -1451; in addition, there is a shifting to a lower frequency of the aluminum-hydrogen stretching vibrations which would be predicted as a result of magnesium expanding the hydride lattice. One of the new absorptions is a small shoulder at approximately 2000 cm^{-1} , which is the same absorption frequency region as that of an aluminum-hydrogen stretching mode in magnesium aluminum hydride. The absorption peak at 1108 cm^{-1} bears no correlation with either infrared spectrum of the hydrides alone.

(C) It is therefore suggested, although the evidence is certainly not conclusive, that the species incorporated into the hydride lattice may be present essentially as magnesium aluminum hydride, the doping agent used for its incorporation.

Table XI

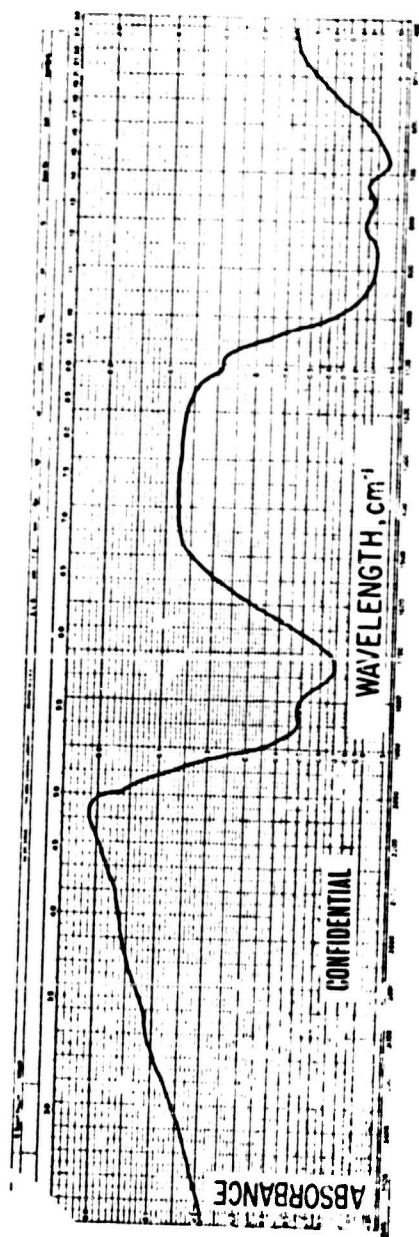
(C) Comparison of Infrared Frequencies of
Magnesium-Doped and Standard Aluminum Hydride-1451

<u>Frequencies, cm^{-1}</u>	
<u>Aluminum</u>	<u>Magnesium-Doped Aluminum Hydride-1451</u>
	2000 (New)
	1840
	1730
	1108 (New)
	875
	755
	675
	590

b. Aging of Magnesium-Doped Aluminum Hydride-1451 (C)

(C) It was discovered from surveillance of magnesium-doped AlH_3 -1451 samples stored at -15°C . under an inert atmosphere that a large improvement in stability occurred unexpectedly after approximately five months' storage. One sample, data shown in Figure 43,

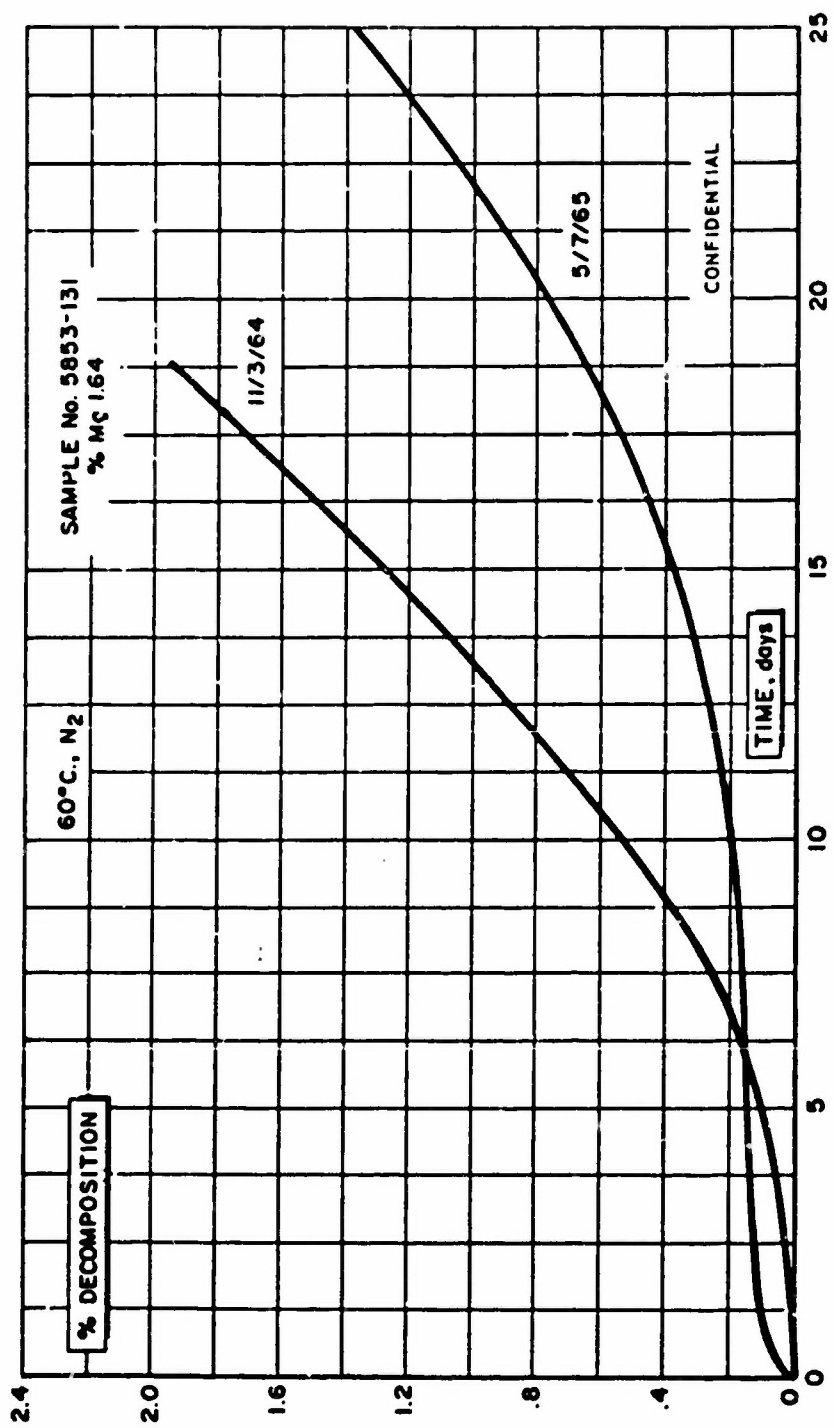
CONFIDENTIAL



(C) FIG. 42 - Infrared Absorption Spectrum of Magnesium-Doped Aluminum Hydride-1451

CONFIDENTIAL

CONFIDENTIAL



(C) Fig. 43 - Effect of Age on the Thermal Stability of a Magnesium-Doped Aluminum Hydride-1451

CONFIDENTIAL

CONFIDENTIAL

increased in stability, as measured by Taliani test, from 13 to 43 days before reaching 1% decomposition at 60°C. Another sample increased from 13 to 75 days before reaching 1% decomposition (Figure 44). These samples currently represent some of the most stable samples of aluminum hydride prepared and evaluated in this laboratory.

(C) The initial rapid gassing exhibited during the first day by aged magnesium-doped AlH_3 -1451 samples, illustrated in Figures 43 and 44, is odd and was originally thought perhaps to be a result of unintentional exposure to moisture, as that type of decomposition curve is typical of an undried sample. More recently, it was discovered that the total amount of gassing during the first day is roughly correlated with the degree of improvement during aging as shown in Table XII. No correlation with the concentration of magnesium in the samples was observed. These initial gassing data imply that at least a portion of the magnesium may be originally incorporated into the hydride lattice as magnesium aluminum hydride, and that this configuration appears to be unstable in the presence of the AlH_3 -1451 lattice, which upon aging undergoes transformation to a more stable configuration, liberating hydrogen in the process. The extent of this transformation could then be approximated by the quantity of gas evolved during aging. Hence, the observed correlation between initial gassing and improved stability can be rationalized by the slow diffusion of hydrogen generated during this transformation from the interior of the crystals. Since this correlation is not normally observed for hydride stored under identical conditions, it is concluded that the enhanced stability is probably a result of an annealing process. However, the effect of surface moisture treatment may still be a consideration.

Table XII

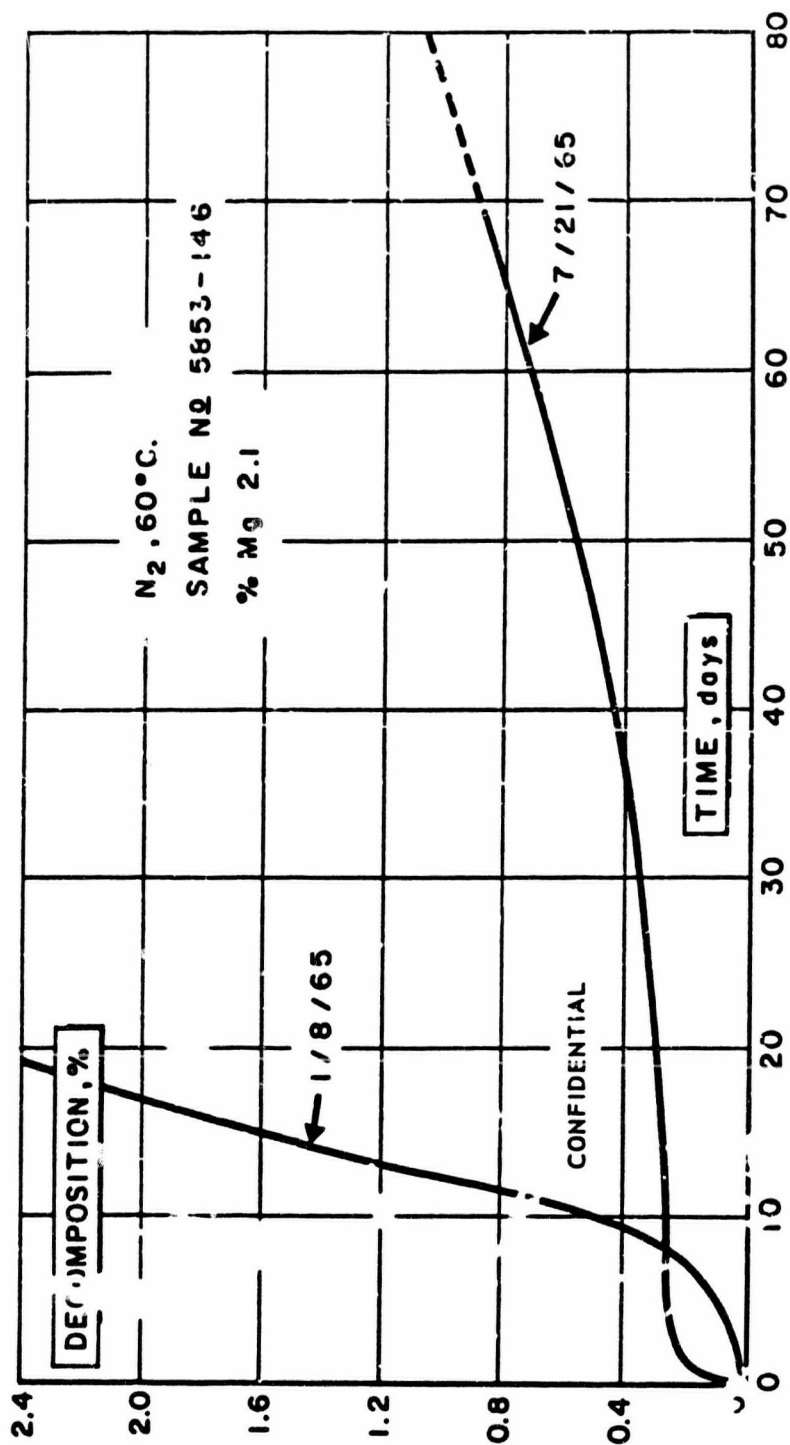
(C) Thermal Stability of Magnesium-Doped,
Aged Samples of Aluminum Hydride-1451

Sample Number	% Mg in Sample	Decomposition During First Day, mole %	Days to Reach % Decomposition		Days Improvement	Age in Months
			Original	Rerun		
5853-145	2.09	0.02	14.3	13.7	None	~5
5853-131	1.64	0.07	13.5	22.5	9	~6
5853-143	1.96	0.10	16.8	29	12	~7
5853-142	1.72	0.13	12.9	42	29	~4
5853-146	2.07	0.17	12.8	75	62	~7

↑
increase

↑
increase

CONFIDENTIAL

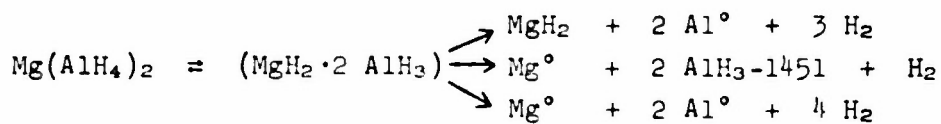


(C) Fig. 44 - Decomposition Rate of Aged Magnesium-Doped Aluminum Hydride-1451 at 60°C.

CONFIDENTIAL

CONFIDENTIAL

(C) Several chemical equations could be written to explain the transformation and generation of hydrogen.



(C) However, it is presently not known which reaction or combination of proposed reactions is taking place. Hence, further speculation at this time does not appear justified because of a lack of supporting data.

(C) Realizing that a transformation of this type can occur with time, it is now suggested that the aging phenomenon of normal $\text{AlH}_3\text{-1451}$ can also be explained by a similar mechanism. Since it is known that all aluminum hydride samples contain lithium which cannot be washed out with ether, it appears likely that an amount of LiAlH_4 and/or LiBH_4 is also incorporated into the hydride lattice in an unstable configuration during crystallization; under suitable aging conditions these species may also undergo transformations and/or readjustment of the atoms in the lattice to a more stable configuration.

c. Kinetic Studies of the Decomposition of Aluminum Hydride-1451 (C)

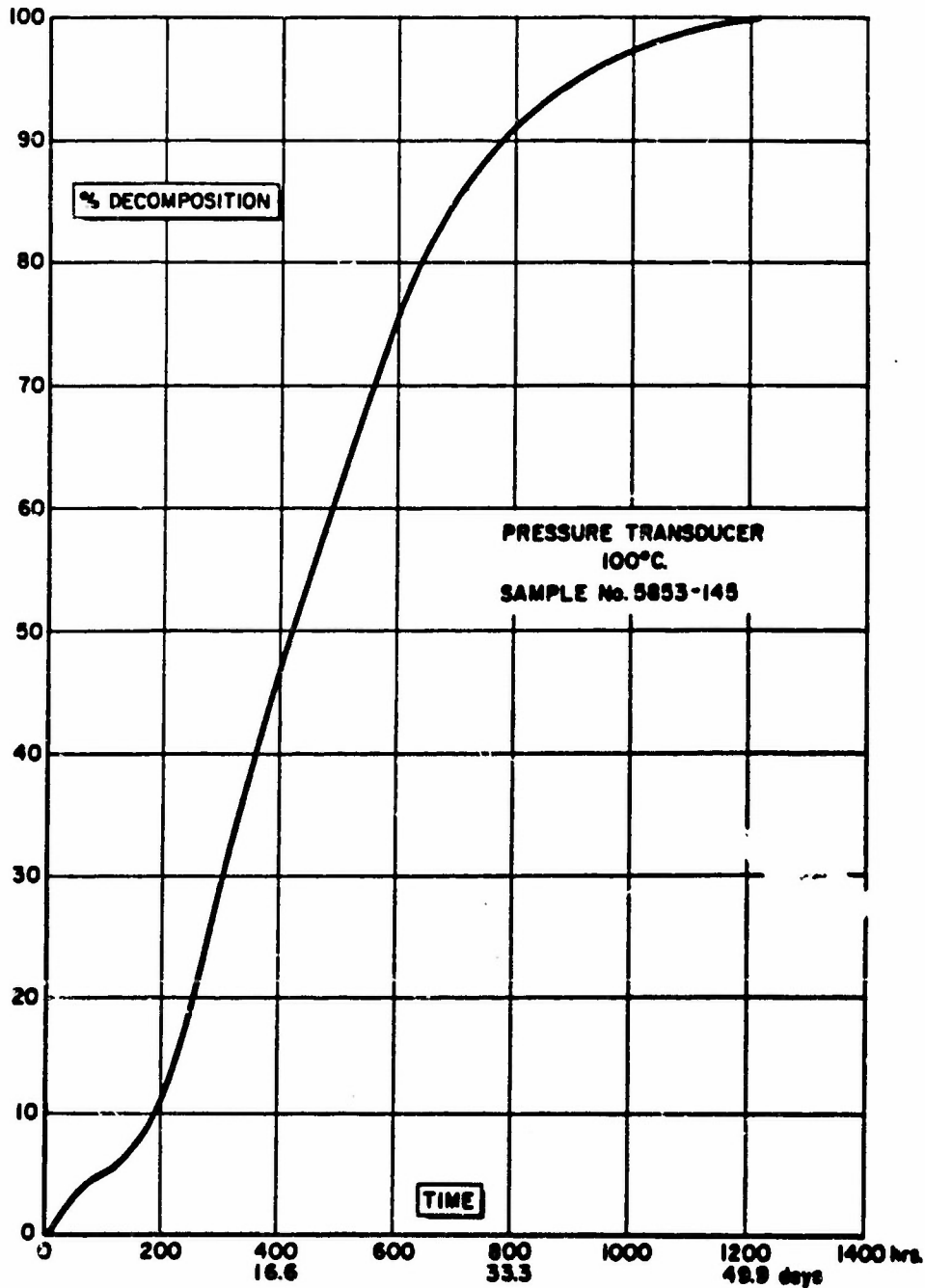
(C) The activation energy for the acceleration period during the decomposition of normal $\text{AlH}_3\text{-1451}$ is 23.0 ± 1.5 kcal./mole as determined by the Prout-Tompkins equation given below:

$$\ln P/P_\infty - P = kt + C$$

(C) It was previously reported (1) that two samples containing 0.9% magnesium yielded an average activation energy of 24.9 kcal./mole, using a mercury manometer to follow the changes in pressure. Recent measurements on magnesium-doped samples containing approximately 2.0% magnesium have yielded much higher activation energies. A typical magnesium-doped sample was decomposed at 100°, 130°, and 150°C. on a pressure transducer apparatus. The results are shown in Figures 45 and 46. Table XIII summarizes the data acquired in obtaining the Arrhenius plot shown in Figure 47. From the slope of the line which is equal to $-E/2.303 R$, the activation energy E was calculated to be 35.8 kcal./mole.

(C) The reason for the difference in previously reported values for magnesium-doped hydride is not presently known, but could be a result of the higher concentrations of magnesium, effect of mercury, or changes during aging. These possibilities are currently under examination.

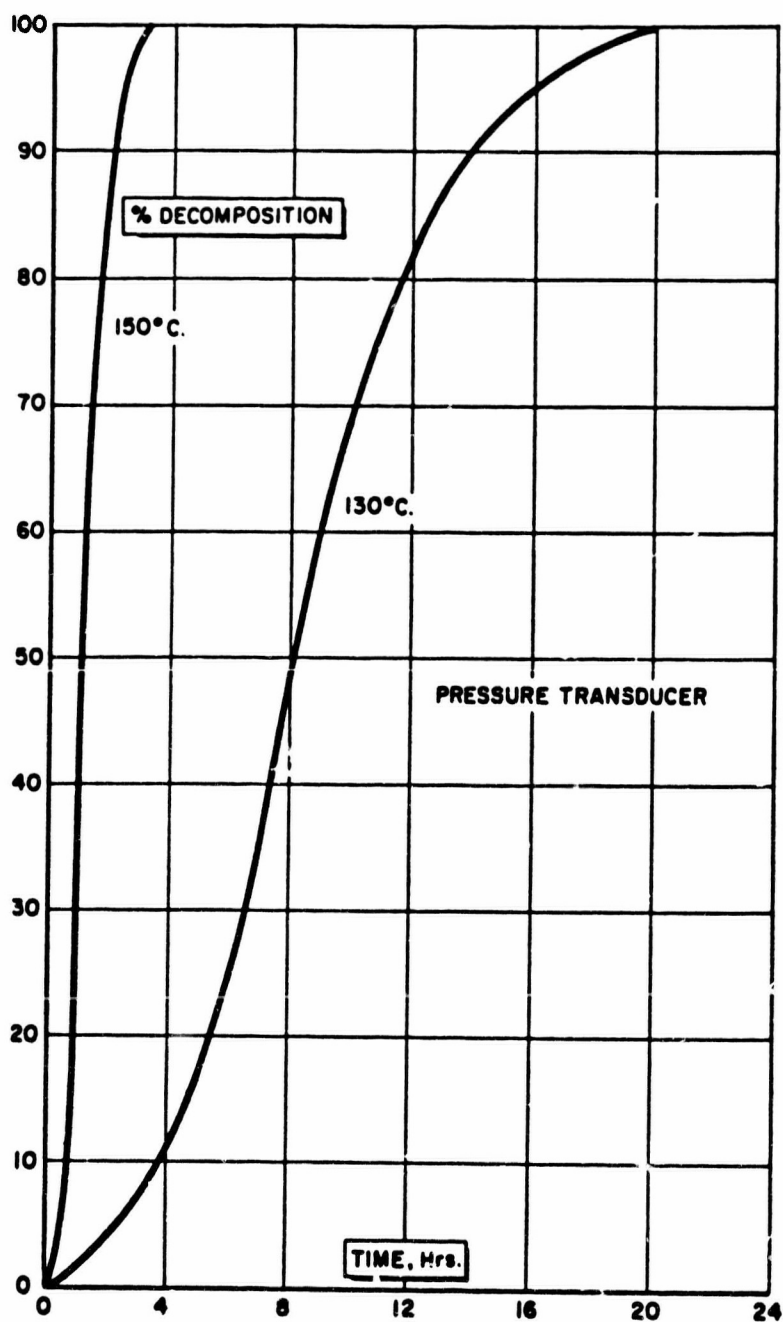
CONFIDENTIAL



(C) Fig. 45 - Decomposition Curve of Aluminum Hydride-1451 at 100°C.

CONFIDENTIAL

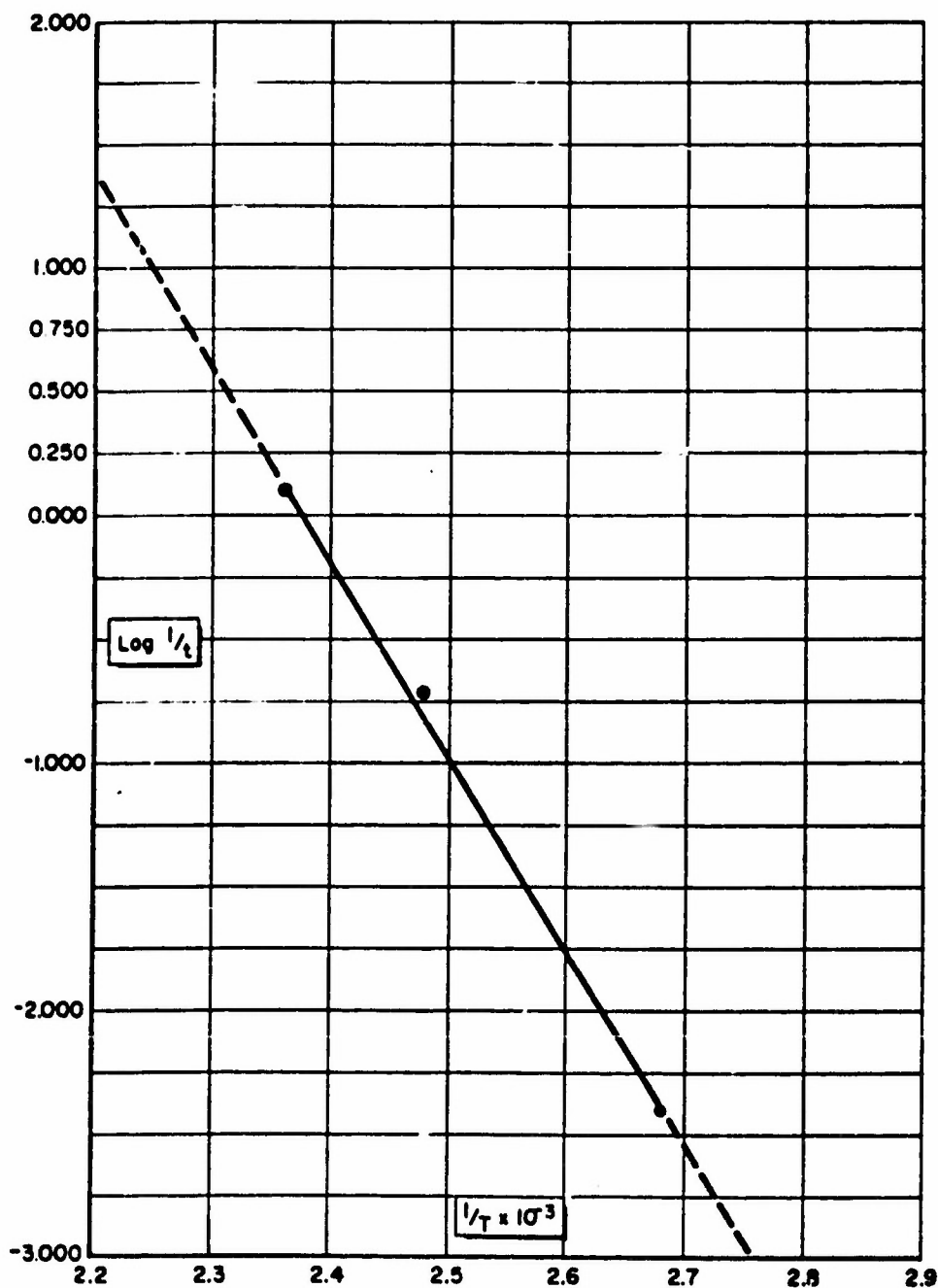
CONFIDENTIAL



(C) Fig. 46 - Decomposition Curve of Aluminum Hydride-1451 at 130°C. and 150°C.

CONFIDENTIAL

CONFIDENTIAL



(C) Fig. 47 - Arrhenius Plot Obtained for the Acceleration Reaction of Aluminum Hydride-1451

CONFIDENTIAL

CONFIDENTIAL

Table XIII

(C) Summary of Decomposition Data of Aluminum Hydride-1451
at Various Temperatures Using Prout-Tompkins Equation

<u>Time^a</u> <u>hours</u>	<u>1/t</u>	<u>Log</u> <u>1/t</u>	<u>Temp.</u> <u>°K.</u>	<u>1/T x 10⁻³</u>
255	0.00392	2.407	373	2.68
5.1	0.1960	0.707	403	2.48
0.8	1.250	0.097	423	2.36

^aTo reach 20% decomposition.

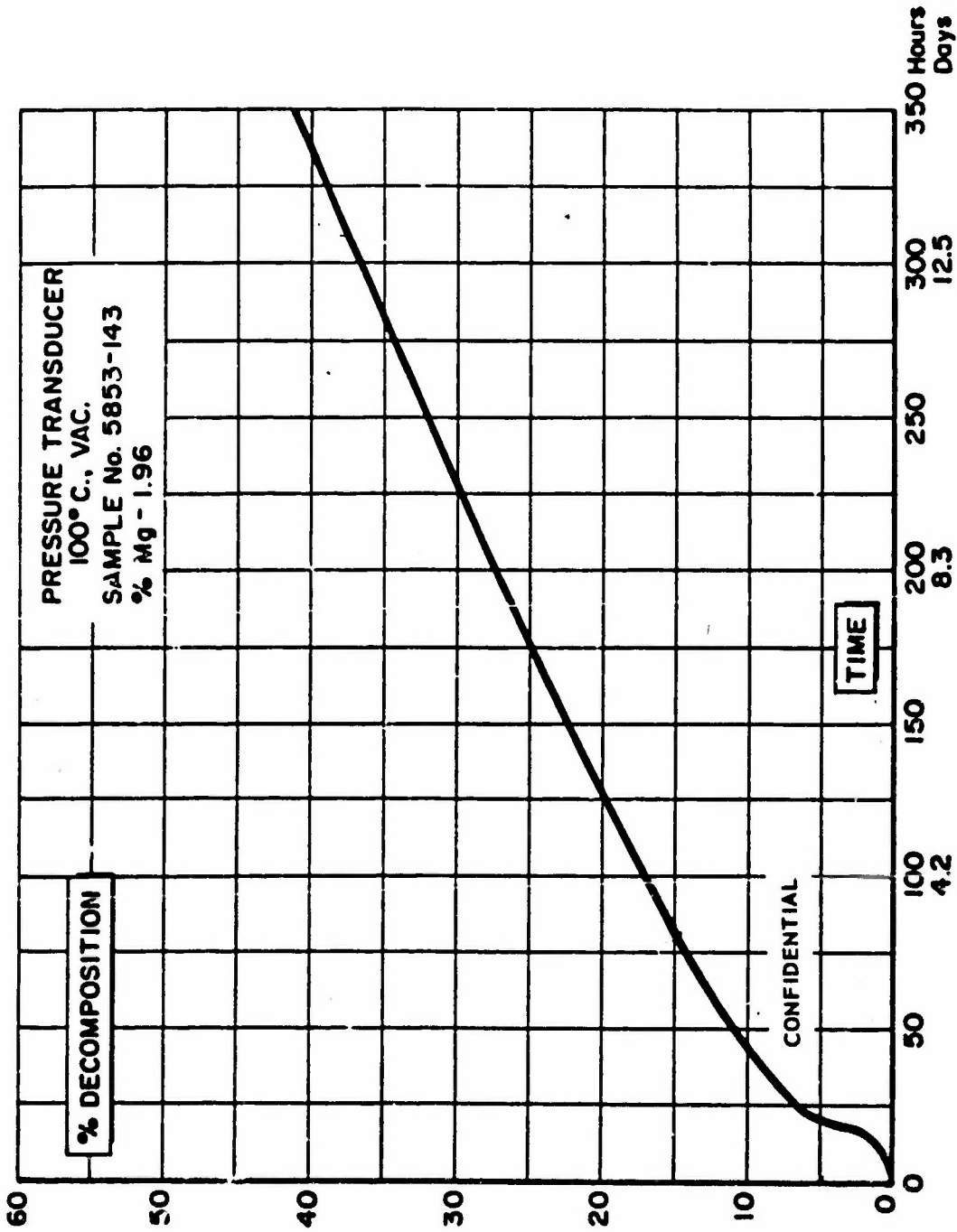
d. Decomposition Rates of Magnesium-Doped Aluminum Hydride-1451 (C)

(C) The decomposition rates observed for two different magnesium-doped samples at 100°C. are shown in Figures 48 and 49. These decomposition rates were measured by a pressure transducer to eliminate any possibility of mercury stabilization that might occur from use of a mercury manometer. These samples represent some of the most thermally stable hydride evaluated at 100°C., with the data shown in Figure 48 demonstrating the smallest sigmoid-shaped decomposition curve observed to date. The accelerated portion of the decomposition curve changed rate at about 6.5% decomposition, after which subsequent decomposition occurred at a greatly reduced rate. A new type of decomposition curve for a magnesium-doped sample not previously observed for aluminum samples at 100°C. is shown in Figure 49. The characteristic sigmoid decomposition curve normally observed from the beginning was absent, although the sample subsequently demonstrated an increased rate of decomposition similar to that illustrated in Figure 45. These decomposition curves indicate that all magnesium-doped hydride samples, in general, exhibit this new type of decomposition curve at 100°C.

3. Long-Term Surveillance Studies of Aluminum Hydride-1451 (C)

(C) A number of macrocrystalline aluminum hydride samples have been under surveillance for long-term storage studies. These studies were necessary to check the accuracy of the predicted shelf life extrapolated from accelerated test data. The samples are stored in taped glass vials under an inert atmosphere at ambient and -15°C. temperatures. In addition, six other lots of hydride are being evaluated at 40°C. The samples are routinely checked for percent decomposition by carbon and hydrogen analysis, and the results are recorded in Tables XIV and XV. Eleven different lots of Dow Pilot Plant material have been stored for a period of from 1.3 to 1.8 years. During this time, less than 1% decomposition has been detected at ambient and essentially no decomposition at -15°C., as determined by hydrogen content. The percentages of decomposition shown in Table XIV are still within the experimental error of analysis. Hence, at this time, these numbers are not absolute

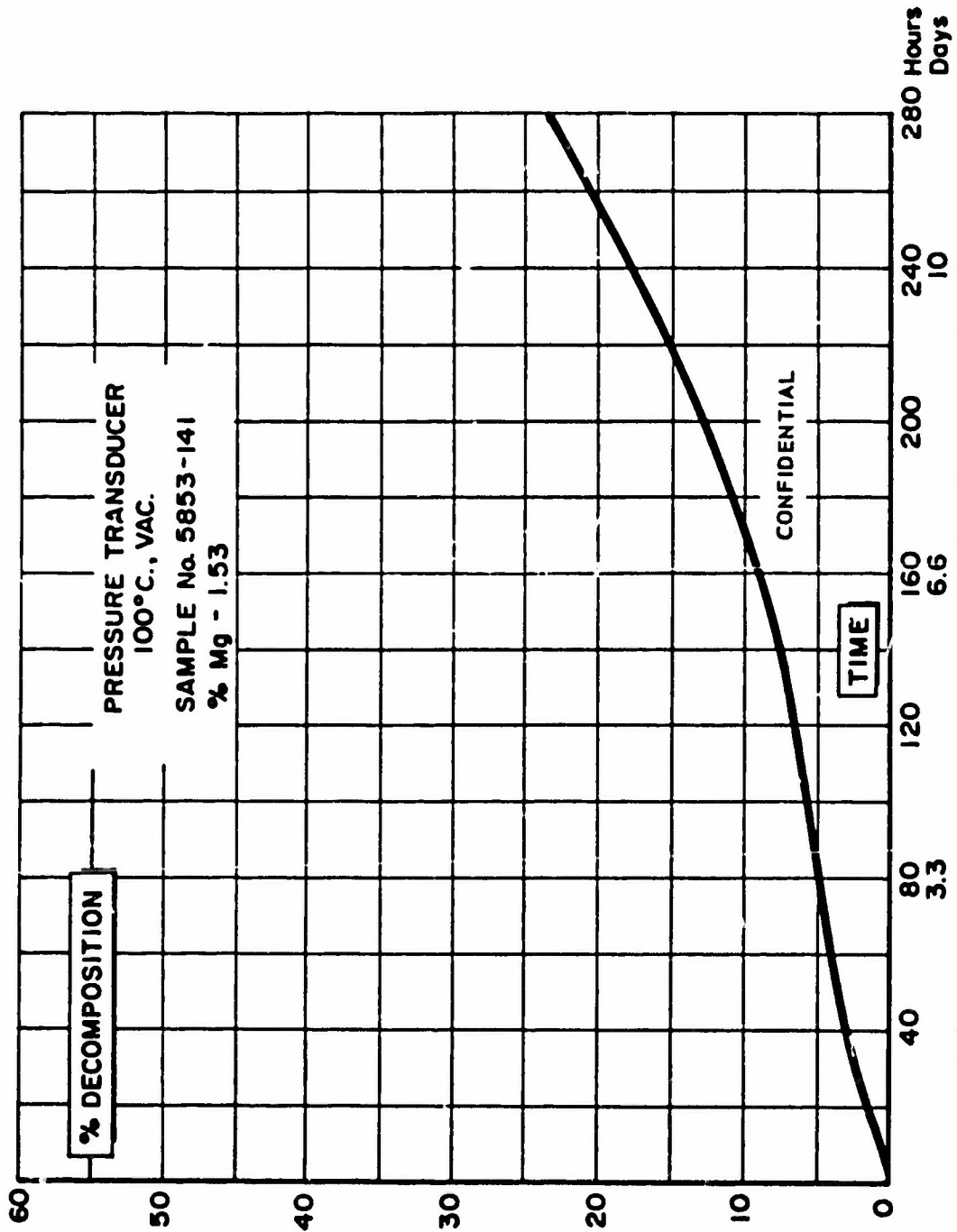
CONFIDENTIAL



(C) Fig. 48 - Thermal Stability of a Magnesium-Doped Aluminum Hydride-1451, Sample 5853-143, at 100°C.

CONFIDENTIAL

CONFIDENTIAL



(c) Fig. 49 - Thermal Stability of a Magnesium-Doped Aluminum Hydride-1451, Sample 5853-141, at 100°C.

CONFIDENTIAL

CONFIDENTIAL

values but represent only an indication of a small amount of decomposition. Visual examination of the samples shows that those stored at ambient temperature have turned light gray, indicating a small amount of decomposition, whereas those stored at -15°C . are still white.

Table XIV

(C) Long-Term Storage Stability of Aluminum Hydride-1451

<u>Sample Number</u>	<u>Age, years</u>	<u>% Decomposition^a</u>	
		<u>Ambient Storage</u>	<u>-15°C. Storage</u>
3655-85	2.6	2.8	2.0
02034A	1.8	0.8	None
02044	1.8	0.4	None
02044	1.8	None	None
02134A	1.8	None	None
03294	1.7	0.9	None
04194	1.6	1.1	None
06014A	1.4	0.7	None
0602A	1.4	1.0	None
06054	1.4	None	None
06104A	1.4	None	None
06104AT(VCN)	1.4	None	None
07084	1.3	1.0	None
07084T(VCN)	1.3	None	None

^aDetermined by carbon and hydrogen analysis; hydrogen $\pm 1\%$ of total.

Table XV

(C) Long-Term Storage Stability of Aluminum Hydride-1451 at 40°C .

<u>Sample Number^a</u>	<u>% Decomposition^b</u>	
	<u>After 80 days</u>	<u>After 97 days</u>
04185A	1.3	1.3
04195	1.8	2.4
04265B	1.1	2.2
06225	0.2	1.7
06275	1.2	2.5
06285	<u>1.0</u>	<u>2.2</u>
Average % Decomp.	1.1	2.1

^aSamples stored 3 months in cold storage prior to evaluation.

^bDetermined by carbon and hydrogen analysis; hydrogen $\pm 1\%$ of total.

CONFIDENTIAL

(C) The oldest sample of macrocrystalline hydride under surveillance has now been stored for a period of 2.0 years. It has exhibited approximately 2.8% decomposition at ambient temperature and 2.0% decomposition at -15°C . However, it is thought that the decomposition for this sample is highly approximately 1% or more, since it is based on an original hydrogen value of 10.12%.

(C) Extrapolated decomposition rates from accelerated decomposition studies had indicated that the hydride should have reached 1% decomposition in about 0.15 years, or 5% in 1.2 years. A comparison of the extrapolated stability data with that obtained under actual storage conditions shows the measured surveillance stability to be currently 5 to 7 times better than originally predicted.

(C) The data presently obtained from six different lots stored at an elevated temperature of 40°C . are summarized in Table XV. It was noted that within a few days the lots had started to change to light gray. After 80 days' storage, the six lots exhibited an average of 1.1% decomposition, and after 97 days' storage an average of 2.05% decomposition. This compares with a predicted decomposition rate of 1% in 30 days or 5% in approximately 100 days.

(C) The need for accuracy on the long-term storage stability data of neat aluminum hydride samples cannot be overemphasized. For that reason, the oxygen content of two different lots of hydride (06014A and 06054) was determined by neutron activation analysis to determine if the samples had absorbed or reacted to any significant degree with moisture and/or oxygen which may be present in the inert atmosphere.

(C) Analysis of both the samples at ambient temperature and -15°C . indicated no significant change from the concentration originally present. Both samples showed 0.3% to 0.4% oxygen with no significant difference between the oxygen concentration found as a result of storage at the two temperatures.

(C) In addition to periodically determining the percent decomposition by carbon and hydrogen analysis, the samples were also examined at 60°C . to determine the change in thermal stability of the material with time.

(C) Tables XVI, XVII, and XVIII summarize the information obtained from the Taliani test at 60°C . on the various lots stored at ambient temperature, -15°C ., and 40°C . over the designated period of time. Figures 50, 51, 52, and 53 represent plotted examples of lots 02044A, 03294, 02134A, and 04194 summarized in Tables XVI and XVII. Plotting the days to reach 1% decomposition at 60°C . versus storage time again dramatically illustrates the aging phenomenon previously reported (1). The samples do not always decrease in stability as is expected or originally observed for the old fine powder products (9), but will sometimes increase in stability with time.

CONFIDENTIAL

(C) The data illustrated in Figures 50, 51, and 53 do suggest this temperature dependency, as the samples stored at ambient temperature have reached a maximum stability prior to that obtained for the same sample stored at -15°C . Figure 52 indicates that the thermal stability at -15°C . is changing at a slower rate than for the corresponding ambient temperature sample as the two lines are diverging with time.

(C) Without further knowledge it would be predicted that the maximum stabilities observed for the samples at ambient temperature might be the maximum stability exhibited by the sample at any temperature. However, this apparently is not true, as some lots stored at -15°C . have shown stabilities greater than originally observed and greater than that exhibited at any time by the samples stored at ambient temperature. The examples shown in Figures 50 and 52 suggest that the annealing process is in competition with the process governing the initiation of decomposition, and if the temperature is too high the detrimental decomposition process will overcome the beneficial effect of the annealing process.

Table XVI

(C) Effect of Storing Aluminum Hydride at Ambient Temperature on Thermal Stability

Sample No.	Days to Reach 1% Decomposition at 60°C . ^a					
	Original	Storage Time, months				
		3	8	11	16	20
3655-95-2	4.2	5.8	3.7	4.5	9.6	8.7
02034A	5.3	3.3	7.2	8.0	9.2	8.6
02044	3.9	3.9	6.6	6.3	6.8	8.3
02044A	4.5	2.8	11.7	12.5	13.0	9.6
02134A	5.3	8.7	11.2	8.5	9.0	7.0
04194	5.5	7.2	6.3	6.0	--	--
03294	8.0	6.9	5.4	4.6	--	--
06014A	6.2	5.0	4.2	4.2	--	--
06024A	6.3	4.7	4.0	4.2	--	--
06054	8.0	5.9	4.5	4.1	--	--
06104A	10.0	8.3	7.4	7.3	--	--
06104AT	10.2	8.5	7.1	6.2	--	--
07084	7.2	6.2	6.3	5.8	--	--
07084T	6.3	5.4	4.1	3.6	--	--

^aTallian test $\pm 0.2\%$ decomposition.

CONFIDENTIAL

Table XVII

(C) Effect of Storing Aluminum Hydride
at -15°C. on Thermal Stability

<u>Sample No.</u>	<u>Original</u>	<u>Days to Reach 1% Decomposition at 60°C.^a</u>				
		<u>Storage Time, months</u>				
		<u>3</u>	<u>8</u>	<u>11</u>	<u>16</u>	<u>20</u>
3655-95-2	4.2	--	--	--	--	--
02034A	5.3	4.7	4.4	4.8	5.3	5.4
02044	3.9	3.7	6.7	7.0	8.9	5.6
02044A	4.5	4.4	5.1	6.8	8.3	9.2
02134A	5.3	4.6	10.5	11.6	13.9	12.6
04194	5.5	7.6	9.0	8.9	--	--
03294	8.0	7.7	7.9	7.6	--	--
06014A	6.2	5.0	5.7	7.1	--	--
06024A	6.3	5.7	5.8	6.8	--	--
06054	8.0	6.2	6.8	7.1	--	--
06104A	10.0	8.7	10.2	9.4	--	--
06104AT	10.2	8.8	8.7	9.6	--	--
07084	7.2	6.7	7.0	7.4	--	--
07084T	6.3	7.1	6.6	7.0	--	--

^aTaliani test \pm 0.2% decomposition.

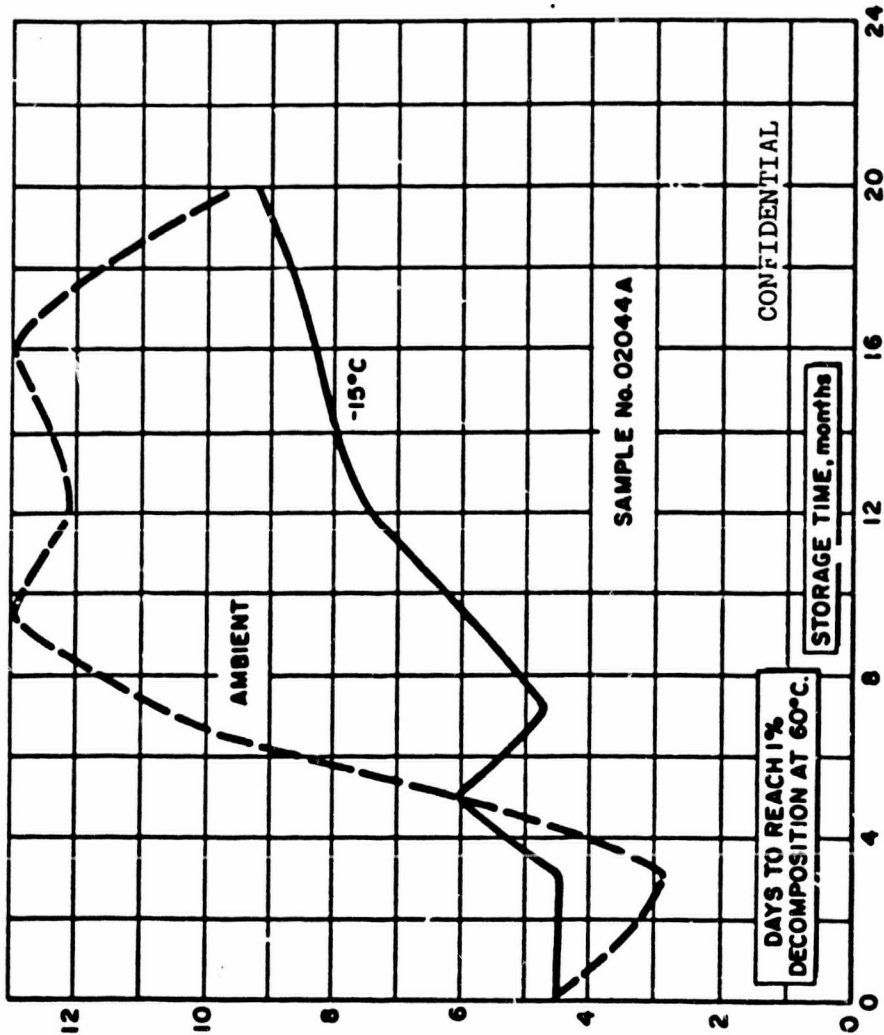
Table XVIII

(C) Effect of Storing Aluminum Hydride
at 40°C. on Thermal Stability

<u>Sample Number</u>	<u>Original</u>	<u>Days to Reach 1% Decomposition at 60°C.^a</u>			
		<u>Storage Time, days</u>			
		<u>16</u>	<u>42</u>	<u>63</u>	<u>96</u>
04195A	6.6	4.9	2.6	3.5	1.25
04195A	6.6	4.8	4.5	3.4	1.1
04265B	7.5	5.8	4.7	3.1	1.1
06225	8.7	8.0	6.2	3.6	2.4
06275	6.2	5.6	4.6	3.9	0.9
06285	6.6	5.9	3.8	2.5	1.4

^aTaliani test \pm 0.2% decomposition.

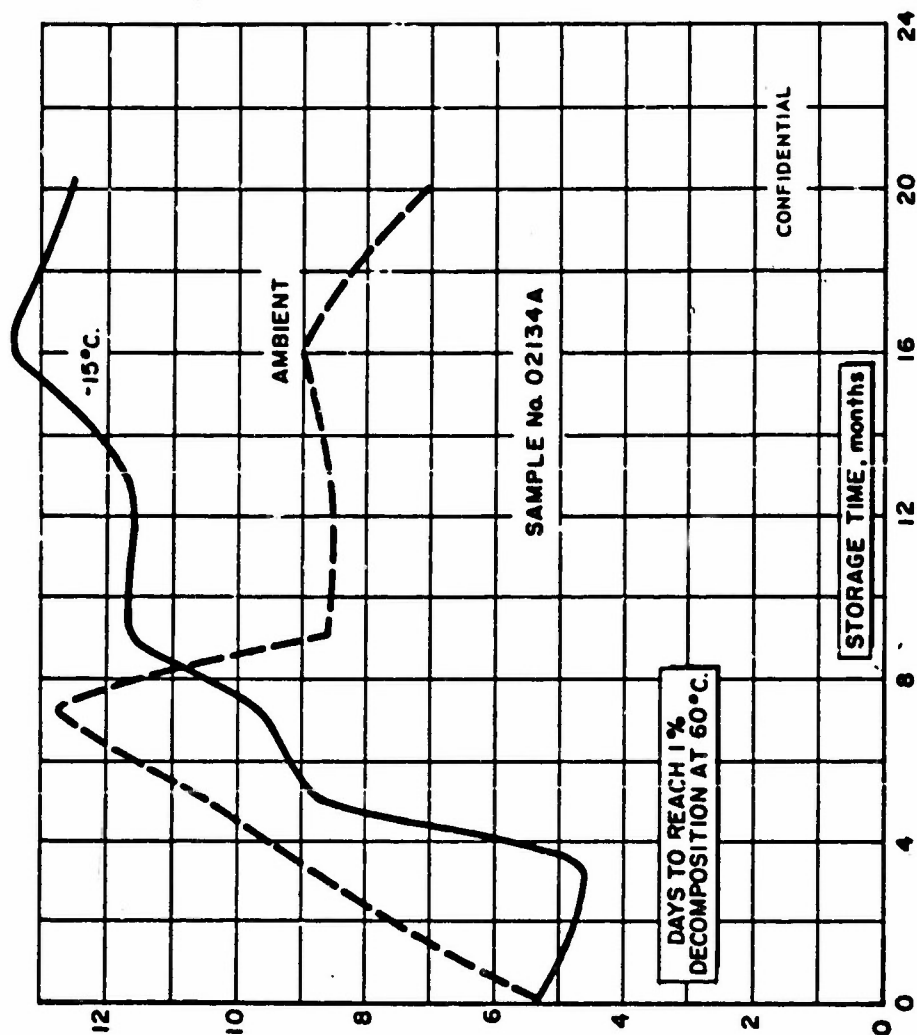
CONFIDENTIAL



(C) Fig. 50 - Effect of Age on the Thermal Stability of Aluminum Hydride-1451, Sample 02044-A, at 60°C.

CONFIDENTIAL

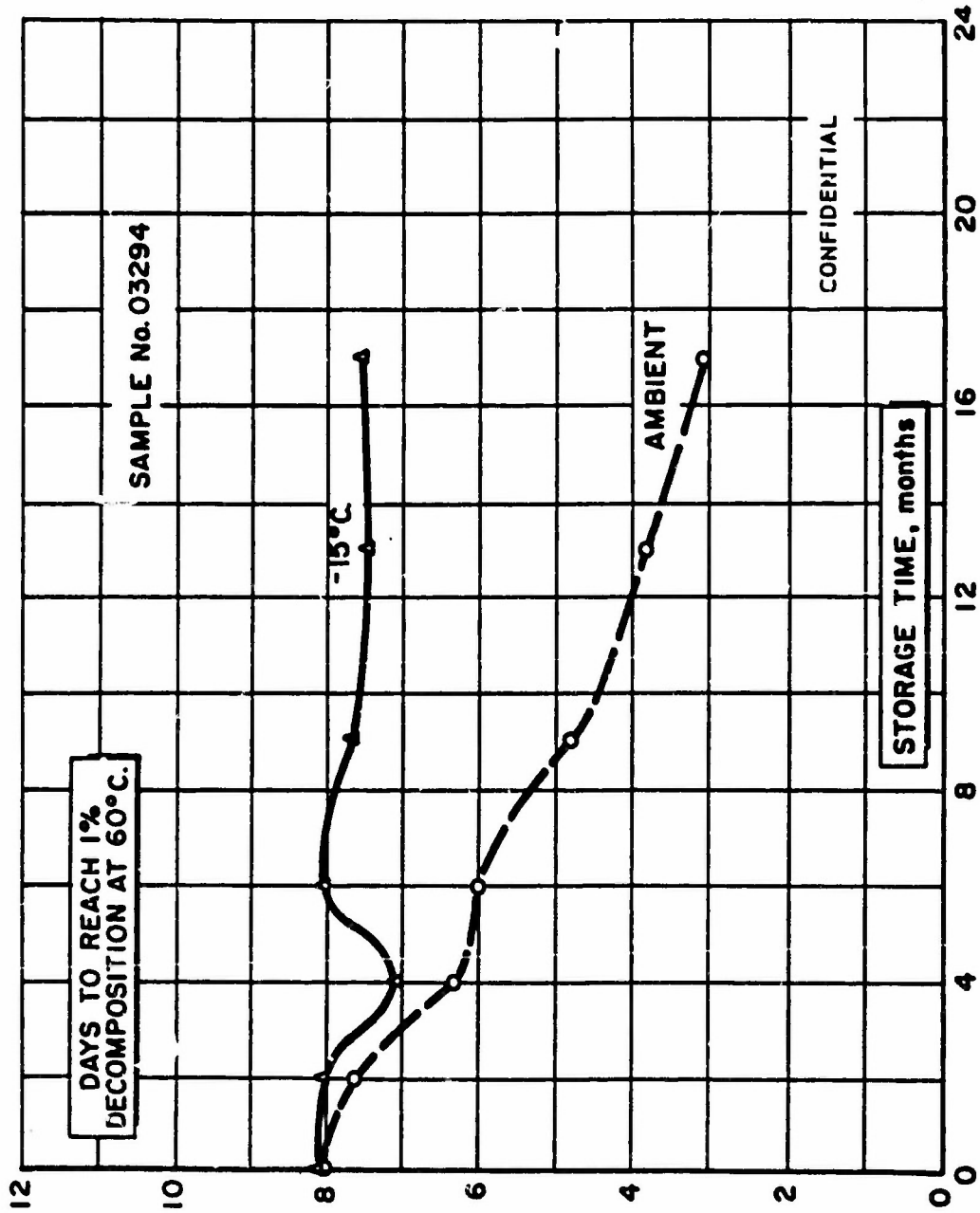
CONFIDENTIAL



(C) Fig. 51 - Change in the Thermal Stability of Aluminum Hydride-1451, Sample 02134A, Measured at 60°C. as a Function of Storage Time

CONFIDENTIAL

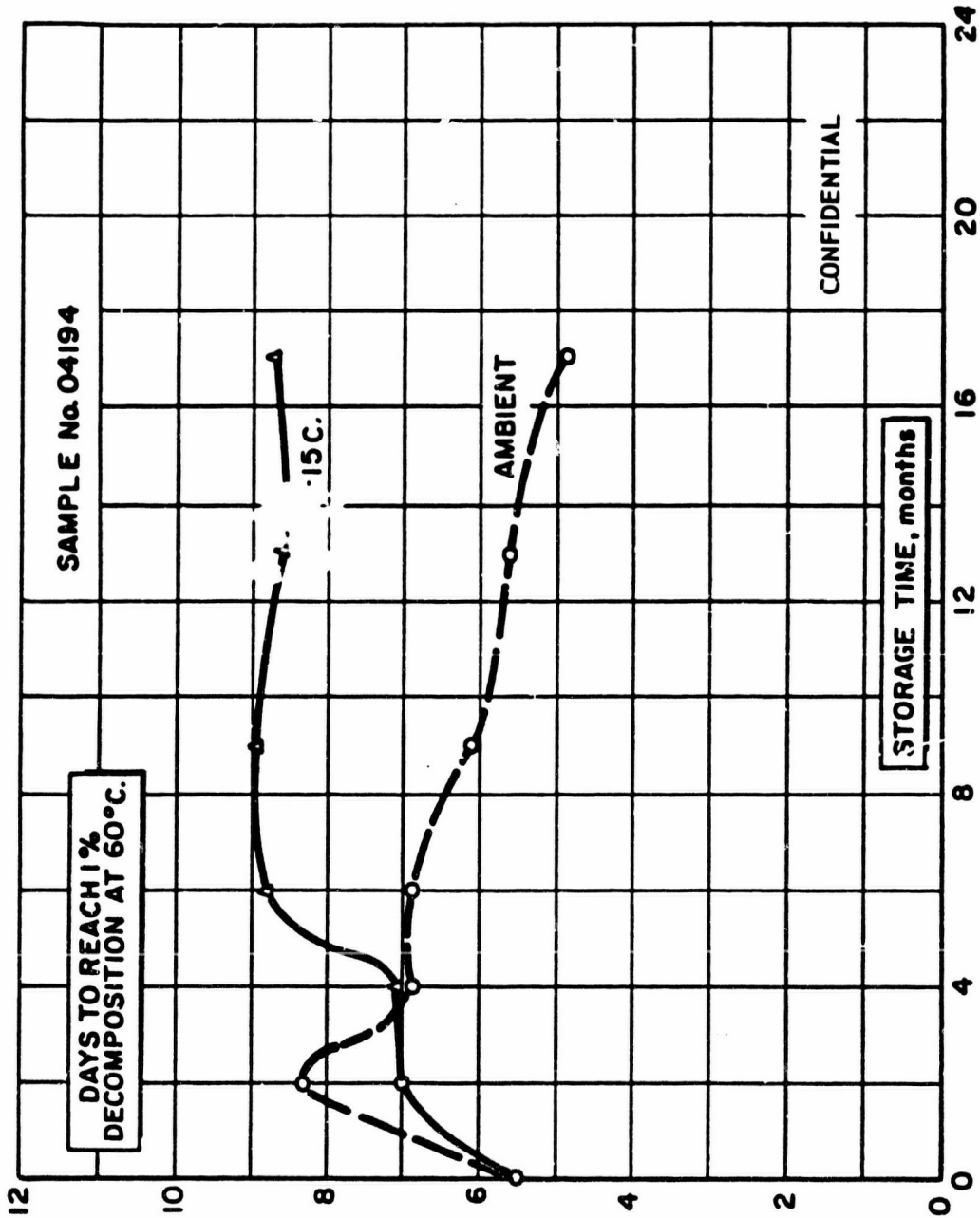
CONFIDENTIAL



(c) Fig. 52 - Change in the Thermal Stability of Aluminum Hydride-1451, Sample 03294, Measured at 60°C. as a Function of Storage Time

CONFIDENTIAL

CONFIDENTIAL



(c) FIG. 53 - Change in the Thermal Stability of Aluminum Hydride-1451, Sample 04194, Measured at 60°C. as a Function of Storage Time

CONFIDENTIAL

CONFIDENTIAL

(C) Two hydride lots yielded yearly a three-fold improvement in thermal stability during a storage period of 16 months. This aging phenomenon may explain the large discrepancy between the observed and predicted shelf life at ambient temperature. The decomposition rate is based on the stability of the sample observed immediately after preparation and does not consider any changes in the hydride with time, which would counteract the process or processes involved in the initiation of decomposition.

(C) This aging phenomenon could be rationalized in several ways; however any further explanation beyond that already discussed in Sections B-1 and B-2 would be speculative at this time. It is presently preferred to think only in terms of a time-temperature dependent annealing process, as it is expected that the annealing process will take place slower at reduced temperatures. However, it must be remembered that as temperature increases, not only does the rate of annealing increase, but also the rate or tendency towards decomposition. Hence, an optimum temperature must exist for each sample at which the rate of initiation of decomposition is small and the rate of annealing large, resulting in a maximum stabilization of the hydride in a minimum length of time. Further supporting data, obtained from hydride lots stored at 40°C., are summarized in Table XVIII. Each of the six lots decreased consistently in stability during a storage period of 96 days, again suggesting if the temperature is too high the decomposition process will indeed dominate.

(C) The data make it quite clear that the aging phenomenon exhibited by the various lots of hydrides differs significantly from lot to lot. This variation between lots must be related to the preparation and environmental history. It is interesting to note that the stability of 9 of 11 samples stored at -15°C. has remained approximately the same or significantly increased, after a storage period of 8 months. Only 5 of 11 lots stored at ambient temperature for the same period of time increased in stability. Four of these lots, 02034A, 02044, 02044A, and 02134A, were made at approximately the same time.

(C) The rate of change in the thermal stability with time for the hydride varies for a given period of time. Sometimes the change in decomposition rate is large for a given period, while other times it is small. This appears to suggest that, due to changes that are occurring in the hydride, the hydride may at certain periods of time be more vulnerable to decomposition. It is hoped that a better understanding of the decomposition mechanism will result from an intensive study of the aging phenomenon.

(C) Two long-term storage samples, lots 06104AT and 07084T, were surface treated with vinyl cyanide. A comparison of these lots with the reference lots 06104A and 07084 showed no significant difference. Data on hydride samples surface treated with various materials and evaluated over a long period of time have been previously reported (1). The results; at that time, demonstrated

CONFIDENTIAL

definite differences in the direction and magnitude of change for the annealing process when the reference was compared to the other surface-treated samples. The older data suggest that the condition of the surface may be playing a role in the long-term stability of the sample.

4. Effect of Doping Aluminum Hydride Crystals with Various Additives (C)

(C) Past experience with crystal lattice additives such as magnesium has proven this to be a valid and fruitful approach toward improving the stability of AlH_3 -1451. For this reason, the study of various elements as crystal lattice additives was conducted with the objective of finding a better additive and/or combination of additives which would produce an even greater increase in the thermal stability of the hydride.

(C) The experimental difficulties encountered in this study center around the incorporation of the desired element. Experience has demonstrated that the doping agent must be carefully chosen if the element is to be successfully incorporated into the hydride crystal lattice.

(C) Results obtained during the year suggest that several factors were involved. It appears that the principal criterion is the solubility of the doping agent in the ether-benzene solution. The presence of large amounts of reducing hydrides in the system restricts the additives to metals with a high oxidation potential (i.e., the alkali and alkaline earths, certain group III-A and IV-A elements, and certain transition metals). It is also known that strong bases such as amines must be excluded because the complex formed with aluminum hydride is too stable.

(C) Experimental results suggest that the ability to form stable hydride complexes is very important because of solubility and redox considerations. Calcium, magnesium, and gallium have given the highest percentages incorporated into the hydride lattice, and this may be attributed to their ability to form complex metal hydrides. The size of the additive ion, atom, or molecule being incorporated into the hydride lattice is also a critical factor determining if the element will be substitutionally or interstitially incorporated. If this size factor is not favorable, solid solution formation will be severely limited. Thus, large complex molecules are generally not suitable doping agents.

(C) The effect of coordination number has not been completely evaluated, but elements such as phosphorus and chromium with a potential coordination number of six have not been effective. However, other considerations probably outweigh the favorable coordination number of these elements. It is also important that the doping agent be of a simple nature because properties such as volatility, ease of hydrolysis, and general purity of reagents may affect the very sensitive hydride system, producing undesirable

CONFIDENTIAL

CONFIDENTIAL

aluminum hydride phases during preparation. Experimental results obtained during the past year in an attempt to incorporate various elements into the hydride lattice are described in the following sub-sections.

a. Phosphorus Pentachloride as a Doping Agent (U)

(C) Attempts were made to incorporate phosphorus into the AlH_3 -1451 lattice by the addition of phosphorus pentachloride during the preparation of an aluminum hydride solution. A maximum concentration of 0.06% phosphorus was incorporated by this method. A characteristic feature of this doping agent was the formation of appreciable turbidity in the hydride solution approximately 10°C . before normal precipitation temperature. This initial turbidity apparently had no detrimental effect on the final product, as AlH_3 -1451 was consistently isolated as the only phase present. The product was always characterized by a phosphine odor. Although an increase in thermal stability was observed at 100°C ., the corresponding increase at 60°C . was insignificant.

b. Lithium Gallium Hydride as a Doping Agent (U)

(C) The use of lithium gallium hydride as a doping agent for the incorporation of gallium proved to be very effective. A maximum of 0.7% gallium was incorporated into the AlH_3 -1451 lattice. The concentration of gallium is noteworthy because few elements have been incorporated into the hydride lattice at concentrations greater than 0.5%. The gallium-doped product gave some increase in product stability at 100°C . and 60°C . The presence of moisture in the starting reagent, gallium trichloride, has prevented a complete evaluation of the stabilizing effect of this element.

c. Germanium Tetrachloride as a Doping Agent (U)

(C) The addition of germanium tetrachloride to the aluminum hydride solution resulted in a maximum incorporated concentration of 0.01% germanium into the hydride lattice. A 75% increase in stability at 100°C . was observed, but phase problems prevented reproducibility. The high volatility of the germanium tetrachloride and hydride appears to make it undesirable as a doping agent.

d. Inorganic Oxides as Doping Agents (U)

(C) In an effort to dope AlH_3 -1451 crystals with greater concentrations of oxygen, the following inorganic oxides were evaluated: TiO_2 , Fe_2O_3 , MoO_3 , and WO_3 . Inorganic oxides are reported to react with ethereal solutions of lithium aluminum hydride in an anhydrous atmosphere to form soluble hydroxides (10). It was hoped that soluble oxygen-containing species would result and remain soluble during the preparation of the hydride. However, no increase in oxygen content or stability was observed.

CONFIDENTIAL

CONFIDENTIAL

e. Chromous and Chromic Chloride as Doping Agents (U)

(C) Attempts were made to incorporate chromium into the AlH_3 -1451 lattice by the addition of chromous and chromic chloride at several different stages throughout the process.

(C) Results indicate that generally these agents are reduced by the lithium aluminum hydride, probably forming some chromium metal or lower valent salts. If this is not removed by the final filtration, it will generally result in the formation of AlH_3 -1444 phase. Emission spectrographic analysis indicated that a maximum concentration of 0.01% chromium had been incorporated. Although some stabilization was achieved, it was attributed to modifications in crystal growth rather than the concentration of chromium found.

f. Ferrocene and Ferric Chloride as Doping Agents (U)

(C) Iron is an impurity occasionally found in hydride samples. For that reason, an early evaluation was made of the effect this element had on aluminum hydride thermal stability.

(C) The effectiveness of ferrocene as a doping agent for the incorporation of iron was evaluated. The addition of ferrocene to the benzene solvent in concentrations of 0.05 and 0.1 g./6g. of AlH_3 produced a slight discoloration of the solution, although the final recovered product was white. Emission spectrographic analysis of the samples indicated 0.005% iron in the sample. The presence of ferrocene in the system had very little effect upon the hydride stability, as the samples exhibited a normal degree of stability at 60°C.

(C) The effectiveness of anhydrous ferric chloride was also evaluated as a potential doping agent. Concentrations of 0.5 and 1.0 g. of FeCl_3 /6 g. of AlH_3 were initially added to the aluminum chloride starting reagent prior to the addition of lithium aluminum hydride. It was determined by emission spectrographic analysis that 0.04% and 0.06% iron had been incorporated into the aluminum hydride sample. However, both the hydride solutions and the final product were colored tan. An evaluation of the thermal stability of the hydride at 60°C. showed no significant change.

g. Nickel Bromide as a Doping Agent (U)

(C) From a surveillance study of trace metal impurities present in aluminum hydride-1451 samples, there appeared a possible relationship between the nickel concentration and the rate of decomposition of the hydride. Three samples indicated that as the nickel concentration increased, the thermal stability of the hydride decreased.

(C) Therefore, work was initiated using nickel bromide as a doping agent in an attempt to incorporate larger concentrations of nickel into the hydride lattice and to further evaluate and confirm

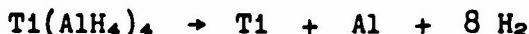
CONFIDENTIAL

CONFIDENTIAL

this proposed relationship. Concentrations of 0.5 and 1.0 g. of NiBr_2 /6 g. of AlH_3 were again added to the aluminum chloride solution prior to the addition of lithium aluminum hydride. Emission spectrographic analysis indicated that 0.02% and 0.04% Ni, respectively, had been incorporated. As with ferric chloride, the doping agent caused the hydride solution and product to be quite brown. In addition, 5% to 10% AlH_3 -1444 was identified by X-ray analysis in the sample containing the 1.0 g. of nickel bromide. An evaluation of the sample containing 0.02% Ni, however, indicated very little effect upon the thermal stability of the hydride sample at 60°C.

h. Titanium Tetrachloride as a Doping Agent (U)

(C) The use of titanium tetrachloride as a doping agent for the incorporation of titanium proved to be very detrimental to the system. The titanium tetrachloride was added to the aluminum chloride as before, prior to the addition of lithium aluminum hydride. However, upon adding the lithium aluminum hydride, the solution turned very black, apparently as a result of the formation and subsequent decomposition of titanium aluminum hydride, which is known to decompose about -85°C. as follows:



(C) The succeeding decomposition of aluminum hydride in solution, as evidenced by gas evolution and the identification of aluminum metal in the flask after reaction, is apparently catalyzed by the presence of the finely divided metals. Therefore, it is assumed that if titanium tetrachloride were present as an impurity in the starting reagent, aluminum chloride, it would cause a very severe decomposition problem in the crystallizing system.

1. Calcium, Strontium, and Barium Chlorides as Doping Agents (U)

(C) Attempts were made to incorporate the group IIA elements of the periodic table into the AlH_3 -1451 lattice in an attempt to obtain a correlation between atomic size of the impurity atom and stability. The success achieved incorporating magnesium into the hydride lattice suggested that this group of elements would probably lend itself to such an evaluation. However, work using calcium, strontium, and barium chlorides as doping agents for AlH_3 -1451 has not been very successful. The maximum incorporated concentrations of these doping agents, as determined by emission spectrographic or atomic absorption techniques, have been 0.5% calcium, 0.03% strontium, and 0.0011% barium. The products obtained using these doping agents appeared normal. An evaluation of the thermal stability of the hydride at 60°C., in general, produced no significant change, although a couple of samples containing calcium appeared to exhibit superior stability. As a result of the limited success in

CONFIDENTIAL

incorporating the group IIA elements, no conclusions could be drawn about the relationship between atomic size and stability. However, it would appear, if other factors are equal, that the larger the group IIA cation, the less tendency towards solid solution formation.

4. Trimethylsilanol as a Doping Agent (U).

(C) Trimethylsilanol reacts with aluminum hydride according to the following equation:



It was anticipated that the presence of small amounts of the trimethylsiloxyaluminum hydride would introduce both oxygen and silicon into the crystal lattice with a resulting effect upon stability.

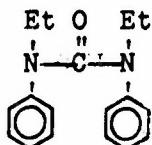
(C) A total of 8 runs was made, varying the amount of trimethylsilanol from 10 ml. to 0.5 ml. per run. The highest concentration added, 0.5 ml./60 mmoles of AlH_3 , resulted in the formation of 5% to 10% 1433. However, reducing this amount to one-half (0.5 ml./120 mmoles AlH_3) resulted in all AlH_3 -1451.

(C) Four samples of AlH_3 -1451 containing trimethylsilanol as an additive produced a 25% to 60% increase in stability compared to normal hydride.

5. New Stabilization Agents for Aluminum Hydride-1451 (C)

a. Ethyl Centralite (U)

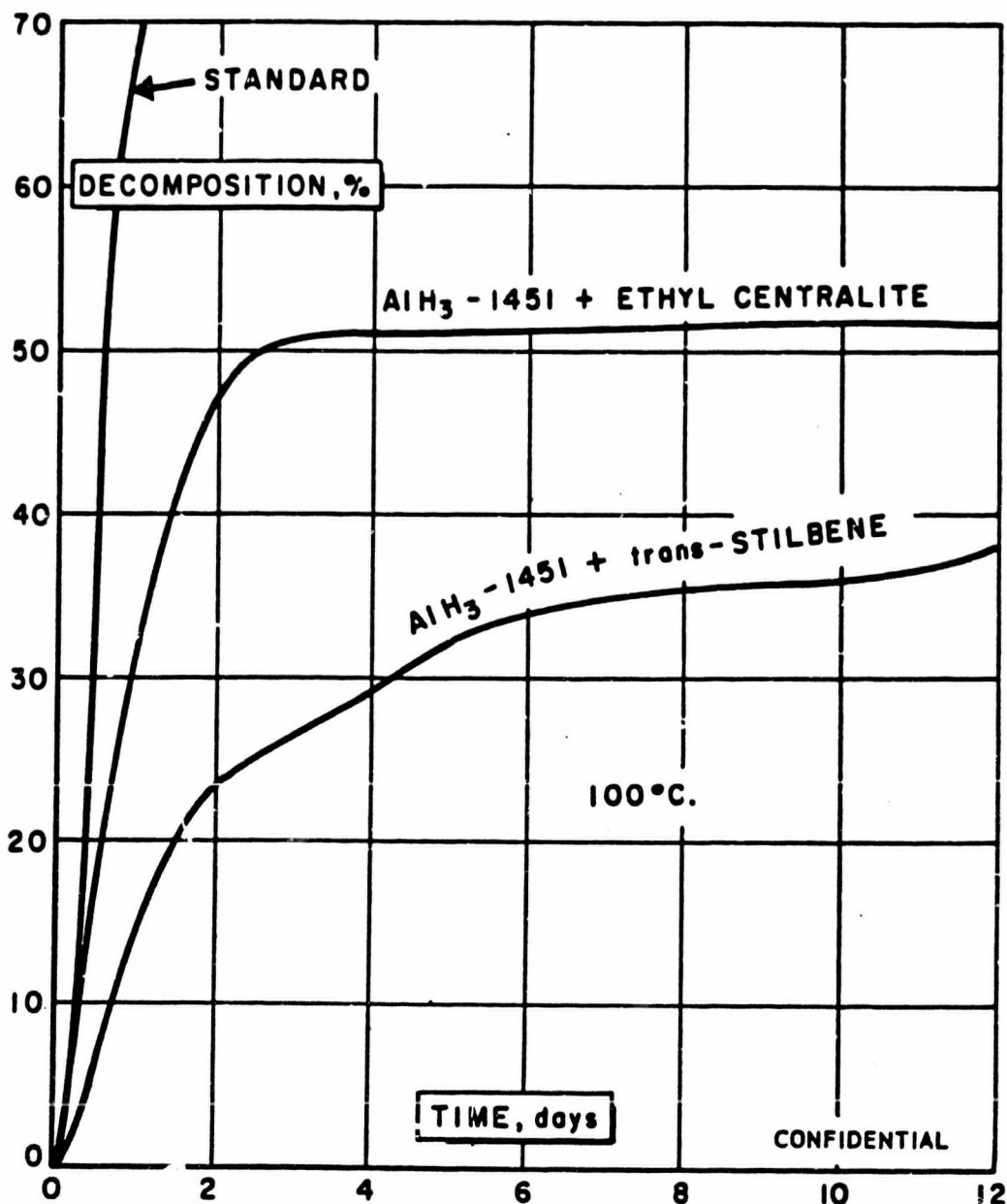
(C) It has been found that symmetrical diethyldiphenylurea,



, designated ethyl centralite (EC), stabilizes AlH_3 -1451

in a completely new and unique manner previously not observed. When aluminum hydride was decomposed in the presence of molten ethyl centralite at 100°C., the characteristic induction period was similar to other hydrides, but the accelerated decomposition of the hydride essentially stopped at approximately 50% decomposition, as shown in Figure 54. The percent decomposition at this level remained constant for several days. The residue was analyzed by X-ray diffraction and found to contain AlH_3 -1451 and aluminum metal in approximately the same amounts as indicated by gas evolution. X-Ray analysis also indicated an expanded crystal lattice. Analysis of the gas evolved showed 0.16 mole % benzene and 0.41 mole % of a C_4 -substituted benzene in addition to the main constituent, hydrogen. It was anticipated, if the decomposition could be completely stopped at 50%, that under the proper conditions this same effect would be applicable at low percentages of decomposition.

CONFIDENTIAL



(C) Fig. 54 - Rate of Decomposition of Aluminum Hydride-1451 Alone and with Ethyl Centralite and trans-Stilbene at 100°C.

CONFIDENTIAL

CONFIDENTIAL

(1) Weight Percent Ethyl Centralite (U)

(C) In all of the early experimental work a weight ratio of approximately 50% with respect to the 0.2 to 0.4 g. of aluminum hydride was used. An attempt was made to determine the minimum amount of EC necessary for stabilization. The results of varying the EC concentration from 15 to 56 weight % are shown in Figure 55. At a weight ratio of 15% EC, the rate of hydride decomposition to 100% showed no deviation from the standard. At 33.5 weight % EC, the decomposition proceeded slower, appearing to taper off at 30%, but then increased sharply, proceeding to nearly 100%. A mixture containing 49% EC exhibited the normal termination of decomposition at 50%; however, after 100 to 120 hours, a slight increase was observed which again stopped at 85% where it continued to remain until termination. The sample containing 56% EC stopped decomposing at ~50% and essentially remained there until termination 14 days later. Hence, it became apparent that a definite threshold concentration of EC was necessary to achieve this degree of stabilization.

(2) Temperature (U)

(C) An attempt was made to determine the maximum temperature at which this stabilizing effect by EC was still operative. Temperatures of 100°, 120°, and 130°C. were evaluated. The results obtained at 100° and 120°C. compared to the decomposition rate of the standard are depicted in Figure 56. The data illustrated that the EC was still effective at 120°C. At 130°C. the hydride did slowly reach 87% decomposition, although it took an additional 18 days after initially reaching 46% in 6 hours. It was, therefore, concluded that this stabilizing effect was still operative at these high temperatures.

(3) Role of Ethyl Centralite (U)

(C) Realizing the unique stabilizing effect of EC on AlH₃-1451, an effort was made to determine the chemical or functional group(s) of the molecule responsible for the observed stabilization. It was found that the presence of urea, H₂N-C(=O)-NH₂, during decomposition

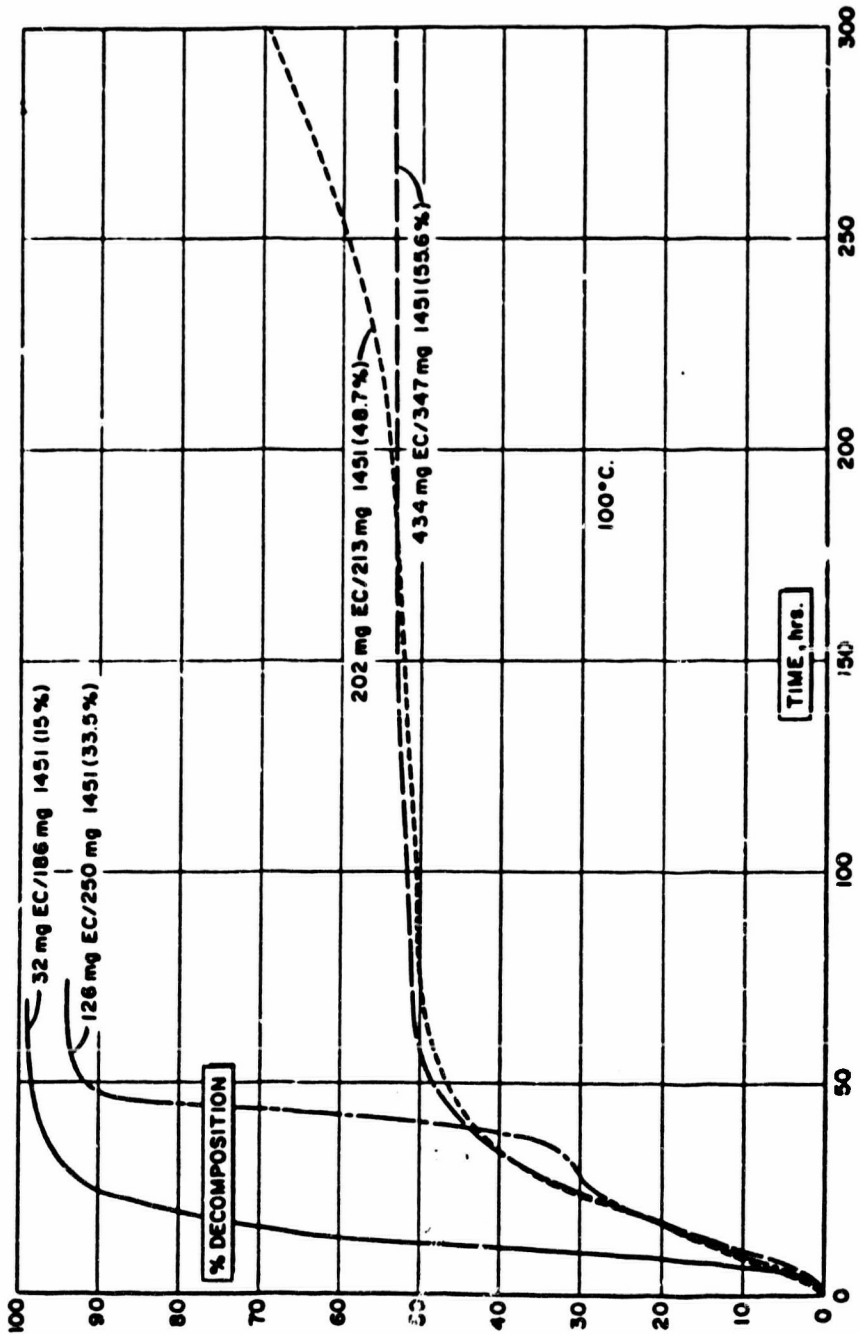
of the hydride produced a slight increase in the rate of decomposition.

Tetramethylurea, $\begin{array}{c} \text{CH}_3 \quad \text{O} \quad \text{CH}_3 \\ \diagdown \quad \parallel \quad \diagup \\ \text{N} - \text{C} - \text{N} \\ \diagup \quad \parallel \quad \diagdown \\ \text{CH}_3 \quad \text{O} \quad \text{CH}_3 \end{array}$, showed no stabilization

of the hydride similar to that observed for EC. These results suggest that the phenyl groups are responsible in some manner for the observed stabilization phenomenon.

(C) It is interesting to note two facts associated with ethyl centralite stabilization of another material, nitrocellulose: (a) it expands the lattice of nitrocellulose (11), and (b) this

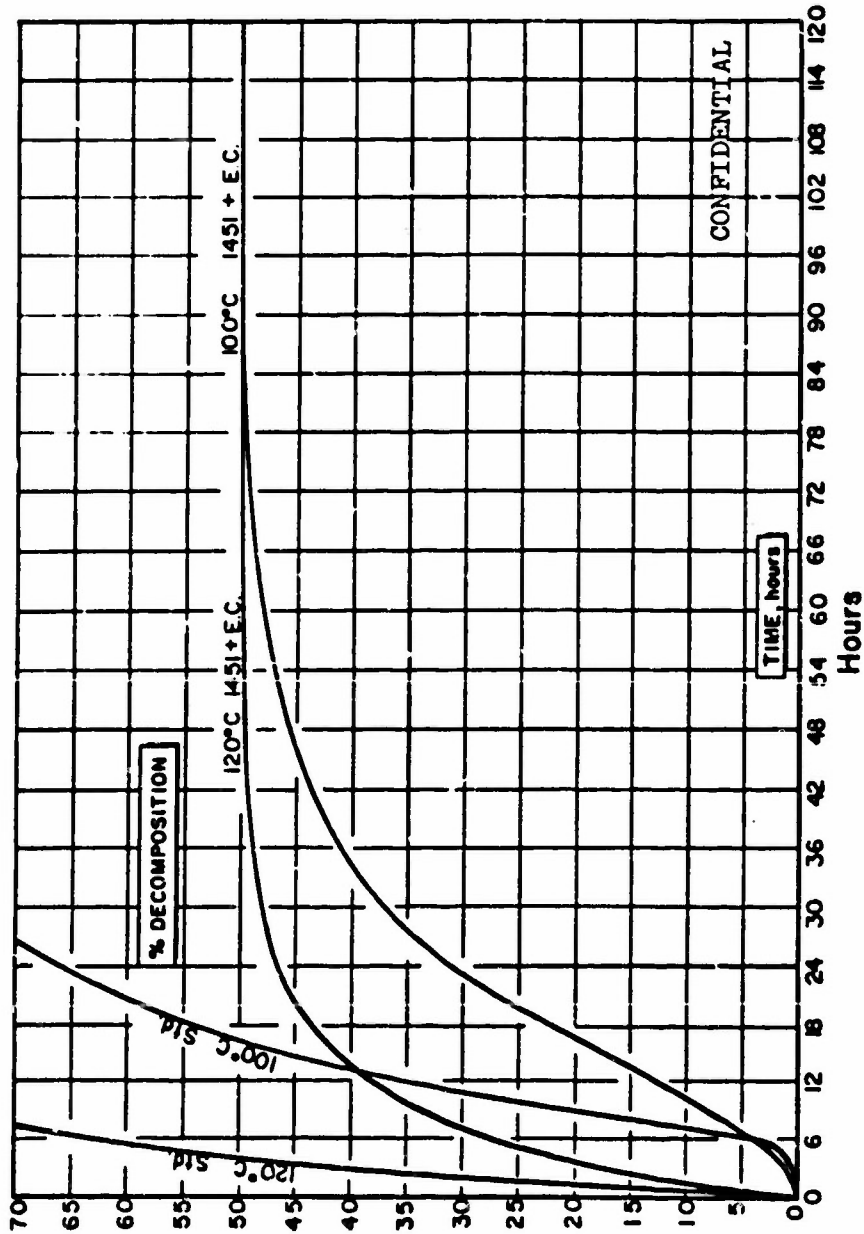
CONFIDENTIAL



(C) Fig. 55 - Effect of Various Weight Percentages of Ethyl Centralite on Decomposition Rate of Aluminum Hydride-1451

CONFIDENTIAL

CONFIDENTIAL



(C) FIG. 56 - Effect of Ethyl Centralite on the Decomposition Rate of Aluminum Hydride at 100°C. and 120°C.

CONFIDENTIAL

CONFIDENTIAL

stabilization of nitrocellulose is usually attributed to free radical scavenging; however, more potent radical scavengers are inferior stabilizers. Hence, it appears that such stabilization may be more closely related to electron absorbing or releasing capability (π acidity) than it is to formal reaction with free radicals.

b. Other Stabilizers (U)

(C) From the aforementioned work, a program was initiated to screen compounds with structural parameters similar to those of ethyl centralite. The results obtained from tetramethylurea indicated that electron absorbing or releasing tendencies as exhibited by the phenyl group are required. Hence, various compounds containing one or more phenyl groups, as listed in Table XIX, were examined and ranked according to their relative effectiveness.

(C) One of the first potential stabilization agents examined

in this group was trans-stilbene $\left[\begin{array}{c} \text{H} \quad \text{H} \\ | \quad | \\ \text{C} = \text{C} \\ | \quad | \\ \text{C}_6\text{H}_5 \quad \text{C}_6\text{H}_5 \end{array} \right]$. As illustrated

in Figure 54, this material was observed to behave in much the same manner as ethyl centralite. The decomposition, in this case, stopped between 30% and 35% rather than 50% as observed for ethyl centralite. One other notable difference between ethyl centralite and trans-stilbene stabilization is that a gross quantity of ethyl centralite is required (50/50 mixture), while in the case of trans-stilbene a gross quantity is mixed initially, but, on heating, the trans-stilbene sublimates away, leaving less than 3% present.

(C) Substituted derivatives of trans-stilbene, dinitrostilbene and diaminostilbene were examined to determine the effect of electron withdrawing and electron donating groups on the compounds' ability to function as a stabilizer for aluminum hydride. Typical results are shown in Figure 57. Both of the substituted derivatives appeared to be less effective than trans-stilbene, terminating rapid decomposition at approximately 60% and 75% for the dinitro- and diaminostilbenes, respectively, compared to 30% for trans-stilbene alone.

(C) If it were assumed that reactivity and electron accepting ability were two major factors playing a role during stabilization of the hydride, then the following comments could be made. The amine substitution on the phenyl group would tend to increase the electron density of the double bond, but decrease the phenyl groups' electron accepting ability, whereas the opposite is true for the nitro substitution, as the electron density of the double bond is decreased while the phenyl groups electron accepting ability increases. The data indicate that these electronic effects are not the principal factor in hydride stabilization by this type of molecule. Therefore, an additional parameter would appear to be necessary.

CONFIDENTIAL

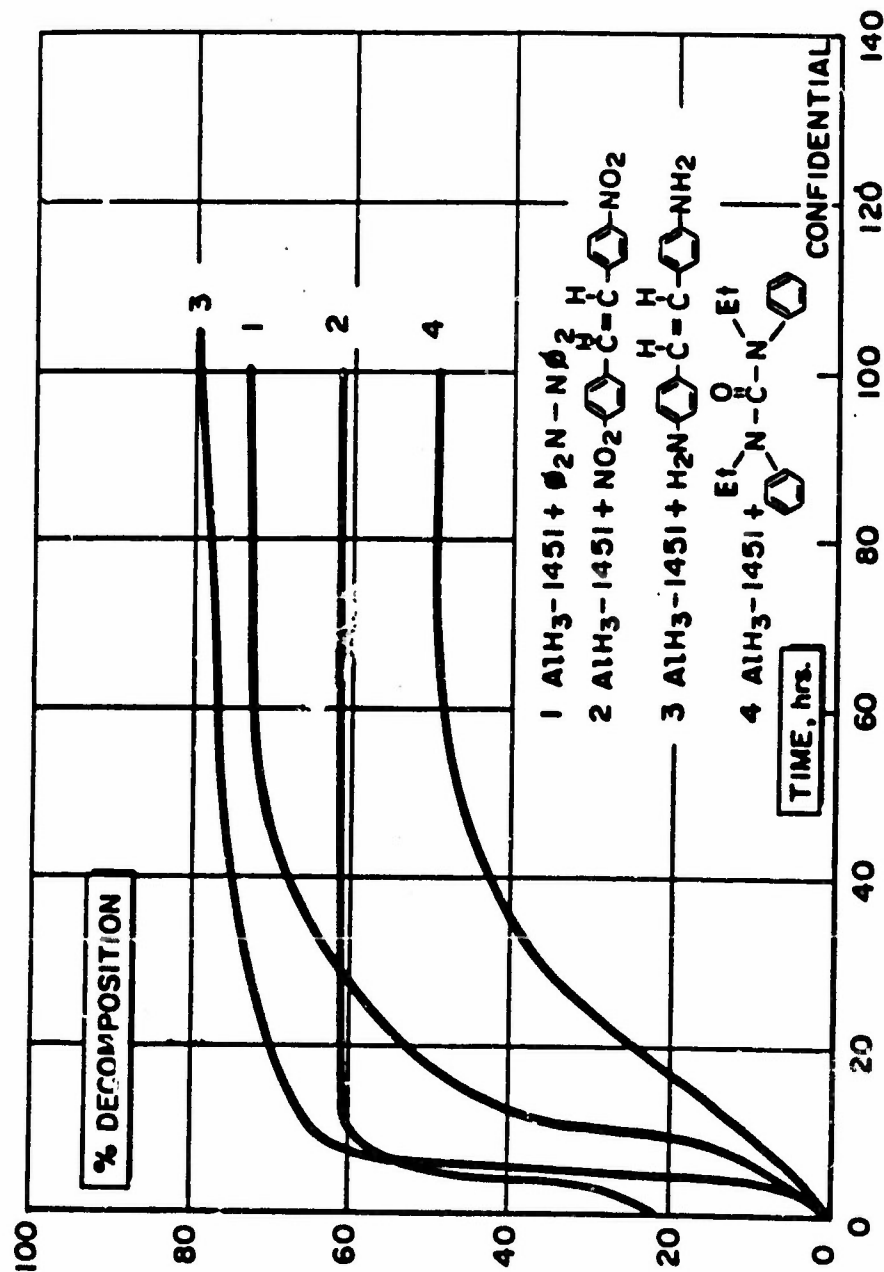
CONFIDENTIAL

Table XIX

(C) Ranking of Various Aluminum Hydride-1451 Stabilizers

Good	Fair	Poor
$\phi-C \equiv C-\phi$	$\begin{array}{c} \text{Et} \quad \text{O} \quad \text{Et} \\ \diagdown \quad \parallel \quad \diagup \\ \text{N}-\text{C}-\text{N} \\ \diagup \quad \quad \diagdown \\ \phi \quad \quad \phi \end{array}$	$\phi_2C \equiv C\phi_2$
$\begin{array}{c} \text{H} \quad \text{H} \\ \quad \\ \phi-\text{C}=\text{C}-\phi \\ \text{cis and trans} \end{array}$	$\begin{array}{c} \text{H} \\ \\ \phi-\text{N}-\phi-\text{N} \equiv \text{N}-\phi \\ \phi \text{N}=\text{N}\phi \end{array}$	$\begin{array}{c} \text{H} \quad \text{H} \\ \quad \\ \text{NH}_2\phi-\text{C}=\text{C}-\phi-\text{NH}_2 \cdot 2 \text{ HCl} \end{array}$
	$\begin{array}{c} \text{NO}_2 \\ \\ \phi-\text{N}-\phi \\ \\ \text{H} \end{array}$	$\begin{array}{c} \text{OCH}_3 \\ \\ \phi-\text{C}=\text{C}-\phi \\ \\ \text{OCH}_3 \end{array}$
	$\phi_2\text{N}-\text{N}\phi_2$	$\begin{array}{c} \text{O} \\ \\ \phi\text{P}(\text{OH})_2 \end{array}$
	$\begin{array}{c} \text{H} \quad \text{H} \\ \quad \\ \text{NO}_2\phi-\text{C}=\text{C}-\phi-\text{NO}_2 \end{array}$	$\begin{array}{c} \text{CH}_3 \quad \text{CH}_3 \\ \quad \\ \text{CH}_3-\text{C}-\text{C}-\text{CH}_3 \\ \quad \\ \text{H} \quad \text{BH}_2 \end{array}$
	$\begin{array}{c} \text{O} \\ \\ \phi-\text{N}-\text{C}-\text{N}-\phi \\ \quad \\ \phi \quad \phi \end{array}$	$\phi_2\text{N}-\text{N}-\phi-\text{NO}_2$
	$\begin{array}{c} \text{N} \equiv \text{C} \quad \text{C} \equiv \text{N} \\ \diagdown \quad \diagup \\ \text{C}=\text{C} \\ \diagup \quad \diagdown \\ \text{N} \equiv \text{C} \quad \text{C} \equiv \text{N} \end{array}$	
	$\text{N} \equiv \text{C}-\phi-\text{C} \equiv \text{N}$	
	$\text{CH}_2(\text{C} \equiv \text{N})_2$	
	$\begin{array}{c} \phi-\text{C} \equiv \text{C}-\phi \\ \quad \\ \phi-\text{N} \quad \text{N}-\phi \\ \quad \\ \phi-\text{C}=\text{O} \quad \text{H} \end{array}$	

CONFIDENTIAL



(C) Fig. 57 - Effect of Various Compounds Containing Phenyl Groups on the Decomposition Rate of Aluminum Hydride-1451

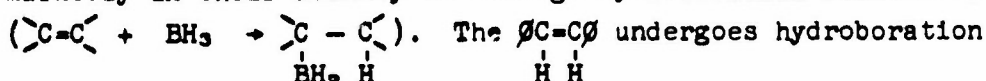
CONFIDENTIAL

CONFIDENTIAL

(C) Evaluation of cis- and trans-stilbene, melting points 1°C. and 124°C., respectively, demonstrated identical stabilizing effects. This indicates either the trans-stilbene had sufficient vapor pressure to make it effective or volatility was not an important parameters.

(C) It is also challenging to try to rationalize the reason tetraphenylethylene, $\phi_2C=C\phi_2$, shows no stabilizing effect on the rate of decomposition, while symmetrical diphenylethylene, $\overset{\overset{H}{|}}{\phi}C=C\overset{\overset{H}{|}}{\phi}$.

is relatively effective. It is known that the two materials differ markedly in their ability to undergo hydroboration reactions,



rapidly while $\phi_2C=C\phi_2$ does not. This does suggest that reactivity may be a very important parameter, although the difference could be accounted for in many different ways. Steric hindrance factors do not appear to be of major importance, since $\phi_2N-N\phi_2$ is fairly effective while $\phi_2C=C\phi_2$ exhibits no effect.

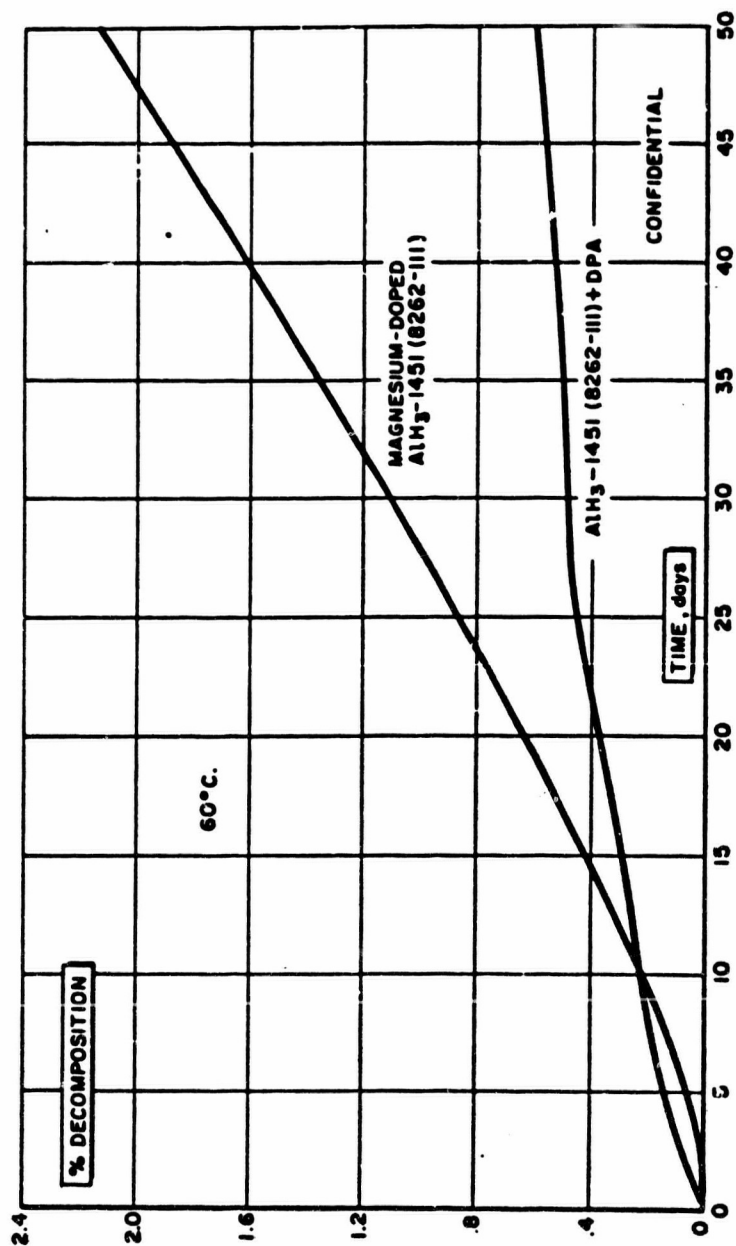
(C) It is clearly apparent from the above discussion that the parameters necessary for a compound to be an effective stabilizer for AlH_3 -1451 are not well understood. It is, however, shown from this screening program that the presence of phenyl groups alone is not sufficient to make an effective stabilizer for aluminum hydride.

(C) A very effective stabilizer for AlH_3 -1451 has, however, been discovered as a result of this screening program. The stabilizer, diphenylacetylene (DPA), has demonstrated a very remarkable stabilization of the hydride, as shown in Figures 58 and 59. Surface treatment with this material has been found to greatly extend the length of the induction period prior to accelerated decomposition of the hydride. For unknown reasons this material is more effective than any of the other compounds studied.

(C) The decomposition curves at 60°C. and 100°C., shown in Figures 58 and 59, respectively, were obtained by using a gross amount of DPA (50/50 mixture). This material, however, at 100°C. again sublimes away from the hydride sample, similar to the trans-stilbene. At 100°C. the induction period was extended from 5 to 300 hours before accelerating its decomposition. The rate of decomposition of a magnesium-doped hydride sample at 60°C. with DPA has exhibited only 0.6% decomposition in 50 days, compared with 20 days for the magnesium-doped hydride alone.

(C) Preliminary results give definite evidence that concentrations as low as 1% DPA are effective for stabilizing the hydride at 60°C. Another very important observation made from these studies indicates that the improvements in stability by using magnesium and DPA are additive. Results indicate the DPA is a more effective stabilizer for magnesium-doped material than for normal hydride.

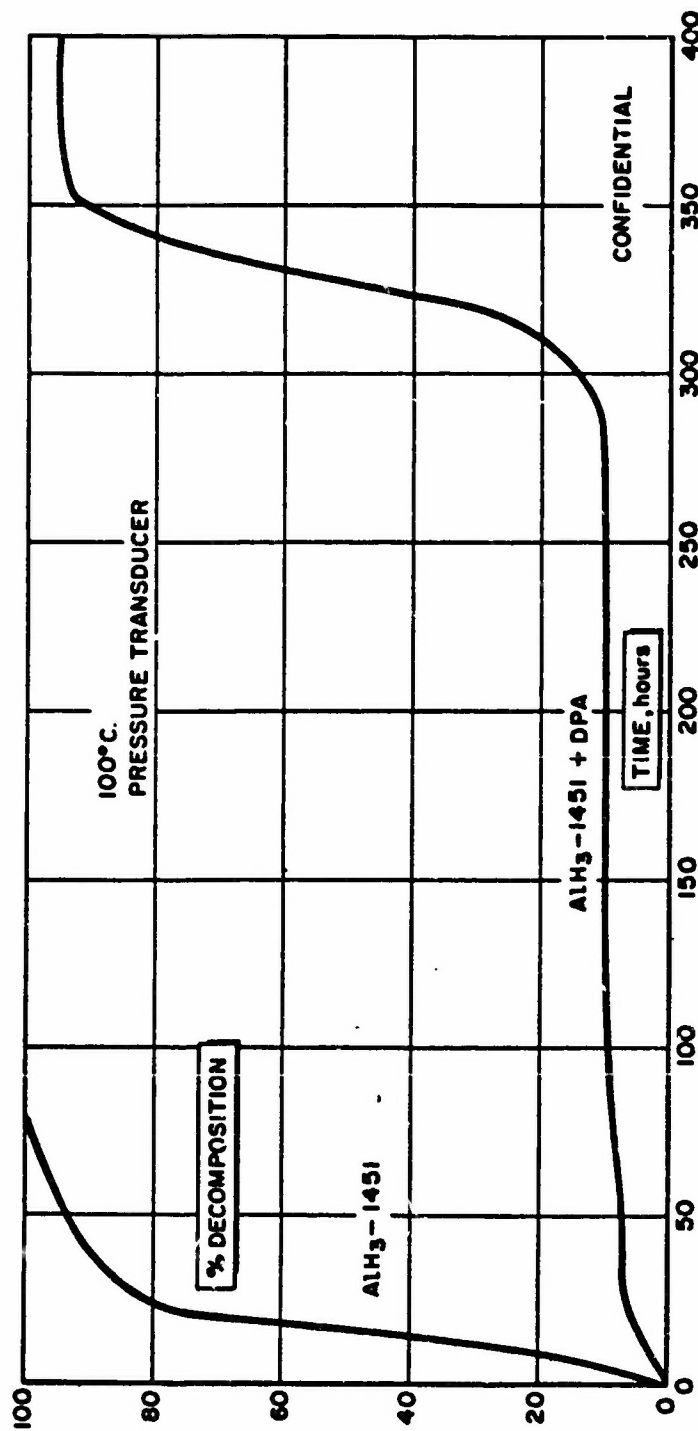
CONFIDENTIAL



(C) Fig. 58 - Effect of Diphenylacetylene on the Decomposition Rate of Magnesium-Doped Aluminum Hydride-1451 at 60°C.

CONFIDENTIAL

CONFIDENTIAL



(C) Fig 59 - Effect of Diphenylacetylene on the Decomposition Rate of Aluminum Hydride at 100°C.

CONFIDENTIAL

CONFIDENTIAL

6. Effect of Electrical Properties on the Decomposition of Aluminum Hydride-1451 (C)

(C) To further elucidate the importance of surface electrical properties, two experiments were performed. Aluminum hydride-1451 was suspended in a lampblack matrix (a conductor) and decomposed at 100°C. The length of the induction period as shown in Figure 60 was greatly reduced under these conditions, and the material decomposed much faster than the standard.

(C) In a second experiment, a sample of AlH_3 -1451 was placed in a sample tube with two platinum electrodes, 1 cm. by 1 cm. and 8 mm. apart. A 45 volt D.C. potential was impressed across the electrodes when the tube was placed in a 100°C. temperature bath. The induction period for the onset of decomposition was greatly reduced and the acceleration period was reached in approximately one hour. The AlH_3 -1451 again decomposed much faster than the standard as shown in Figure 60. During decomposition, the aluminum metal agglomerated into a solid mass.

C. MISCELLANEOUS STUDIES OF ALUMINUM HYDRIDE-1451 (C)

1.. Effect of Oxygen and Water on the Preparation and Stability of Aluminum Hydride-1451 (C)

(C) It has been known for some time that AlH_3 -1451 samples contained oxygen varying in amounts from 0.2% to 1.5%. Since this represented the largest impurity in aluminum hydride, a systematic study of its effect on AlH_3 -1451 was investigated. This study was made possible by the development of analytical methods to monitor both oxygen and water in the dry boxes, and of means to maintain them at very low levels.

a. Description of Equipment and Methods Used to Remove, Analyze, and Monitor the Water and Oxygen Content (U)

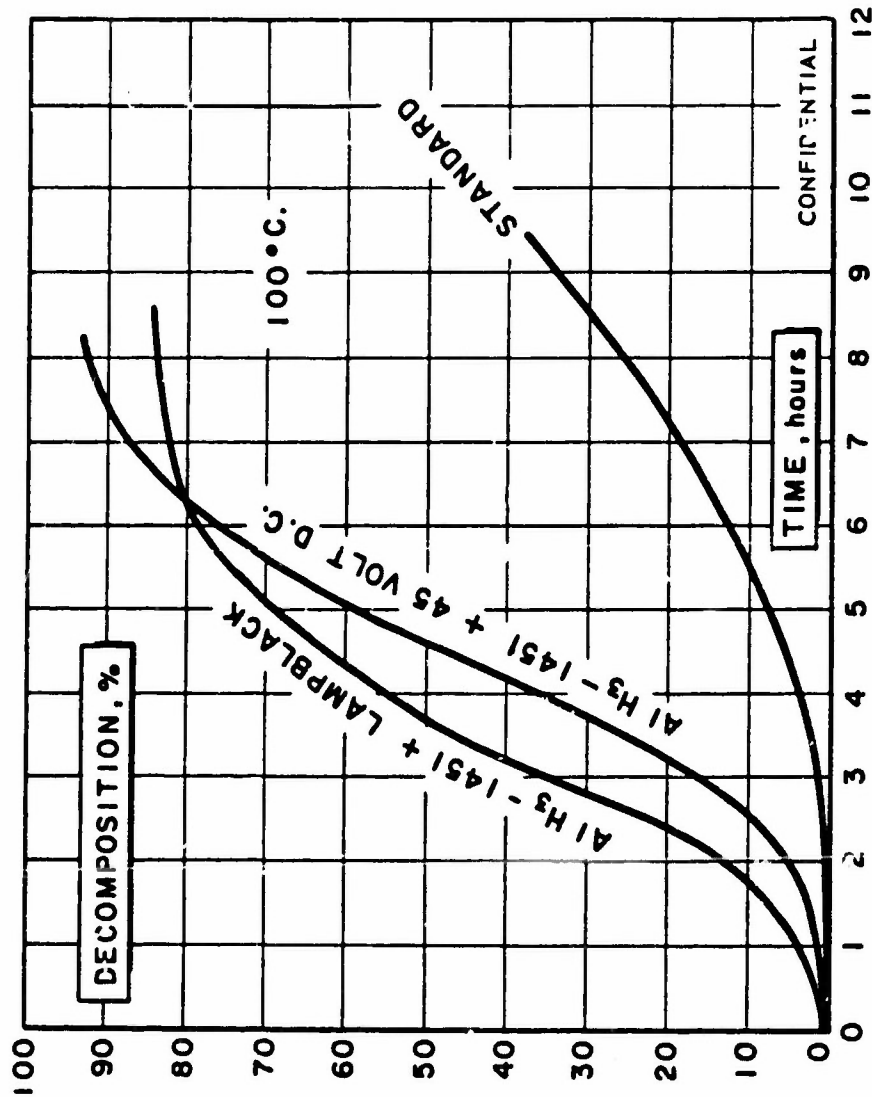
(U) It was thought that the hydride was being contaminated with oxygen during its preparation under partially hydrolytic or oxidative conditions. Hence, the following methods and equipment were designed and used to control both water and oxygen concentrations in the dry box atmospheres and purge nitrogen.

(U) The analysis problem was solved by investigating methods presently in use, experimenting with new ones, and developing an integrated system so that the atmosphere of each dry box could be conveniently analyzed by instruments placed in a central location.

(U) Previous Dow experience had demonstrated that the Analytix Systems Company Model 603W oxygen analyzer was both accurate and reliable for the determination of oxygen in nitrogen atmospheres. A further check in our laboratories confirmed these findings and a unit was purchased from Analytix Systems Company.

CONFIDENTIAL

CONFIDENTIAL



(C) Fig. 60 - Rate of Decomposition of Aluminum Hydride-1451 Alone and with Lampblack and Electric Potential at 100°C.

CONFIDENTIAL

CONFIDENTIAL

(U) Water analyzers using electrolysis have previously been used to monitor water in dry box atmospheres, but when benzene and ether vapors are present, as in our dry boxes, the P_2O_5 coating on the cell becomes contaminated and the instrument no longer gives accurate results. During the early part of 1964, Gilbert and Barker Manufacturing Company began marketing a quartz crystal water analyzer which covered a range of 1 to 2,500 ppm. and appeared to be free from the disadvantages of the electrolytic type. The instrument, the Gilbarco Sorption Hygrometer, model SHL-100, was purchased.

(U) The oxygen and water analyzers illustrated in Figure 61 can simultaneously monitor both oxygen and water in either the incoming line nitrogen or any selected dry box by use of a manifold in a few minutes.

(U) Subsequent to developing methods of analyzing and monitoring the oxygen and water concentrations, a study was initiated to find the most satisfactory and efficient method of removing these two contaminants from the dry boxes.

(U) Molecular sieves and Dow "Q" Catalyst were found to be most effective for the removal of water and oxygen, respectively. This combination can maintain an atmosphere containing less than 1 ppm. oxygen and water if desired. Generally, our dry box atmospheres contain less than 20 ppm. of water and 5 ppm. of oxygen during normal operation. All the nitrogen used by the laboratory for dry box work is purified by the above methods and consistently contains less than 0.5 ppm. oxygen and water.

(U) Using information furnished by Gilbarco Company, the Gilbarco Sorption Hygrometer was modified to analyze water in the low ppm. range in solvents such as benzene and ether. The sensitive quartz crystal is used, in effect, as a GLC detector to measure the height of the water peak. Calibration curves were made for both ether and benzene with known amounts of water and showed a straight line relationship between the peak height and water in ppm. This arrangement is very useful for determining when significant amounts of water are present; however, it is not sufficiently accurate below 10 ppm., due mainly to the sensitivity of the oscillators to slight changes in temperature.

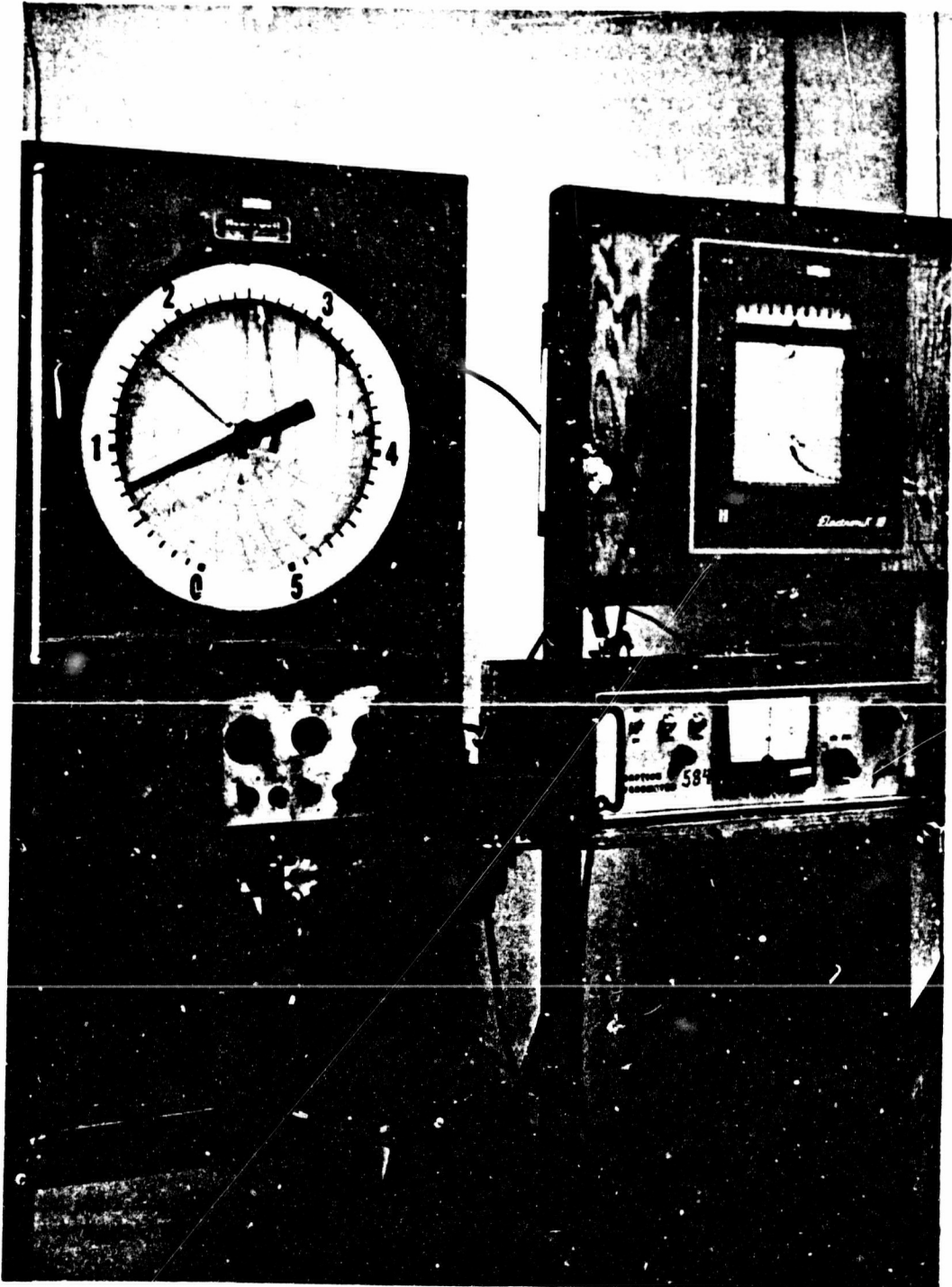
b. Preparation of Aluminum Hydride-1451 in the Presence of Water and Oxygen (C)

(C) The oxygen in samples of AlH_3 -1451 is believed to be present in the crystal lattice as well as on the surface. Our ability to use doping agents which increase the oxygen concentration, and the large amount of surface oxidation required to generate material with a high oxygen content, suggest this is the case. In addition, hydride samples carefully prepared under conditions of less than 1 ppm. of oxygen and water contain 0.2% to 0.3% oxygen, of which very little could have been the result of surface contamination.

CONFIDENTIAL

CONFIDENTIAL

(This page is Unclassified)



(U) Fig. 61 - Photograph of Oxygen and Water Analyzers

-145-

CONFIDENTIAL

(This Page is Unclassified)

CONFIDENTIAL

(C) A dry box was contaminated with molecular oxygen to determine its effect upon the preparation and stability of aluminum hydride. The dry box atmosphere was held constant at approximately 10,000 ppm. oxygen during a large series of runs. In 15 preparations under this environment, the oxygen concentration averaged 0.32% with 0.2% and 0.4% representing the maximum deviation. During this series of preparations, four reference samples had an average stability of 4.8 days before reaching 1% decomposition at 60°C. Two reference samples made prior to contaminating the box with 10,000 ppm. of oxygen averaged 0.17% oxygen and required only 3 days before reaching 1% decomposition. These data suggest that oxygen content affects stability, although the changes described are only changes in degree.

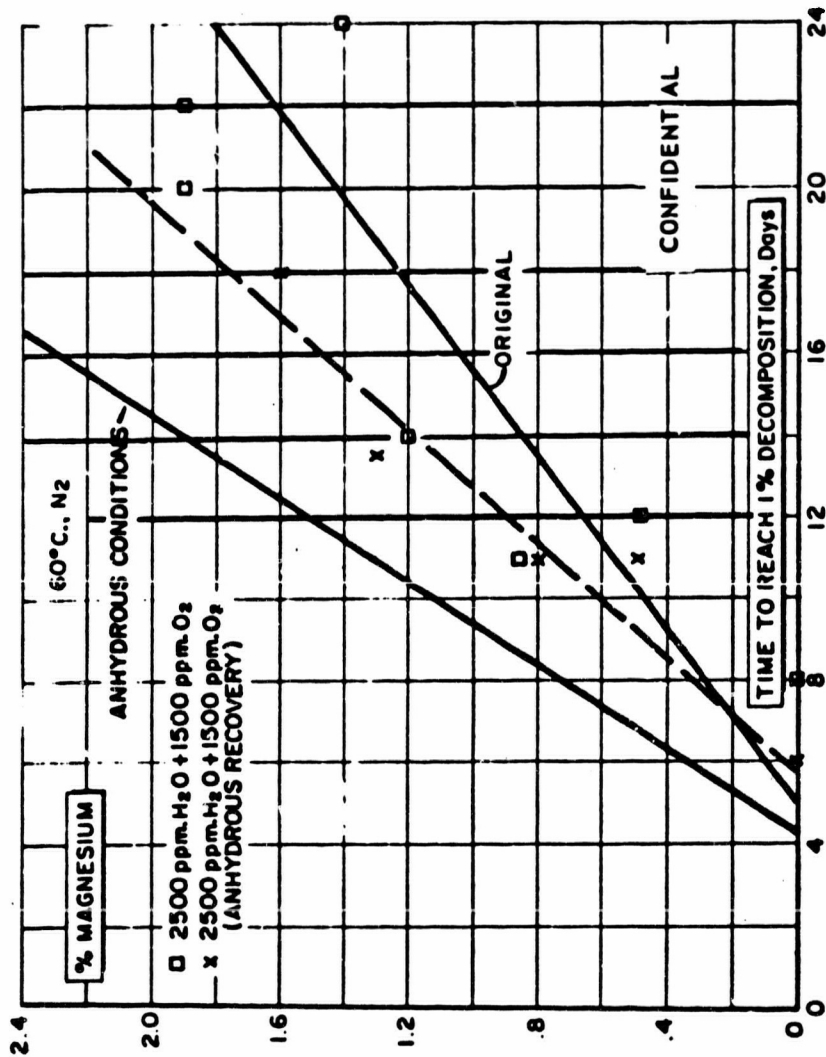
(C) It was later discovered that magnesium-doped materials prepared under water- and oxygen-free conditions were not as stable as originally observed. The relationship between magnesium concentration and stability as originally found is shown in Figure 62 along with the same relationship obtained under water- and oxygen-free conditions. The data indicate that the stability of the hydride prepared under oxygen- and water-free conditions again increases as magnesium concentration increases, but the slope and magnitude of improvement are not as great as originally observed. However, upon storage, these samples have become extremely stable with age. The resulting oxygen content of these samples was approximately 0.3%.

(C) In an attempt to determine the cause of change in this relationship, several preparations were made under an anhydrous (25 ppm. H_2O) nitrogen atmosphere containing 10,000 ppm. oxygen. The stabilities of 9 samples made under these conditions were nearly identical to those obtained under water- and oxygen-free conditions, suggesting that water was probably responsible for the change in relationship depicted in Figure 54. The average oxygen concentration in the samples was 0.59% with 0.43% and 1.07% representing the maximum deviation. The increased oxygen concentration appeared to have little effect upon the stability. It was also observed that it was more difficult to convert AlH_3-1433 to AlH_3-1451 when prepared under an atmosphere containing oxygen.

(C) Additional experiments were then carried out under controlled moisture conditions to further substantiate the effect of water. Several preparations were made in an inert atmosphere containing 2,500 ppm. water and 1,500 ppm. oxygen. The oxygen concentration was higher than desired because the oxygen scavenger also removed appreciable amounts of water making it impossible to maintain both a high water and low oxygen concentration. Preparation and hydride recovery under these conditions approximately duplicated the original relationship obtained between magnesium concentration and stability, as shown in Figure 62. The oxygen concentration in the final product under these conditions averaged 0.62%, with 0.5% and 0.75% representing the maximum deviation.

CONFIDENTIAL

CONFIDENTIAL



(C) Fig. 62 - Comparison between the Original and New Stabilization Obtained under Anhydrous Conditions of Aluminum Hydride-1451 as a Function of Magnesium Concentration at 60°C.

CONFIDENTIAL

CONFIDENTIAL

(C) To further elucidate the role played by water, a series of preparations was made under the same conditions, except the product was recovered under anhydrous conditions. The data are shown in Figure 62 with a dotted line drawn through the resulting points. This relationship was found to be intermediate between that obtained under completely anhydrous conditions. The oxygen concentrations from these experiments averaged 0.36%, with 0.25% and 0.47% representing the maximum deviation. There appeared to be a slight tendency towards increased oxygen concentration as the magnesium concentration increased. The data suggest that, in addition to magnesium, water is playing the major role in determining this relationship. The results indicate that water must have been originally present during preparation and recovery. The change in relationship obtained when the product was recovered under anhydrous conditions illustrates that surface treatment of the hydride with moisture is affecting the results. Independent surface treatment of magnesium-doped materials as well as normal hydride with water, as described in Section C.2.a., has indicated that it can significantly improve the stability of the hydride. A significant amount of the increased oxygen concentration appears to be a result of this surface treatment.

c. Reaction of Oxygen with Lithium Aluminum Hydride, Lithium Borohydride, and Aluminum Hydride (C)

(C) Since the removal of both oxygen and water from the aluminum hydride systems reduced the resulting oxygen concentration from approximately 0.7% to 0.3%, as determined by neutron activation analysis, it was decided that the reaction of each of the components with oxygen should be examined.

(1) Lithium Aluminum Hydride (U)

(C) Higuchi (12) reported a reaction of oxygen with lithium aluminum hydride which reduced the amount of active hydride in solution. When oxygen was passed through an ether - benzene solution containing 7.5 mmoles of lithium aluminum hydride, a precipitate was formed. Analysis of the filtered solution showed a decrease in both lithium and aluminum content as oxygen was added, and after 2500 cc. was bubbled through the solution practically all the lithium aluminum hydride was removed. Evaporation of the above solution to dryness left no solid residue, indicating that molecular oxygen does not form a soluble compound with lithium aluminum hydride in the binary mixture. The solid which precipitated from the above reaction was found to be amorphous by X-ray diffraction analysis.

(2) Lithium Borohydride (U)

(U) No precipitate was formed when oxygen was bubbled through a binary solvent containing lithium borohydride, in contrast to the experiment performed with lithium aluminum hydride. After the solvent was stripped away, a solid residue was obtained

CONFIDENTIAL

and found by X-ray analysis to be an unknown pattern, designated UP-1476. Hence, it appears that a soluble oxygen-containing species is formed when oxygen reacts with lithium borohydride.

(3) Aluminum Hydride (C)

(C) To investigate the effect of oxygen on aluminum hydride-ether solutions, oxygen was also bubbled through a solution of the hydride in an ether-benzene solvent. With a limited amount of oxygen, a white precipitate formed, which was very reactive with water, amorphous, and showed an AlH absorption peak at 5.2μ in the infrared spectrum, as shown in Figure 63. After drying under vacuum at 75°C ., the elemental analysis was 49.1% aluminum, 13.9% carbon, 4.89% hydrogen and 32.1% oxygen (by difference). Assuming that the carbon is due to diethyl ether and correcting the hydrogen and oxygen content for ether, the ratio of the non-etherated molecule is 1 aluminum:1.09 hydrogen:0.95 oxygen. Therefore, within experi-

mental error, a structure of $\left[\begin{array}{c} \text{Al-O} \\ | \\ \text{H} \end{array} \right]_x$ is suggested with the ether molecules coordinated to the aluminum.

(C) The compound is insoluble in diethyl ether, benzene, and tetrahydrofuran. In preliminary experiments with hydrogen fluoride, it reacted violently to produce aluminum fluoride. When the reaction was moderated by Freon-11 and a limited amount of HF used, a compound possessing a novel X-ray pattern resulted.

2. Surface Treatment Studies of Aluminum Hydride (C)

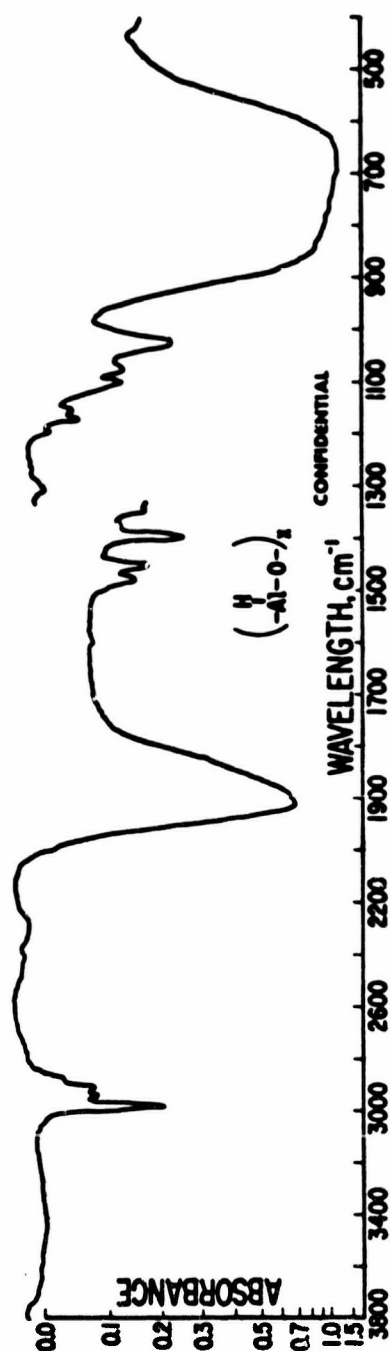
a. Effect of Surface Hydrolysis on Aluminum Hydride-1451 (C)

(C) Aluminum hydride will react with water and generate hydrogen, as given by the following equation:



The rate of hydrolysis is affected by pH, particle size, etc. Recently the rates of hydrolysis of various lots of Dow Pilot Plant material were examined. The rates of hydrolysis of 0.25 g. samples in 25 ml. of water are illustrated in Figure 64. A large difference in rate of hydrolysis under these conditions was observed ranging from 1.3 hours to 7.6 hours before reaching 10% hydrolysis based on the above equation. The corresponding oxygen content of the samples obtained from neutron activation analysis is given in Table XX. These samples differed very little in the oxygen content, suggesting that variations in surface oxidation were not responsible for these large differences in hydrolysis rate. However, it should be pointed out that neutron activation analysis does not differentiate between surface oxygen, oxygen incorporated into the lattice, or oxygen present in impurities. It is still possible that differences in surface oxidation existed.

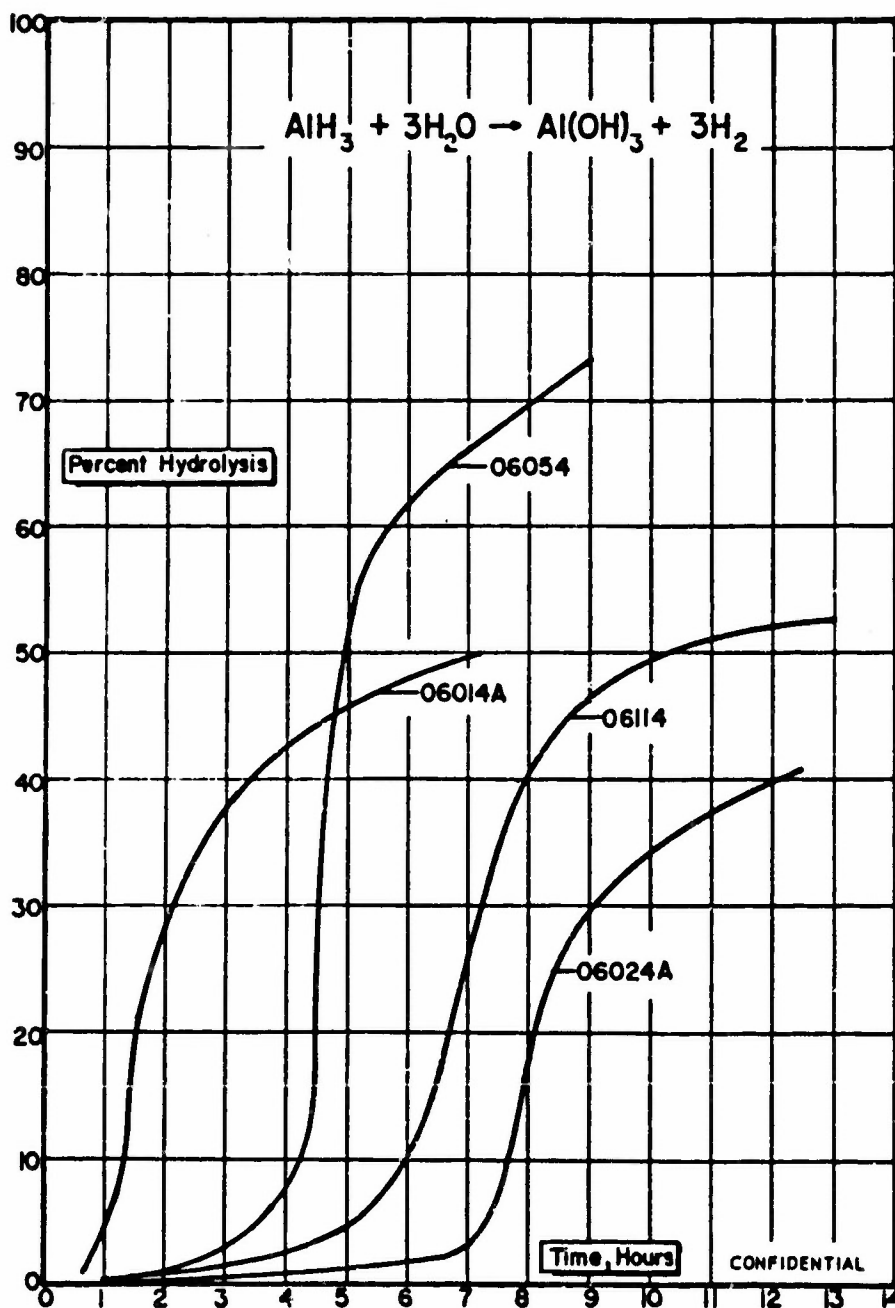
CONFIDENTIAL



(C) Fig. 63 - Infrared Absorption Spectrum of Solvated (AlHO)_x

CONFIDENTIAL

CONFIDENTIAL



(C) Fig. 64 - Hydrolysis Rate of Various Samples of Aluminum Hydride-1451

CONFIDENTIAL

CONFIDENTIAL

Table XX

(U) Oxygen Analysis of Dow Pilot Plant Samples

<u>Sample Number</u>	<u>Percent Oxygen^a</u>
06054	0.27 ± 0.019
06014A	0.22 ± 0.053
06114	0.18 ± 0.032
06024A	0.23 ± 0.018

^aBy neutron activation analysis.

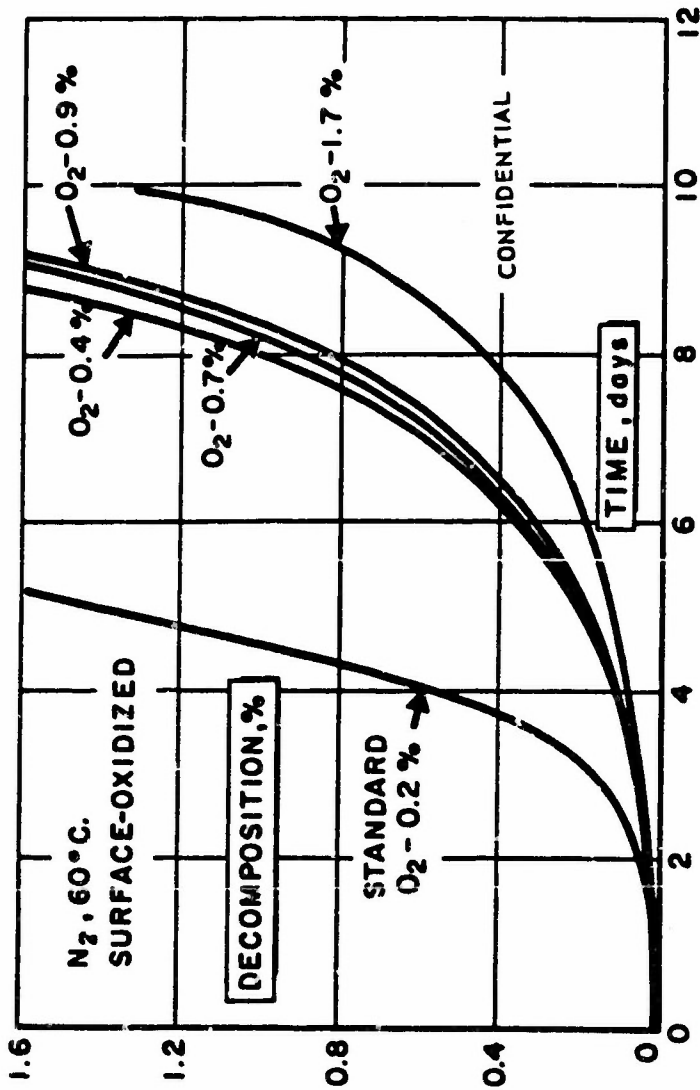
(C) It is also known from electron diffraction work done early in 1952 (9) that an aluminum hydride surface will become oxidized, forming an amorphous surface layer much like that formed by aluminum metal. More recently, work done by Allegany Ballistics Laboratory has very clearly documented that the surface of current aluminum hydride is not virgin. Various surface treatments used by the industry in passivating the hydride to improve compatibility, such as air exposure, wet VCN, etc., and our own recent efforts in evaluating the effect of oxygen and water on the preparation and stability of aluminum hydride have generated a new interest in surface oxidized hydride.

(C) The concept of improving stability through surface treatment has proven to be a valid approach toward improving stability. However, many different techniques and materials have been tried by our group and others in the industry with only a few surviving due to inconsistency of results. Currently, it does appear that an oxidized surface may be one of the best surface coatings available for the hydride. This surface condition has, to a degree, been characteristic of aluminum hydride and has probably affected the consistency of results by other surface treatments in the past.

(C) In an attempt to determine the amount of surface oxidation necessary to effectively improve stability, a hydride sample was partially hydrolyzed as previously described. Figure 65 illustrates the stabilities obtained on the various hydrolyzed portions of the original sample after being dried at 40°C. under vacuum for approximately 16 hours. The elemental analyses as a function of the degree of hydrolysis are given in Table XXI. It is interesting to observe that little improvement was gained by surface hydrolysis in excess of 0.1%. Electron diffraction studies of the surface at this level of oxidation, as well as the samples possessing correspondingly larger amounts of oxygen, showed it to be completely amorphous. A clear diffraction pattern of aluminum hydride-1451 was obtained from the reference sample. Table XXI shows that the elemental analysis changes slightly, but definitely, for small degrees of surface hydrolysis.

CONFIDENTIAL

CONFIDENTIAL



(C) FIG. 65 - Effect of Various Degrees of Surface Oxidation on the Stability of Aluminum Hydride-1451

CONFIDENTIAL

CONFIDENTIAL

Table XXI

(C) Elemental Analysis of Aluminum Hydride-1451
as a Function of Degree of Surface Hydrolysis

<u>Hydrolysis</u> <u>%</u>	<u>% O^a</u>	<u>% C</u>	<u>% H</u>	<u>% Al^b</u>	<u>Electron Diffraction</u> <u>Studies of Surface</u>
0	0.2	0.2	10.1	89.7	Crystalline
0.12	0.4	<0.1	9.9	89.0	Amorphous
0.35	0.7	<0.1	9.9	89.0	Amorphous
0.5	0.9	<0.1	9.9	89.0	Amorphous
1.3	1.7	0.1	9.8	88.1	Amorphous

^aBy neutron activation analysis.

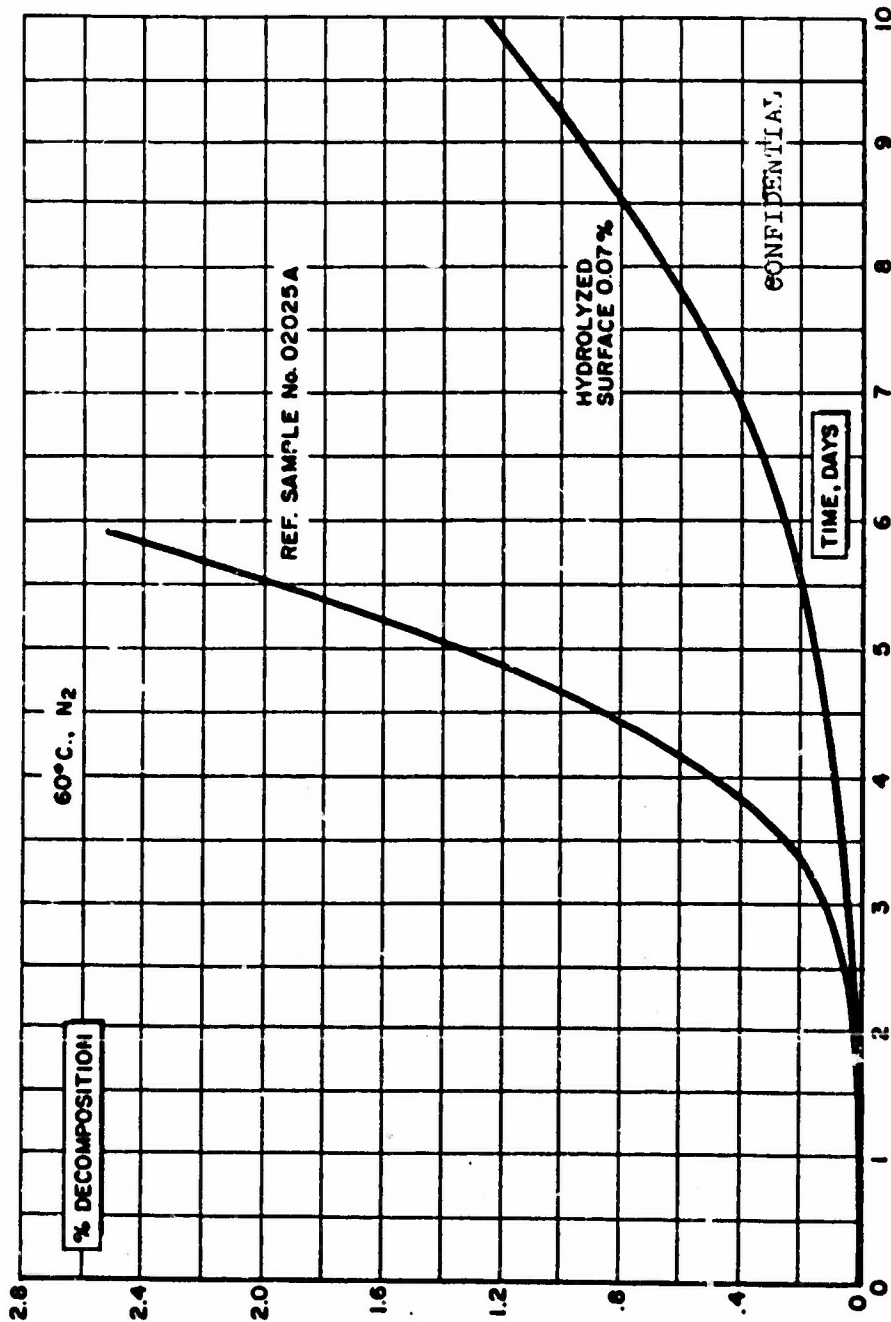
^b± 0.25%.

(C) The effect of a different aluminum hydride reference, lot 02025A surface hydrolyzed 0.07%, upon stability is shown in Figure 66. Both samples produced nearly a 100% improvement in thermal stability when compared before and after treatment. This, of course, does not evaluate any beneficial effects of such a treatment which might occur over long periods of time as previously discussed in Section B.3.

(U) The consistency of results in improving stability from partial surface hydrolysis is very encouraging. This material has also been formulated and found to be completely compatible with the ingredients, yielding theoretical densities. Experience with moisture treatments in formulation work by the industry has actually indicated an improvement in compatibility.

(C) A magnesium-doped hydride composite sample was surface-oxidized to further check results obtained under anhydrous conditions and also to determine if material possessing very good thermal stability could be improved. Experience with surface treatment such as VCN in the past has indicated that large improvements in stability could be obtained from poor samples, but very little benefit was obtained from a sample already possessing good stability. A comparison of the stabilities obtained before and after treatment is illustrated in Figure 67. The magnesium-doped sample hydrolyzed 1.8% improved in stability from 20 to 30 days before reaching 1% decomposition at 60°C. Hence, surface treatment and magnesium-doped hydride with moisture is certainly capable of affecting its rate of decomposition and complements the studies discussed in Section C.1.b.

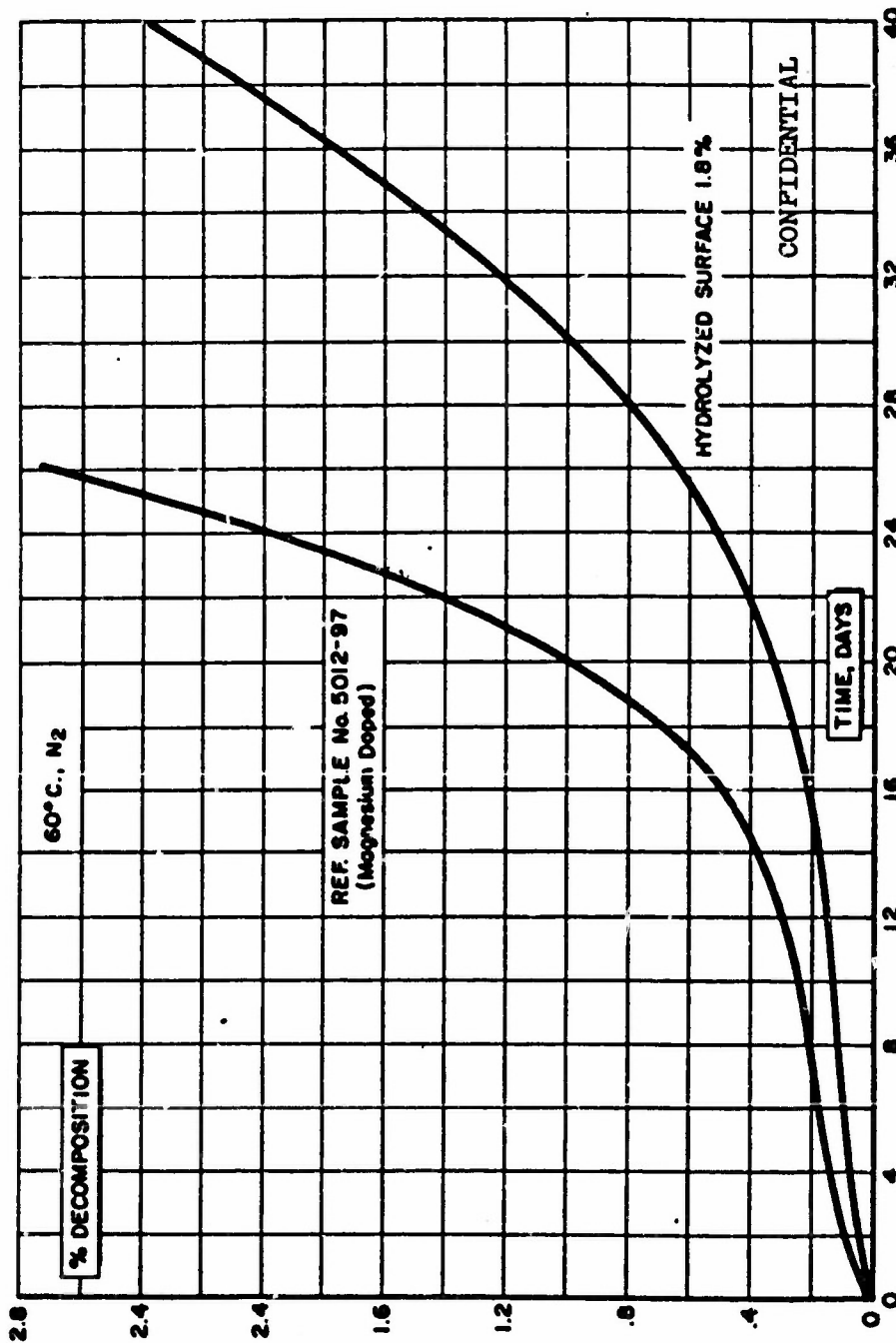
CONFIDENTIAL



(C) Fig. 56 - Effect of Surface Oxidation on the Stability of Aluminum Hydride-1451, Sample 02025A

CONFIDENTIAL

CONFIDENTIAL



(C) FIG. 57 - Effect of Surface Oxidation on the Stability of a Magnesium-Doped Aluminum Hydride-1451 Sample

CONFIDENTIAL

CONFIDENTIAL

b. Effect of Hydrogen Fluoride, Fluorine, Hydrogen Cyanide, and Carbon Monoxide on Aluminum Hydride-1451 (C)

(C) Attempts were made to stabilize commercial samples of AlH_3 -1451 by surface treatment with hydrogen fluoride, hydrogen cyanide, fluorine, and carbon monoxide. Liquid-solid and solid-gas phase interactions were used with hydrogen fluoride, hydrogen cyanide, and carbon monoxide. Anhydrous hydrogen fluoride was condensed upon AlH_3 -1451, and the liquid state maintained by using an ice bath. Ether and benzene suspensions of AlH_3 -1451 were used with hydrogen cyanide and carbon monoxide, respectively. Only a solid-gas phase interaction was attempted using fluorine.

(C) Surface treatment with hydrogen fluoride gave no evidence for fluorinated aluminum compounds. No significant improvement in stability, however, was observed at 100°C ., and metallographic studies suggested that surface cleaning took place rather than surface coating, as increased surface decomposition was noted.

(C) Surface treatment with fluorine gas was also attempted by allowing the sample to stand in the presence of the gas for approximately 35 minutes at ambient temperature. Again, as in the case of hydrogen fluoride, no fluorinated aluminum compounds were isolated. The sample, however, exhibited an increased rate of decomposition at 100°C . and a metallographic study of the sample again indicated an increase in surface decomposition.

(C) Surface treatment with hydrogen cyanide resulted in an acceleration of decomposition at 100°C . Mass spectrometric analysis of the gaseous product from thermal decomposition failed to detect hydrogen cyanide, although a yield of hydrogen greater than 100% was observed. Heating the solid AlH_3 -1451 during the run apparently increased the amount of surface interaction because the volume of evolved gas and the rate of decomposition increased.

(U) Treatment of a sample with carbon monoxide gave no appreciable change in decomposition rate at 100°C . No carbonyl bands could be detected by infrared analysis and no noticeable change resulted from temperature variations between ambient and 65°C .

3. Surface Studies of Aluminum Hydride-1451 (C)

(C) It has been demonstrated that the surface of AlH_3 -1451 is hydrophilic. Results of a survey of the surfaces of samples currently under long-term surveillance by electron diffraction examination indicate that the hydride surfaces have reacted with atmospheric moisture. The data are summarized in Table XXII. It was noted during examination of sample 02134A with a very low electron beam intensity that a pattern different than $\gamma\text{-Al}_2\text{O}_3$ was observed. Upon increasing the electron beam intensity, the pattern faded and $\gamma\text{-Al}_2\text{O}_3$ appeared. The d values of the unknown pattern corresponded very closely to those of the bayerite, $\alpha\text{-Al}(\text{OH})_3$. Bayerite starts to decompose at approximately 60°C ., transforming to $\gamma\text{-Al}_2\text{O}_3$ at approximately 300°C . It is known that a sample can be heated to this range simply by increasing the beam intensity.

CONFIDENTIAL

Table XXII

(C) Electron Diffraction Studies of the Surface
of Long-Term Surveillance Samples of Aluminum Hydride

<u>Sample Number</u>	<u>Analysis of Surface</u>
02034A	γ - or η - Al_2O_3
02044	γ - or η - Al_2O_3
02044A	γ - or η - Al_2O_3
02134A	γ - or η - Al_2O_3
03294	γ - or η - Al_2O_3
04194	γ - or η - Al_2O_3
06014A	Amorphous
06024A	γ - or η - Al_2O_3
06054	Amorphous
06104A	Amorphous
06104AT(VCN)	γ - or η - Al_2O_3 and Al°
07084	γ - or η - Al_2O_3 and Al°
07084T(VCN)	Amorphous
02055A	Amorphous
02125A	Amorphous
04185A	Amorphous (possibly LiAl_5O_8)
04195A	Amorphous
04265B	Amorphous
06225	Amorphous
06275	Amorphous
06285	γ - or η - Al_2O_3
8262-103I(Mg)	Amorphous
5853-141(Mg)	Amorphous (MgAl_2O_4)

(C) The surface of several samples, as shown in Table XXII, appeared to be completely amorphous, as no pattern could be obtained, with the exception of a pattern of aluminum found after prolonged searching. The aluminum, which is not reported in Table XXII, is believed to represent decomposition generated by the electron beam as the sample is heated during examination. In some instances, however, weak patterns of aluminum metal, which are thought to represent original decomposition of the hydride at the surface, are found during scanning of the samples.

CONFIDENTIAL

(C) It should also be pointed out that these samples are not ground or exposed to air prior to examination. The large crystal size ($\sim 100 \mu$) of the hydride does, to a degree, limit our ability to characterize the surface, since the electron beam examines only an area 1μ in width. Hence, a probability factor exists in examining the surface of the hydride; this implies that the condition of the surface reported in Table XX is not a complete characterization, but that the condition reported represents the probability of a greater portion of the surface existing in that state.

(C) It is known that if the samples are ground, a clear pattern of AlH_3 -1451 is immediately observed.

(U) In sample 04185A, a different pattern was observed which could possibly represent the formation of LiAl_5O_8 . The examination of the surface of a magnesium-doped sample (5853-141) also yielded a different pattern which closely resembles MgAl_2O_4 . This phase was not believed to be originally present, but was produced as a result of prolonged examination of the surface.

(C) Therefore, it is concluded that aluminum hydride possesses a hydrophilic surface. The surface developed as a result of this property consists of oxides (Al_2O_3), oxy-hydroxides (AlOOH), and hydroxides [$\text{Al}(\text{OH})_3$] varying in degree of molecular order from completely amorphous to crystalline Al_2O_3 .

4. Effect of Magnesium on Unit Cell Dimensions of Aluminum Hydride-1451 (C)

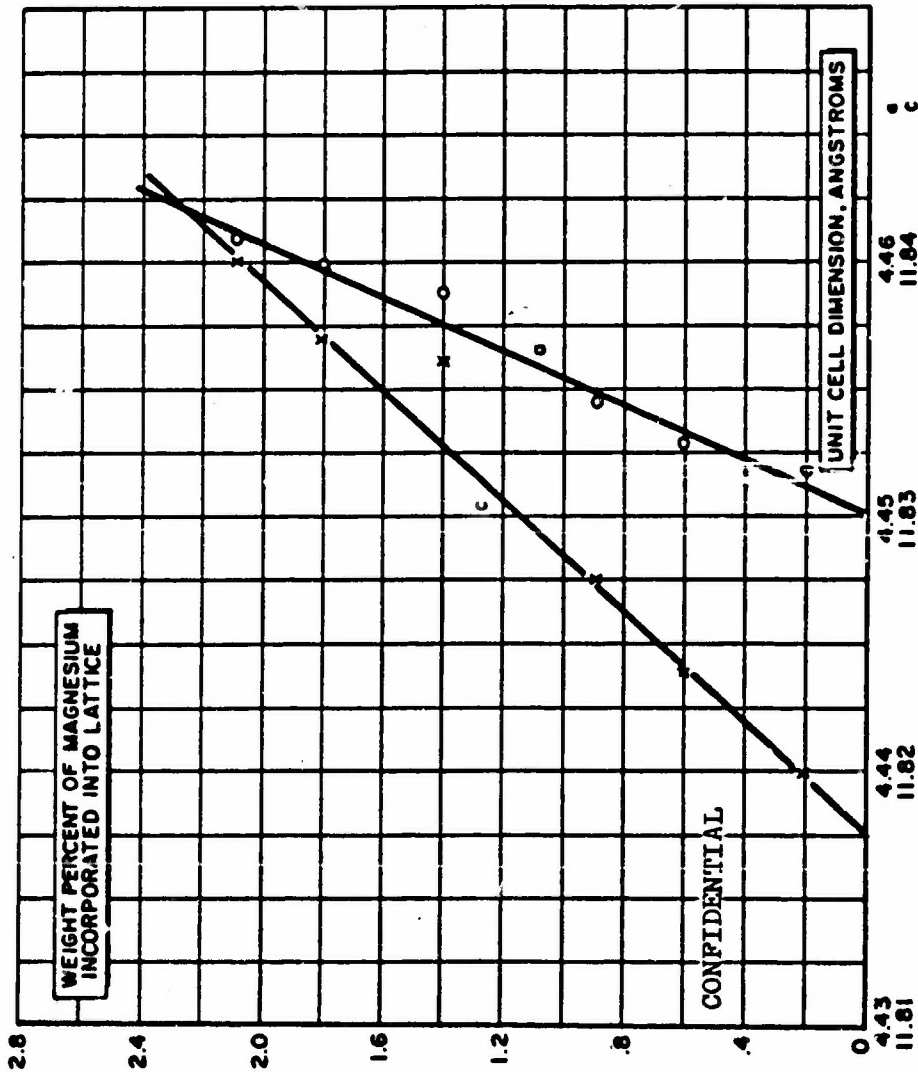
(C) It was pointed out by Dr. Bock of Edwards Air Force Base (8) that the incorporation of magnesium into the lattice of AlH_3 -1451 resulted in an expanded unit cell. An example of this phenomenon was previously reported (1); however, it was not known at that time if the lattice constants increased as the magnesium concentration increased or if the expansion was a linear function of percent magnesium.

(C) Subsequent to these original observations, a series of samples doped with various amounts of magnesium was obtained and evaluated. The unit cell dimensions of each sample were carefully determined from X-ray patterns taken on an AEC Guinier type focusing camera with aluminum as the reference. The resulting data are summarized in Table XXIII.

(C) The data clearly indicate that the lattice constants a and c increase as the magnesium concentration increases. The changes in lattice constants are reasonably small but easily detectable. The data also indicate that both the a and c lattice constants show approximately the same percent expansion although the c axes are changing more than the a axes. A plot of the data in Figure 68 shows that the unit cell expansion is nearly a linear function of the percent magnesium incorporated into the lattice.

CONFIDENTIAL

CONFIDENTIAL



(C) Fig. 68 - Unit Cell Dimensions of Aluminum Hydride as a Function of Weight Percent Magnesium Incorporated into Lattice

CONFIDENTIAL

CONFIDENTIAL

Table XXIII

(C) Unit Cell Dimensions of Aluminum Hydride
as a Function of Magnesium Concentration

<u>Sample No.</u>	<u>Wt. % Mg</u>	<u>a, Å</u>	<u>c, Å</u>
Original	0.3	4.4498	5.9062
5853-40	0.6	4.4518	5.9098
5853-23	0.6	4.4528	5.9118
5853-127	0.9	4.4544	5.9137
5853-128	1.38	4.4589	5.9180
5853-137	1.80	4.4598	5.9184
5853-145	2.09	4.4607	5.9200

5. Test Apparatus (U)

(C) The decomposition rate of aluminum hydride is known to be affected by mercury. The accuracy of the 100°C. vacuum decomposition apparatus was previously reported and found to be reliable for samples possessing "normal" stability, but unreliable for samples possessing improved stability such as magnesium-doped material (1). Therefore, all magnesium-doped samples are currently being evaluated at elevated temperatures with a pressure transducer apparatus.

(C) However, most other samples are currently evaluated at 60°C. by a modified Taliani apparatus. This apparatus has demonstrated relatively good precision, but the accuracy has not been completely established (13). Currently, this apparatus is being examined by comparing the measured decomposition rate with that measured by a pressure transducer apparatus. Using a pressure transducer, two of the samples were examined under vacuum and two under N₂, as shown in Table XXIV. Differences in the measured rates of decomposition at 60°C. have been observed; however, additional data are necessary before any definite conclusions regarding the accuracy of the modified Taliani apparatus can be drawn. It can be stated, though, that the results in general are similar.

D. CRYSTAL STRUCTURE STUDIES OF ALUMINUM HYDRIDE³ (C)

1. Comparison of Proposed Aluminum Hydride-1451 Structures (C)

(C) At the meeting of the Working Group on Analytical Chemistry of the Interagency Chemical Rocket Propulsion Group, February 24-26, 1965, three papers concerning the structure of AlH₃-1451 were presented. In particular, J. R. C. Duke of the Ministry of Aviation,

³Work by Dr. J. W. Turley of the Chemical Physics Research Laboratory of The Dow Chemical Company.

CONFIDENTIAL

Table XXIV

(C) Comparison of Decomposition Rates of Aluminum Hydride
as Measured by the Taliani and Pressure
Transducer Apparatus at 60°C.

Sample No.	Test	Decomposition, %					
		Days					
		1	2	3	4	5	6
8506-95	Transducer ^a	0.21	0.55	0.66	0.77	0.94	1.7
	Taliani ^a	0.02	0.05	0.23	0.46	0.66	0.90
5012-41-1	Transducer ^a	0.08	0.18	0.31	0.45	0.57	0.73
	Taliani ^a	0.07	0.15	0.29	0.49	0.75	1.7
8262-54	Transducer ^b	0.50	0.70	0.90	1.2	1.6	2.3
	Taliani ^a	0.02	0.04	0.30	1.2	2.2	---
8262-59	Transducer ^b	0.0	0.10	0.14	0.20	0.23	0.24
	Taliani ^a	0.02	0.05	0.18	0.65	1.72	---

^aNitrogen atmosphere

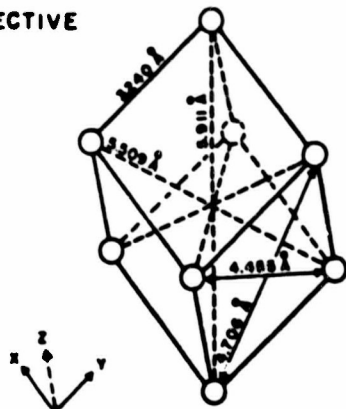
^bVacuum

Explosives Research and Development Establishment, Waltham Abbey, England, discussed the results of an X-ray diffraction analysis of this structure which conflicted with previously postulated structures. The excellent state of refinement of Duke's data, together with additional evidence from wideline proton NMR ("Configuration of LMH-2 by Wideline Proton NMR", by R. E. Swarbrick, Esso) reported at the same meeting, strongly suggests that the Al atoms are in the configuration as described by Duke and shown in Figure 69. In this structure, the aluminum atoms are at the points of the rhombohedral lattice and equidistant from each other. The Al-Al distance of 3.240 Å is considered to be due to hydrogen bridging, and Duke has assigned the hydrogens to positions midway between each pair of aluminum atoms on the edges of the rhombohedral cell. This arrangement leaves a fairly large cage-like hole in the center of the unit cell. The dimensions of this hole are given by the body diagonals, three of which measure 5.509 Å and one of which measures 5.911 Å. If the aluminum atom has a radius of 1.43 Å, then the largest dimension of this space is 3.051 Å; the shorter dimension is 2.649 Å. The second and third closest Al-Al distances are given by the two face diagonals 4.455 Å and 4.706 Å.

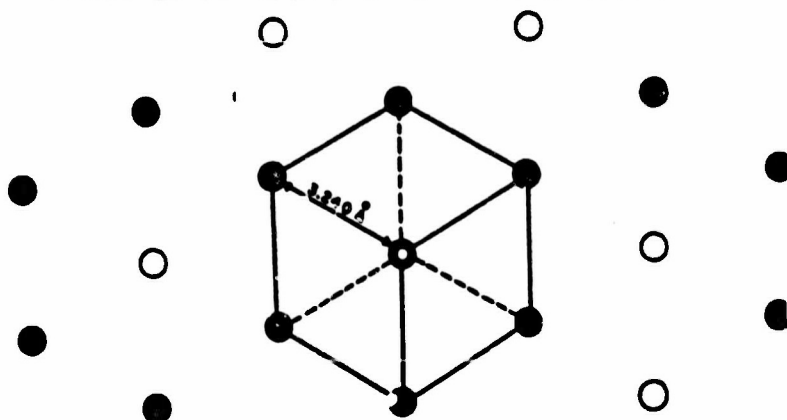
(C) The hexagonal structure for AlH₃-1451 reported by Dow earlier is shown in Figure 70. In this unit cell, the c-axis of 5.911 Å and the a-axis of 4.455 Å correspond to the 5.911 Å body

CONFIDENTIAL

IN PERSPECTIVE



PROJECTED ON THE (111) PLANE WITH UNIT CELL SHOWN



CONFIDENTIAL

RELATIVE HEIGHT
ALONG (111) AXIS

●	3.941 Å
◐	1.970 Å
○	ZERO

Approx. Scale : 1 in. = 2 Å

(C) Fig. 69 - Aluminum Hydride-1451 Structure
Proposed by Duke

CONFIDENTIAL

CONFIDENTIAL

diagonal and the 4.455 Å face diagonal respectively in Duke's rhombohedral cell. For further comparison, the corresponding distorted rhombohedral cell has been sketched in with four 3.470 Å and two 2.869 Å edges. It is to be noticed that in both structures the atoms lie on planes which are perpendicular to the c-axis or to the body diagonal, which are 1.970 Å apart. In these planes, the aluminum atoms have the same positions with respect to each other in both structures; the difference lies in the positioning of the planes with respect to each other. In the Dow structure, each aluminum atom has one 2.869 Å approach and two 3.470 Å approaches to aluminum atoms in both the plane above it and the plane below it. In Duke's structure, each aluminum atom has six 3.240 Å approaches, three to aluminum atoms in the plane above and three to aluminum atoms in the plane below. Thus, the transformation from the Dow structure to Duke's structure can be visualized as a horizontal shifting of the planes of atoms above and below a given plane until all of the atoms are equidistant and 3.240 Å apart. During this maneuver, the configuration within the planes is held constant.

(C) Although the evidence for Duke's structure is convincing with respect to the aluminum atoms, the evidence for the hydrogen positions is not nearly so strong. Because of the basic difficulty of obtaining reliable information about hydrogen atoms from X-ray diffraction data, neutron diffraction data have been obtained.

(C) The structure based on the interpretation of these data is discussed in Section D.2. The structure of aluminum metal is shown in Figure 71. This was previously compared with the Dow AlH_3 -1451 structure but Duke's structure shows an even closer relation. In the metal, the atoms in a plane are 2.86 Å apart, and in the hydride they are 4.455 Å apart; the configuration of the aluminum atoms is the same in both. In the metal the planes are 2.338 Å apart, and in the hydride they are 1.970 Å apart. Therefore, the net result of the decomposition of the hydride to the metal is an increase in the interlayer distance and a decrease in the interatomic distances within the layer.

2. X-Ray and Neutron Powder Diffraction Data (U)

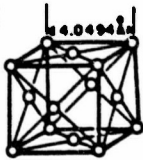
a. X-Ray Powder Diffraction Data for Aluminum Hydride-1451 and Aluminum Deuteride-1451 (C)

(C) Although the AlH_3 -1451 crystal structure reported by Duke (6) appeared to be acceptable and reasonably well-substantiated, analysis of the neutron powder diffraction data shows unequivocally that the X-ray powder pattern line at 1.93770 Å, which was disregarded by Duke, belongs to the 1451 pattern and must be included in any refinement of the structure. It also follows from this that the c-dimension of the crystal unit cell is twice the value reported by J. R. C. Duke. Further consideration has also been given to the choice of a space group for this structure. The fact that $R\bar{3}m$ requires two sets of equivalent positions to describe the aluminum atoms, which are almost certainly equivalent, leads to the choice

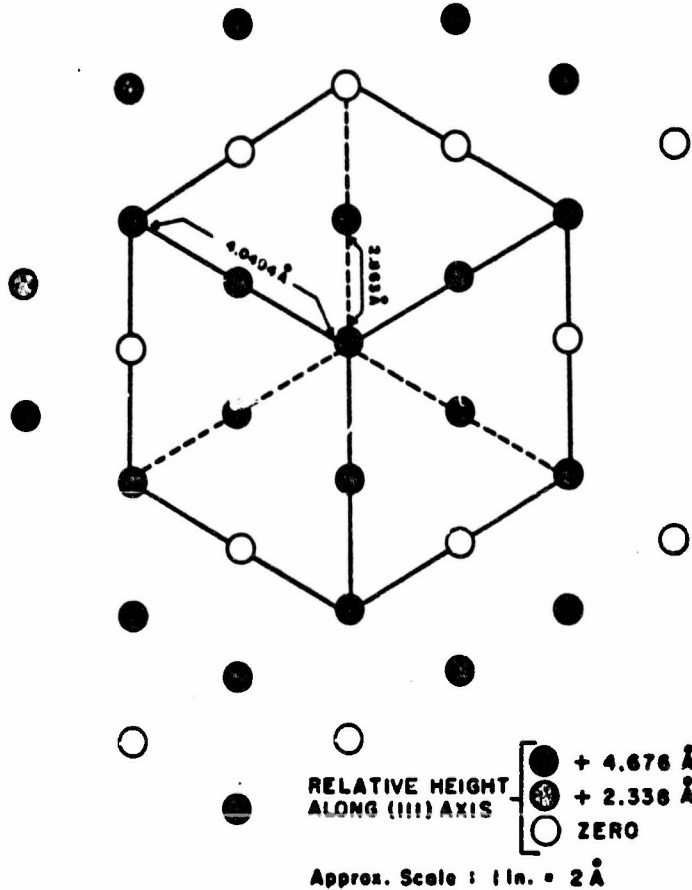
CONFIDENTIAL

(This page is Unclassified)

IN PERSPECTIVE



PROJECTED ON THE (111) PLANE WITH UNIT CELL SHOWN



(U) Fig. 71 - Face-Centered Cubic Structure
of Aluminum Metal

-166-

CONFIDENTIAL

(This page is Unclassified)

CONFIDENTIAL

of the higher symmetry space group $R\bar{3}c$. Special positions 6(a) and 18(e) in this space group are being used for the Al and H (or D) atoms, respectively. The unit cell dimensions for both the hydride and deuteride have been refined using Frevel's methods of axial ratios (14) with observed d-spacings measured from a film obtained with an AEG focusing camera. The new values below are expressed in both the hexagonal and rhombohedral systems:

	Hexagonal	Rhombohedral
AlH ₃ -1451	a = 4.4498 Å, c = 11.8123 Å	a = 4.7015 Å, α = 56.49 Å
AlD ₃ -1451	a = 4.431 Å, c = 11.774 Å	a = 4.6848 Å, α = 56.45 Å

Table XXV compares observed and calculated d-spacings for both crystals, indexed in the hexagonal system.

b. Neutron Powder Diffraction Data for Aluminum Deuteride-1451 and Aluminum Hydride-1451 (C)

(C) Neutron powder diffraction data for AlH₃-1451 and AlD₃-1451 were obtained at Argonne National Laboratory through the courtesy of Dr. S. S. Sidhu. A 10-12 gram sample was required for the experiment and the diffracted intensities were recorded using counter techniques. A 0.1°, 2θ step-scan technique was used for the 1451 compounds. The experimental results were obtained in the form of a list of 2θ values and corresponding counts plus a strip chart record used to monitor the experiment.

(C) The AlH₃-1451 data showed a high background with only 5 or 6 peaks. The AlD₃-1451 pattern was much more complex, showing at least 15-20 peaks. Sets of hydride-deuteride data are generally used to solve for phase angles of reflections common to both sets. The method is based on knowing the scattering length for H is negative and that for D is positive, so that enhancement or diminution of a peak in one pattern in comparison with the same peak in the other pattern can be interpreted in terms of positive and negative phase angles. However, this hydride data will not be processed because a trial structure is already available for AlH₃-1451. The deuteride data have been plotted (counts vs. 2θ), and the overlapping peaks resolved by "peeling." The graphical integrations have been carried out using a planimeter, and indexing of the peaks has been satisfactorily completed. Indexing in both the rhombohedral and hexagonal systems is shown in Table XXVI. The observed and calculated 2θ values as well as the normalized intensities are given. Aluminum and deuterium each have about the same scattering power for neutrons in contrast with the strong scattering power of Al and weak scattering power of deuterium for X-rays. As a result, the neutron diffraction intensities are very sensitive to shifts in position of the deuterium atoms, and a structure refinement should give reliable information about these positions.

CONFIDENTIAL

Table XXV

(C) X-Ray Powder Diffraction d-Spacings for Aluminum Hydride-1451 and Aluminum Deuteride-1451^a

Aluminum Hydride-1451			Aluminum Deuteride-1451		
hkl	d(obs)	d(calc.)	hkl	d(obs)	d(calc.)
012	3.2284	3.2274	012	3.217	3.2147
104	2.3445	2.3440	104	2.336	2.3355
110	2.2252	2.2249	110	2.215	2.2155
006	1.9686	1.9687	006	1.962	1.9623
113	1.9377	1.9370	113 (weak)	1.920	1.9293
202	1.8316	1.8318	202	1.824	1.8242
024	1.6134	1.6137	024	1.607	1.6074
116	1.4743	1.4744	116	1.469	1.4690
122	1.4140	1.4142	122	1.408	1.4083
018	1.3788	1.3788	018	1.375	1.3742
214	1.3064	1.3063	214	1.301	1.3010
300	1.2846	1.2846	300	1.279	1.2791
1·0·10	1.1292	1.1294	208	1.168	1.1678
220	1.1124	1.1124	119	1.126	1.1265
306	1.0765	1.0758	220	1.108	1.1078
312	1.0526	1.0517	306	1.072	1.0716
128	1.0374	1.0369	312	1.047	1.0473
0·2·10	1.0071	1.0070	128	1.033	1.0330
134	1.0045	1.0050	0·2·10, 134	1.002	1.0035, 1.0009
0·0·12	0.9833	0.9844	0·0·12	0.980	0.9812
			226	0.965	0.9647
			042	0.947	0.9468
			2·1·10, 404	0.913	0.9141, 0.9121
			1·1·12, 137	0.878	0.8994, 0.8971
			232	0.871	0.8707
			318	0.863	0.8624
			324	0.841	0.8434
			410	0.838	0.8374
			235	0.829	0.8246
			048	0.804	0.8037

^aObserved data were recorded with an AEG focusing camera and represent averages of five Norelco charts.

CONFIDENTIAL

CONFIDENTIAL

Table XXVI

(C) Neutron Powder Diffraction Data for
Aluminum Deuteride-1451 Space Group R $\bar{3}$ c

<u>I/I₀(obs)</u>	<u>2θ(obs)</u>	<u>2θ(calc)</u>	<u>(hexagonal) hki</u>	<u>(rhombohedral) hkl</u>
18.34	18.98	19.14	012	110
7.93	27.80	{26.46 27.92	104 110	211 10 $\bar{1}$
100.00	32.03	{31.61 32.17	006 113	222 210
10.66	38.84	38.85	024	220
29.42	42.68	42.67	116	321
6.19	43.58	43.59	211	20 $\bar{1}$
3.51	44.26	{44.61 45.78	122 018	21 $\bar{1}$ 332
27.87	49.42	{48.51 49.40	214 300	310 2 $\bar{1}$ $\bar{1}$
2.91	51.52	51.29	125	320
4.87	54.60	54.48	208	422
27.17	56.80	{56.65 56.70 57.70 58.24	119 10010 220 217	432 433 20 $\bar{2}$ 421
40.31	60.40	{59.84 60.18 60.56 61.37 62.32	306 223 131 312 128	411 31 $\bar{1}$ 21 $\bar{2}$ 30 $\bar{1}$ 431
17.02	67.09	{66.02 66.89 67.29 68.74	00012 315 226 042	444 410 420 222

CONFIDENTIAL

Table XXVI (Contd.)

<u>I/I₀(obs)</u>	<u>2θ(obs)</u>	<u>2θ(calc)</u>	(hexagonal) <u>hkl</u>	(rhombohedral) <u>hkl</u>
3.98	73.18	71.57	2·1·10	532
		71.75	404	400
		72.93	137	430
		73.14	1·1·12	543
		75.01	321	302
0.31	75.90	75.74	232	312
		76.60	318	521
13.49	78.81	76.72	1·2·11	542
		78.43	229	531
		78.65	324	411
		79.33	410	312
		80.81	235	421
6.69	81.71	81.18	0·1·14	544
		81.49	413	401
		85.22	1·3·10	541
11.63	87.45	86.52	327	520
		86.72	0·3·12	552
		87.88	2·0·14	644
		87.89	416	510
		88.18	2·1·13	643
		89.23	502	411
		90.06	238	530
		90.18	3·1·11	632
		91.89	4·0·10	622
		92.06	054	332
9.52	92.45	92.51	1·1·15	644
		92.73	330	303
		93.39	2·2·12	642
		94.56	1·2·14	653
		94.86	333	412
		95.20	241	313
		95.39	1·0·16	655
		95.91	422	402

CONFIDENTIAL

3. Present State of Refinement of the Aluminum Deuteride-1451 Structure (C)

(C) From the discussion of space group symmetry in Section D.2.a., it is seen that all atoms in this structure are in special positions. The aluminum atoms are at fixed lattice points with no variation in position allowed, and the position of the deuterium atoms is a one-parameter problem. Intensity ratios for a set of six uniquely indexed peaks were used to give and obtain a trial solution to this problem. The unrefined parameter gives a value of about 1.8 Å for the Al-D bond distance in the bridge. In the boron hydrides, this bridging distance is approximately equal to the sum of the covalent radii of the atoms. For the AlD_3 , $1.18 (\text{Al}) + 0.3 (\text{D}) = 1.55 \text{ Å}$, although, in this case, the use of the 1.43 Å atomic (or metallic) radius for aluminum gives better agreement. Figure 72 is a schematic drawing of the structure as viewed along the hexagonal c-axis. The aluminum atoms are octahedrally coordinated to six bridge-forming hydrogens, as shown by the drawing of the coordination polyhedron for the central atom at $Z = 1/2$ with three hydrogens at $Z = 0.42$ and three hydrogens at $Z = 0.58$. In this figure, the solid lines outline the unit cell, and the numbers at atom positions give Z coordinates for those atoms. The bridging at the central aluminum at $Z = 1/2$ to the six nearest aluminum neighbors is shown in Figure 73. In one unit cell, the structure is represented by three different columns, parallel with the Z-axis, of two aluminums each, and by two different columns, also parallel with Z, of three hydrogens each. The bridging of the three hydrogens on one column to the surrounding three columns of aluminum atoms is shown in Figure 74. Each column of aluminum atoms is surrounded by six columns of hydrogen atoms (three of each kind).

(C) In Figure 75, the motion of hydrogen atoms which is required to transform Duke's proposed structure into the above-discussed structure is shown with arrows. The change produces a configuration which appears to fill the lattice more uniformly than that proposed by Duke (6); however, further comment will be withheld until refinement of the structure is completed.

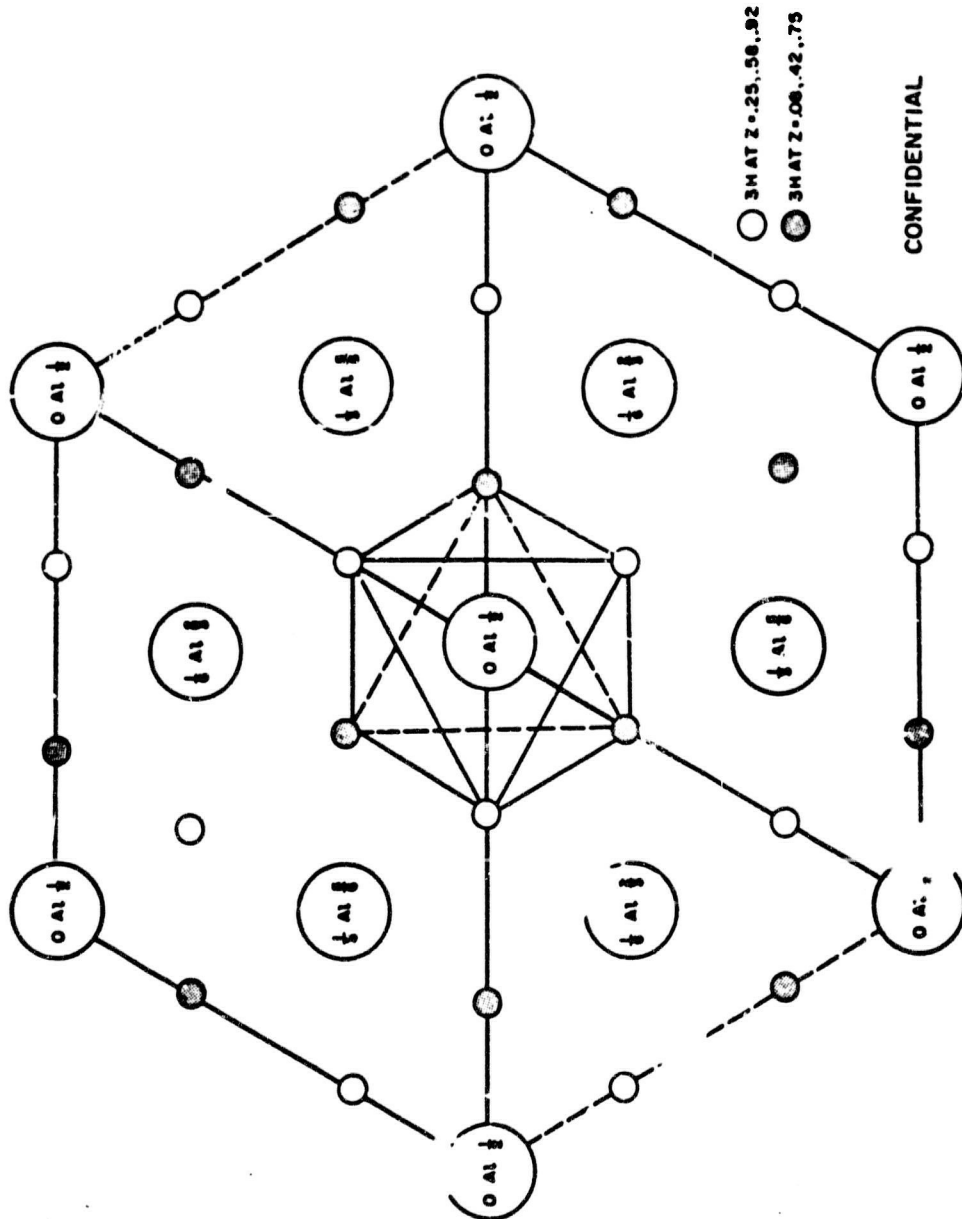
4. Characterization of Aluminum Hydride-1717 and Aluminum Hydride-1563 (C)

(C) Microscopic examination of some recent samples showed large crystals of two different polymorphs. These were separated under the microscope and then used for further identification by single crystal methods. Crystals of AlH_3 -1717 and AlH_3 -1563 have been separated from a mixture of AlH_3 -1451, AlH_3 -1717, and AlH_3 -1563.

(C) Crystals of AlH_3 -1717 are colorless and tablet-shaped, approximately square, and about 1/5 to 1/10 as thick as they are wide. They are of orthorhombic symmetry and crystallize in space group $\text{C}21\text{cm}$, $\text{Cmc}2_1$, or cmcm with extinction rules

$hkl,$	$h + k = 2n,$	c-centered unit cell
$hol,$	$l = 2n,$	c-glide plane

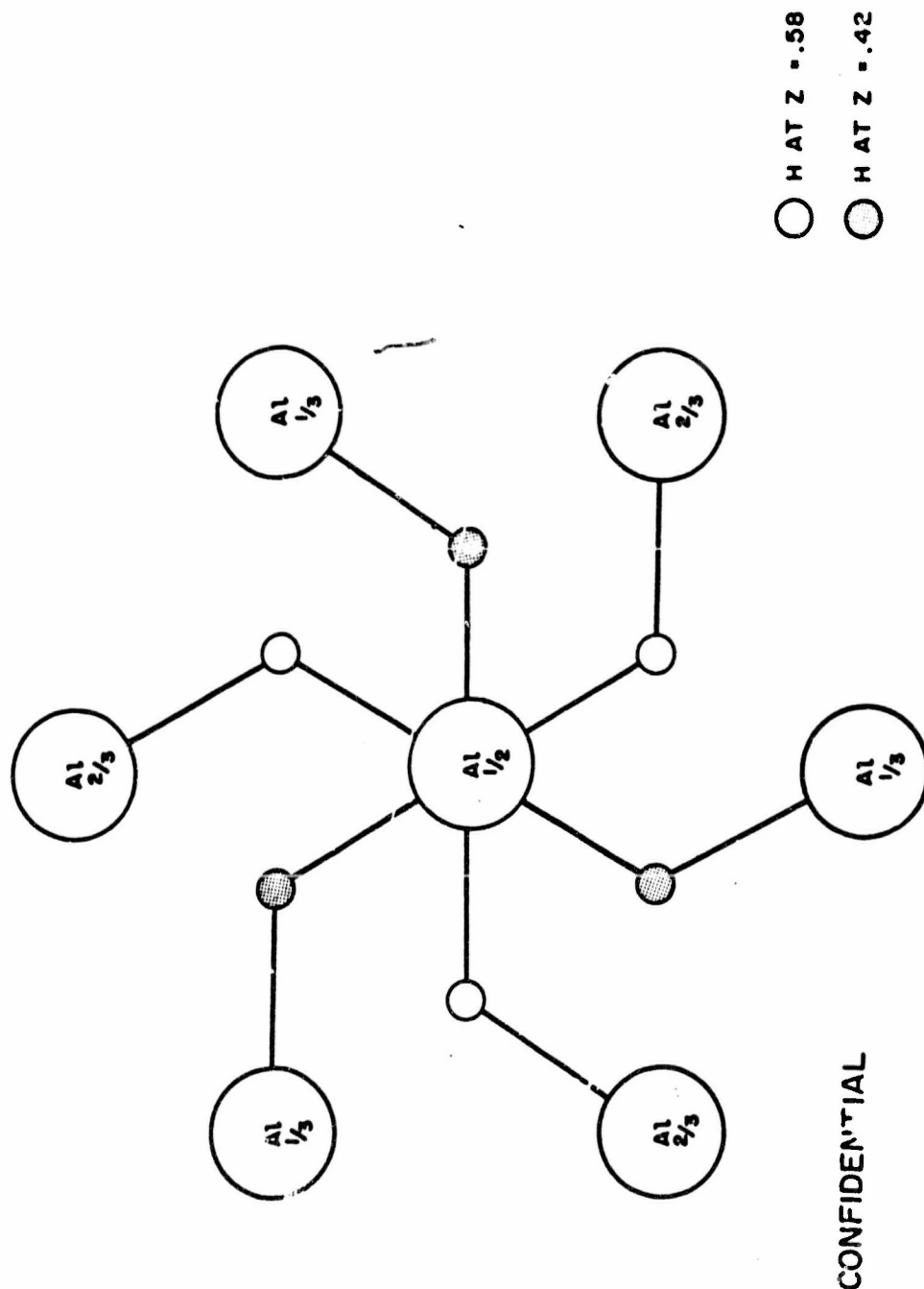
CONFIDENTIAL



(c) Fig. 72 - Schematic Drawing of the Structure of Aluminum Hydride-1451 in Projection on the (001) Plane Showing the Aluminum Coordination

CONFIDENTIAL

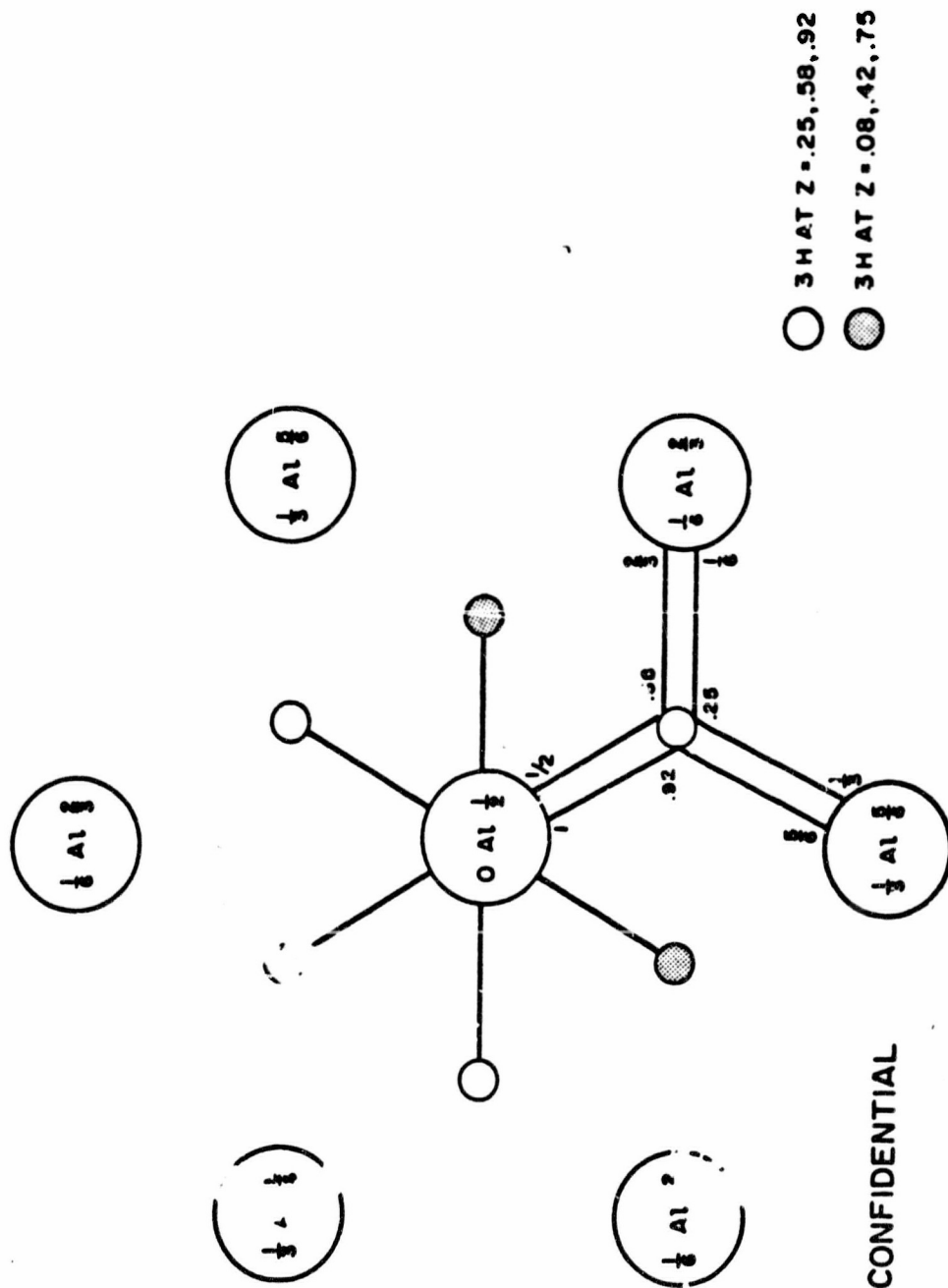
CONFIDENTIAL



(C) Fig. 73 - Schematic Drawing of the (001) Projection of Aluminum Hydride-1451 Structure Showing the Al-H-Al Bridging for one Aluminum

CONFIDENTIAL

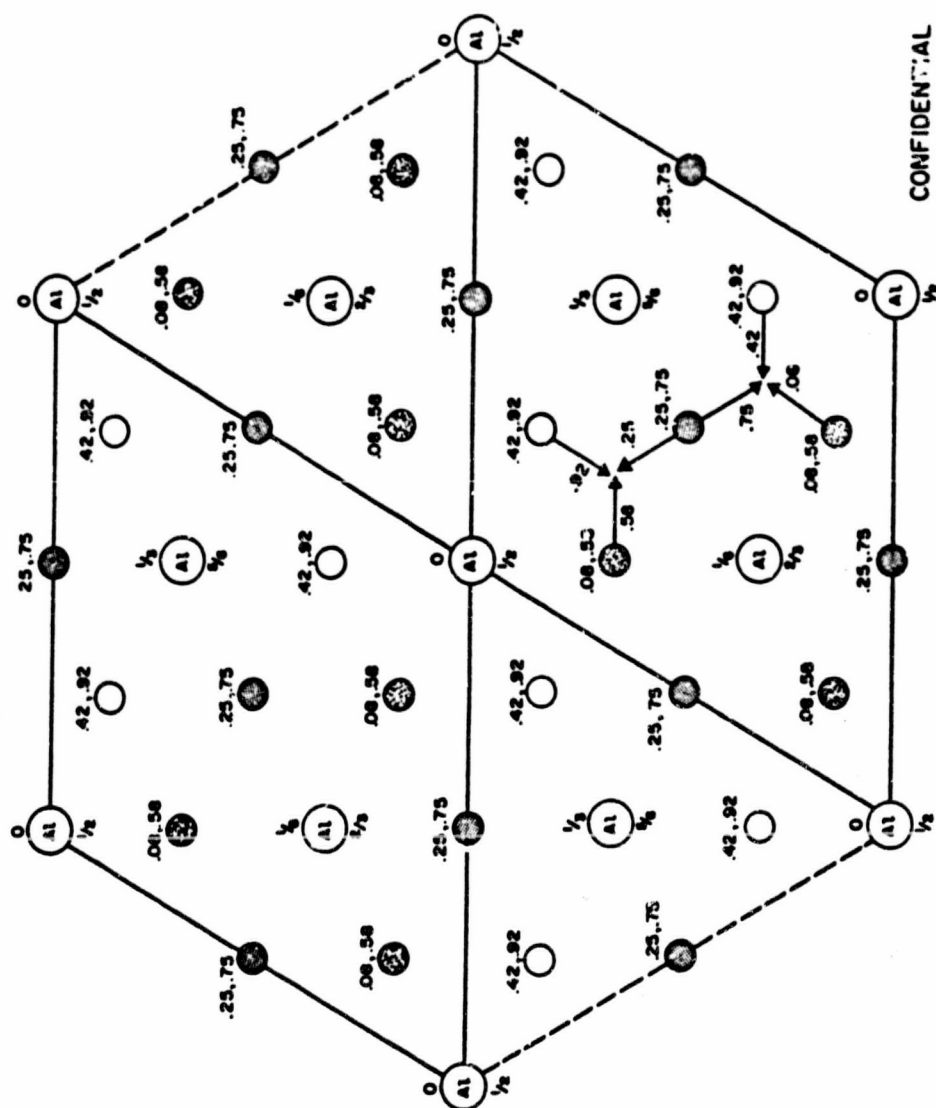
CONFIDENTIAL



(C) Fig. 74 - Schematic Drawing of the Structure of Aluminum Hydride-1451 in Projection on the (001) Plane Showing the Bridging of the Three Hydrogens on one Column

CONFIDENTIAL

CONFIDENTIAL



CONFIDENTIAL

(U) Fig. 75 - Schematic Drawing Illustrating the Relationship Between 'Dukes' and the Newly Proposed Structure as Viewed from the Projection on the (001) Plane

CONFIDENTIAL

CONFIDENTIAL

and unit cell dimensions:

$$a = 8.661 \text{ \AA}, \quad b = 9.923 \text{ \AA}, \quad c = 12.755 \text{ \AA}$$

(C) Although the indexing of the observed X-ray diffraction pattern is not yet complete, agreement between calculated and observed d-spacings appears to be satisfactory. A calculation of d-spacings out to the limit of the Cu reflecting sphere shows that 700 non-equivalent X-ray diffraction lines are allowed.

(C) Crystals of AlH_3 -1563 are colorless and rectangular, with an approximately diamond cross-section. Efforts to mount one of these crystals have not yet been successful.

E. EVALUATION OF ALUMINUM HYDRIDE-1451 AS A PROPELLANT INGREDIENT

(C) A program of study encompassing the stability, compatibility, formulatability, and aging characteristics of propellant containing AlH_3 -1451 fuel was undertaken. The purpose of this work was to detect and identify those reactions or processes taking place in the propellant system which could significantly affect the performance of rocket propellants containing AlH_3 -1451. The study included both double base and composite propellant systems. Normal hydride, as well as some of the most recently synthesized improved AlH_3 -1451, was evaluated.

(C) The study was divided into two parts, formulation-compatibility investigations and long-term stability surveillance. Compatibility studies were conducted on samples of double base and composite propellant. These were first formulated in the dry box, then cured in the Taliani apparatus at 60°C . Observations were made of the rates of gas evolution as indicators of system incompatibility. Long-term aging studies at 25°C . and 40°C . were also conducted on larger samples, 1/4-lb. motors and 1/5-lb. slabs, stored in surveillance bombs. Periodically, analyses were made of the gas in these bombs to determine the onset of decomposition. From time to time the ballistic and physical properties of samples of propellant were also studied. In this work, however, only double base propellant was surveyed because of the limited compatibility of the composite formulations.

(C) Formulations and compatibility studies have indicated the relative compatibility of AlH_3 -1451 with the different propellant ingredients. Epoxies and BDNPA, bis(2,2-dinitropropyl)-acetal, were found to increase the rate of decomposition of the hydride when compared to the neat AlH_3 -1451, but nitrocellulose (which contained ethyl centralite) and other nitro esters (TMETN) exhibited a stabilizing influence.

(C) Surveillance studies have provided decomposition rates of AlH_3 -1451 in double base propellant of approximately 1.12×10^{-3} percent per day at 25°C . after 125 days, and 3.00×10^{-3} percent per day at 40°C . after 100 days. If the gassing rate remained

CONFIDENTIAL

constant at these values the hydride would be expected to exhibit 0.4% decomposition per year, or 2% decomposition in five years at 25°C. At 40°C. the hydride should show 1.1% decomposition per year or 5.5% decomposition in five years. In addition, some insight into the aging characteristics of the propellant has been gained. A slight hardening and embrittlement of the AlH_3 -1451 double base propellant occurs with age, but voids formed in the propellant by decomposition of the AlH_3 -1451 were not observed.

(C) A procedure has been developed for recovering the AlH_3 -1451 from a cured propellant sample of double base propellant. A solvent is used to remove the other ingredients, leaving the insoluble crystals of AlH_3 -1451. Analytical results from the recovered AlH_3 -1451 indicate that a coating consisting of oxides of nitrogen has formed on the surface of the AlH_3 -1451.

1. Compatibility Studies of Aluminum Hydride-1451 (C)

(C) As a complementary program to the surveillance program, studies have been conducted on the reactivity of typical propellant ingredients with various types of AlH_3 -1451. This work has already been conducted in the Taliani gas evolution apparatus at 60°C. with the rates of gas evolution giving a quantitative indication of compatibility. Qualitative analyses by mass spectroscopy of the off-gases have also been made. The solid residues from these tests have been analyzed by X-ray diffraction. Chemical methods have been developed to allow a more complete study of these residues to indicate the nature of AlH_3 -1451 decomposition in a propellant grain. The solubility of hydrogen in the propellant ingredients was determined but found to be negligible.

(U) Work is also in progress to develop data on the diffusivity of hydrogen in the propellant. This work should provide the corrective factors needed for accurate interpretation of Taliani and formulation data.

(C) The Taliani studies have included magnesium-doped and surface-hydrolyzed samples of AlH_3 -1451 as well as a standard lot (02055) of the hydride. The hydride was combined with propellant ingredients in various combinations. The weight ratio of hydride to the other propellant ingredients was maintained at the concentrations listed in Table XXVII. In all cases, 0.25 g. of AlH_3 -1451 was combined with the corresponding amount of propellant component being checked. No special preparation of the ingredients other than removal of shipping solvents was used, with the exception of the Epon 82 epoxy resin which will be discussed later. The Taliani tests were run at 60°C. under an inert atmosphere. A list of these tests is presented in Table XXVIII. Some of the corresponding off-gas analysis results are listed in Table XXIX. In an effort to correlate the Taliani results to propellant ingredient contaminants, analyses were run to determine water and free hydroxyl content of some of the ingredients. The results of these determinations are given in Table XXX.

CONFIDENTIAL

Table XXVII

(C) Composition of Propellant Formulations

<u>Material</u>	<u>Double Base Propellant, %</u>	<u>Composite Propellant, %</u>
HX 735	---	9.4
PGNC	12.0	---
MAPO	---	1.2
Epon 812	---	0.8
TMETN	---	14.2
NG	26.2	---
TEGDN	4.4	--
BDNPA	4.4	---
2-NDPA	1.0	---
Resorcinol	1.0	---
1451	25.0	25.0
AP	26.0	49.4

(C) The early Taliani results, shown in Figure 76, indicated that the composite propellant system increased the decomposition rate of the AlH_3 -1451 as compared with neat AlH_3 -1451; however, the double base propellant system exhibited a reduced decomposition rate. This suggested a possible incompatibility of the AlH_3 -1451 with an ingredient in the composite system and a possible stabilization of the hydride by an ingredient in the double base formulation. Studies were then directed at identifying and determining the cause and ingredients responsible for these phenomena.

(C) The composite system was first examined on the Taliani apparatus by combining each of the ingredients with AlH_3 -1451. The rate of gas generation from these studies is plotted in Figures 77 and 78. Generation of 300 mm. mercury pressure very closely approximates 1% decomposition in the AlH_3 -1451. These figures indicated some incompatibility with the Epon 812 epoxy resin, causing acceleration of the decomposition of the AlH_3 -1451. Other ingredients of this composite system demonstrated a negligible or slightly beneficial effect. It was first thought that the behavior of the Epon 812 was due to its relatively high water content as shown in Table XXX. However, reducing the water content by degassing the resin showed only a slight improvement in compatibility with AlH_3 -1451. Studies were then attempted to relate rates of gassing with epoxide content of the base polymer. Examination of a high purity, greater functionality, Dow epoxy resin again demonstrated a degree of incompatibility with the AlH_3 -1451, but no quantitative relationship could be shown.

CONFIDENTIAL

Table XXVIII

(C) Composition of Formulations Tested on the Taliani Apparatus at 60°C.

Test Number	Ingredient, g.										
	HA 7%	PONC	MAPO	Epon 812	Dow Epoxy	TMCTN	NO	TEODM	BDNPA	1451	AP
III-1,2	0.094	---	0.012	0.008	---	0.142	---	---	---	0.250 ^a	0.495
III-3,4	0.094	---	0.012	0.008	---	0.142	---	---	---	---	---
III-5,6	0.094	---	0.012	0.008	---	0.142	---	---	---	0.250 ^a	---
III-7,8	---	---	---	---	---	---	---	---	---	0.250 ^a	---
IV-1,2	---	---	0.012	---	---	---	---	---	---	0.250 ^a	---
IV-3,4	0.094	---	0.012	0.008	---	0.142	---	---	---	0.250 ^a	---
IV-5,6	0.094	---	0.012	0.008	---	0.142	---	---	---	---	0.4947
IV-7,8	---	---	---	---	---	---	---	---	---	0.250 ^a	---
V-1,2	0.094	---	---	---	---	---	---	---	---	0.250 ^a	---
V-3,4	---	---	---	0.008	---	---	---	---	---	0.250 ^a	---
V-5,6	---	---	---	---	---	0.142	---	---	---	0.250 ^a	---
V-7,8	---	---	---	---	---	---	---	---	---	0.250 ^a	---
VI-1,2	---	---	---	0.008	---	---	---	---	---	0.250 ^a	---
VI-3,4	---	---	---	---	---	0.142	---	---	---	0.250 ^a	---
VI-5,6	---	---	---	---	0.073	---	---	---	---	0.250 ^a	---
VII-11,12 ^h	---	0.12	---	---	---	---	0.263	0.044	0.044	0.250 ^a	0.260
VII-13,14 ^h	---	0.12	---	---	---	---	0.263	0.044	0.044	0.250 ^a	---
VII-15,16 ^h	---	0.12	---	---	---	---	0.263	0.044	0.044	---	0.260
VII-17,18	---	---	---	---	---	---	---	---	---	0.250 ^a	---
VIII-1,2	---	0.12	---	---	---	---	---	---	---	0.250 ^a	---
VIII-3,4	---	---	---	---	---	---	---	0.044	---	0.250 ^a	---
VIII-5,6	---	---	---	---	---	---	---	---	0.044	0.250 ^a	---
VIII-7,8	---	---	---	---	---	---	0.263	---	---	0.250 ^a	---
IX-15,16	---	---	---	0.008 ^b	---	---	---	---	---	0.250 ^a	---
IX-17,18	---	---	---	---	---	---	---	---	---	0.250 ^a	---
X-1	---	---	---	---	---	---	---	---	---	0.250 ^c	---
X-2 ^h	---	0.12	---	---	---	---	0.263	0.044	0.044	0.250 ^c	0.260
X-3	0.094	---	0.012	0.008	---	0.142	---	---	---	0.250 ^c	0.495
X-4 ^h	---	0.12	---	---	---	---	0.263	0.044	0.044	0.250 ^d	0.260
X-5	0.094	---	0.012	0.008	---	0.142	---	---	---	0.250 ^d	0.495
X-6	---	---	---	0.008	---	---	---	---	---	0.250 ^d	0.495
X-7	---	---	---	---	---	---	---	---	---	0.250 ^d	---
X-8	---	---	---	---	---	---	---	---	0.044	0.250 ^e	---
X-9 ^h	---	0.12	---	---	---	---	0.263	0.044	0.044	0.250 ^e	0.260
X-10	0.094	---	0.012	0.008	---	0.142	---	---	---	0.250 ^e	0.495
X-11	---	---	---	---	---	---	---	---	---	0.250 ^f	---
X-12	---	---	---	---	---	---	---	---	---	0.250 ^f	---
X-13	---	---	---	---	---	---	---	---	0.044	0.250 ^f	---
X-14 ^h	---	0.12	---	---	---	---	0.263	0.044	0.044	0.250 ^f	0.260
X-15	0.094	---	0.012	0.008	---	0.142	---	---	---	0.250 ^f	0.495
X-16	---	---	---	---	---	---	---	---	---	0.250 ^g	---
X-17	---	---	---	---	---	---	---	---	0.044	0.250 ^g	---
X-18 ^h	---	0.12	---	---	---	---	0.263	0.044	0.044	0.250 ^g	0.260
X-19	0.094	---	0.012	0.008	---	0.142	---	---	---	0.250 ^g	0.495

^aLot No. 02055.

^bSample of Epon 812 vacuum degassed prior to testing.

^cLot No. 5009, magnesium-doped sample containing 1.0% magnesium.

^dLot No. 5009, hydrolyzed surface, 0.14% oxygen.

^eLot No. 02055, hydrolyzed surface, 0.20% oxygen.

^fLab run 07085, magnesium-doped sample containing 0.64% magnesium.

^gLab run 07085, hydrolyzed surface.

^hThese formulations contained 0.010 g. of both 2-MDPA and resorcinol.

CONFIDENTIAL

(This Page is Unclassified)

Table XXIX

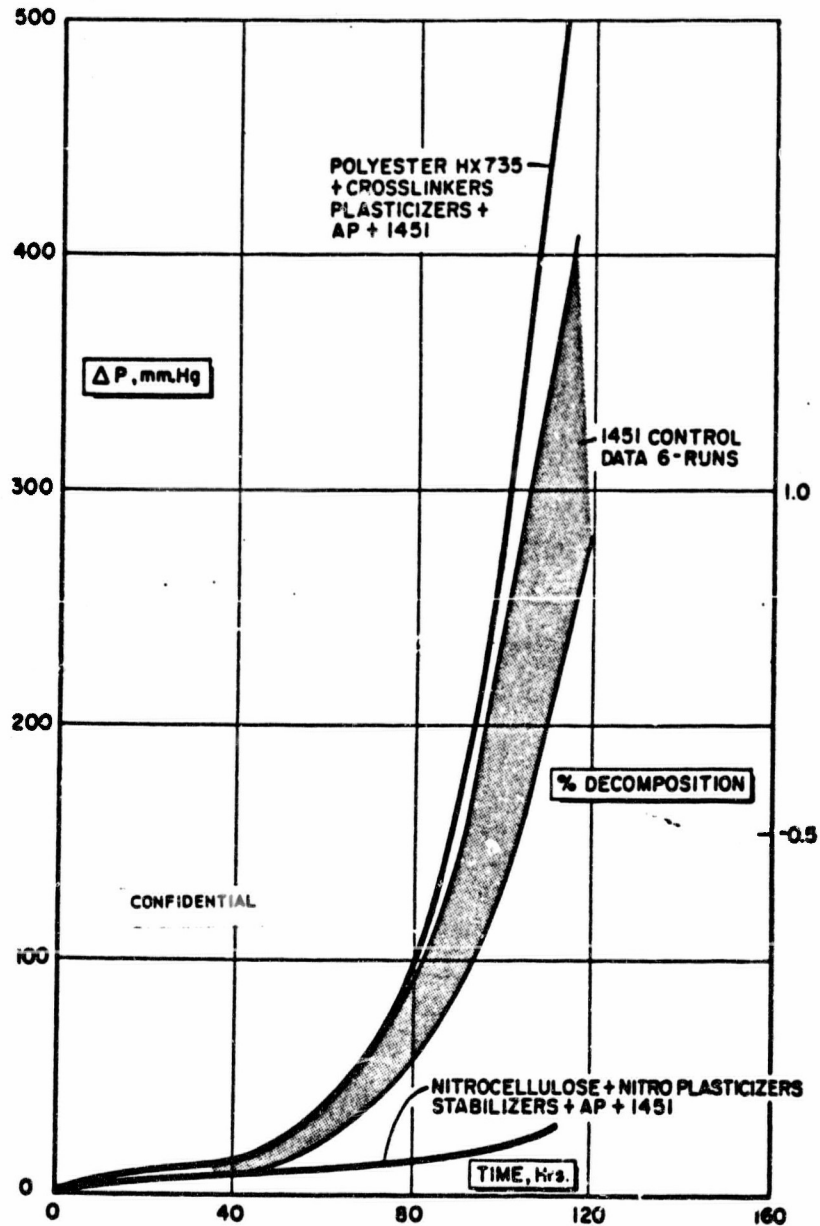
(U) Gas and X-Ray Diffraction Analysis of Components and Residues of 60°C. Taliani Tests after 96 Hours

Test Number	Gas Analysis, cc.					Total Pressure, mm.	Total Vol. Gas, cc.	Residue, g
	H ₂	CO	CO ₂	N ₂	NO			
III-2	2.11	---	Trace	0.04	---	425	2.20	Not run
III-3	---	---	Trace	Trace	---	16	Nil	Not run
III-5	1.87	---	0.017	0.370	---	385	2.37	Not run
IV-1	0.452	---	---	0.02	---	152	0.512	100, 1451
V-1	0.541	---	0.002	0.007	---	158	0.57	100, 1451
V-5	Trace	---	---	---	---	52	Nil	Not run
V-8	0.52	---	---	Nil	0.03	157	0.55	93, 1451 7, Al
VI-1	2.64	---	0.02	0.78	---	520	3.56	Not run
VI-5	1.5	---	0.019	0.181	---	302	1.7	Not run
VII-12	Trace	---	Trace	---	---	17	Nil	50, AP 50, 1451
VII-16	---	Trace	---	---	---	10	Nil	Not run
VIII-2	Trace	---	---	Trace	---	38	Nil	95, 1451 5, Al
VIII-4	0.11	Trace	---	---	Trace	105	0.13	Not run
VIII-6	1.246	---	---	---	0.002	256	1.28	Not run
VI-I-7	0.175	---	---	0.002	Trace	112	0.179	Not run
IX-16	1.795	---	---	0.010	---	320	1.81	Not run

CONFIDENTIAL

(This Page is Unclassified)

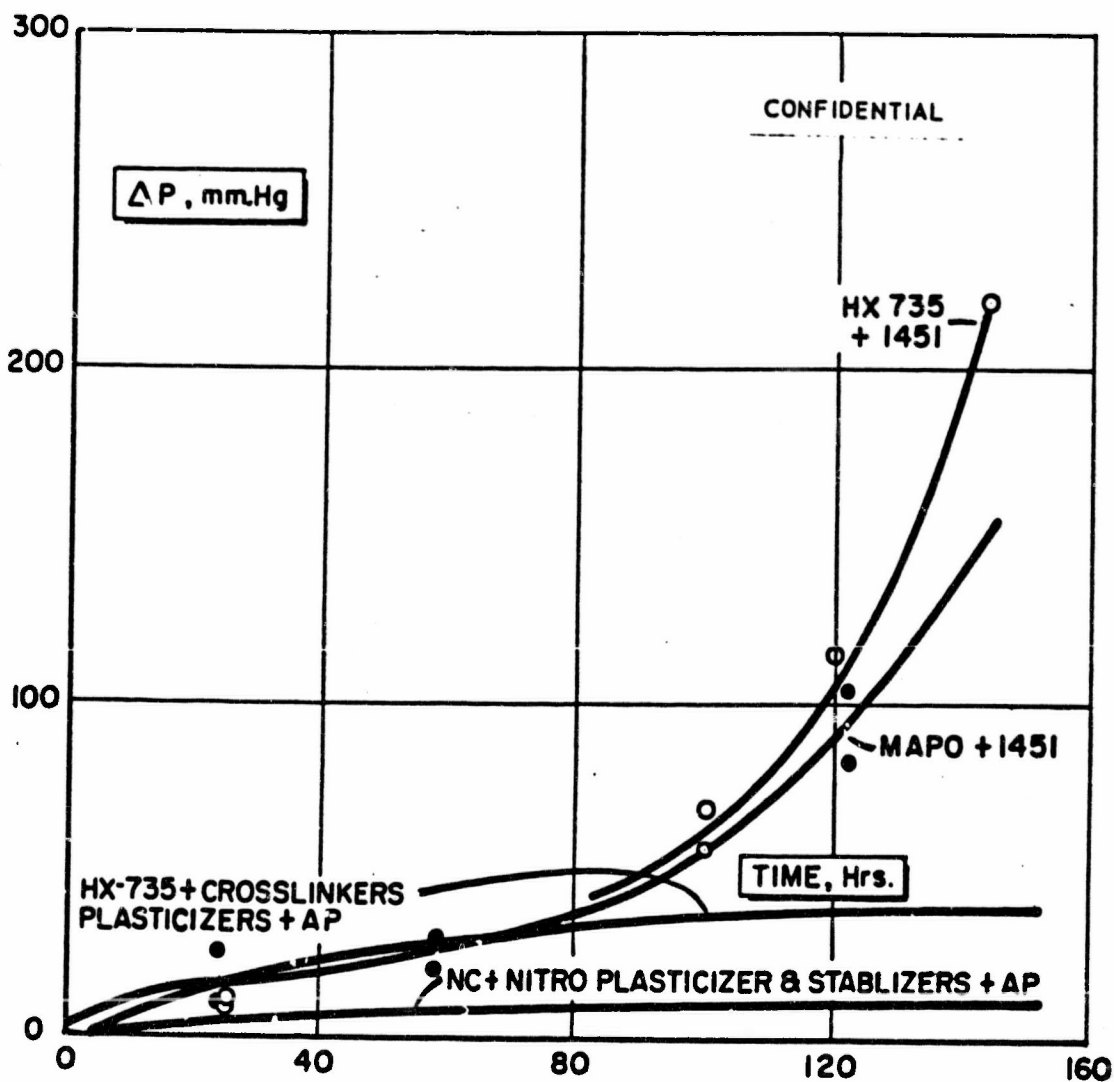
CONFIDENTIAL



(C) Fig. 76 - Taliani Data on Aluminum Hydride-1451 (Lot 02055), Typical Composite, and Double Base Propellants at 60°C.

CONFIDENTIAL

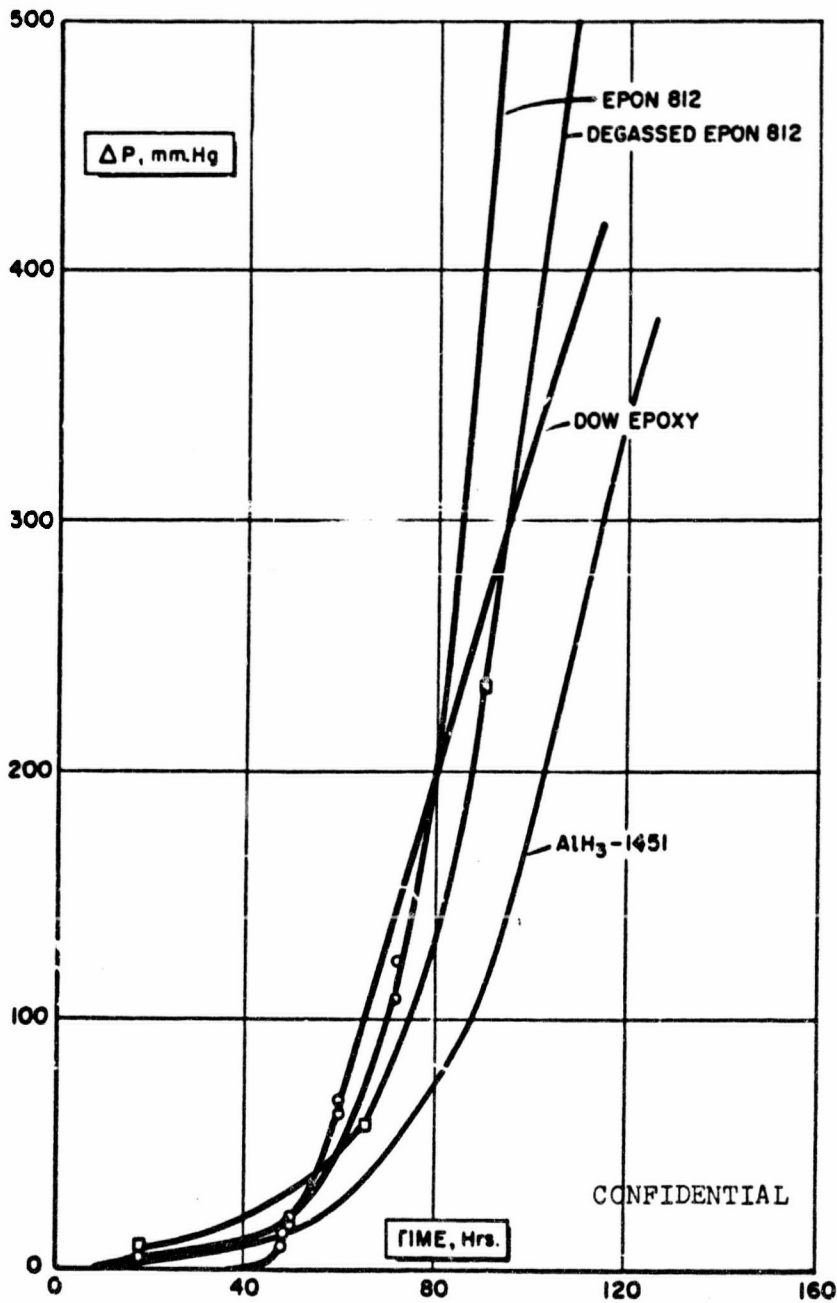
CONFIDENTIAL



(C) Fig. 77 - Taliani Data on Polymer Systems With and Without Aluminum Hydride-1451 (Lot 02055)

CONFIDENTIAL

CONFIDENTIAL



(C) Fig. 78 - Taliani Data on Epoxy Systems with Aluminum Hydride-1451 (Lot 02055)

CONFIDENTIAL

CONFIDENTIAL

Table XXX

(U) Moisture Analyses of Propellant Ingredients

<u>Component</u>	<u>% H₂O (Karl Fischer)</u>	<u>% OH</u>
TMETN	0.09	0.36
PGNC	0.75	4.91
Dow Epoxy	0.129	0.25
Dow Epoxy (degassed)	0.032	---
Epon 812	0.93	2.92
Epon 812 (degassed)	0.16	2.78
HX 735	0.40	0.11
TEGDN	0.197	---
AP	0.01	---

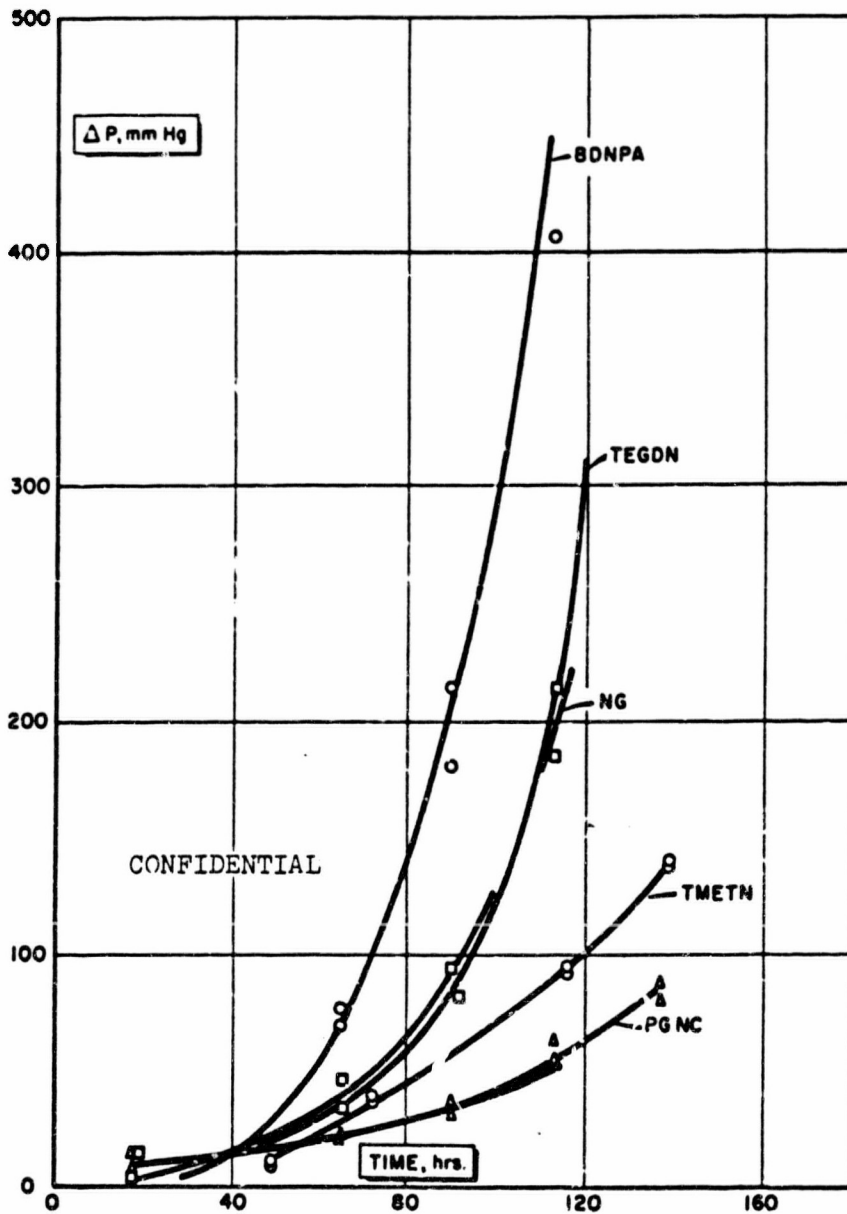
(C) The gas analysis data, as shown in Table XXIX, are limited in accuracy by the small quantities of gas generated during the Taliani test. Results did not indicate any definite trends for the composite propellant system. X-Ray diffraction data are also presented in Table XXIX. However, X-ray analysis was found not to be applicable for the detection of small amounts of aluminum as a result of hydride decomposition.

(C) Interpretation of the Taliani results on the composite propellant formulation shows that AlH₃-1451 may be reacting with the epoxide group of epoxy resins. The other ingredients of this system did not seem to accelerate the decomposition of AlH₃-1451 and therefore are considered compatible with hydride. The hydroxyl and water content of the ingredients may have some effect on compatibility, but these effects seem to be less than those of the reactive groups on the ingredient molecules.

(C) The double base propellant system was similarly examined. The effect of each of its constituents on the decomposition rate of AlH₃-1451 was determined, and the results are shown in Figure 79. This plot shows that BDNPA accelerates the decomposition of the AlH₃-1451 while TMETN and PGNC (containing 5% ethyl centralite) have a stabilizing effect.

(C) The gas analysis data from the samples were again limited in accuracy due to the small quantities of gas evolved. The appearance of NO and N₂O was detected in the gas generated from the double base system. Analytical work on AlH₃-1451 recovered from the double base propellant after aging has yielded strong evidence of a coating consisting of oxides of nitrogen on the AlH₃-1451 surface. This in situ surface coating may be responsible for the stabilization of AlH₃-1451 observed in double base

CONFIDENTIAL



(C) Fig. 79 - Taliani Data on Aluminum Hydride-1451 (Lot 02055), and Nitro Compounds at 60°C.

CONFIDENTIAL

CONFIDENTIAL

propellant. The analytical work done on the propellant will be more fully discussed in connection with the long-term surveillance of the propellant. These results substantiate earlier indications that nitro esters and ethyl centralite have a stabilizing influence on AlH_3 -1451. The detrimental effect of the BDNPA is as yet unexplained.

(C) Some of the most recently improved AlH_3 -1451 samples have also undergone some compatibility testing in Taliani test apparatus with propellant ingredients. Figure 80 shows the relative stability of the four types of hydride evaluated. The improvement in compatibility achieved with magnesium-doped hydride is shown in Figure 81.

(C) The following results and conclusions were obtained from these tests:

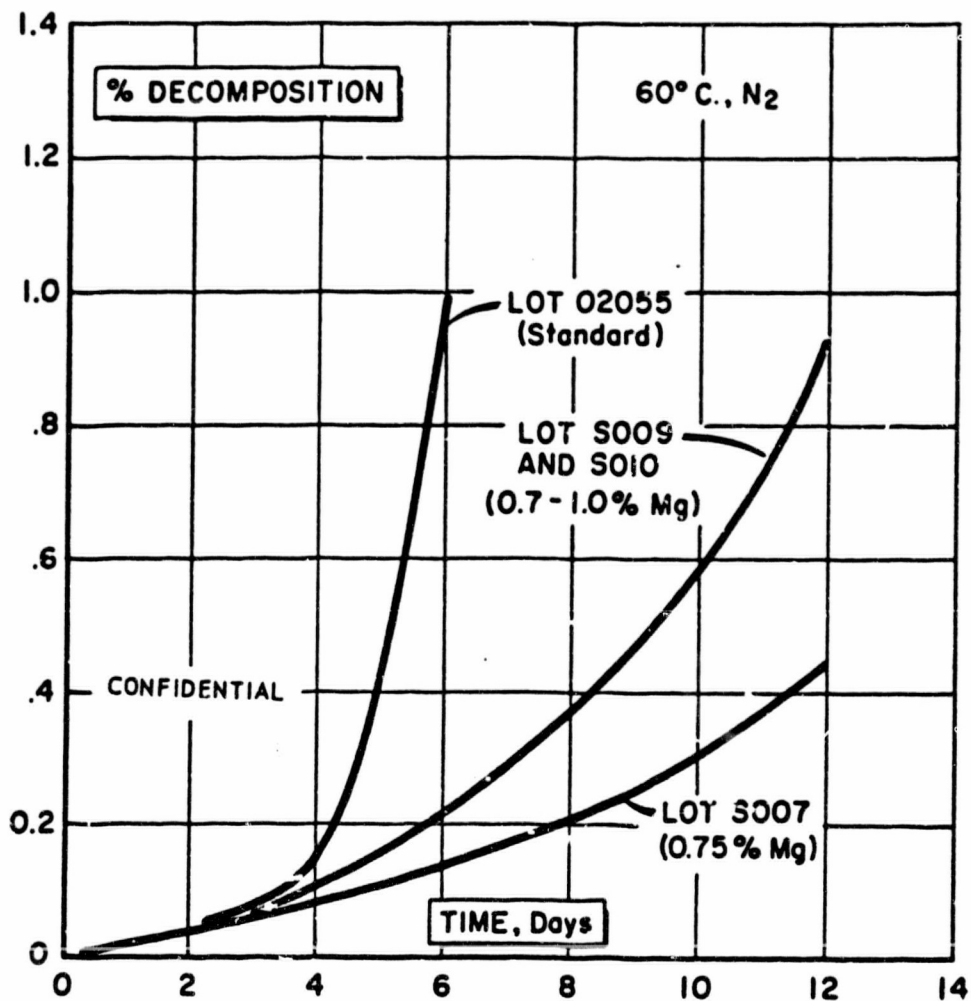
- (C) (i) Regardless of propellant type, significant improvements both in compatibility and stability were observed in mixtures containing the magnesium-treated hydride. The degree of improvement in propellant stability was observed to correlate with the increased stability of the neat hydride.
- (C) (ii) Surface oxidation of aluminum hydride, whether magnesium-doped or not, appeared to improve stability of the neat AlH_3 -1451. Surface-oxidized material took roughly 24 to 30 hours longer to reach 1% decomposition compared to normal hydride. The result of this treatment is to delay the initiation of decomposition of the hydride.
- (C) (iii) Propellants formulated with a surface-oxidized sample (02055) and a magnesium-doped, surface-oxidized sample (5009) exhibited a degree of improvement in stability over that formulated with non-hydrolyzed forms. This improvement was most distinct in the double base propellant system.

2. Surveillance of Aluminum Hydride-1451 in Propellant Grain (C)

(U) A large amount of effort was directed at modification of facilities for remote formulation and surveillance of propellant during the first part of the year. These facilities, with a capability of remote formulation, mixing, and curing, as well as surveillance of twelve samples at 25°C. and twelve samples at 40°C., were completed in July and aging studies initiated.

(U) Figure 82 shows a picture of the surveillance bombs, disassembled and assembled, into which are placed nearly one-half pound of propellant. Next to these vessels are the 1/4-lb., 2 in. x 3 in. CIB test grain and an 80-gram slab, both of which are placed into the bomb and aged. The test grain is aged in place in its motor case.

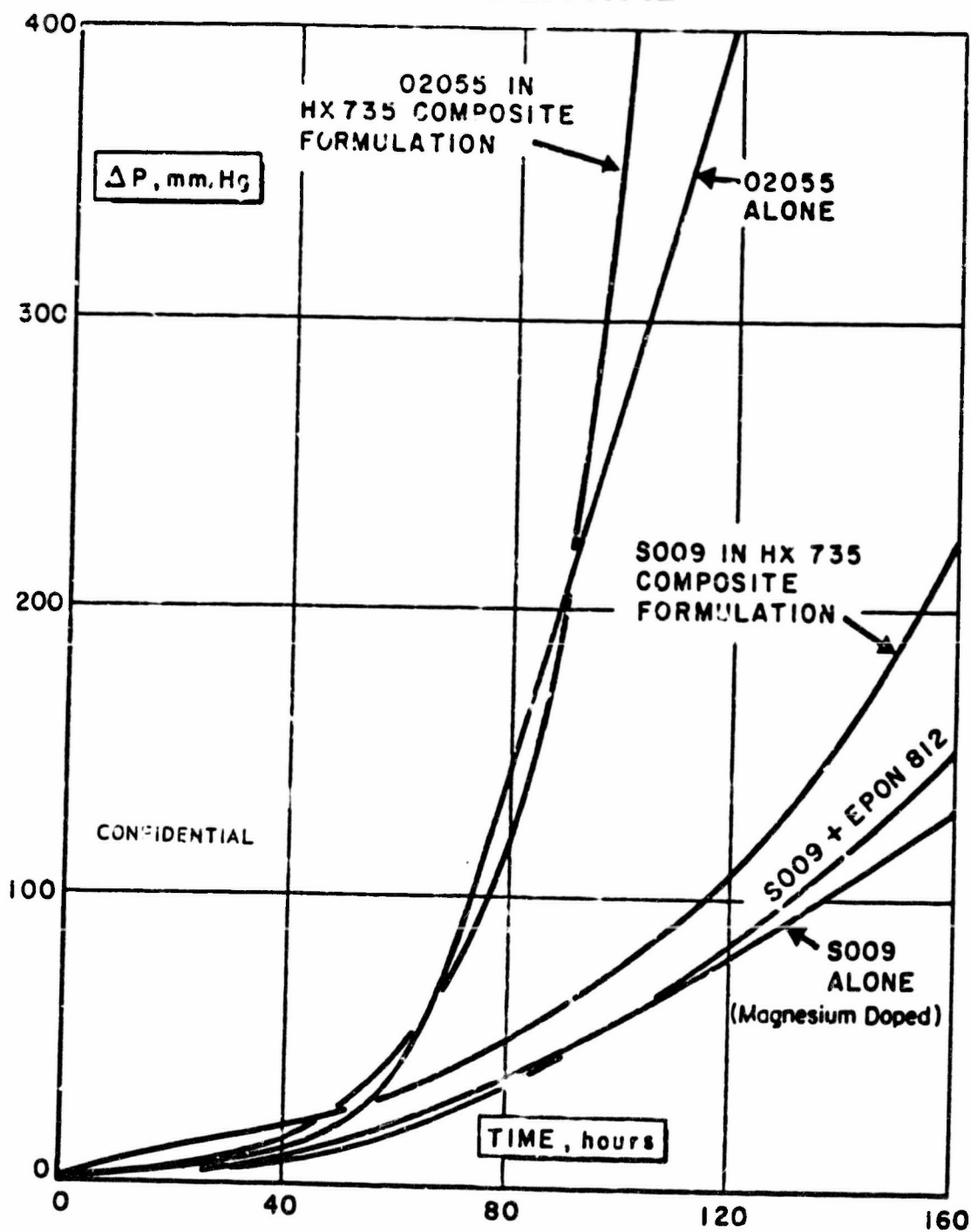
CONFIDENTIAL



(C) Fig. 80 - Decomposition Rate of Neat Aluminum Hydride

CONFIDENTIAL

CONFIDENTIAL

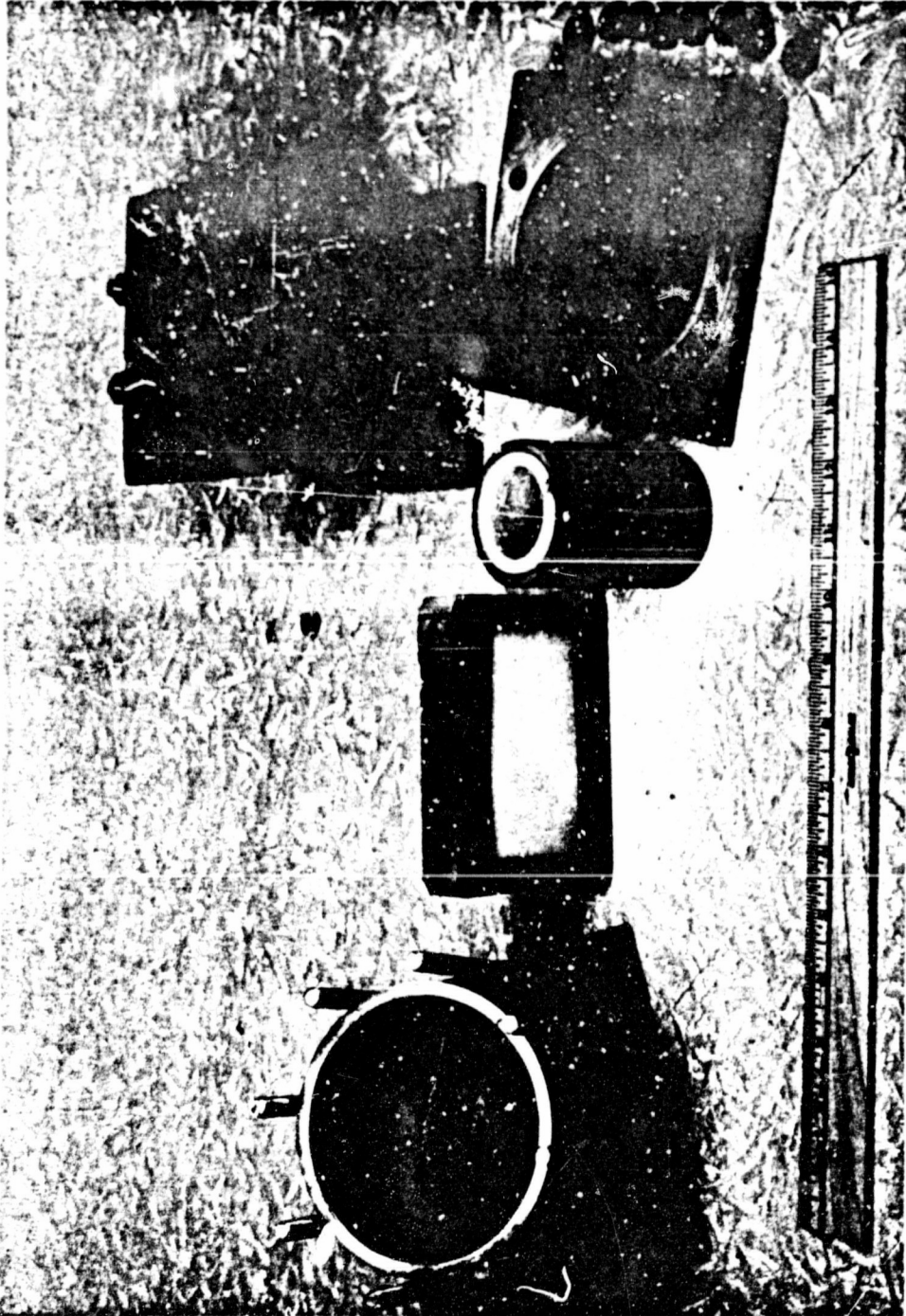


(C) Fig. 81 - Taliani Data Obtained at 60°C.
on the Compatibility and Stability
of Magnesium-Doped Aluminum Hydride
Alone and in Formulations

CONFIDENTIAL

CONFIDENTIAL

(This Page is Unclassified)



(U) Fig. 82 - Propellant Samples and Aging Bomb

CONFIDENTIAL

(This Page is Unclassified)

CONFIDENTIAL

(U) Figure 83 is a photograph of the cubicle where the units are undergoing aging at room temperature. The conditioning cabinet surrounding the twelve bombs is controlled to $25^{\circ}\text{C.} \pm 1^{\circ}\text{C.}$ The bank of manometers in front of the bombs monitors the gasses developed during surveillance. Careful leak checks have been made on these units.

(U) Figure 84 shows the cubicle and heated baths into which the bombs are placed for elevated temperature ($40^{\circ}\text{C.} \pm 1^{\circ}\text{C.}$) aging. Very small diameter stainless steel tubing interconnects the bombs in these baths with manometers mounted on the outside cubicle wall.

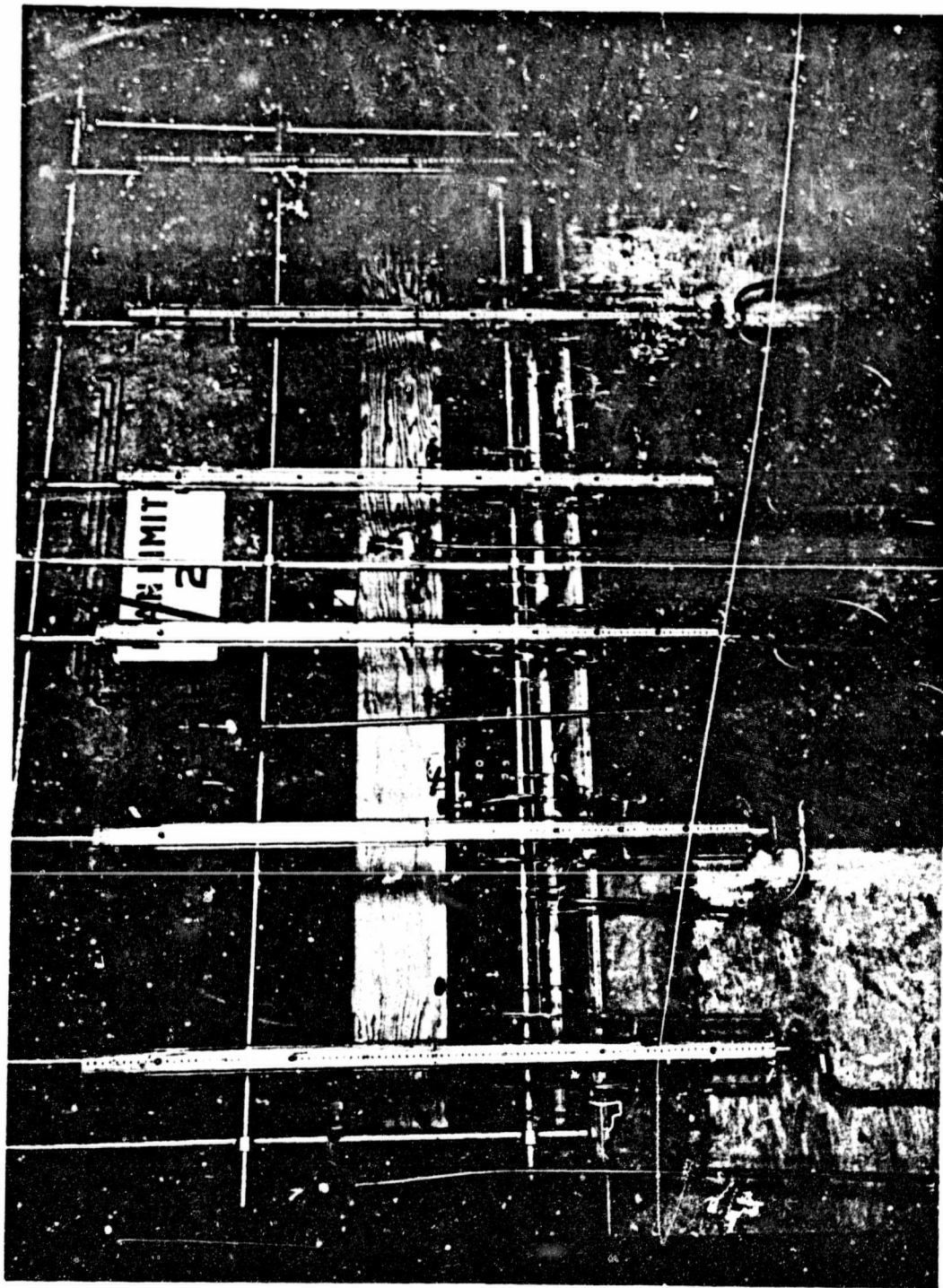
(C) During the past year, fifteen 1/4-lb. samples of double base type propellant grain were placed on test in the surveillance equipment. Six samples were formulated and are being tested in pairs, with one Al metal propellant sample being prepared with each AlH_3 -1451 sample. Of these six pairs, three are being studied at 25°C. and three at 40°C. In addition, two 1/4-lb. samples of propellant formulated with surface-hydrolyzed AlH_3 -1451 have been placed on test, one at 25°C. and the other at 40°C. Another sample has been formulated with magnesium-doped AlH_3 -1451 and is on test at 25°C. All samples are under an argon atmosphere. Table XXXI lists the samples placed on test. The propellant formulation used is the same as that given in Table XXVII.

(C) Initially, gaseous results were erratic, with a negative pressure change observed in the bombs containing an argon atmosphere. The problem was traced to the slow diffusion of argon through a silicone rubber gasket used in the surveillance bombs. Metal gaskets were used to replace the rubber and the samples were again placed on test. This did not interfere with the decomposition calculations, since the slow loss of argon was relatively constant in many of the bombs, including the standard Al propellant, allowing a standard correction.

(C) The pressure generation and off-gas analysis data have been related to percent decomposition of AlH_3 -1451. These measured decomposition rates at 25°C. and 40°C. are shown in Figures 85 and 86, respectively. The calculated values for percent decomposition were obtained by subtracting the moles of gas generated by the aluminum propellant from the moles of gas generated by the AlH_3 -1451 propellant and then assuming the remainder to be all hydrogen generated from the decomposition of AlH_3 -1451. A check on the validity of this assumption was made, calculating the percent decomposition directly from the gas analysis data by use of the mole percent hydrogen observed and the ideal gas law. The results agree very well, suggesting that the difference in pressure does represent hydrogen and not some other gas resulting from hydride catalytic decomposition of the other ingredients.

(C) The decomposition rates observed from propellant containing surface-hydrolyzed and magnesium-doped AlH_3 -1451 at 25°C. are presented in Figure 87. The surface-hydrolyzed sample of AlH_3 -1451 at 40°C. is shown in Figure 88. These preliminary results

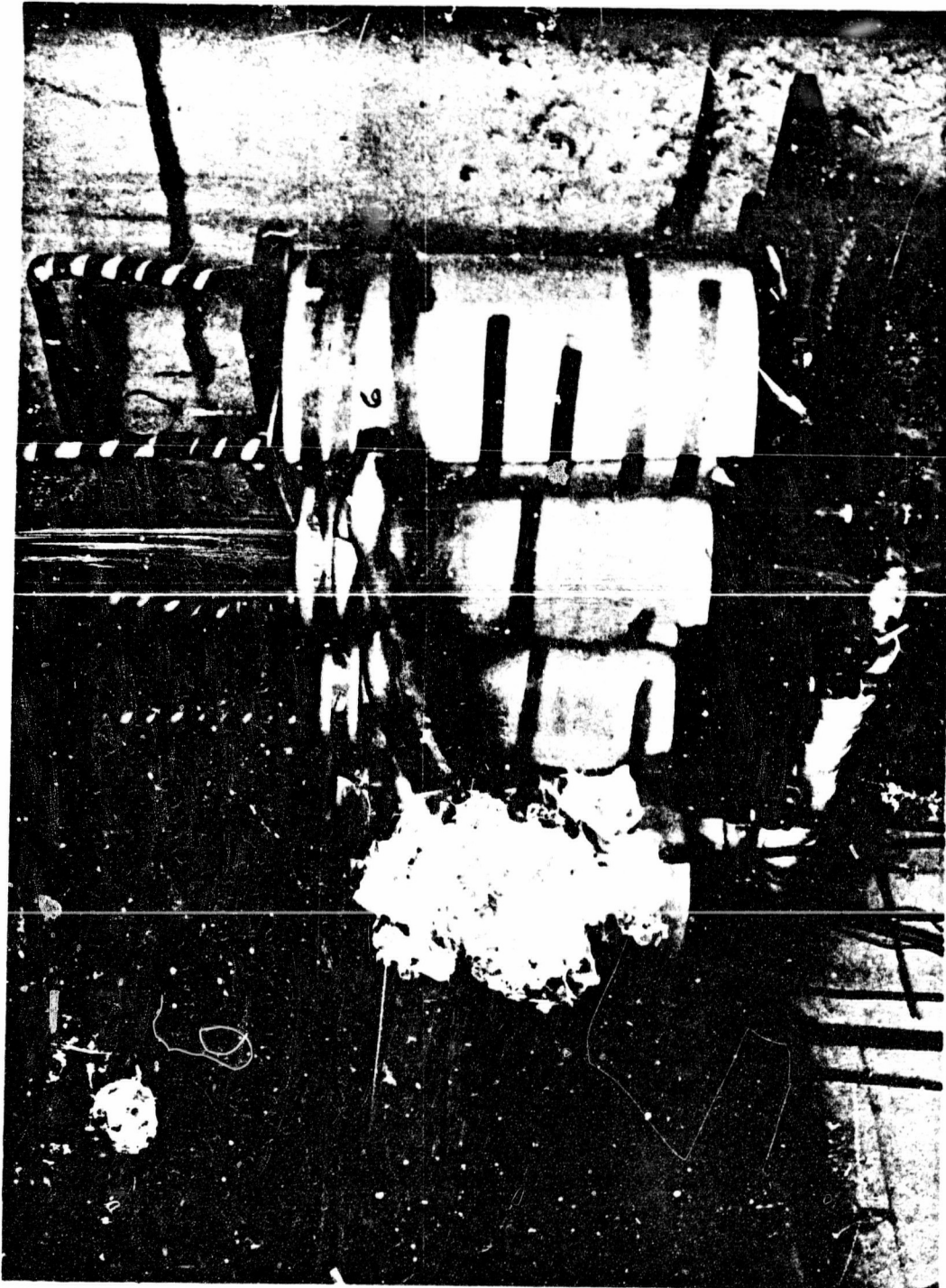
UNCLASSIFIED



(U) Fig. 83 - Room Temperature Surveillance Facility

UNCLASSIFIED

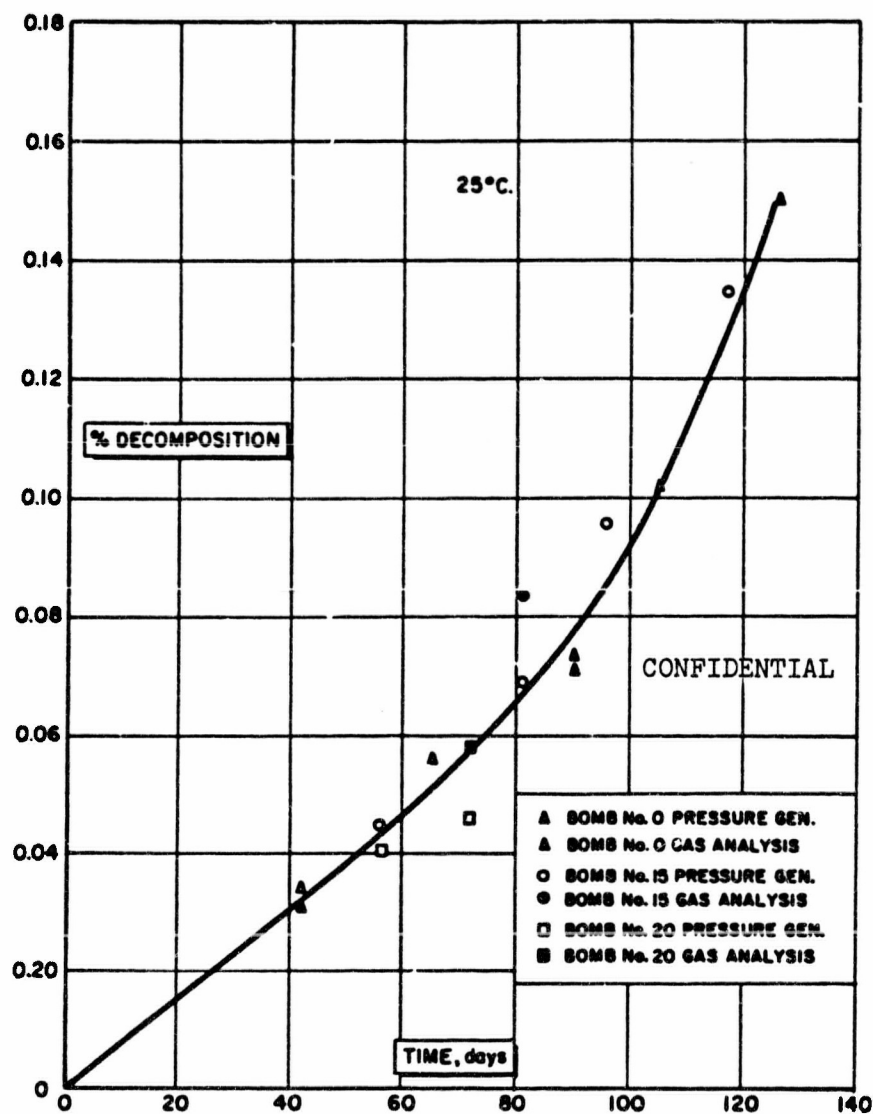
UNCLASSIFIED



(U) FIG. 84 - High Temperature Aging Baths

UNCLASSIFIED

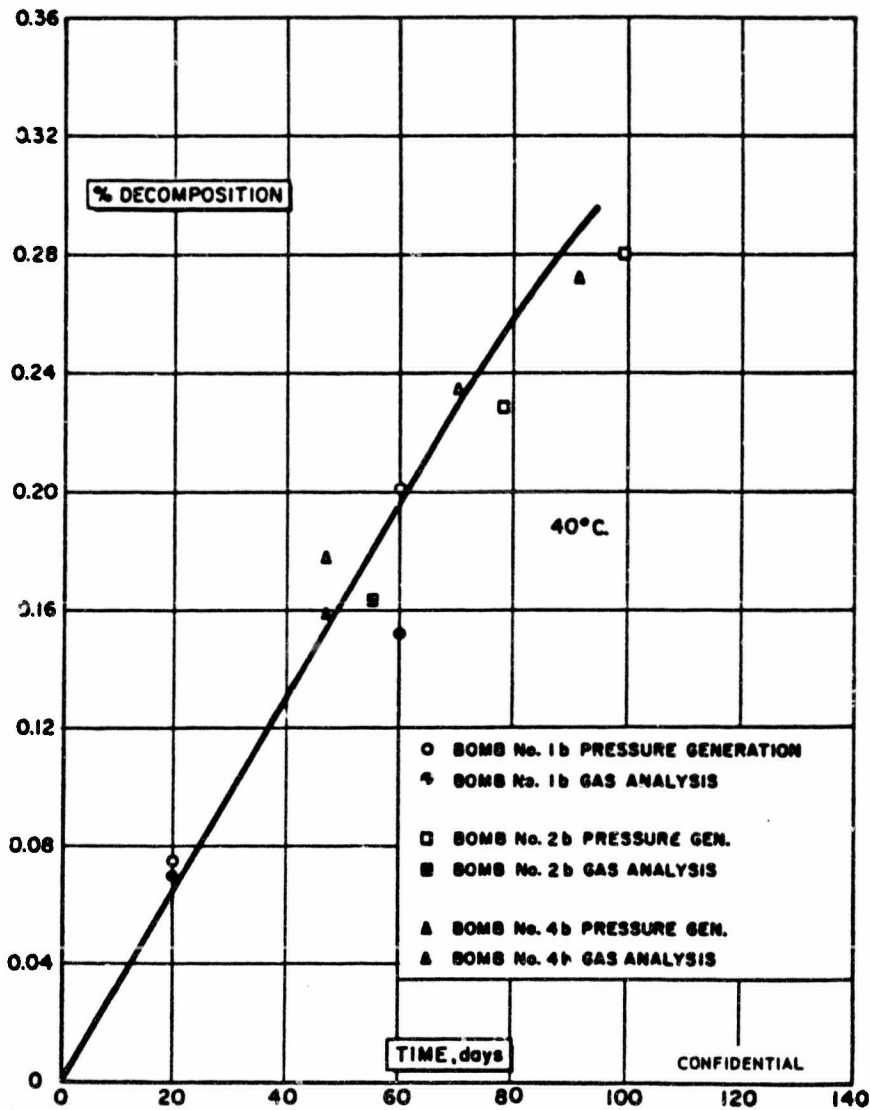
CONFIDENTIAL



(C) Fig. 85 - Decomposition of Aluminum Hydride-1451 (Lot 02055) in Double Base Propellant at 25°C.

CONFIDENTIAL

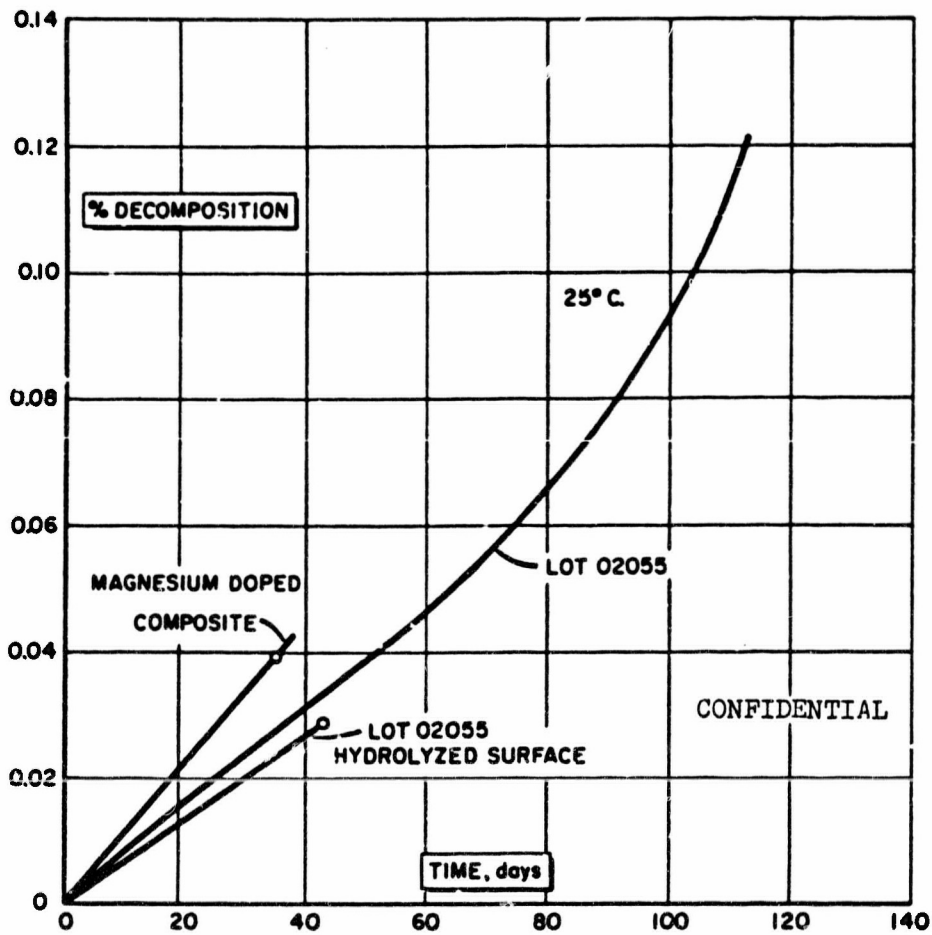
CONFIDENTIAL



(C) Fig. 86 - Decomposition of Aluminum Hydride-1451 (Lot 02055) in Double Base Propellant at 40°C.

CONFIDENTIAL

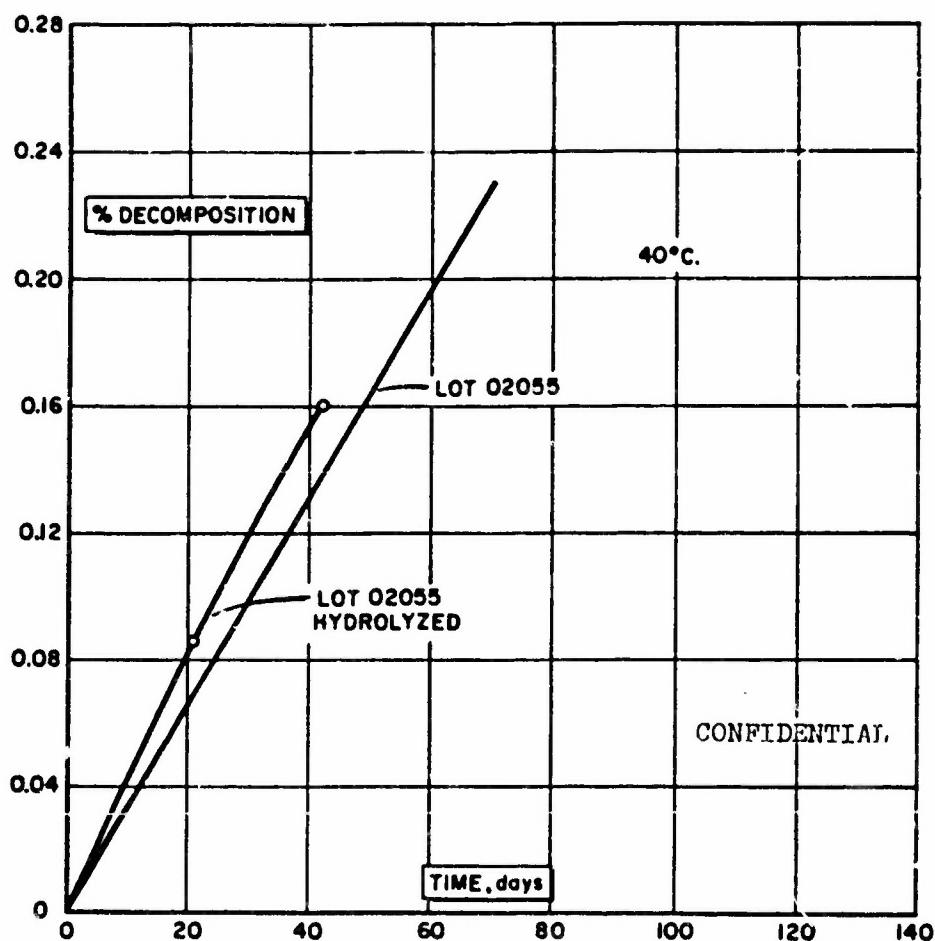
CONFIDENTIAL



(c) Fig. 87 - Decomposition of Aluminum Hydride-1451
(Magnesium-Doped or Surface Hydrolyzed)
in Double Base Propellant at 25°C.

CONFIDENTIAL

CONFIDENTIAL



(C) Fig. 88 - Decomposition of Aluminum Hydride-1451 (Surface Hydrolyzed) in Double Base Propellant at 40°C.

CONFIDENTIAL

CONFIDENTIAL

show insufficient deviation from the standard data at this time to predict the long-term storage stability in propellant of these special hydride samples.

(C) The gas analysis data accumulated from the surveillance samples show the presence of H_2 , N_2 , O_2 , Ar, CO_2 , and a trace of an unidentified species of mass 45. The data indicate a slow generation of N_2 and O_2 , probably from binder decomposition or desorption of these gases. Carbon dioxide is also being slowly generated. It has been noted that in seven out of eight cases a greater amount of CO_2 has been generated from the AlH_3 -1451 propellant when compared with the standard aluminum propellant. A comparison of the amount of CO_2 and O_2 generated from the hydride and aluminum propellants is shown in Table XXXI. No trend in O_2 generation from the hydride or aluminum propellants is indicated. The CO_2 gas generation phenomenon may be important in detecting a possible slow binder decomposition reaction which is increased by the presence of AlH_3 -1451.

(C) Table XXXII presents the physical property, burning rate, and heat of explosion data obtained from the surveillance studies. The heat of explosion and burning rate studies have been hampered by incomplete and erratic combustion of the small samples. No trends in the results of these tests can be seen due to scatter of the data. The physical property data do show some effect of propellant age. The aluminum-containing propellant shows no significant change in tensile, elongation, or hardness properties with age. However, the AlH_3 -1451 containing propellant has somewhat poorer initial properties and does show some slight hardening and embrittlement with age. No change in density of the propellant was observed although decomposition of the AlH_3 -1451 would have reduced the density nearly 20% of theory had the hydrogen been trapped in the grain. This indicates that H_2 readily diffuses through the propellant grain and does not create voids in the cured propellant.

3. Chemical Analysis of Aluminum Hydride-1451 Double Base Propellant* (C)

(C) Chemical analysis studies were initiated to devise separation and analytical methods for the various components in the AlH_3 -1451 double base propellant formulation. The primary objective was to isolate and recover the AlH_3 -1451 from the formulation for subsequent physical and chemical evaluation. A complementary objective was to devise analytical methods for the known components of the double base formulation.

(C) The formulation was extracted with a number of different solvents. Dry acetone was found to be the most promising solvent for readily and completely dissolving the double base formulation. The dry acetone did not appear to alter the AlH_3 -1451 to any extent.

⁴ Work by M. C. Kelly of the Analytical Laboratory of The Dow Chemical Company.

CONFIDENTIAL

(This page is Unclassified)

Table XXXI

(U) Surveillance Gas Analysis Data Comparison

Temperature, °C.	25	25	25	25	40	40	40	40
Bomb Numbers								
A1 Propellant	13	13	16	21	1a	1a	2a	4a
1451 Propellant	0	0	15	20	1b	1b	2b	4b
Time Aged, days	42	90	81	71	20	60	55	47
CO ₂ Off-Gas from A1 Propellant g. moles/g. Propellant x 10 ⁷	3.01	4.52	3.43	2.49	4.97	8.68	13.9	6.01
CO ₂ Off-Gas from 1451 Propellant g. moles/g. Propellant x 10 ⁷	3.50	5.60	3.56	2.80	5.80	7.25	17.8	13.9
Comparison	+	+	+	+	+	-	+	+
O ₂ Off-Gas from A1 Propellant g. moles/g. Propellant x 10 ⁷	68.5	104.5	89.3	101.0	21.6	57.0	51.6	45.4
O ₂ Off-Gas from 1451 Propellant g. moles/g. Propellant x 10 ⁷	70.0	95.4	87.0	108.2	31.9	89.9	47.6	54.4
Comparison	+	-	-	+	+	+	-	+

-198-

(This page is Unclassified)

CONFIDENTIAL

CONFIDENTIAL

(This page is Unclassified)

Table XXXII
(U) Evaluation of Propellant

Type of Propellant	Results of Evaluation				
	Al	Al	Al	1451	1451 ^a
Temp. of Aging, °C.	---	25	40	---	40
Days Aged	0	71	60	0	60
Percent Decomp. at Evaluation	---	---	---	---	0.20
Physical Properties					
Tensile Strength, psi	108.5	103.9	106.5	55	84.0
Elongation, %	49.7	43.7	47.5	43.7	28.6
Heat of Explosion ^b , cal./g.	1855	1801	1786	1447	1666
Shore Hardness	69	68	69	55	70
Density % of Theory	99.5	99.9	100.5	97.0	97.9
Burning Rate ^c , in./min.					
At 500 psi	0.360	0.364	0.440	0.350	0.290
At 1000 psi	0.500	0.502	0.480	0.510	0.465
n	0.45	0.48	0.125	0.55	0.687

^aNo detectable Al by X-ray analysis.

^bIncomplete combustion of 1451 propellant.

^cExperimental accuracy prevents interpretation.

(This page is Unclassified)

CONFIDENTIAL

CONFIDENTIAL

(C) A number of samples from the same double base formulation were extracted with dry acetone to determine the extracting efficiency. The weight of formulation varied from 0.1 to 0.5 g. After a three-hour extraction, the residue for all samples consisted of AlH_3 -1451 coated with a material initially believed to consist of 2-NDPA plus a small amount of nitrocellulose. Further study indicates that the 2-NDPA is present in a much smaller concentration than previously suspected. Extraction of the residue with glacial acetic acid readily removes the coating which subsequently analyzes less than 0.001% 2-NDPA. The small concentration of 2-NDPA detected indicated the presence of another impurity.

(C) It was also found that the 2-NDPA is more soluble in acetone than in glacial acetic acid, again suggesting that the bulk of the coating associated with the residue consisted of another substance.

(C) The solubility of the coating in glacial acetic acid and the resulting color plus the conditions under which it is formed are indicative of a possible oxide of nitrogen being present. Decomposition of nitroglycerine, nitrocellulose, and TEGDN would account for the presence of NO_2 and NO . The confined gases in the propellant during storage could easily contact and react with AlH_3 -1451. To determine the presence of an organic nitrogen compound or the presence of a possible oxide of nitrogen, the tests tabulated in Table XXXIII were made. Duplicate samples of freshly prepared AlH_3 -1451 double base propellant, and a sample of the same propellant partly decomposed (0.05% decomposition) were extracted with acetone, dried and analyzed. Samples 1 and 2 are duplicate samples of the same material. Sample 3 represents the partly decomposed sample.

Table XXXIII

(C) Elemental Analysis of Recovered
Aluminum Hydride-1451

<u>Sample</u> <u>No.</u>	<u>% C</u>	<u>% N</u>	<u>% H</u>	<u>% Al</u>
1	0.38	0.10	9.91	88.2
2	0.32	0.15	9.90	87.8 ^a
3	0.13	0.45	9.90	88.3

^aSuspect this value to be low.

(C) The consistency of the hydrogen and aluminum concentrations is indicative that the concentration of AlH_3 -1451 has not been altered and is fairly uniform between samples.

CONFIDENTIAL

(U) Sample No. 3 analyzes one third as much carbon and three times as much nitrogen. If the nitrogen is due to presence of an organic compound such as 2-NDPA, the carbon and hydrogen should be proportionately higher. The only explanation for the results obtained would be that a nitrogen-bearing addend is present. The most logical answer would be an oxide of nitrogen since such an entity is present and organic nitrogen compounds are ruled out.

(C) The AlH_3 -1451 could react with an $-\text{ONO}_2$ group of a nitric acid ester or with the NO_2 or NO which are decomposition products of the esters. The former does not seem likely, since a solution of double-base propellant in intimate contact with the AlH_3 -1451 did not react. However, the NO_2 and NO gas could easily contact the AlH_3 -1451 and react. This discovery is extremely interesting because independent studies have shown nitric oxide to stabilize AlH_3 -1451. Hence, the in situ surface treatment of the hydride with oxides of nitrogen evolved from the double-base propellant may be a contributing factor to the enhanced stabilization of the hydride sometimes observed in this environment. If the AlH_3 -1451 does react with the oxides of nitrogen evolved from the decomposition of the nitric esters, the AlH_3 -1451 would be functioning as a stabilizer for the esters as well.

(U) Analysis of the various components present in the acetone filtrate can be accomplished as follows. An aliquot of the acetone extract is dried and then extracted with methylene chloride or acetic acid. The residue is then washed with water to remove water solubles. The washed residue is nitrocellulose. The nitrocellulose can be dried in a vacuum desiccator and calculated on a gravimetric basis. Alternatively, the nitrocellulose can be analyzed by the ferrous ammonium sulfate and titanous chloride system.

(U) TEGDN, NG, BDNPA and 2-NDPA can be extracted with formula 30 alcohol from the dried acetone extract. The four are electro-reducible and have overlapping polarographic waves in tetramethylammonium chloride electrolyte. It is possible to determine the BDNPA by hydrolyzing the TEGDN and NG with alkaline sodium hydroxide and correcting for the 2-NDPA which can be found independently (visible spectrophotometry). The total I_0 before hydrolysis can be used to calculate the sum of the TEGDN and NG. The TEGDN and NG may be separated by thin layer chromatography or by using a column of alumina.

(U) The ammonium perchlorate can be determined by titrating the NH_4 by the caustic-formaldehyde method. The perchlorate can be titrated amperometrically with tetraphenylstibonium sulfate. Chloride and chlorate, if present, do not interfere and can be analyzed by conventional methods: AgNO_3 and spectrophotometry, respectively.

(U) Ethyl centralite can be found spectrophotometrically in the far U.V.

CONFIDENTIAL

(U) Resorcinol can be separated by thin layer chromatography and analyzed spectrophotometrically.

(U) Therefore, the quantitative analysis of the components can be achieved. However, additional study is necessary to determine solvent systems or other physical separations needed to isolate the components for individual tests. Standard curves and optimal conditions would also be required for all tests.

F. COMBUSTION AND DECOMPOSITION KINETICS OF HYDRIDE FUELS (U)

1. General Consideration (U)

(C) The purpose of this work is to identify the reactive intermediates and end-products of beryllium hydride combustion and decomposition in the hope of eventual development of combustion mechanisms in rocket propellants. In order to minimize highly exploratory work with toxic beryllium hydride, preliminary work was conducted with aluminum hydride as a prototype.

(C) The combustion of beryllium hydride could conceivably involve species such as BeH , BeH^+ , and BeOH as reactive intermediates. Although at first glance one would expect a diatomic hydride as the transient species, other compounds cannot be ruled out on purely speculative grounds. In addition to the intermediate reactants in the combustion of the hydride propellants, the identification and the distribution of the products, as well as the stable oxide, play an important role in the thermal and chemical make-up of the exhaust products.

(U) The recent work of Nelson (15, 16, 17) and others has shown the technique of flash heating to be well-suited to the preparation and the detection of short-lived atomic and molecular species. The technique involves the heterogeneous flash heating of small grids or strips suspended in an absorption cell in such a manner that 98% to 99% of the background light passes through the cell before entering the spectrograph used for detection. The grids or strips are efficiently heated by absorption of an intense light pulse from a source similar in design and operation to that employed in conventional flash photolysis experiments.

(C) Nelson and Lungberg (18) have estimated that temperatures of 5000°K. can be approached if the grid materials have diameters or thicknesses of 100 μ or less. The short flash durations and high temperatures reached in a cell allow vigorous thermal reactions to occur, such as vaporization or desorption of the grid materials themselves, or rapid thermal pyrolysis of any material suspended on the grid or strip. The cell can be evacuated or filled with any gas, and a study made of the reaction between the gas and grid or suspended material. In this manner, the combustion of beryllium hydride can be studied in an oxygen and/or nitrogen atmosphere, and the thermal pyrolysis of the hydride in an inert gas can be examined.

CONFIDENTIAL

(U) It is worthwhile to point out that flash heating can be used in a manner analogous to flash photolysis but with the following important exceptions:

- (i) Flash heating utilizes the infrared, visible and ultraviolet region of the flash irradiation to heat the grid. Photochemical reactions use only the ultraviolet and are inherently less efficient.
- (ii) There is a threshold flash energy below which no reaction occurs due to flash heating. Thus, the activation energies can be roughly derived from reaction temperatures. No such threshold exists in flash photolysis.
- (iii) Pyrolytic processes do not depend upon the absorption coefficient of the reactant. Thus, weakly or non-absorbing reactants having an electronic spectra will not interfere with those of the intermediate being studied.

(c) The above stated properties of flash heating make the method very amenable to the study of the combustion of hydride propellants.

(U) The photochemical process recorded on the spectrographic plate is that of absorption of the source of background light by the reactant intermediate formed around the grids or strips during flash heating. The limitations of identification of reactant intermediate in the proposed work as well as in any absorption spectroscopy are due to two causes:

- (i) Insufficient concentration of reactive species.
- (ii) Overlap of the spectra of more than one intermediate.

(U) Under the conditions of flash heating the first problem is resolved. The second problem may be made more difficult by the proliferation of species formed at the high temperatures possible in flash heating. Time resolved spectroscopy may, however, represent a solution to this difficulty. The time resolution will initially be of the order of microseconds, but in some extreme cases, the reactions may have to be followed for a number of seconds. It is possible that the first appearance of some of the intermediates may be orders of magnitude later than those of the more reactive species. In this case, it may be feasible to detect different species at different intervals after the initial heating flash.

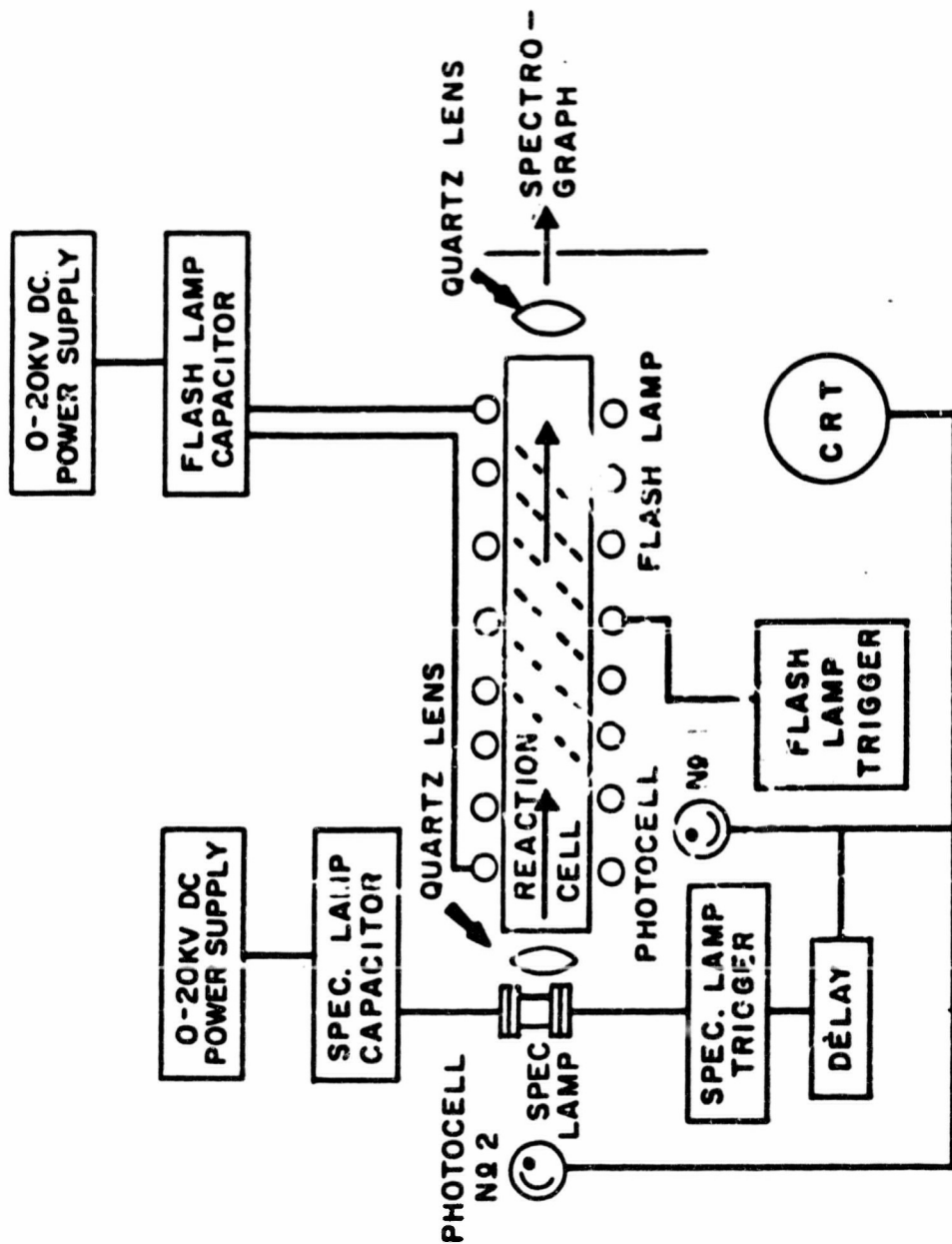
2. Experimental Approach (U)

(U) The various components of the flash heating apparatus, as shown in Figure 89, along with the necessary auxiliary experiment will be described in some detail.

CONFIDENTIAL

CONFIDENTIAL

(This age is Unclassified)



(U) Fig. 89 - Block Diagram of Flash Heating Apparatus

CONFIDENTIAL

(This Page is Unclassified)

UNCLASSIFIED

a. High Voltage Circuit (U)

(U) A high-voltage circuit, shown in Figure 90, has been designed and constructed. The high-voltage capacitor discharge circuit is coupled to an ignitron-activated crowbar circuit by waveform generators.

(U) It has been found that a faster response of the thyatron (6288) is obtained if the matching impedance resistor and its associated capacitor are removed.

(U) The function of the ignitron (GL-7171) is to hold off the voltage applied to the capacitor. In a sense, one has two spark gaps in series (the spectroscopic lamp and the ignitron). The purpose of the circuit in the upper part of Figure 90 is to break down the spark gap of the ignitron in as short a time as possible, i.e., submicroseconds. This then transfers the full potential across the lamp which will break down in a matter of microseconds, provided the potential exceeds the hold-off voltage of the lamp. One cause of misfires in the spectroscopic lamp is an incomplete breaking down of the ignitron caused by too rapid a dissipation of the potential on the 2 microfarad capacitor across the pulse transformer between the capacitor and the ignitron. A new pulse transformer was constructed of 12 turns of RG-58A/U coaxial cable wrapped on two C-shaped cores of high permeability iron obtained from Arnold Engineering Company, Marengo, Illinois. This transformer now delivers a 1700 volt pulse for 3 to 4 microseconds causing sufficient ionization to break down the ignitron in 0.5 microseconds.

(U) Another cause of misfires in the spectroscopic lamp is the relatively high resistance (<0.2 ohms) of the leads between the lamp and ground. The B & S gauge No. 12 wire has been replaced by B & S gauge No. 4 cable between the lamp and ground. The resistance of the flashing lamp is about 0.3 ohms. The current in the lamp is a direct function of the lamp resistance and an inverse function of the total resistance. Hence, the total resistance should be as small as practical. The resistance of the No. 4 cable is 0.00025 ohms/ft. as compared to 0.0016 ohms/ft. for No. 12 wire.

b. Spectrograph (U)

(U) The McPherson Model 216 spectrograph has been installed and calibrated. The linear dispersion of the grating has been found to be 7.75 Å/mm. A spread of about 1600 Å per exposure in the first order has been recorded. The dispersion of the instrument from 2200 Å (air cut-off) to 6000 Å has been calibrated. The resolution is sufficient that two lines 0.28 Å apart have been observed. The spectroscopic lamp provides sufficient radiation to record absorption in the range 2200-6000 Å.

c. Dry Box (U)

(U) A small two-glove dry box has been renovated and installed. The circulation system of the dry box contains an absolute filter on



UNCLASSIFIED

CONFIDENTIAL

the exit side to keep combustion products from contaminating the air in the laboratory. The dry box proper and interchange can be purged separately. The absolute pressure in the dry box is slightly less than atmospheric, which will allow the atmosphere to leak into the contaminated dry box in the event of a slow leak.

d. Reaction Box (U)

(U) A steel box, 2' x 3' x 2', with a quartz window has been fabricated to house the flash heating apparatus. The function of the box is to contain the propellant sample in the event of an explosion of the glass apparatus. Two 2-inch holes have been cut into the bottom of the box on a diagonal to serve as connections to a 50 CFM recirculating fan and an absolute filter. The flow of air is downward into one orifice, which is directly under the flash heating apparatus, and upward from the other. The reaction box table also serves to hold the high-voltage capacitors for the flash and spectroscopic lamps in addition to supporting the recirculating fan and absolute filter. All of the high-voltage circuit is contained either on the shelf of the table or is terminated by the flash lamps in the steel box.

e. Optical Train (U)

(U) The optical train, shown in Figure 91, consists of the following lettered parts: A, quartz spectroscopic lamp filled with 5 mm. argon; B, collimator section; C, reaction cell.

(U) A six-inch focal length quartz lens mounted in a soft iron shell is fitted into the collimator section. Another lens is placed between the reaction cell and the spectrograph. The lens in the collimator section is used to render the light from the spectroscopic lamp parallel before it traverses the reaction cell. The quartz lens between the reaction cell and the spectrograph condenses the light coming from the reaction cell and brings it to a focus on the entrance slit of the spectrograph.

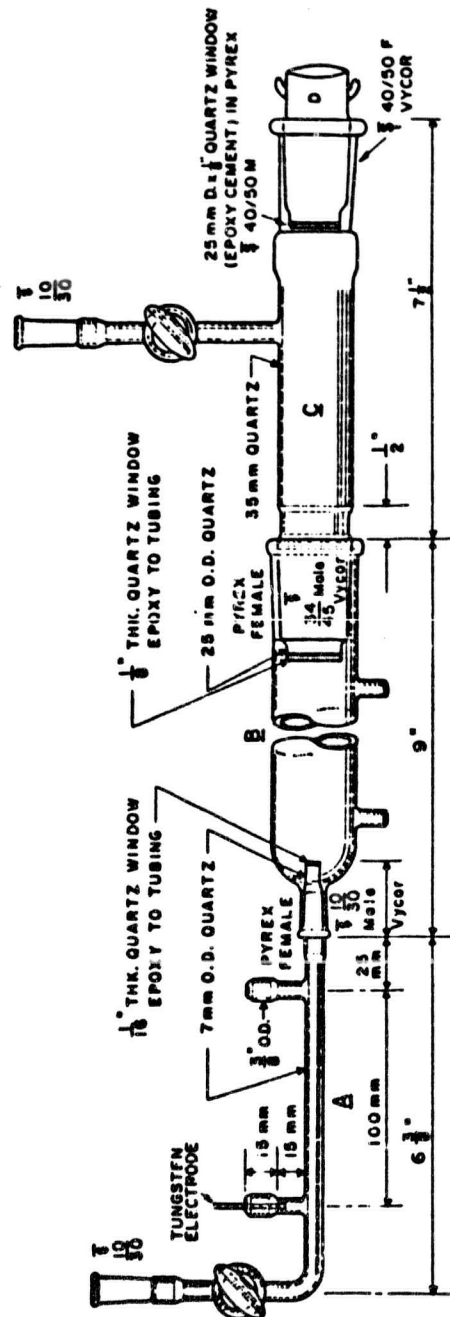
(U) The reaction cell is in two parts, joined by an O-ring seal. The seal and windows at each end of the cell allow the cell to be evacuated. The quartz strip holders have been constructed and have been fused to hold 0.8" x 0.1" x 0.001" graphite strips. The flash lamp is placed around the cell between the stopcock and the tapered joint. The flash lamp is a 4-1/2 turn helix of 10 mm. ID quartz tubing. The electrodes in it and also in the spectroscopic lamp are 1/8 inch tungsten rods. The electrodes are held in the lamps by epoxy cement. The three parts of the optical train are nested together by tapered joints along a common line of center. This facilitates the alignment of the train with the spectrograph.

3. Experimental Results (U)

(C) The flash heating apparatus was first used to study the vacuum decomposition of aluminum hydride-1451. Subsequently, the

CONFIDENTIAL

(This page is Unclassified)



(U) Fig. 91 - Flash-Heating Optical Train

CONFIDENTIAL

CONFIDENTIAL

apparatus has been used to study the decomposition of beryllium hydride in a vacuum or nitrogen atmosphere. Additional studies involved the decomposition of beryllium hydride in atmospheres of oxygen, carbon monoxide, and chlorine.

a. Decomposition of Aluminum Hydride-1451 (C)

(C) The thermodynamic quantities necessary for a discussion of the decomposition of aluminum hydride-1451 are given in Table XXXIV.

Table XXXIV

(C) Heats of Formation of Aluminum-Hydrogen Compounds

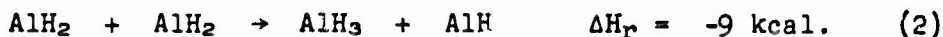
<u>Compound</u>	<u>ΔH_f, kcal./mole</u>	<u>References</u>
AlH ₃	-3	Dow Thermal Laboratory
AlH ₂	+34	R. V. Petrella (est.)
AlH	+62	JANAF Thermochemical Tables
H	+52	JANAF Thermochemical Tables
H ₂	0	JANAF Thermochemical Tables

(C) Two probable primary decomposition routes under flash pyrolytic conditions for AlH₃-1451 are:



(C) The existence of AlH and H₂ in the flash decomposition of AlH₃-1451 in a vacuum has been verified, as seen in Figure 92. The existence of AlH₂ cannot presently be ruled out completely, as a known spectrum has not been reported for this species in the literature. Thermodynamic consideration would favor reaction (1a) over (1b) as the primary step in the decomposition of AlH₃-1451.

(C) Subsequent steps in the reaction scheme may be:



(U) The high radical concentration around the grids in adiabatic flash heating is conducive to radical-radical reaction. This is in contrast to the situation in flash photolysis. In the latter, the reactants are highly diluted with an inert gas, leading to bimolecular collisions with the diluent and subsequent reduction of radical-radical reactions.

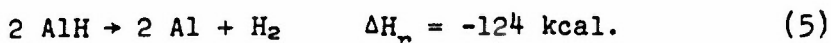
CONFIDENTIAL



(C) Fig. 92 H_2 Spectrum of Aluminum Hydride after Flashing

(C) On a thermodynamic basis it can be shown that reaction (1.b.) will be immediately followed by reaction (3) in preference to reaction (2) or (4), assuming that most of the aluminum hydride present in the gas phase has already been decomposed by reaction (1.a.) or (1.b.).

(C) Both reactions (1.a.) and (1.b.), followed by reaction (2) and/or (3), lead to the intermediate AlH and H_2 as reaction products. The final reaction products are, of course, Al and H_2 . One route to their formation from AlH is:



Aluminum metal has been identified in the residue from the flash heating experiments.

b. Decomposition of Beryllium Hydride (C)

(C) The pyrolytic decomposition of beryllium hydride was studied at a temperature of $2477 \pm 20^\circ\text{K.}$ as determined from the intensity of four iron lines.

(C) The dry beryllium hydride was observed to have an electrostatic charge which originally made it difficult to place the hydride on the graphite strips. This difficulty was overcome by first coating the strips with a small amount of Apiezon "M" stop-cock grease dissolved in benzene.

(C) Adequate spectral data were obtained when the material was subjected to a flash of 1500 joules (10 KV x 30 $\mu\text{fd.}$). The beryllium hydride was found to decompose to BeH, BeH^+ , and H_2 . The products were the same in a nitrogen atmosphere as in a vacuum. Pressure broadening in the inert nitrogen made some of the lines difficult to read.

(C) Two distinct regions of absorption were detected in the decomposition of beryllium hydride. One was in the blue-green region around 5000 Å, the other in the ultraviolet at about 3000 Å. The upper wavelength region corresponds to O-O bond of the $2\Sigma \rightarrow 2$ transition of BeH. The observed lines and their rotational fine structure are shown in Table XXXV. The rotational transition is unresolved doubles. The J_K values are given in half quantum values to conform to the literature reference of Watson (19).

(C) The lower absorption region corresponds to the O-1, O-3, 1-3, and 1-4 bands of the $^1\Sigma \rightarrow ^1\Sigma$ system of BeH^+ . The observed bands and their rotational assignments are shown in Table XXXVI.

CONFIDENTIAL

Table XXXV

(C) Observed Rotational Band for 0-0 Transition
of BeH in Absorption at $2477 \pm 20^\circ\text{K}$.^a

J_K^a	$R(J_K), \text{\AA}$	$P(J_K), \text{\AA}$
1 1/2	4987.4	
2 1/2		4997.5
3 1/2	4975.0	5003.7
4 1/2		5008.4
5 1/2 ^b		5013.8
6 1/2		
7 1/2		5020.0
8 1/2		5027.7
9 1/2		
10 1/2		5037.0
11 1/2		5039.2
12 1/2		5041.7
13 1/2		5046.9
14 1/2		
15 1/2		
16 1/2		
17 1/2		
18 1/2		5064.2
19 1/2		
20 1/2		
21 1/2		
22 1/2		
23 1/2		
24 1/2		5081.2
25 1/2	4862.5	
26 1/2		
27 1/2		
28 1/2		5089.7

^aEach line is an unresolved doublet
This $R(J_K)$ for $J_K = 1/2$ corresponds to
J transition of 0-1 and 0-2.

^b $Q(J_K), \text{\AA}$ is 4992.1.

CONFIDENTIAL

Table XXXVI

(C) Observed Rotational Bands of BeH in
the Ultraviolet at $2477 \pm 20^\circ\text{K}^a$

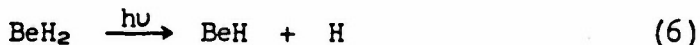
J	0-1		0-3		1-3		1-4	
	R	P	R	P	R	P	R	P
1/2							3082.9	
1/2								
2 1/2		2885.8						3087.5
3 1/2								3090.6
4 1/2				3051.9				3093.7
5 1/2								
6 1/2				3059.6				
7 1/2			3044.7	3065.0				
8 1/2				3068.9		2940.1		
9 1/2				3075.1				
10 1/2		2745.6						
11 1/2		2751.8		3087.5				
12 1/2								
13 1/2								
14 1/2			3071.2					
15 1/2			3077.4					
16 1/2						2994.4		
17 1/2								
18 1/2								
19 1/2						3021.6		
20 1/2					2983.5			
21 1/2								
22 1/2					3000.6			
23 1/2						3065.0		
24 1/2								
25 1/2	2834.7					3087.5		
26 1/2					3038.7			
27 1/2		2912.2			3048.8			
28 1/2								
29 1/2					3059.6			
30 1/2		2955.6						

^aAngstrom Units.

CONFIDENTIAL

CONFIDENTIAL

(C) The inherent electronic instability of the BeH molecule at 2500°K. causes it to lose an electron and degrade into the charged BeH⁺ species. An analysis of this system has been carried out by Watson and Humphreys (20). The pyrolytic decomposition of BeH₂ can be visualized as proceeding by the initial step:



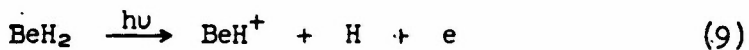
(C) The subsequent steps are the radical reactions:



and



The BeH⁺ is formed by the reaction:



and also to a greater extent by the reaction:



(C) This conclusion was reached by an analysis of the time dependency of each species. The BeH disappeared at a faster rate than did the BeH⁺ with no apparent increase in the rate of production of hydrogen. Analysis time ranged between 7.5 and 200 microseconds after initial heating.

(C) All subsequent reactions reported have shown only BeH as a reactant, although BeH⁺ is the ever-present companion reactant.

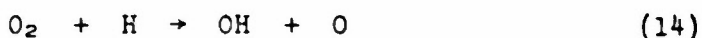
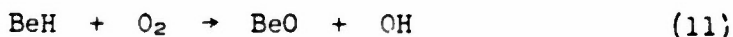
(U) The primary effect of the nitrogen was to suppress radical-radical reaction. Collisional deactivation was increased proportionately as the pressure of the nitrogen was increased from 10 to 700 mm.

c. Beryllium Hydride-Oxygen System

(C) Flash pyrolytic reactions of beryllium hydride were carried out in oxygen in the pressure range of 0-15 mm. oxygen. The analysis time ranged from 17.5 to 100 microseconds after the heating flash. The reaction temperature was calculated to be 2495 ± 30°K. The predominant species seen in the reaction were BeH, BeH⁺, O₂, O₃, OH, and BeO.

(C) The ozone can be visualized as arising from the flash photolysis of oxygen. The OH and BeO are products of the oxidation of the hydride. The proposed mechanism for the reaction of BeH₂ with oxygen is:

CONFIDENTIAL

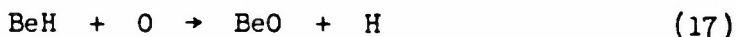
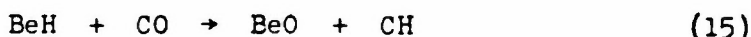


Steps (11), (13), and (14) are chain propagation steps as far as the oxygen is concerned. The species BeH^+ seems to be less reactive than BeH . In an actual motor firing, this species may not react in the combustion chamber but in the exit gas stream, depriving the motor of the enthalpy of Steps (11), (12), and (13) causing low motor efficiencies. Spectroscopic studies of an actual motor firing would validate this supposition.

d. Beryllium Hydride - Carbon Monoxide System (C)

(C) Great amounts of carbon monoxide are formed by the combustion of solid binders, suggesting a reaction between the carbon monoxide and beryllium hydride fuel. To determine the extent of this reaction, beryllium hydride was flash pyrolyzed in 150 mm. of carbon monoxide. The analysis was carried out 100 microseconds after the initial heating flash.

(C) The only products seen were CO , BeO , CH^+ , and CH . A tentative reaction scheme following Step (6) is:



e. Beryllium Hydride - Chlorine System (C)

(C) One of the products from the pyrolysis of AP and NP is chlorine. It seemed prudent, therefore, to study the reaction between beryllium hydride and chlorine. This study was undertaken as a preliminary step before studying the ternary system beryllium hydride - chlorine - oxygen. This latter system offers some interesting alternatives. The toxicity problem would be greatly compounded if beryllium hydride reacted preferentially with chlorine to form beryllium chloride rather than with oxygen to form the potentially non-toxic BeO . Additionally, the efficiency of the engine would be impaired if BeCl or BeCl_2 were an intermediate product even if only for a relatively short duration (0.1 - 1.0 seconds).

CONFIDENTIAL

(C) The main products seen from our study are Cl_2 , Cl_2^+ , and Cl^+ . A few bands corresponding to BeCl are observed, as is one intense band which we have assigned to BeO . This latter band is believed to be due to a reaction between the gaseous BeH and some O_2 which was adsorbed on the cell walls. If this is true, the implication is that BeH would preferentially react with O_2 (or O) rather than with Cl_2 (or Cl). This problem will be clarified when the ternary system is studied.

CONFIDENTIAL

CONFIDENTIAL

SECTION IV

(U) OXIDIZER SYNTHESIS

Work by: D. A. Rausch, R. D. Daniels, H. E. Doorenbos, J. P. Flynn, K. O. Groves, C. I. Merrill, and J. S. Skelcey.

(C) During the past year, the effort in oxidizer synthesis has been concentrated on the study of the preparation and properties of compounds containing the tris(difluoroamino)methyl group.

(C) The major objective was the preparation of ionic $-C(NF_2)_3$ compounds using nucleophilic displacement techniques, e.g., to displace Br from tris-Br. With this approach, it was thought possible to prepare such target compounds as $(F_2N)_3C^+C^-(NO_2)_3$, $(F_2N)_3C^+ClO_4^-$, and $(F_2N)_3C^+ClF_4^-$. A secondary objective involved the preparation of $HC(NF_2)_3$ from $HC(NCO)_3$ by fluorination.

(U) The role of the impurities in the sensitivity of NF compounds was determined during this past year. The compounds studied included PFG, Delta, R, H, tris-bromide, and tris-azide.

(U) The preparation of inorganic compounds containing no fuel atom such as carbon was also explored to obtain oxidizers having decreased sensitivity.

A. PREPARATION OF NF COMPOUNDS (U)

(U) The primary object of the gram-scale preparation of NF compounds was to supply research quantities of these materials for reaction studies in the laboratory. Compounds produced this year include: PFG, tris-Cl, tris-Br, tris-I, tris-A, and tris-fluoro-sulfonate.

(C) Perfluoroguanidine was prepared by the aqueous fluorination of guanidine hydrofluoride. Standard operating conditions and procedures were used. Yields averaged 12-15%, based on the consumed fluorine. The total recovery of 95% pure PFG was approximately 750 grams. Only six of fifty runs were terminated by explosions, five of which occurred during purification and transfer.

(U) During the past year, a process was developed for the preparation of tris-bromide. This process involved the reaction of equimolar amounts of PFG and HBr at $-70^\circ C$. for 16 hours, followed by the direct fluorination of the adduct at $-60^\circ C$. The tris-bromide was isolated by gas chromatography. Yields have been as high as 62% based on PFG. Sulfur dioxide was used as the solvent for both adduct formation and fluorination, eliminating the stripping operation formerly done before fluorination. Sulfur dioxide is satisfactory as a

CONFIDENTIAL

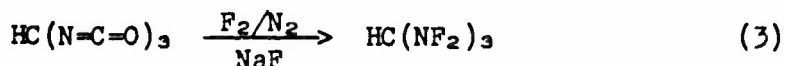
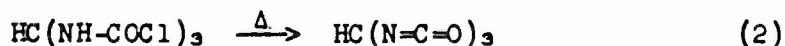
solvent for low temperature fluorinations. At slightly higher temperatures some SO_2F_2 was formed. At least five moles of SO_2 were required during adduct formation for 100% utilization of PFG.

(C) Some effort was made to optimize the amount of HBr charged, and the use of excess HBr, up to 100%, was investigated. Increasing the excess resulted in the formation of larger amounts of the principal by-product, bromoperfluoroformamidine, $\text{BrC}(=\text{NF})\text{NF}_2$, but results indicated that the yield of tris-bromide did not change. Because only tris-bromide was desired, a 1:1 ratio of PFG and HBr was used, since the reaction was cleaner (fewer by-products) and chromatographic separations were easier. Another by-product, sulfurylbromofluoride, SO_2FBr , was also obtained when an excess of HBr was used and when the adduct was allowed to stand for more than 24 hours. If either of these conditions were not met, SO_2FBr was not formed. Sulfurylbromofluoride contaminated the tris-bromide fraction, but could easily be removed by allowing the mixture to stand in glass at room temperature, at which time the SO_2FBr was decomposed to SiF_4 , SO_2 , and Br_2 . These could readily be separated chromatographically.

(U) Reaction and fluorination conditions were studied extensively in the laboratory; therefore, a minimum amount of study was carried out in the gram-scale unit. However, since the method of fluorination was different, the first parameter evaluated was the fluorination time. Using a 2:1 mixture of fluorine to nitrogen and a total flow rate of 125 ml./min., the fluorination time was varied from 60 minutes (200% excess F_2) to 120 minutes using the same flow rate. Incomplete fluorination was noted at both 60 and 90 minutes as shown by the presence of PFG and Br_2 in the product. Fluorination was complete, however, after 120 minutes.

(U) The results in the preparation of tris-bromide on the gram-scale have been comparable to those obtained in the laboratory with yields of 40-45% (3.5-4.0 g./run) based on PFG. The yield of tris-bromide in the initial run was comparatively low (12%); however, a significant quantity of the by-product, bromoperfluoroformamidine, was recovered. In subsequent runs, the ratio of tris-bromide to by-product on a weight basis was approximately 7:1.

(C) Several attempts were made to prepare tris-H, $\text{HC}(\text{NF}_2)_3$, by the following set of reactions:

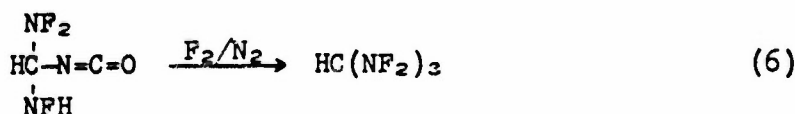
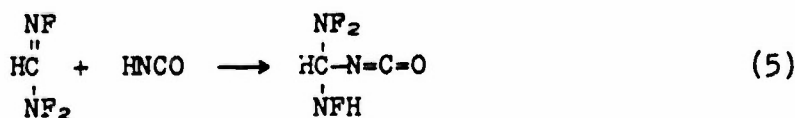
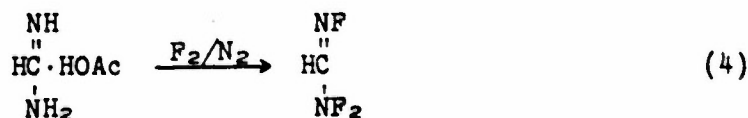


(U) It was found that the above reactions did not take place, however, since polymerization occurred in Step 2. This was indicated by the evolution of CO_2 and the formation of a white gum-like

CONFIDENTIAL

material. Fluorination of the chlorinated product formed COF_2 , SiF_4 , and NF_2Cl , along with an unknown CF-containing compound. This line of investigation was terminated.

(C) The following alternate set of reactions for the possible synthesis of tris-H was also explored:



(U) When Step 4 above was carried out, the desired product was not obtained, but instead a product, $\text{HC}(\text{F})(\text{NF}_2)_2$, was formed in approximately 70% yields. This compound has been previously reported by the Minnesota Mining and Manufacturing Company (21). Since the desired product was not obtained, the work was terminated.

(C) The various PFG-acid adducts were made in a single reactor train, designed to facilitate both the adduction and fluorination steps. The processes for these compounds are similar, except for reaction conditions, and have been discussed in previous reports. Most of these materials were produced at reaction conditions delineated in the laboratory. Yields in most processes were comparable to those reported in the laboratory. The results of those runs are summarized in Table XXXVII. The explosions were random and could not be related to any particular operation.

Table XXXVII

(C) Summary of PFG-Adduct Reactions

<u>tris(Difluoroamino)- methyl Compounds</u>	<u>Number of Runs</u>	<u>Number of Explosions</u>	<u>Product, g.</u>	<u>Yield, %</u>
Chloride	9	3	10	30-40
Bromide	15	3	42	40-50
Isocyanate	13	2	26	15-25
Amine	3	-	6	80
Flucrosulfonate	2	-	<1	12

CONFIDENTIAL

B. REACTIONS OF NF COMPOUNDS (U)

(U) In order to maximize the efforts on the preparation of stable solid oxidizers with decreased sensitivity, there has been a minimum amount of work on the fluorination of organic compounds. Most of the work, therefore, has used known and available tris-compounds as starting materials with the aim of converting these into stable solids.

(C) Many reactions were carried out in attempts to prepare ionic compounds containing the $-C(NF_2)_3$ groups. Among these have been reactions with PFG, reactions with other tris-compounds and miscellaneous reactions.

(U) In the case of PFG, many attempts were made to oxidize PFG using such reagents as permanganyl fluoride as osmium tetroxide. Adduct formations were attempted through the use of oximes, amines, silanols, formic acid and water. The reactions of tris-compounds included reactions with tris-bromide, tris-chloride, tris-fluoro-sulfonate, and tris-isocyanate.

(U) Perhaps the two most important studies conducted during the past year involved the reaction of oximes with tris-bromide and the reaction of tris-isocyanate with nitroform. In the latter case, a stable adduct has been formed and characterized. The impact sensitivity of this compound appears to be substantially lower than that of nitroglycerine.

1. Reactions of tris-Compounds (U)

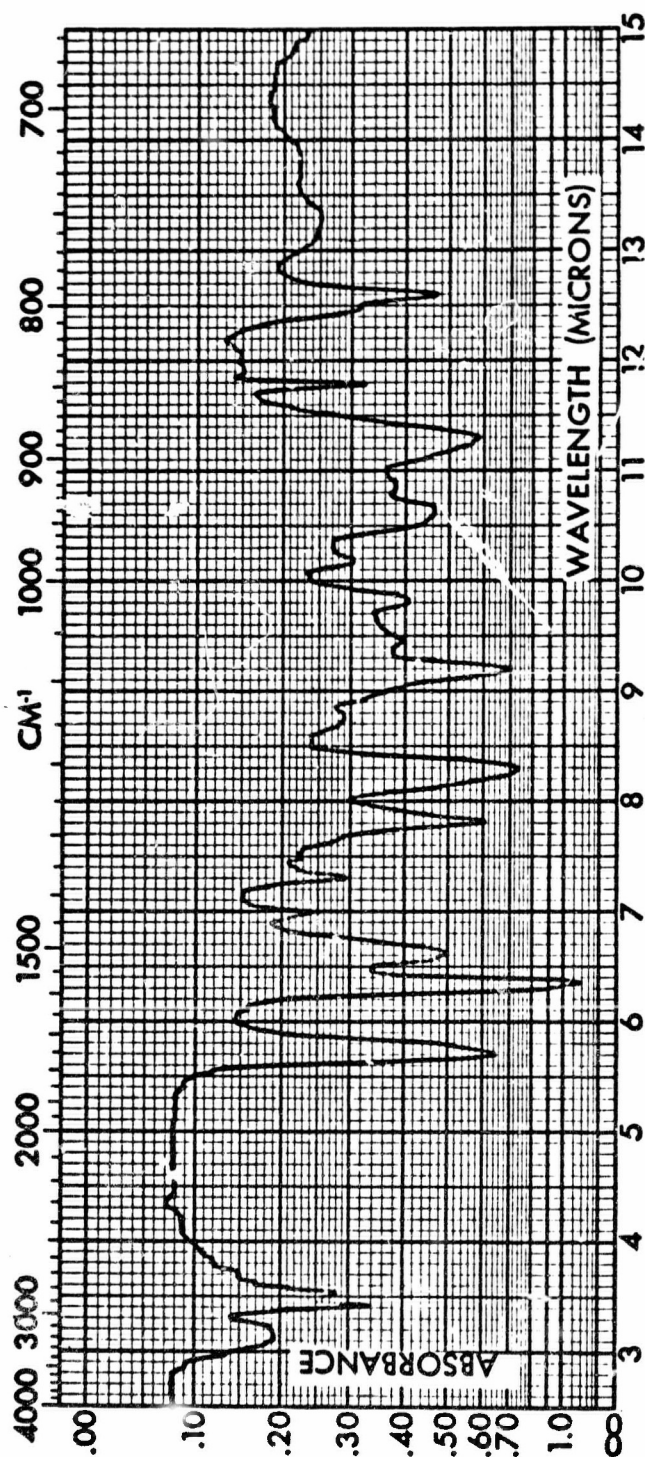
a. Reactions of tris-Isocyanate (U)

(U) Tris-I reacts in a normal manner with alcohls and compounds containing enolizable hydrogens. Since nitroform contains an acidic proton, it was felt that the product from the reaction of tris-I and nitroform should be an excellent oxidizer.

(C) Tris-I reacted with nitroform to give a liquid product,
$$(F_2N)_3C-\overset{\overset{H}{|}}{\underset{\underset{O}{||}}{N}}-\overset{\overset{H}{|}}{\underset{\underset{O}{||}}{C}}-\overset{\overset{O}{|}}{C}(NO_2)_3 \text{ and/or } (F_2N)_3C-\overset{\overset{H}{|}}{\underset{\underset{O}{||}}{N}}-\overset{\overset{H}{|}}{\underset{\underset{O}{||}}{C}}-O-\overset{\overset{O}{|}}{N}=C(NO_2)_2.$$
The reaction was carried out in the presence of dry ether at 25°C. for 50 hours. The product, which formed in quite good yields with little decomposition, was characterized by infrared, mass, and NMR spectroscopy. An infrared spectrum of the product is shown in Figure 93, and its properties are seen in Table XXXVIII. The product is a thick, dark yellow, liquid, and soluble in ether, alcohols, carbon tetrachloride and chloroform.

(C) Impact sensitivity tests on impure samples of this product have been obtained using an Olin Mathieson test apparatus. Under these conditions, the 50% fire level appears to be around 8 cm. using a 2-kg. wt. This compares with a 50% fire level of DEGDN at

CONFIDENTIAL

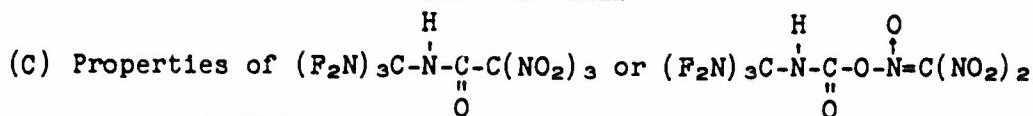


(c) Fig. 93 - Infrared Spectrum of $(F_2N)_3C-\overset{\overset{H}{|}}{\underset{\underset{O}{||}}{N}}-C-\overset{\overset{H}{|}}{\underset{\underset{O}{||}}{N}}-C(NO_2)_3$ or $(F_2N)_3C-\overset{\overset{H}{|}}{\underset{\underset{O}{||}}{N}}-C-\overset{\overset{H}{|}}{\underset{\underset{O}{||}}{N}}-C(NO_2)_2$

CONFIDENTIAL

CONFIDENTIAL

Table XXXVIII



Appearance: Yellow to amber, viscous liquid.

B. P. (est.): >150°C.

F^{19} NMR Spectrum: Single broad peaks at -26.92 δ and -27.18 δ in ratio of 85:15 (probably due to the two isomers).

Mass Spectrum:

Mass Number	211	201	178	168
Rel. Intensity	2.6	16.3	14.9	7.8
Assignment	$(F_2N)_3CNHCO$	$(F_2N)_2CNHCCNO_2$	$COC(NO_2)_3$	$C(NF_2)_3$
Mass Number	158	140	132	107
Rel. Intensity	100	9.6	224	8.0
Assignment	$(F_2N)_3CNCO$	$F_2NCNCFN_2CC$	$COC(NO_2)_2$	$F_2NCNHCO$
Mass Number	106	92	88	87
Rel. Intensity	96	18	44	116
Assignment	F_2NCNCO	$NC(NF)_2$	$FNCNHCO$	$FNCNCO$
Mass Number	86	78	73	70
Rel. Intensity	13	11	57	27
Assignment	$COCNO_2$	CN_2F_2	$FCNCO$	HCF_3 or $COCNO$
Mass Number	69	68	65	64
Rel. Intensity	59	22	20	81
Assignment	CF_3	$NCNCO$	$HCNF_2$	CNF_2
Mass Number	61	59	55	54
Rel. Intensity	88	185	21	47
Assignment	$CONF$	$HCNO_2$	$CNHCO$	$CNCO$
Mass Number	53	52	46	45
Rel. Intensity	12	70	272	380
Assignment	HNF_2	NF_2	NO_2	CNF
Mass Number	43	33	31	30
Rel. Intensity	268	52	274	223
Assignment	$NHCO$	NF	CF	NO

Plus several smaller fragments.

CONFIDENTIAL

2.1 cm. and a 50% fire level of TEGDN at 2.6 cm. under the same conditions. The product appears to be quite stable although it may be slightly sensitive to moisture upon standing. It is felt that this product warrants further investigation, either as a plasticizer for high energy polymers, or as an oxidizer in itself.

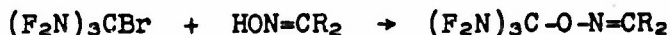
(C) Several attempts have been made to prepare salts of $(F_2N)_3C-NH-CO-C(NO_2)_3$, under the assumption that the hydrogen attached to the nitrogen would be slightly acidic. When the ammonia or hydrazine was allowed to react with the above product in ether, a solid was produced rapidly. An infrared mull of this solid indicated very little NF present; the solid was not impact sensitive.

(C) The reaction of tris-I with peroxydisulfuryl difluoride produced white, crystalline needles, along with $F_2N-O-SO_2F$, $S_2O_5F_2$ and CO_2 . An elemental analysis of the white solid indicated the product to be nitrosyl fluorosulfonate, $NO^+SO_3^-F$. The neat reaction was carried out at $80^\circ C$. for 48 hours.

b. Reactions of tris-Bromide (U)

(1) With Oximes (U)

(C) Recent studies in this laboratory have shown that oximes are capable of displacing bromine from tris-bromide, $(F_2N)_3CBr$. The product of this reaction was believed to be of the type, $(F_2N)_3C-O-N=CR_2$, as indicated below:



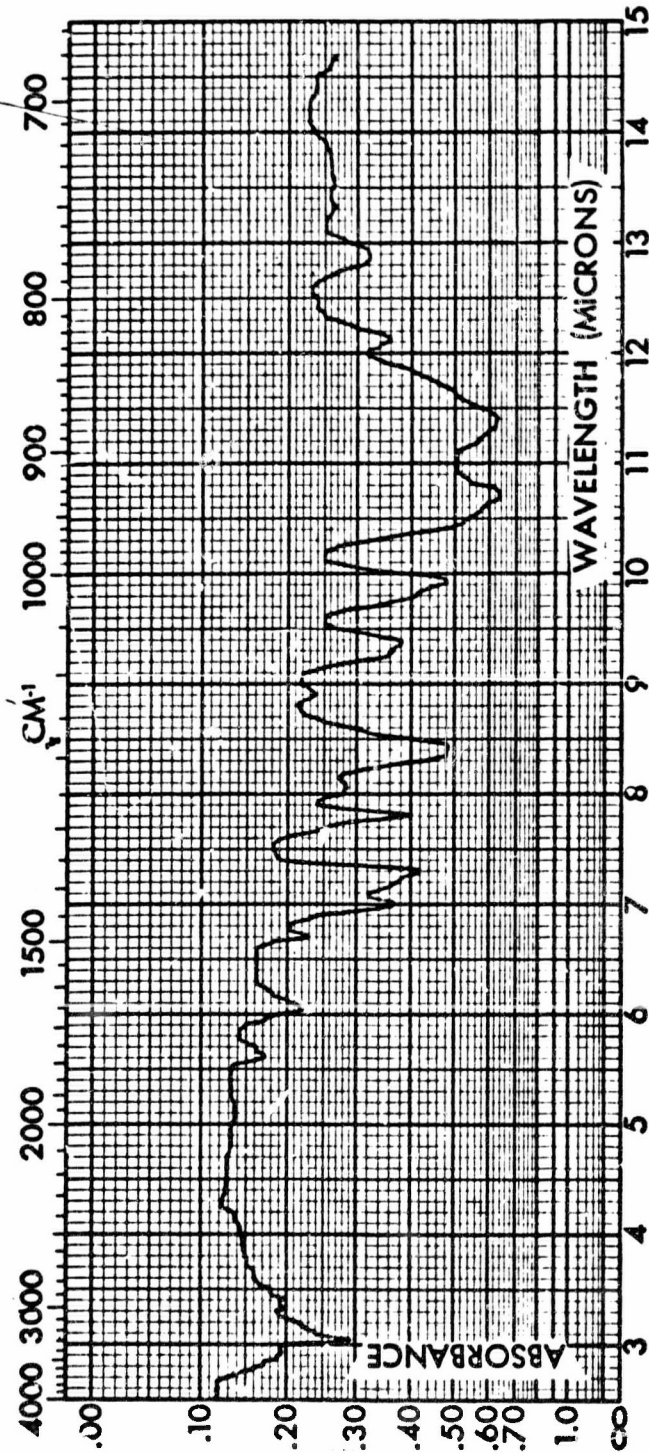
(C) Compounds of this type would be highly desirable, since they could provide the means for preparing $(F_2N)_3C-O-NH_2$ by hydrolysis of the oxime-O-tris compound according to the following general equation:



(C) The above reaction was carried out with four different oximes. The reaction proceeded readily at room temperature to form a product in excellent yield. When difunctional oximes were used, the reaction proceeded stepwise and stoichiometrically, to form a liquid product. Infrared spectra appeared to substantiate the formation of the desired product, viz., $(F_2N)_3C-O-N=CR_2$.

(C) NMR data, which later became available, indicated that the product was not as expected, but actually was $FHNC(NF_2)_2-O-N=CR_2$. A representative spectrum of the above product, where $R = CH_3$, is shown in Figure 94. Although a variety of oximes was employed (acetoxime, glyoxime, dimethylglyoxime and oxamidoxime), NMR evidence conclusively indicated the presence of an NHF group, although this was not indicated by the infrared spectra. All above products were impact sensitive.

CONFIDENTIAL



(C) Fig. 94 - Infrared Spectrum of $\text{NHF}-\text{C}(\text{NF}_2)_2-\text{O}-\text{N}=\text{C}(\text{CH}_3)_2$

CONFIDENTIAL

CONFIDENTIAL

(C) After a careful study, it appears that, during the course of the reaction, one NF_2 group is converted smoothly and quickly into an NHF group without giving any detectable evidence of fragmentation of the tris group during the fluorine abstraction and subsequent hydrogenation. Evidence obtained by following the reaction with NMR indicates that this is not simply a bromine displacement followed by a loss of fluorine from the tris group, but appears to be a concerted reaction wherein one NF_2 group is converted to an NHF group with the concurrent loss of the bromine from the tris group. This evidence is based on the fact that (a) mild bases did not eliminate the above reaction by neutralizing the HBr as it was formed, and (b) in carrying out the same reaction with compound Delta, only starting materials were covered. It seems evident then that oximes do not react with NF_2 groups directly, but may react with tris-bromide by the elimination of bromine and fluorine concurrently, with the subsequent formation of BrF_3 and Br_2 from the eliminated BrF . Bromine is always found as one of the reaction products.

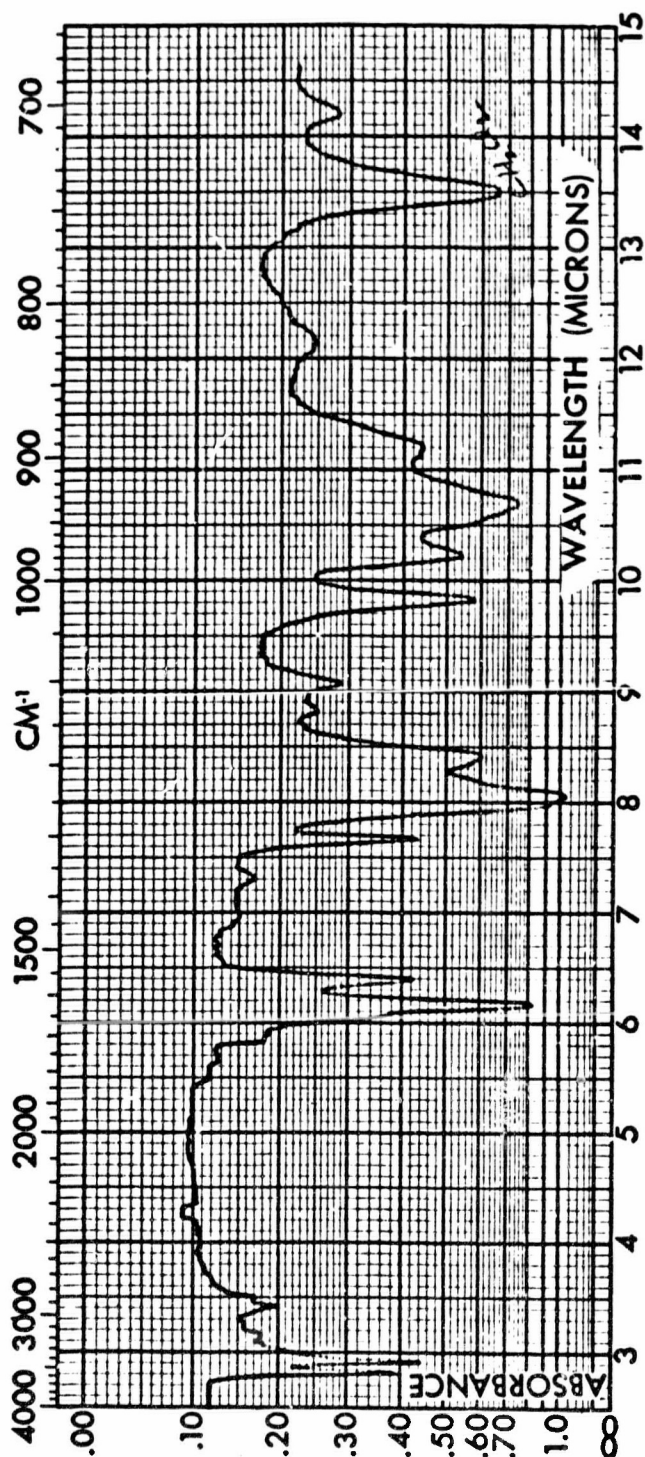
(C) In pursuing the reactions of oximes with tris-bromide, it became evident that nitration reactions with N_2O_4 were possible, since many unsaturated oximes are readily nitrated. This should lead to products having both the tris(difluoroamino)methyl function and a highly nitrated function. Compounds of this type should be solids and also excellent oxidizers. Moreover, shock sensitivity of INFO-635 is reduced in a nitroalkane.

(C) Using a 1:1 molar ratio of oxamidoxime to tris-bromide, the product $(\text{F}_2\text{N})_2\text{C}(\text{NHF})\text{O}-\text{N}=\text{C}(\text{NH}_2)-\text{C}(\text{NH}_2)=\text{NOH}$ was prepared. Nitration of the product occurred readily with N_2O_4 in Freon-11 at -30°C . An infrared spectrum of this product is shown in Figure 95. However, since it was discovered at this time that the oxime-tris-bromide product did not have the tris-moiety intact, but was in reality a PFG adduct, the studies were terminated.

(2) With Hydroxylamine Perchlorate (C)

(C) Since oximes had been found to react with tris-bromide, the reaction of hydroxylamine perchlorate with tris-bromide was investigated for the purpose of preparing INFO-615, directly. Specially prepared hydroxylamine perchlorate (from the reaction of hydroxylamine hydrochloride with barium perchlorate) was allowed to react with tris-bromide in a variety of solvents, including DMF, acetonitrile, ether, ethanol, and methanol, at temperatures from -60°C . to room temperature and over a period of time from 1 to 3 hours. In no case was a shock-sensitive compound made that would be indicative of the desired salt. The products obtained were bromine, unreacted tris-bromide and an unidentified NF -containing compound. When DMF, ether, and acetonitrile were used as solvents, substantial quantities of nitrous oxide from the decomposition of the tris-bromide were obtained. When ethanol and methanol were employed as solvents, ethyl and methyl nitrites were produced as well as nitrous oxide. No hydrogen bromide was ever observed, nor

CONFIDENTIAL



(C) Fig. 95 - Infrared Spectrum of Product from Nitration
of Adduct of tris-Br and Oxamidoxime

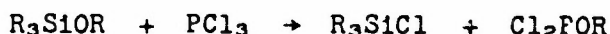
CONFIDENTIAL

CONFIDENTIAL

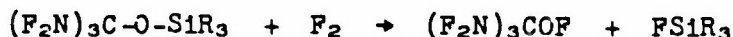
was the expected product found. The above data indicated that the reaction was not proceeding in the desired manner and, therefore, this study was dropped.

(3) With Triphenylsilanol (U)

(C) The discovery that tris-bromide would undergo displacement reactions with slightly acidic hydroxylic compounds, led to attempts at displacement of the bromine from tris-bromide with compounds other than oximes. For example, if tris-bromide reacted with silanols in the same manner as it was originally thought to react with oximes, it should be possible to prepare $(F_2N)_3C-O-SiR_3$ compounds. Fluorination of these compounds should lead to the formation of $(F_2N)_3C-OF$, since it is known that organosilicon alkoxides undergo reactions with various reagents to cleave the Si-O-C linkage at the Si-O bond and never at the C-O bond. Two examples of this are seen below:



Therefore, fluorination of $(F_2N)_3C-O-SiR_3$ should lead to the following:



Moreover, once formed, the $(F_2N)_3COF$ should be capable of transformation into $(F_2N)_3C-ONF_2$ by treatment with HNF_2 .

(C) When tris-bromide and triphenylsilanol were mixed in ether at room temperature, no reaction took place. However, when combined in the absence of a solvent and stirred at room temperature for two hours, the reactants exploded. Finally, pyridine was used as a solvent and proton acceptor to force the reaction to completion. In this case, tetrafluorohydrazine and triphenylsilyl fluoride were produced. Thus, attempts to prepare the silanol derivative of tris-bromide were not successful.

(4) With Nitroform (U)

(C) The reaction of tris-bromide with nitroform should produce tris-nitroformate, $(F_2N)_3C-C(NO_2)_3$, if simple displacement of the bromide by enolic (or slightly acidic) compounds was successful. When it was first discovered that oximes reacted with tris-bromide, the reaction of nitroform with tris-bromide was also carried out in ether at room temperature. An infrared analysis of the products showed the presence of bromonitroform, $BrC(NO_2)_3$. The only other isolable product appeared to be $FC(NF_2)_2NHF$; no free bromine was observed.

(C) Attempts were made to prepare $(F_2N)_3C-C(NO_2)_3$ as a solid oxidizing material by the reaction of tris-bromide and a metal

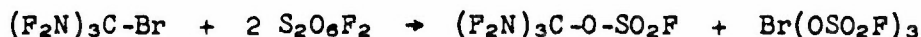
CONFIDENTIAL

salt of nitroform, $\text{MC}(\text{NO}_2)_3$. Both mercury and potassium salts of nitroform were prepared and used.

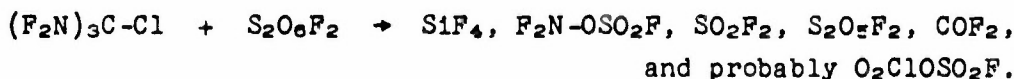
(C) When tris-bromide and the mercury salt of nitroform were allowed to react in diethyl ether at -8°C . for 1-1/2 hours, followed by 2 hours at 25°C ., only unreacted starting material and some decomposition products were observed, e.g., HNF_2 and N_2F_4 . In the case of the potassium salt, only starting materials were recovered from the reaction medium.

(5) With Peroxydisulfuryldifluoride (U)

(C) It was desirable to displace the bromine from tris-bromide by conventional means. However, neither $\text{S}_\text{N}1$ nor $\text{S}_\text{N}2$ displacement techniques had proven satisfactory. Therefore, explorations were made to determine whether free radical techniques could be employed. A successful displacement of bromine from tris-bromide was accomplished in a reaction with peroxydisulfuryl difluoride, $(\text{FSO}_2\text{OOSO}_2\text{F})$. When tris-bromide and peroxydisulfuryl difluoride were allowed to react for 48 hours at 70°C ., the following reaction took place:



(C) Additional quantities of the tris-fluorosulfonate were prepared in 70% yield at 90°C . for 16 hours. Molecular weight, infrared, NMR, mass spectra, and gas density data all corresponded to the product $(\text{F}_2\text{N})_3\text{COSO}_2\text{F}$, and are shown in Figure 96 and Table XXXIX. Employing the same reaction conditions and reagent with tris-chloride gave only the following:



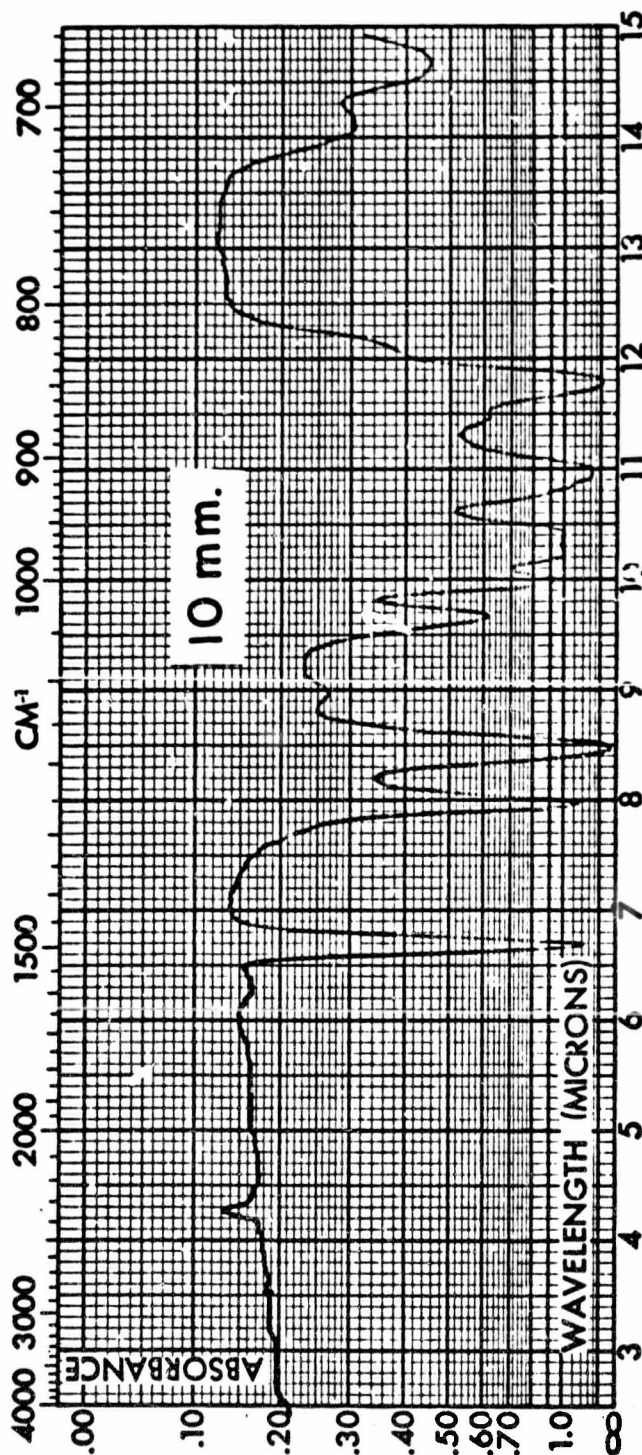
(C) Attempts to fluorinate the tris-fluorosulfonate, $(\text{F}_2\text{N})_3\text{COSO}_2\text{F}$, from the reaction of tris-bromide with peroxydifluorodisulfonate, yielded only the products CF_3OF and NF_3 in quantitative yield. Hydrolysis studies of the tris-fluorosulfonate in aqueous sulfuric acid led to no reaction; the starting material was recovered unchanged.

(U) Since peroxydisulfuryl difluoride apparently acts in a peroxide manner upon tris-bromide, other free radical addition reactions were carried out on tris-bromide employing either azobisisobutyronitrile, AIBN, or 98% H_2O_2 . No reaction was observed in any of these cases.

(6) With Compound A (U)

(C) Since Compound A, ClF_5 , is a powerful fluorinating agent, attempts to react Compound A with tris-bromide were carried out to obtain $(\text{F}_2\text{N})_3\text{C}^+\text{ClF}_4^-$. The product of the reaction was invariably decomposition products of Compound A such as FClO_3 and ClO_2 ; the tris-bromide was recovered unchanged.

CONFIDENTIAL



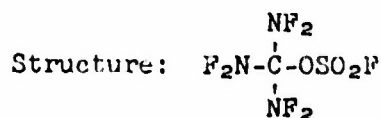
(C) Fig. 96 -- Infrared Spectrum of tris(Difluoroamino)methyl Fluorosulfonate

CONFIDENTIAL

CONFIDENTIAL

Table XXXIX

(C) Properties of tris(Difluoroamino)methyl Fluorosulfonate



Appearance: Colorless liquid.

B. P. (est.): 75°C.

Molecular Weight (by vapor density): Calc., 267; Found, 271.

	<u>Group</u>	<u>Peaks, δ</u>	<u>Area Ratio</u>
F^{19} NMR Spectrum: (CFCl_3 as ref.)	NF_2	-28.2	6
	SF	-52.0	1

SF peaks split into 7 lines with $J = 3.2$ cps.

Mass Spectrum:

M/e	215	168	144	97
Abundance	2.8	3.9	6.0	4.9
Assignment	$(\text{F}_2\text{N})_2\text{COSO}_2\text{F}$	$(\text{F}_2\text{N})_3\text{C}$	$\text{FN}=\text{COSO}_2\text{F}$	$\text{FN}=\text{CNF}_2$

M/e	83	80	78	67
Abundance	100	15	3.4	9.2
Assignment	SO_2F	SO_3^+ and F_2NCO	FNCNF	SOF

M/e	64	61	59	52
Abundance	13	47	1.9	25
Assignment	SO_2	FNCO	FNCN	NF_2

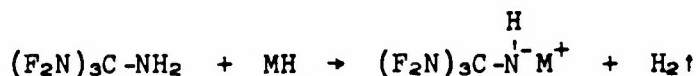
CONFIDENTIAL

c. tris-Chloride (U)

(U) Several displacement reactions were carried out on tris-chloride similar to those performed on tris-bromide. In reactions involving hydrazine, perchloric acid, silver perchlorate, silver nitrate, and fuming nitric acid, either no displacement or decomposition occurred. In the reaction of tris-chloride with oximes, the starting materials were recovered after three days.

d. tris-Amine (U)

(C) With the intention of investigating the possible acid character of tris-amine, the following reaction with a metal hydride was proposed for investigation:



(C) tris-Amine was treated with lithium aluminum hydride for 1 to 2 hours at $-50^\circ\text{C}.$, and the solid residue resulting therefrom was examined and was found to be shock-insensitive. The product consisted chiefly of lithium fluoride with a small quantity of Compound AlH₃-1451. Since it appeared evident that the reaction involved decomposition of the difluoroamino group, no further work was done.

(C) In order to prepare $(F_2N)_3CNO_2$, the oxidation of tris-A was carried out with ozone at room temperature. Analysis of the products indicated the presence of Compound H and PFG, plus various nitrogen oxides. The oxidation of tris-A with peracetic acid was similarly unsuccessful. An alternate approach involved the ozonization of the Schiff base, $(F_2N)_3C-N=CHNH_2$, available from the reaction of tris-A with formamide. Oxidation of this Schiff base with peracetic acid yielded a rearranged product containing $-CF_3$ and $-CF_2-$ groups as well as NF_2 groups. This study was therefore terminated.

e. Compound Delta (U)

(C) Since it had previously been shown that oximes react with tris-bromide to form an adduct with a concomitant elimination of bromine and fluorine from the tris group, a study of the reaction of Compound Delta with oximes was undertaken to determine if the oxime group reacts with NF_2 groups. Equimolar quantities of Compound Delta and acetone oxime were mixed in carbon tetrachloride and allowed to react 18 hours at room temperature. After this time, only unreacted starting materials were recovered. Ohtersolvents and catalysts did not facilitate a reaction between these reagents.

CONFIDENTIAL

(C) It was observed that Compound Delta decomposes photochemically when irradiated with ultraviolet light. If photochemical decomposition of Compound Delta is similar to thermal decomposition and proceeds through a $(F_2N)_3C$ free radical, it was thought possible to trap the free radical with a compound such as nitric oxide. When vapor phase mixtures of these two compounds were mixed and irradiated for 40 minutes, no reaction occurred; the starting materials were recovered unchanged.

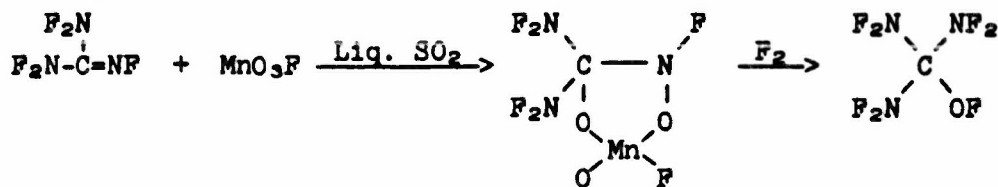
2. Reactions of PFG (U)

a. With Peroxydisulfuryl Difluoride (U)

(C) Since it has been shown that prototropic compounds such as HCl, HBr, HNCN, and HN_3 will form adducts with PFG, several other reactions of this type and others were carried out in order to obtain a solid oxidizer. Successful reactions were carried out with equimolar quantities of PFG and peroxydisulfuryl difluoride, in which case F_2NOSO_2F , $F_2NC(N^-)OSO_2F$, and $(FSO_2O)_3CN(F)OSO_2F$ were formed. Each of these products has been characterized by infrared, nuclear magnetic resonance and mass spectral methods, and these data are found in Figures 97 and 98 and Tables XL and XLI. Although these products in themselves are not useful as oxidizers, the above reaction does indicate that a presumed free radical attack may be employed to prepare useful oxidizers from PFG. Thus, additional research in this area with free radical formers was undertaken. However, neither azoisobutyronitrile (AIBN) nor 100% H_2O_2 proved successful.

b. With Permanganyl Fluoride (U)

(C) Since PFG had been found capable of undergoing the Diels-Alder reaction, it was thought that it would undergo other reactions peculiar to the carbon-nitrogen double bond. The specific reaction considered was the hydroxylation of olefins with metal oxides. The desired reaction sequence was as follows:

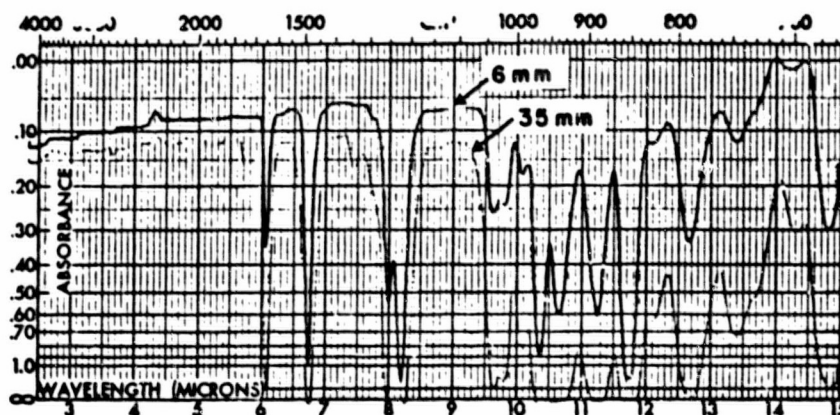


(U) The permanganyl fluoride was prepared by the reaction of fluorosulfonic acid with potassium permanganate as indicated below:



(U) Reactions with both MnO_3F and OsO_4 gave no indication of an adduct, and the direct fluorination gave no evidence that an OF-containing material had been produced.

CONFIDENTIAL



(C) Fig. 97 - Infrared Spectrum of Perfluoroformamidine Fluorosulfonate

Table XL

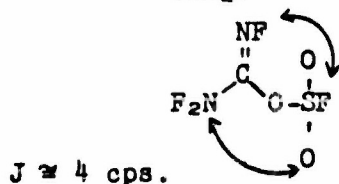
(C) Properties of Perfluoroformamidine Fluorosulfonate

Structure: $\text{F}_2\text{N}-\overset{\text{NF}}{\underset{\text{||}}{\text{C}}}-\text{OSO}_2\text{F}$
 Appearance: Colorless liquid
 B. P. (est.): 60°C.
 Molecular Weight (by vapor density): Calc., 196; Found, 195.

F^{19} NMR Spectrum:

Group	Peaks, δ	Ratio
NF_2	-7.33	2
$=\text{NF}$	-45.4	1
OSO_2F	-48.5	1

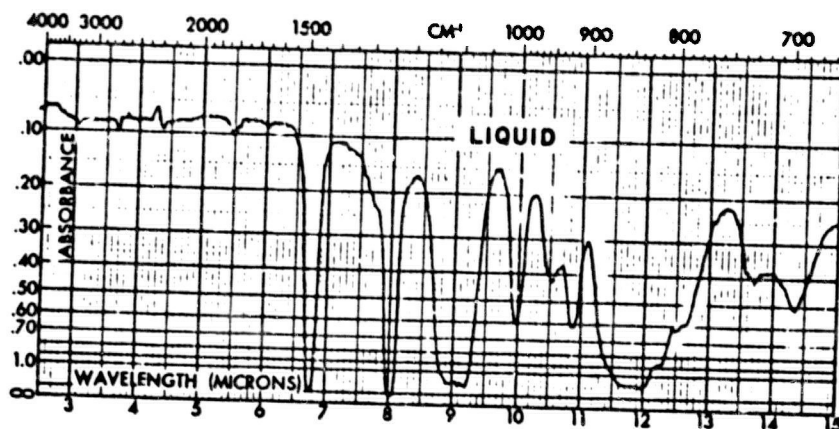
$J \approx 15$ cps.



Mass Spectrum:

M/e	144	97	83	80			
Abundance	8.7	1.2	100	5.4			
Assignment	FNCOSO ₂ F	FNCNF ₂	SO ₂ F	SO ₃ and OCNF ₂			
M/e	78	67	64	61	59		
Abundance	1.2	9.7	7.5	9.2	1.0		
Assignment	F ₂ NCN and FNCNF	SOF	SO ₂	OCNF	NCNF		
M/e	52	51	48	45	42	40	33
Abundance	2.9	1.0	10.2	0.6	5.8	1.3	9.0
Assignment	NF ₂	SF	SO	FNC	NCO	NCN	NF

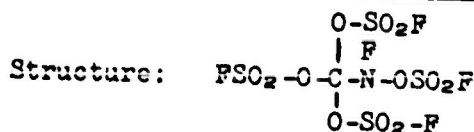
CONFIDENTIAL



(C) Fig. 98 - Infrared Spectrum of [tris(Fluorosulfonate)-methyl] Fluorosulfonatefluoroamine

Table XLI

(C) Physical Properties of [tris(Fluorosulfonate)methyl]-Fluorosulfonatefluoroamine



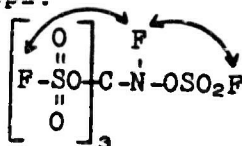
Appearance: Colorless liquid

B. P. (est.): >200°C.

¹⁹F NMR Spectrum:

Group	Peaks, δ	Ratio
NF	-18.6	1
NOSO ₂ F	-42.5	1
C(OSO ₂ F) ₃	-52.6	3

$J = 4.7$ cps. $J = 4.1$ cps.



Mass Spectrum:

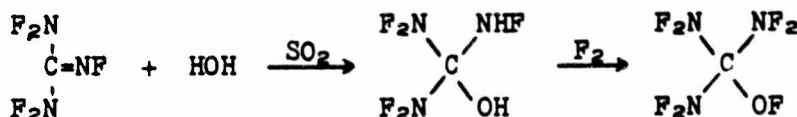
M/e	127	125	83	67	64
Abundance	24	24	39	20	100
Assignment	OCOSO ₂ F	NCOSO ₂ F	SO ₂ F	SOF	SO ₂

M/e	61	44	33
Abundance	3	97	6
Assignment	OCNF	CO ₂	NF

CONFIDENTIAL

c. With Water (U)

(C) Since the reaction of PFG with HCl or HBr to form tris-Cl and tris-Br, respectively, had proven successful, several attempts were made to react PFG with water in liquid SO₂ in the hope that this solvent might modify the hydrolysis reaction and allow water to add across the double bond to form an adduct.



(C) The reaction was carried out by starting at -80°C. and slowly raising the temperature over a period of several days. No hydrolysis was evidenced until the temperature reached -10°C., at which time the material hydrolyzed to yield HNF₂ in a matter of one or two hours.

d. With Formic Acid (U)

(C) Since it might be possible to obtain tris-OF by the fluorination of the formic acid adduct of PFG, FHNC(NF₂)₂-O-CH₃,
 $\text{O} \cdot$

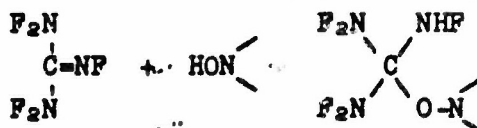
this reaction was investigated. When PFG was allowed to react with formic acid in liquid SO₂, no reaction was observed at temperatures up to room temperature over a period of time. Therefore, aluminum chloride was added as a catalyst, at which time a very rapid reaction was observed. Separation and identification of the products indicated the main product to be tris-chloride. The HCl was formed presumably in the hydrolysis reaction of aluminum chloride with water due to the wet formic acid. Upon drying the formic acid, the presence of aluminum chloride in the reaction media had no catalytic effect and no adduct formation was detected.

e. With Hydrogen Iodide (U)

(U) Since reactions of PFG with HCl and HBr had produced tris-chloride and tris-bromide, respectively, several attempts were made to prepare tris-iodide by the reaction of PFG with hydrogen iodide. Although a variety of techniques were used, such as low temperature addition of HI, dilution of the reaction medium, and the use of catalysts, no adduct formation was observed; instead, the hydrogen iodide was almost immediately oxidized to iodine.

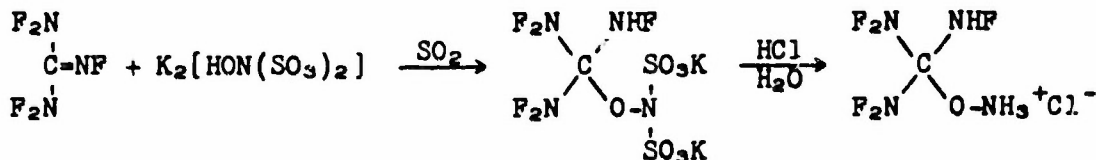
f. With Oximes (U)

(C) It has been shown in the past that oximes will form adducts with PFG, according to the following general equation:



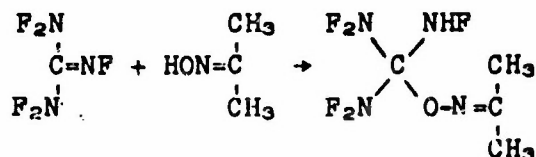
CONFIDENTIAL

(C) By analogy, therefore, it should be possible to form the hydroxylammonium adduct of PFG, using the following procedure:

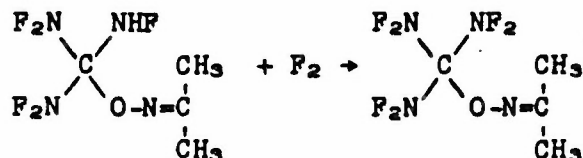


(U) PFG was allowed to react with potassium hydroxylamine disulfonate in liquid SO_2 as indicated above. However, no adduct formation was observed, probably due to the insolubility of the potassium salt.

(C) Acetone oxime forms an adduct with PFG quite easily in a variety of solvents. The general reaction is:

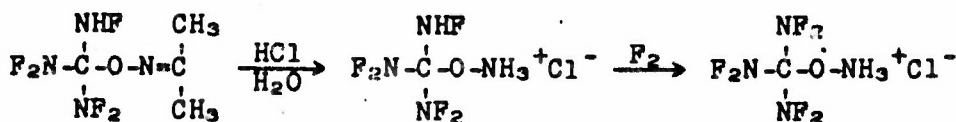


(C) The product has been identified by infrared and NMR spectroscopy. However, the difficult step in obtaining the desired product occurs in the fluorination of the adduct.



(U) Only poor yields could be obtained in this fluorination reaction.

(C) Because of the difficulty experienced in fluorinating the adduct, the feasibility of hydrolyzing the adduct to give the desired hydroxylamine salt was explored. Fluorination of this salt should then result in the desired product as indicated below:



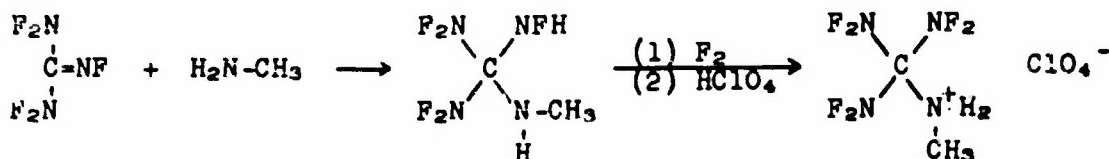
(U) Hydrolysis was therefore attempted with stoichiometric quantities of gaseous HCl and water in a variety of solvents. Ethanol was found to be the best solvent for this reaction and observable amounts of acetone were formed after hydrolysis; however, a large amount of N_2F_4 was also produced in the reaction.

CONFIDENTIAL

(U) Since the oxime adduct apparently decomposes under the conditions used for hydrolysis, this study was terminated.

g. With Amines (U)

(C) Although tris-A has been shown to be insufficiently basic to form salts, it was thought that the methylamine or dimethylamine adducts of PFG would be sufficiently basic to form salts, e.g., with HClO_4 , due to the positive inductive effect of the methyl groups. Several reactions, therefore, were carried out in order to prepare the methylamine and the dimethylamine adducts of PFG so that the perchlorate salt could be formed therefrom.



(C) The reaction between PFG and methylamine or dimethylamine was studied in the presence of solvents as well as neat, and under a variety of temperatures. These studies showed that when the reaction occurred, a light yellow, shock-insensitive solid was obtained. Elemental analysis was obtained on the products, all of which showed too low a fluorine content. The infrared spectrum showed the presence of CH, CF, and CN bonds. Only very weak peaks were found in the NF_2 region. Thus, it appeared that the essential reaction taking place was one of oxidation of the dimethylamine by the NF_2 group of the PFG rather than the desired adduct formation.

h. With Triphenylsilanol (U)

(C) Attempts were made to prepare the triphenylsilanol, $(\text{C}_6\text{H}_5)_3\text{SiOH}$, adduct of PFG as an intermediate, in the synthesis of tris(difluoroamino)methoxyfluoride, $(\text{NF}_2)_3\text{COF}$, and tris(difluoroamino)oxydifluoroaminomethane, $(\text{NF}_2)_3\text{CONF}_2$. At -80°C ., PFG and triphenylsilanol were combined in liquid SO_2 ; however, after one hour no reaction was observed. The reaction mixture was warmed to room temperature and maintained there for one hour. Again, no reaction was observed. In the presence of nitromethane and urea, the silanol reacted to form tetrafluorohydrazine, N_2F_4 , and triphenylsilanylfluoride, $(\text{C}_6\text{H}_5)_3\text{SiF}$. Similar results were obtained when PFG and triphenylsilanol were allowed to react in acetonitrile with urea as the catalyst at 0°C . for two hours. Since the desired results were not obtained, this reaction study was terminated.

(C) Recent literature discloses the preparation of anhydrous carbonic acid etherate. Since the cesium fluoride catalyzed fluorination of carbon dioxide yields $\text{CF}_2(\text{OF})_2$, it was thought that fluorination of free carbonic acid might yield $\text{CF}(\text{OF})_3$. Free carbonic acid was fluorinated with elemental fluorine at -80°C . for one hour. The reaction products were collected at -183°C .

CONFIDENTIAL

Upon warming the collected products to room temperature and while expanding them into a vacuum system, they ignited to yield a carbonaceous deposit. Infrared analysis of the remaining gases indicated that no material with OF bonds was present. No further work was done on this system.

C. FLUORINATION OF INORGANIC COMPOUNDS (U)

(C) In the past, attempts have been made to prepare C-OF compounds, since these appear to be less shock-sensitive than the corresponding NF compounds [cf. $(F_2N)_2CF_2$ vs. $(FO)_2CF_2$]. On the whole, these attempts have not been particularly fruitful. An alternative to this approach has been to completely eliminate the carbon (fuel) from the molecule. This idea has resulted in the fluorination of several salts in efforts to produce new oxidizers or oxidizer intermediates. The potassium, cesium, and ammonium salts of perchloryl amide, H_2NClO_3 , have been examined as a means of producing the possible oxidizer, NF_2ClO_3 . Fluorination of K_2NClO_3 and Cs_2NClO_3 at low temperatures resulted in explosions at $-20^\circ C.$ to $-30^\circ C.$ during a very gradual warm up of the reactor. Aqueous fluorination of $NH_4^+NHCLO_3^-$ at $0^\circ C.$ resulted in the production of $NOCl$, CO_2 , N_2O , FNO_3 , $FCLO_3$, ClO_2 , and trans- N_2F_2 . Upon fluorination calcium hypochlorite gave CaF_2 , ClO_2 , and Cl_2 as the main products, with $FCLO_3$ appearing as a minor product. Attempts to produce $FON=NOF$ from sodium hyponitrite and silver hyponitrite were unsuccessful. Since NF_2CF_2OF would be useful as a model in predicting the stability of compounds containing both NF_2 and OF groups, potassium cyanate was fluorinated at $-40^\circ C.$ About 95% of the gaseous product mixture was NF_3 and CF_3OF with the remaining 5% composed of equal quantities of CF_4 and OF_2 .

(C) Using cesium fluoride as a catalyst (generated by the fluorination of cesium carbonate), several runs have been made attempting to fluorinate nitrosyl fluoride, FNO_2 , to the oxidizer, $F_2N(O)OF$. No fluorination of FNO_2 was observed in the temperature range of $-30^\circ C.$ to $125^\circ C.$ At $150^\circ C.$ an unknown substance was detected. However, carbon compounds such as CO_2 , CF_3OF , and $CF_3(OF)_2$, derived from the catalyst, complicated isolation of the substance in a pure form. Table XLII lists the reactions carried out together with the conditions, the product expected, and the products observed.

D. EFFECT OF IMPURITIES ON THE IMPACT SENSITIVITY OF DIFLUOROAMINO COMPOUNDS (C)

(C) Since no further work of an extended nature is contemplated on sensitivity of difluoroamino compounds, this report will summarize the entire effort in this area.

1. Summary (U)

- (1) NF_2 compounds are inherently impact sensitive and appear to increase in sensitivity with the number of NF_2 groups per carbon.

CONFIDENTIAL

Table XLII

(1) Summary of Fluorination of Inorganic Compounds

Reaction Conditions	Expected Product	Products Found
$\text{PWO}_3 + \text{F}_2 \xrightarrow[\text{0.1 to 600 atm.}]{\text{CaF}_2 \text{ cat. Monel, } -80^\circ\text{C. to } 360^\circ\text{C.}}$	F_2NOF	No reaction
$\text{PWO}_3 + \text{F}_2 \xrightarrow[\text{0.1 to 0.5 atm.}]{\text{CaF}_2 \text{ cat. Monel, } -80^\circ\text{C. to } 25^\circ\text{C.}}$	$\text{PF}(\text{OF})_2$	$\text{PWO}_3 + \text{O}_2$
$\text{Na}_2\text{H}_2\text{O}_2(\text{trans}) + \text{F}_2 \xrightarrow{\text{metal}}$	Attempted to prepare PFM-NOF cis- or trans-	NO_2 , NOCl , SiF_4
$\text{Na}_2\text{H}_2\text{O}_2(\text{trans}) + \text{F}_2 \xrightarrow{\text{aqueous}}$	Attempted to prepare PFM-NOF cis- or trans-	CO_2 , OF_2
$\text{Ca}_2\text{H}_2\text{O}_2(\text{trans}) + \text{F}_2 \xrightarrow{\text{metal}}$	Attempted to prepare PFM-NOF cis- or trans-	NO_2 , NOCl , SiF_4
$\text{K}_2\text{H}_2\text{O}_2(\text{cis}) + \text{F}_2 \rightarrow$	Attempted to prepare PFM-NOF cis- or trans-	PWO_3 , H_2O
$\text{CaCO}_3 + \text{F}_2 \xrightarrow[\text{monel}]{-60^\circ\text{C.}}$	$\text{FC}(\text{OF})_2$	$\text{CF}_2(\text{OF})_2$ 64% + CF_3OF 36% + OF_2 + O_2CaF 36%
$\text{PClO}_2 + \text{F}_2 \xrightarrow[\text{nickel } 500 \text{ atm.}]{25^\circ\text{C. to } 300^\circ\text{C.}}$	$\text{F}_2\text{Cl}(\text{OF})_2$	PClO_2
$\text{PClO}_3 + \text{F}_2 \xrightarrow[\text{nickel } 500 \text{ atm.}]{25^\circ\text{C. to } 360^\circ\text{C.}}$	$\text{F}_2\text{Cl}(\text{OF})_2$	No reaction
$\text{Ca}(\text{OCl})_2 + \text{F}_2 \xrightarrow[\text{stainless steel}]{-80^\circ\text{C.}}$	F_2ClOF	CaF_2 + ClO_2 + PClO_2 + Cl_2
$\text{NaClO}_2 + \text{F}_2 \xrightarrow[\text{stainless steel}]{\text{room temperature}}$	$\text{F}_2\text{Cl}(\text{OF})_2$	ClO_2 , PClO_2
$\text{K}_2\text{MnClO}_4 + \text{F}_2 \xrightarrow[\text{stainless steel}]{-25^\circ\text{C.}}$	MnF_2ClO_2	PClO_2 , PWO_3 , H_2O , NOCl , ClO_2 , PWO_3
$\text{Ag}_2\text{MnClO}_4 \xrightarrow{\text{room temperature}}$	MnF_2ClO_2	Same as with potassium salt
$\text{NH}_4\text{MnClO}_4 + \text{F}_2 \xrightarrow{\text{aqueous}}$	cis- and trans- MnF_2ClO_2	CO_2 , PWO_3 , H_2O , NOCl , PClO_2 , H_2F_2
$\text{K}_2\text{OCH}_2\text{NHO}_2 + \text{F}_2 \xrightarrow[\text{stainless steel}]{-80^\circ\text{C.}}$	$\text{MnF}_2\text{CF}(\text{OF})_2$	CO_2 , H_2O , PWO_3
$(\text{NH}_4\text{OH})_2 \cdot \text{H}_2\text{SO}_4 + \text{F}_2 \xrightarrow{\text{aqueous}}$	F_2NOF	PWO_3 , H_2O , SiF_4
$\text{KOCN} + \text{F}_2 \xrightarrow{-40^\circ\text{C.}}$	MnF_2CFOF	CF_3OF + MnF_2 (quant.) + KF
$\text{KOCN} + \text{F}_2 \xrightarrow{\text{aqueous}}$		CO_2 , MnF_2 , OF_2 , H_2F_2
$(\text{MnF}_2)_2\text{OOSO}_2\text{F} + \text{F}_2 \xrightarrow[\text{-60}^\circ\text{C.}]{\text{CaF}_2}$	$(\text{MnF}_2)_2\text{COF}$	MnF_2 + CF_3OF + SO_2F_2 (quant.)
$(\text{F}_3\text{SO})_2\text{CHFCO}_2\text{F} + \text{F}_2 \xrightarrow[25^\circ\text{C.}]{\text{NaF}}$	$\text{FC}(\text{OF})_2$	SO_2F_2 , $\text{MnF}_2\text{OSO}_2\text{F}$, CO_2

CONFIDENTIAL

- (ii) Although there is an effect of impurities on the sensitivity of R and PFG, it is small. Furthermore, the impurities are mainly NF-containing compounds.
- (iii) The sensitivity of the tris-compound (formed upon fluorinating the HZ adduct of PFG) is substantially dependent upon the character of the Z group.
- (iv) In some cases, increased purity results in a lower sensitivity (e.g., R and PFG), whereas in others, the result is an increase in sensitivity (e.g., Delta).
- (v) A mixture or condition has not yet been found which exhibits an outstandingly lower sensitivity.

2. Introduction

(U) The objectives of this work have been two-fold:

- (i) To determine the degree of shock sensitivity of NF compounds.
- (ii) To determine whether impurities increase or decrease shock sensitivity of NF compounds.

(U) It is believed that both of these objectives have been met and were accomplished in an empirical approach.

(U) The NF compounds were subjected to an impact test in an "as received" or impure condition, and again after the materials were purified with a chromatograph having a thermal conductivity cell detector.

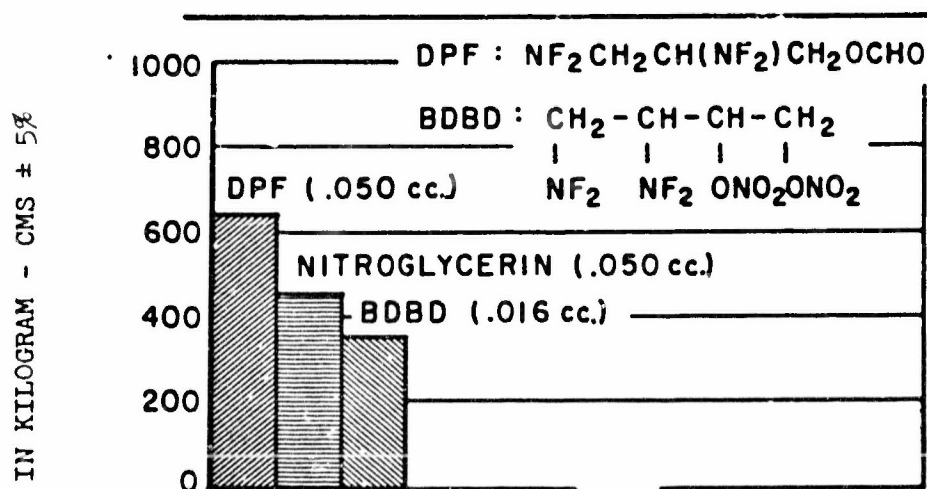
(U) To ascertain the purity of the compounds, an analytical gas chromatograph was used with accessory gas sampling and vacuum line apparatus. The analytical chromatograph, containing an electron capture detector which was especially sensitive to organic halides, was used to determine the extent of purification obtained from the preparative chromatographic column. Although numerous column absorbents were investigated, siloxane (FS-1265) and Kel-F 8126 oil in 30 percent concentration on Chromosorb W. were almost exclusively used. The former served as an excellent polar substrate and the latter a non-polar absorbent. Both columns were used with any single NF compound, usually several times. The degree of purity attained was estimated to be greater than 99.5%. To obtain a more accurate figure would be a very lengthy procedure because of the number of calibrations required on generally unavailable compounds.

(C) To determine the impact sensitivity of a sample, a special comparative method was employed in which samples of the NF₂ compound were sealed into copper capsules, placed in a specially constructed anvil, and then impacted with the dropped weight on a Bureau of Mines

CONFIDENTIAL

impact tester. The test capsules were fabricated from previously passivated 1/8 in. OD, soft copper tubing by using a jig to cut and crimp-seal the capsules in a uniform manner. The capsules were fitted with a Nupro stainless steel valve through which they could be loaded by condensing the volatile NF_2 compounds from the vacuum line. The design of the anvil insured that the liquid being tested would be at the bottom of the capsule and would be positively displaced upon impact compression. The test capsule was not completely closed following impact. From knowledge of the experimental parameters, it was known that the same liquid volume of sample was condensed into the capsule each time. Unless otherwise noted, the liquid volume used in the impact test was 0.016 ml. The impact levels reported are minimum fire levels, that is, the level at which at least five no-fires were recorded.

(C) Since it was of interest to compare data obtained by this method on more generally known compounds, three such compounds were included. The results are shown in Figure 99. It was found that DPF, nitroglycerin and du Pont's BDBD would detonate in the range of our apparatus. However, in order to get DPF and nitroglycerin to detonate at all, the volume required for impact testing had to be increased from 0.016 ml. to 0.050 ml.



(C) Fig. 99 - Minimum Fire Levels for DPF, Nitro, and BDBD

3. Experimental Work with D. Fluoroamino Compounds (C)

(C) Most of our effort involved a detailed examination of compounds R and PFG. Impact data were obtained on these impure and highly purified compounds and most of the impurities identified. Table XLIII shows that data on compound R as obtained from Minnesota

CONFIDENTIAL

Mining and Manufacturing. The five impurities were identified as (1) Compound H, $(F_2N)_2CF_2$, (2) PFF, F_2NCFNF , (3) FC-43, (4) F_2NCF_2NCO , (5) $CF_3NFCF_2NF_2$. A trace of a sixth impurity was present but has not been identified. The impure R was found to have a minimum impact level about 2.5 times lower than the highly purified compound.

Table XLIII

(U) Sensitivity Data on R and PFG

<u>Property</u>	<u>R</u>	<u>PFG</u>
Source	Minnesota Mining and Manufacturing 96% as received	American Cyanamid 92% as received
Minimum fire level kg. cm.		
Pure	381	258
As received	150	150

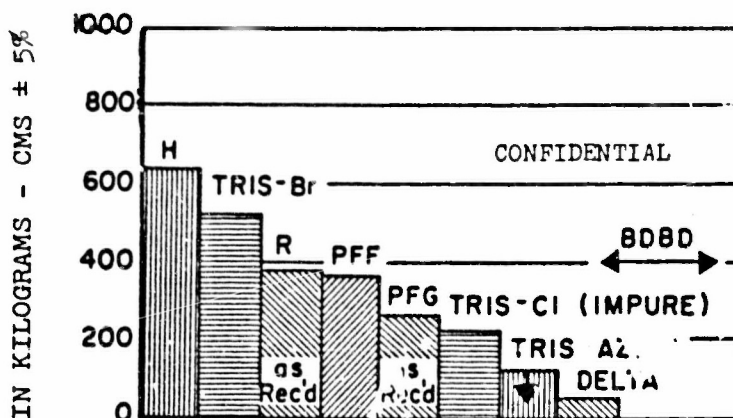
(C) In Table XLIII are shown the data on compound PFG received from American Cyanamid. The following impurities were identified: (1) N_2O , (2) CO_2 , (3) CF_4 , (4) N_2F_4 , (5) F_2N-CN , (6) F_2NCFN_2 , (7) $F_2NCF=NF$, (8) F_2NCF_2NHF , (9) HNF_2 , (10) $CF_2=NF$, and (11) F_2N-CF_2NCO .

(U) For both R and PFG, the isolated and identified impurities were reinserted singly into the purified material to determine which impurity might be responsible for initiating the detonations. There were indications that PFF might in some way affect the sensitivity of R and PFG. (In early work, the reinsertion of an impurity fraction containing mainly PFF gave an increased sensitivity to pure R. In another instance, insertion of PFF into PFG gave detonations at lower levels than pure PFG). However, since the impact sensitivity of PFF was determined to be nearly that of R, the effect of PFF on the sensitivity is not clear.

(U) In addition to PFG, and R, several other available compounds shown in Figure 100 were investigated. With the exception of tris-chloride, these compounds were purified chromatographically before testing.

(U) Tris-chloride could not be purified as highly as the others. Because of the limited supply of tris-azide, a minimum fire level was not obtained. The impact level for about 98% as-received Delta was less sensitive than the highly purified material by 6 kg. c. i.

CONFIDENTIAL



(C) Fig. 100 - Minimum Fire Levels for Various Difluoroamino Compounds

(C) The increasing sensitivity of the compounds as the progression is made from compound H to compound R, to Delta is to be noted. It had been conjectured, by analogy to tetranitromethane, that Delta, once made, would be less sensitive than other difluoroamino compounds. This was not found to be the case.

(U) The sensitivity relation between tris-bromide, tris-chloride, and tris-fluoride (compound R) is not immediately clear. Until more is known about the molecular structure and potential functions of compounds containing such highly electronegative groups, it may not be possible to clarify this apparent anomaly.

(U) Several additives have been used in attempts to reduce the impact sensitivity of PFG and R. Compounds such as N_2F_4 , N_2O_4 , HF , BF_3 , and NO were used in concentrations of 10 volume percent. A major decrease in the impact sensitivity was not achieved by any of these additives.

E. SUMMARY AND CONCLUSIONS (U)

(U) The studies on the role of the impurities in the shock sensitivity of NF compounds have shown that there appears to be no simple solution for the sensitivity problem. While careful purification of some NF compounds did reduce their sensitivity, in others there was an increased sensitivity with purification. The addition of certain inhibitors also did not decrease their sensitivity to a useful level.

CONFIDENTIAL

(C) The tris-halogen compounds are available by known synthetic routes and appear to be stable on storage. However, they are atypical in their reactions. They fail to undergo the simple displacement, Grignard, or addition reactions. Although reactions occur with slightly acidic compounds, e.g., oximes, the reactions can also form rearranged NF products.

(C) There now appears to be two routes open for further investigation. The first involves the preparation of multiple OF-containing compounds; e.g., $C(OF)_4$, $C_2(OF)_6$, etc., for which no synthesis route is presently available. The shock sensitivity of these compounds is presently unknown. The second route involves the preparation of mixed oxidizers such as those containing two or more of the groups, $-NO_2$, NO_2 , OF , ClF_4 , and NF_2 . Such a product, containing both NO_2 and NF_2 , is reported herein. Because of the limited time, this product has not been fully examined; however, its properties seem to warrant further investigation.

(U) Since additional stability could be available as a result of the crystal lattice energy, ionic crystalline solids should also be investigated.

(C) Several experiments were carried out to prepare $-O-NF_2$ type compounds starting with the reaction of PFG with oximes. None of these was successful. An alternate method for the preparation of an $O-NF_2$ compound might be the transformation of INFO-615 into tris- $-ONF_2$ by fluorination, if INFO-615 were readily prepared. To date, only one method is known for the preparation of $-O-NF_2$ compounds. This method requires the corresponding $-OF$ compound as the starting material, for which, again, there is no known suitable method of preparation. However, the potential energy available in a compound such as $C(O-NF_2)_4$ makes it highly desirable as an oxidizer.

CONFIDENTIAL

CONFIDENTIAL

(This page is Unclassified)

SECTION V

(U) PHYSICAL CHEMISTRY

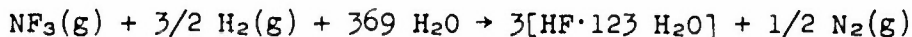
Work by: . Carr, J. Chao, A. T. Hu, B. H. Justice, G. C. Karris,
R. A. McDonald, F. L. Oetting, E. W. Phillips, H. Prophet,
G. C. Sinke, D. R. Stull, A. C. Swanson, A. N. Syverud,
L. C. Walker, and S. K. Wollert

A. THERMAL MEASUREMENTS (U)

1. Heats of Formation (U)

a. Nitrogen Trifluoride

(U) Nitrogen trifluoride has proved to be a useful oxidizer in reaction calorimetry. The technical grade material on hand contains 0.3% N₂O and 1.8% N₂. A batch of 20 g. was purified by low temperature codistillation. Careful analysis of this sample by infrared spectrometry and gas chromatography showed N₂O and SiF₄ content to be less than 0.01%. Mass spectrometer analysis had earlier (1) been interpreted as 0.05% N₂O and up to 0.1% SiF₄ but it now appears this is normal background. The work on the heat of reaction of NF₃ and H₂ was therefore revised once more with the only impurity correction being 0.02% CF₄. Details of this work have been published in the open literature (22). The new results are:



$$\Delta E = -198.31 \text{ kcal./mole}$$

$$\Delta H = -199.49 \text{ kcal./mole}$$

In order to calculate the heat of formation of NF₃, the heat of formation of aqueous HF is required. Two sets of values have recently been published (23, 24). These differ by about one kcal./mole and current opinion is that the best value is an average of the two. For (HF·123 H₂O)_{aq} this yields -76.9 kcal./mole, and employing this value gives for NF₃ a $\Delta H_{f298}(\text{g}) = -31.2 \text{ kcal./mole}$. This will be used in subsequent calculations in this report.

b. Aluminum Borohydride

(U) Details of measurements on the heat of explosion of mixtures of Al(BH₄)₃ vapor and NF₃ have been performed earlier in 1965 in this laboratory. Since then new information has become available on the heats of formation of the products (25) AlF₃(c)

CONFIDENTIAL

(This Page is Unclassified)

and $\text{BF}_3(\text{g})$ as well as the reactant* $\text{NF}_3(\text{g})$. The data were, therefore, recalculated using -360.8 kcal./mole for $\text{AlF}_3(\text{c})$, -271.65 kcal./mole for $\text{BF}_3(\text{g})$, and -31.2 kcal./mole for $\text{NF}_3(\text{g})$. Excess NF_3 in the experiments dissociated to N_2 and F_2 ; the new value for $\Delta E_{\text{dissoc.}}$ is -30.6 kcal./mole. The fluorine produced by dissociation reacted to some extent with Teflon gaskets used in the bomb to produce CF_4 . Analysis of the bomb gases for free fluorine indicated not all the CF_4 could have been formed by fluorine reaction; therefore, it was assumed that some CF_4 was produced by decomposition of Teflon into carbon and CF_4 . This was evidenced by patches of soot on the gaskets and the bomb walls near the gaskets. The analytical data were not accurate enough to exactly define the extent of each reaction and the best estimate was that 50% of the CF_4 was due to each. Infrared spectrometer analysis showed an average of 0.00026 mole CF_4 per $\text{Al}(\text{BH}_4)_3$ experiment and 0.000038 mole CF_4 per comparison experiment. The correction for fluorine reaction with Teflon is -123.7 kcal./mole of CF_4 formed (26), while the heat of decomposition to carbon and CF_4 was calculated as -24.8 kcal./mole of CF_4 . The total correction is then 19.3 calories in the $\text{Al}(\text{BH}_4)_3$ experiments and 2.8 calories in the comparison experiments. The uncertainty introduced by these corrections is about ± 5 kcal./mole in the heat of formation of $\text{Al}(\text{BH}_4)_3$.

(U) The recalculated experimental results are given in Tables XLIV and XLV.

Table XLIV

(U) Heat of Explosion of Aluminum Borohydride -
Nitrogen Trifluoride Mixtures

Run No.	Total Cal.	Corrections, Calories				ΔE_R kcal./mole
		NF_3 Dissoc.	Teflon Attack	Pt. Ign.	Sample moles	
1B	-2492.1	-65.4	19.3	3.3	0.001454	1741.0
2B	-2488.9	-65.3	19.3	6.4	0.001457	1735.4
4B	-2492.4	-65.8	19.3	6.6	0.001457	1738.0
5B	-2495.2	-65.9	19.3	6.0	0.001456	1740.9
6B	-2487.0	-66.7	19.3	6.0	0.001453	1740.1
					Average	1739.1

*See Section A.1.a.

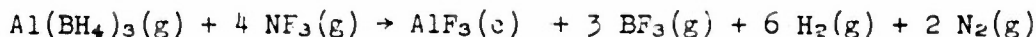
CONFIDENTIAL

Table XLV

(U) Nitrogen Trifluoride - Hydrogen Comparison Experiments

Run No.	Total Cal.	<u>Corrections, Calories</u>			Moles H ₂	<u>-ΔE_R</u> kcal./mole
		<u>NF₃</u> <u>Dissoc.</u>	<u>Teflon</u> <u>Attack</u>	<u>Pt</u> <u>Ign.</u>		
1C	- 981.0	-18.6	2.8	0.7	0.008607	115.7
2C	-1004.7	-14.1	2.8	0.6	0.008710	116.6
3C	- 993.4	-18.9	2.8	0.9	0.008694	116.0
5C	-1000.2	-16.8	2.8	0.6	0.008752	115.8
6C	- 999.2	-24.2	2.8	1.1	0.008739	116.7
Average						116.16

Combining the average values, this yields:



$$\Delta E = -1042.1 \text{ kcal.}$$

$$\Delta H = -1038.6 \text{ kcal.}$$

(C) From this result and the heats of formation of AlF₃, BF₃, and NF₃ discussed earlier, there is derived for Al(BH₄)₃:

$$\Delta H_f^\circ_{298} [\text{Al}(\text{BH}_4)_3] = -12.4 \text{ kcal./mole}$$

The total uncertainty is estimated as not more than 10 kcal./mole including uncertainties in the heats of formation of AlF₃, BF₃, and NF₃. The result is in reasonable agreement with recent work at the National Bureau of Standards.

c. Hybaline A-4 (U)

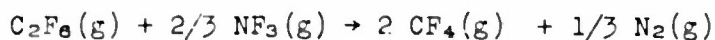
(C) Two experiments were carried out in which Al(BH₄)₃ vapor and (CH₃)₂NH vapor were reacted to form the liquid complex, known as Hybaline A-4. The average result was originally reported earlier this year as -43 kcal./mole. This included a correction for 4% hydrocarbon which was believed present in the Al(BH₄)₃. Later analysis showed no hydrocarbon to be present and the revised heat of reaction is -41 kcal./mole. Using the heat of formation of -12.4 kcal./mole for Al(BH₄)₃ just derived and -4.5 kcal./mole for (CH₃)₂NH vapor, there is calculated for liquid Hybaline A-4

CONFIDENTIAL

$\Delta H_{f298} = -57.9$ kcal./mole. This is in good agreement with -54.6 kcal./mole reported earlier, obtained by direct acid hydrolysis of a sample of Hybaline A-4. The heats of formation of $Al(BH_4)_3$ and its dimethylamine addition product are now reasonably well fixed. No further work is planned.

d. Hexafluoroethylene (U)

(U) To further develop techniques in the use of NF_3 as an oxidizer in calorimetry as well as to better define the thermochemistry of C_2F_6 , the heat of reaction of NF_3 and C_2F_6 was determined. An account of this work has been accepted for publication in the Journal of Physical Chemistry. The final result is repeated here:



$$\Delta H_{r298} = -103.9 \text{ kcal./mole}$$

(U) Accurate heats of formation cannot be calculated because of the uncertainty in $HF(aq)$ and $CF_4(g)$, but a test for consistency can be made using the latest NBS values (24). Using this reference, $\Delta H_{f298}(g) = -318.2$ kcal./mole, Tschuikow-Roux (27) measured the (CF_3-CF_3) dissociation energy as 93 ± 4 kcal. by direct observation in a shock tube. Combination of these data yields for the CF_3 radical a $\Delta H_{f298} = -112.6$ kcal./mole. Recent work on the (CF_3-H) dissociation energy has been summarized by Tarr, Coomber, and Whittle (28) who selected 105 ± 1 kcal./mole. Combination of this with the heat of formation of $CHF_3(g)$ for the CF_3 radical a $\Delta H_{f298} = -111.6$ kcal./mole, in excellent agreement with the value based on our heat of formation of C_2F_6 . These results are of theoretical interest as well as better defining thermal data for the JANAF Thermochemical Tables. Techniques developed for this problem should prove useful in determining heats of formation of any volatile C-H-F-N compound.

e. INFO-635 (U)

(C) The heat of formation of INFO-635 was determined by measuring the heat of combustion of a methanol solution as well as the heat of solution in methanol. The final result is:

$$\Delta H_{f298}(\text{INFO-635, c}) = -114.8 \text{ kcal./mole}$$

This value is in good agreement with work reported by Minnesota Mining and Manufacturing Company and by United Aircraft Company.

CONFIDENTIAL

f. Bis [tris(difluoroamino)methyl] Urea (BTU) (C)

(U) The BTU was supplied to us by the American Cyanamid Company (29) in a halocarbon wax medium. The directions, supplied by the above Company, necessary for purification of this product were followed in general, i.e., extraction with n-hexane followed by sublimation. Best results were obtained by subliming the BTU onto a gold or platinum foil thimble at a pressure of 1.2 microns and at an oil bath temperature of 110°C. After sublimation, all transfer work was carried out in a dry box having a low oxygen and water vapor content.

(U) Because BTU is explosive and hygroscopic, a suitable technique had to be developed for obtaining accurate sample weights. The thimble and deposited BTU were transferred in a dry box from the sublimation apparatus to a weigh bottle with a ground glass stopper. The dry box pressure was adjusted close to that of the outside atmosphere, the weigh bottle was closed and placed in a spare combustion bomb which was then also closed and removed from the dry box. An analytical balance was available which had a wire connected to one arm. The wire passed through a hole in the balance floor into an enclosure below the balance table. The spare combustion bomb was opened, the weigh bottle hung on the wire, and the weight recorded as a function of elapsed atmosphere exposure time. The bottle was then returned to the bomb which was in turn locked into the dry box along with a calorimetric platinum lined combustion bomb. The thimble and deposited BTU were transferred to the calorimetric bomb which was then closed. A tare weight was obtained on the empty weigh bottle in the same fashion as described for the sample. Repeating the cycle three times each for the full and empty weigh bottle indicated a reproducibility of 0.1 mg. in the same weight. Weights were corrected to mass in vacuum using a density of 1.88 g./cc. for BTU.

(U) The calorimetric bomb containing the thimble and deposited BTU was attached to a vacuum line and evacuated. High purity hydrogen was then charged to the bomb to a pressure of 800.0 mm. The bomb was then placed in a calorimeter. One valve stem had been replaced by a length of 1/8" stainless steel tubing and a Hoke needle valve; the tubing projected through the lid of the calorimeter so that the needle valve was outside the calorimeter and could be connected to a cylinder of oxygen. After initial drift rate readings, the needle valve was opened and the bomb charged with oxygen to a total pressure of 5 atm. The valve was closed and the mixture ignited by an electrically heated fuse wire. The explosion of the hydrogen-oxygen mixture set off the BTU. The heat of the overall reaction was measured. The addition of oxygen just prior to ignition was necessary because hydrogen and oxygen react slowly in a platinum lined bomb. To eliminate the effects of this oxygen charging, comparison runs were made in which hydrogen but no BTU was charged to the bomb. Oxygen was added just as in the BTU experiments and the heat of the explosion measured.

CONFIDENTIAL

(This page is Unclassified)

(U) After the calorimetry, 50 ml. of water was forced into the bomb and the bomb was shaken to wash down the walls and lid. The gaseous combustion products were analyzed for CO_2 by passage through magnesium perchlorate and absorption in Ascarite. Samples of the gas after passage through the absorption train showed no detectable CF_4 by mass spectrometry. A trace of CF_4 was observed by infrared in both the BTU and the comparison experiments; this was attributed to reaction of Teflon gaskets, and any effect cancelled out. The solution remaining in the bomb was analyzed for total acidity, fluoride, and nitrate.

(U) The calorimeter was calibrated by combustion of NBS benzoic acid 391. An average of 0.234 g. was used, the bomb volume was 0.35 l., the initial pressure 30 atm. of oxygen, and 1 ml. of water was added. At 25°C . the heat of combustion under these conditions was calculated as 6317.24 cal./g. mass. Three determinations agreed within ± 1.9 cal./ $^\circ\text{C}$. The calorimeter equivalent adjusted to experimental conditions was calculated for each individual experiment.

(U) Four acceptable comparison experiments gave an average of 1036.87 cal./experiment, with a maximum deviation of 1.06 cal. and an average deviation of 0.67 cal.

(U) Results of the BTU experiments are listed in Table XLVI. The corrected temperature rise, calorimeter equivalent, and sample mass need no further explanation. The "volume correction" allows for the hydrogen displaced by the thimble and the BTU. The "vapor correction" allows for the difference in vapor pressure of the pure water formed in comparison experiments and the HF solutions formed in the BTU experiments. Vapor pressure data for this correction are from Brosheer et al. (30). Heats of vaporization of water and HF were taken as 10 and 11 kcal./mole, respectively. The "dilution correction" allows for adjustment to a final state of $\text{HF} \cdot 3\text{H}_2\text{O}$, and the " HNO_3 correction" allows for formation of nitric acid from oxygen, nitrogen, and water. The " C_2F_4 correction" allows for slight reaction of Teflon gaskets to form CO_2 and HF. The extent of this reaction was calculated from the CO_2 analysis and the sample weight. The total CO_2 found, less the theoretical amount from the sample, gave the amount due to Teflon reaction. The assumption of Teflon reaction was tested in one BTU experiment by placing an extra unprotected Teflon washer in the bomb. A large excess of CO_2 over the calculated amount from BTU was recovered and the washer was almost completely consumed. CF_4 was also found in the product gas from this experiment. From Table XLVI the average $-\Delta E_c/M$ is 2004 cal./g. with a standard deviation of 5 cal./g. It should be noted that all runs except the last were made on freshly sublimed samples. The last run involved a sample which was stored for over a week. Further work would be needed to determine if the rather low value for this run was due to decomposition or reaction during storage.

CONFIDENTIAL

(This page is Unclassified)

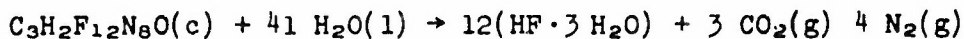
CONFIDENTIAL

Table XLVI

(U) The Heat of Combustion of BTU

Δt °C.	Calor. Equiv. cal./°C.	Sample Mass g.	Correction, cal.					Net Cal.	$\Delta E^{\circ}C/M$ cal./g.
			Vol.	Vapor	Dil'n.	HNO ₃	C ₂ F ₄		
0.43590	-3169.7	0.1664	-0.47	-1.71	-0.44	4.97	6.03	-333.0	2001
0.41358	-3170.6	0.1334	-0.42	1.41	-0.15	3.41	2.20	-367.7	2007
0.43171	-3170.6	0.1607	-0.36	1.65	-0.33	4.36	3.28	-323.3	2012
0.43134	-3170.6	0.1602	-0.36	1.67	-0.33	4.86	2.05	-322.9	2016
0.44675	-3170.6	0.1860	-0.38	1.86	-0.79	5.91	3.63	-369.4	1986
Average									2004

(C) Employing a molecular weight of 394.08, there is derived:



$$\Delta E = -789.74 \text{ kcal.}$$

$$\Delta n(\text{gas}) = +7 \text{ moles}$$

$$\Delta H = -785.59 \text{ kcal.}$$

$$\text{Uncertainty} = 2 \sigma = 4 \text{ kcal./mole}$$

(U) The heat of formation depends on the value for HF(aq), as shown in Table XLVII. Values based on work reported by American Cyanamid Company are given for comparison. The difference is larger than the combined uncertainties by about 15 kcal. We are unable to account for the discrepancy.

Table XLVII

(U) Heat of Formation of BTU Using Selected Auxiliary Data

	ΔH_{f298}° , kcal./mole		
	NBS		
	NBS Circular 500	Technical Note 470-1	Current Best Value
Dow	-59.6	-90.7	-73.7
American Cyanamid	-85.8	-93.4	-100.4

UNCLASSIFIED

2. High Temperature Enthalpies (U)

a. Thermodynamic Properties and Allotropy of Beryllium Chloride from 13°K. to 750°K.

The investigation of beryllium chloride has been completed this year.

The heat capacities of the α' and β forms of beryllium chloride have been measured in an adiabatic calorimeter from 13°K. to 304°K. The absolute entropy at 298.15°K. is 19.76 ± 0.06 cal./mole °K. for the α' form and 18.12 ± 0.05 cal./mole °K. for the β form.

Using a copper block drop calorimeter, enthalpies were determined for the β form (relative to the β form) from 298°K. to 676°K., the α form (relative to the α' form) from 676°K. to 688°K., and the liquid (relative to the α' form) from 688°K. to 713°K. The α' form and the α form are considered to be identical. The heat of the α - β transition at 676°K. was calculated to be 1490 ± 150 cal./mole. The heat of fusion of the α form at 688°K. was found to be 2070 ± 60 cal./mole.

The heat of the α - β transition was earlier reported erroneously as 1320 ± 100 cal./mole. This changes the Table of Thermodynamic Functions above 676°K. and corrected values are given in Table XLVIII presented here.

A schematic phase diagram was proposed.

b. Thermodynamic Properties of Aluminum from 298°K. to 1650°K.

Published values for the enthalpy and heat capacity of liquid aluminum are widely discordant and cover only a small part of the liquid temperature range. There is also some uncertainty in the value of the heat of fusion of aluminum. This work was undertaken to obtain more definitive data and to extend the measurements on liquid aluminum to higher temperature.

Cylindrical samples were machined from high purity aluminum purchased from the United Mineral and Chemical Corporation. Spectrographic analysis detected only 2.0 ppm. Si, 1.8 ppm. Fe, and 2.7 ppm. Cu.

Two crucibles, one of titanium diboride and one of boron nitride, were used to contain the aluminum. An X-ray diffraction analysis of a titanium diboride crucible manufactured by the

UNCLASSIFIED

Table XLVIII

(U) Thermodynamic Functions^a of α -Beryllium Chloride^b

T °K.	C_p cal./mole °K.)	S° cal./mole °K.)	$-(F_T-H_0)/T$ cal./mole °K.)	H_T-H_0 cal./mole
13	0.476	0.162	0.040	1.6
15	0.641	0.241	0.062	2.7
20	1.114	0.489	0.136	7.1
25	1.605	0.790	0.236	13.9
30	2.130	1.129	0.356	23.2
35	2.689	1.499	0.493	35.2
40	3.217	1.893	0.643	50.0
45	3.718	2.301	0.804	67.3
50	4.202	2.717	0.975	87.1
55	4.691	3.141	1.152	109.4
60	5.144	3.569	1.336	134.0
70	5.968	4.425	1.716	189.6
80	6.747	5.273	2.108	253.2
90	7.541	6.109	2.506	324.3
100	8.045	6.925	2.907	401.8
110	8.619	7.719	3.309	485.1
120	9.189	8.494	3.709	574.2
130	9.74	9.251	4.106	666.9
140	10.26	9.992	4.500	768.9
150	10.76	10.72	4.891	874.0
160	11.24	11.43	5.277	984.1
170	11.68	12.12	5.659	1099
180	12.07	12.80	6.037	1218
190	12.46	13.46	6.411	1340
200	12.80	14.11	6.780	1466
210	13.14	14.74	7.144	1596
220	13.46	15.36	7.504	1729
230	13.74	15.97	7.859	1865
240	14.01	16.56	8.209	2004
250	14.28	17.14	8.554	2145
260	14.55	17.70	8.895	2290
270	14.81	18.26	9.232	2436
273.15	14.89	18.42	9.336	2484
280	15.06	18.80	9.564	2586
290	15.31	19.33	9.891	2738
298.15	15.50	19.76	10.16	2863
300	15.54	19.85	10.22	2892
310	15.76	20.37	10.53	3048

UNCLASSIFIED

Table XLVII (Contd.)

T °K.	C_p cal./mole °K.)	S° cal./mole °K.)	$-F_T-H_0)/T$ cal./mole °K.)	H_T-H_0 cal./mole
B-a-Liquid Beryllium Chloride ^b				
13	0.209	0.898	0.011	0.7
15	0.300	1.208	0.020	1.2
20	0.600	1.546	0.055	3.4
25	1.008	1.904	0.106	7.4
30	1.499	2.274	0.173	13.6
35	2.038	2.654	0.257	22.5
40	2.610	3.433	0.356	34.1
45	3.138	4.217	0.469	48.5
50	3.647	4.995	0.595	65.4
55	4.137	5.761	0.730	84.9
60	4.606	6.514	0.875	106.8
70	5.496	7.252	1.185	157.4
80	6.259	7.977	1.515	216.2
90	6.951	8.688	1.858	282.3
100	7.595	9.385	2.210	255.1
110	8.202	10.07	2.567	434.1
120	8.771	10.73	2.927	519.0
130	9.344	11.38	3.288	609.6
140	9.857	12.02	3.648	705.6
150	10.33	12.65	4.008	806.6
160	10.78	13.26	4.365	912.1
170	11.21	13.86	4.720	1022
180	11.62	14.45	5.072	1136
190	12.02	15.02	5.421	1254
200	12.38	15.58	5.767	1377
210	12.73	16.13	6.110	1502
220	13.03	16.67	6.448	1631
230	13.32	16.83	6.782	1763
240	13.60	17.19	7.115	1897
250	13.86	17.71	7.442	2035

UNCLASSIFIED

Table XLVII (Contd.)

T °K.	C _p cal./[(mole °K.)]	S° cal./[(mole °K.)]	-(F _T -H ₀)/T cal./[(mole °K.)]	H _T -H ₀ cal./mole
260	14.11	16.13	7.766	2175
270	14.34	16.67	8.086	2317
273.15	14.41	16.83	8.186	2362
280	14.56	17.19	8.402	2461
290	14.76	17.71	8.714	2608
298.15	14.92	18.12	8.965	2729
300	14.96	18.21	9.022	2756
350	15.76	20.58	10.51	3525
400	16.42	22.73	11.97	4330
450	16.90	24.69	13.22	5166
500	17.40	26.50	14.46	6024
550	17.78	28.18	15.63	6904
600	18.12	29.74	16.74	7801
650	18.44	31.20	17.80	8715
676(b)	18.60	31.97	18.33	9197
676(a)	19.39	34.11	18.33	10687
680	19.41	34.25	18.42	10764
684	19.42	34.36	18.51	10842
688(a)	19.44	34.47	18.60	10920
688(1)	29.02	37.48	18.60	12990
700	29.02	37.99	18.94	13338
750	29.02	39.99	20.27	14789

^aTo retain internal consistency, some of the values in this table are given to more places than would be justified by experimental accuracy.

^bMolecular weight, 79,927.

UNCLASSIFIED

National Carbon Company, Division of Union Carbide Corporation, revealed the only crystalline phase present in detectable amounts to be TiB_2 . Spectrographic analysis indicated the presence of 0.02% Al, 3% Cr, 1.2% Fe, 0.07% Mo, and 0.04% V.

Two crucibles of boron nitride were obtained from Cerac, Incorporated. A glaze was found on the first crucible after measuring its enthalpy. The glaze contained boric acid, identified by X-ray diffraction, and was soluble in methanol. Undoubtedly boron oxide is present in the boron nitride, either as an impurity or as part of a proprietary oxide binder.

Extraction of the boron nitride crucibles and covers with A.C.S. grade methanol in a Soxhlet extractor for 22 hours resulted in a weight loss of 11% to 12%. This eliminated the glazing and lowered the enthalpy of the crucible, but the treatment was not sufficient to remove all of the boron oxide as shown by subsequent reaction with the aluminum sample.

The enthalpy, $H_T - H_{298.15}$, was measured in a copper block calorimeter previously described (31).

The first titanium diboride crucible with cover (8.736 g.) was sealed in a platinum - 10% rhodium alloy capsule (15.029 g.) by arc welding under helium at about 8 cm. mercury pressure. The enthalpy of the empty crucible was determined, but the top and bottom of the crucible stuck to the metal capsule and therefore it was not used again. An aluminum cylinder (6.072 g.) was contained in the second titanium diboride crucible (12.554 g.) sealed in a platinum - 10% rhodium capsule (14.406 g.) for the first series of measurements on aluminum. This series ended when the crucible cracked, allowing molten aluminum to attack the capsule.

Additional titanium diboride crucibles could not be purchased and, upon the advice of Dr. William B. Frank of the Alcoa Research Laboratories, boron nitride was selected as the crucible material for further experiments.

One of the methanol extracted boron nitride crucibles, with cover, weighing 5.344 g., was sealed in a 14.728 g. platinum - 10% rhodium alloy capsule for the empty crucible runs. For the second series of aluminum enthalpy measurements, 5.869 g. Al, 5.336 g. BN crucible, and 14.962 g. capsule were used. The second series of measurements was terminated when corrosion of the capsule became evident. The capsule was opened. The area of attack of the capsule was located at the juncture of the crucible and its cover. There was also a blackening of the inner wall of the boron nitride crucible and some coating of parts of the aluminum slug. X-Ray diffraction analyses have identified $9 \text{ Al}_2\text{O}_3 \cdot 2 \text{ B}_2\text{O}_3$, AlN , $\alpha\text{-Al}_2\text{O}_3$, and H_3BO_3 in the reaction products. Evidently not all of the boron oxide had been removed from the boron nitride by the methanol extraction.

UNCLASSIFIED

After mechanically cleaning the aluminum sample slug, a hydrogen gas evolution analysis indicated that at least 98.5% of the original aluminum sample still was present as aluminum metal after the final measurement.

Even though the titanium diboride crucible was not pure titanium boride, the observed enthalpy is in agreement with the data of Walker, Ewing, and Miller (32) who indicated a sample purity of 99.7%, and with values given by Mexaki, Tilleux, and Barnes (33). There is also reasonable agreement with the work of Osment (34) up to about 1650°K. The observed enthalpies of "titanium diboride," Table XLIX, were smoothed as suggested by Shomate (35) to obtain the values in Table I. Figure 101 and Table XLIX show the percent deviation of the observed values from the smoothed data.

The enthalpy of the extracted boron nitride crucibles was found to be somewhat higher (2.5% maximum) than published values (36) up to about 1500°K. This is attributed to the presence of impurities in the boron nitride crucible.

The observed enthalpy data for aluminum are listed in Table LI. The heat content of the solid aluminum was about 32% of the total heat measured in the titanium diboride crucible series and about 40% of the total in the boron nitride crucible series. With liquid aluminum the proportion is somewhat more favorable at about 40% and 46%, respectively.

Rough average heat capacities of solid aluminum were obtained at 50°C. intervals from the "best curve" of a large scale enthalpy vs. temperature plot. The rough heat capacities were then graphically smoothed, taking into account the low temperature heat capacity studies of Giauque and Meads (37) [lowered slightly to apply to the multicrystalline state as indicated by the work of Maier and Anderson (38), and Griffiths and Griffiths (39)]. The smoothed heat capacities at 20°C. intervals were then integrated by a computer to obtain the smoothed enthalpies given in Table LII. Deviations of the observed from the smoothed data are shown in Table LI and Figure 102.

Also shown in Figure 102 are the values from Awbery and Griffiths (40), Eastman, Williams and Young (41), Glaser (42), Kendall and Hultgren (43), Magnus (44), Naccari (45), Satoh (46), Tilden (47), Umino (48), and Wust, Meuthen, and Durrer (49). The smoothed data are in general agreement with Awbery and Griffiths, Eastman et al., Kendall and Hultgren, Satoh, and Wust et al. The rest found generally lower values. The evaluations of Kelley (50), which were adopted by Stull and Sinke (51), and of Hultgren et al. (52), are only slightly lower than the smoothed enthalpies presented here, except near the melting point where the deviation increases to about one percent.

UNCLASSIFIED

UNCLASSIFIED

Table XLIX

(U) Observed Enthalpy of Titanium Diboride^{a, b}

T, °K.	H _T -H _{298.15} cal./mole	Deviation from Smooth Curve	
		cal./mole	%
326.7	326.1	+16	+5.10
441.8	1,769	-1	-0.06
445.3	1,822	+4	+0.22
558.0	3,483	-11	-0.31
667.8	5,266	+10	+0.19
757.1	6,742	-10	-0.14
890.0	9,082	+26	+0.29
954.7	10,155	-37	-0.36
970.4	10,478	+2	+0.02
1,072.1	12,373	+77	+0.63
1,155.5	13,821	+21	+0.15
1,246.7	15,419	-33	-0.21
1,305.7	16,453	-87	-0.52
1,320.5	16,770	-40	-0.24
1,385.1	17,991	-7	-0.04
1,457.2	19,346	+8	+0.04
1,544.0	20,944	-8	-0.04
1,642.3	22,926	+126	+0.55
1,765.6	25,176	+32	+0.13

^aNot greater than 95.7% pure.

^bGram mole wt. = 69.54.

Table L

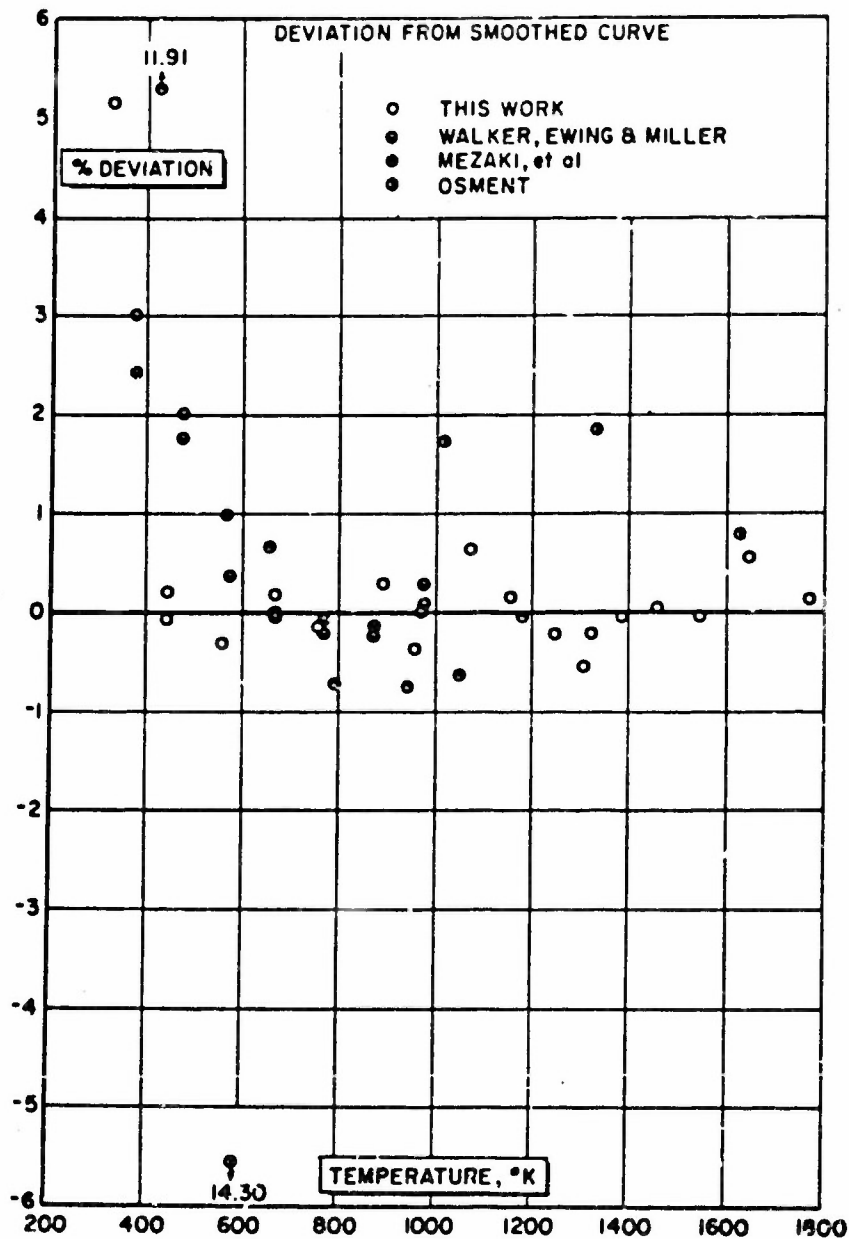
(U) Smoothed Enthalpy of Titanium Diboride^{a, b}

T, °K.	H _T -H _{298.15} cal./mole	T, °K.	H _T -H _{298.15} cal./mole
298.15	0	1,100	13,800
300	19.47	1,200	14,610
400	1,210	1,300	16,431
500	2,608	1,400	18,272
600	4,152	1,500	20,126
700	5,791	1,600	22,005
800	7,492	1,700	23,894
900	9,233	1,800	25,808
1,000	11,005		

^aNot greater than 95.7% pure.

^bGram mole wt. = 69.54.

UNCLASSIFIED



(U) Fig. 101 - Deviation of Enthalpy of Titanium Diboride from Smoothed Curve up to 1800°K.

UNCLASSIFIED

UNCLASSIFIED

Table LI

(U) Observed Enthalpy of Aluminum^a

T, °K.	HT-H _{298.15} cal./mole	Deviation from Smooth Curve	
		cal./mole	%
365.8	380.9	-19	-4.75
426.0 ^b	762.4	- 9	-1.17
431.1 ^b	921.6	+20	+2.49
486.7	1,137	-17	-1.47
528.9 ^b	1,459	+30	+2.10
595.6	1,852	-18	-0.96
656.8 ^b	2,301	+18	-0.79
727.5 ^c	2,776	- 4	-0.01
762.1 ^b	2,990	-36	-1.19
775.6 ^b	3,137	+15	+0.48
777.1	3,111	-22	-0.70
805.5 ^b	3,351	+10	+0.30
870.7 ^b	3,867	+36	+0.94
895.4 ^b	3,966	-60	-1.45
909.1	4,114	-21	-0.51
920.8	4,265	+36	+0.85
(933.0)	(m.p.)	---	---
941.4	6,974	+22	+0.32
998.6 ^b	7,342	-43	-0.58
1,011.5 ^b	7,500	+17	+0.22
1,081.0 ^b	7,980	-30	-0.38
1,097.8	8,152	+14	+0.17
1,208.4 ^b	9,027	+50	+0.55
1,244.9	9,247	- 8	-0.08
1,384.2	10,298	-14	-0.13
1,512.1	11,254	-28	-0.25
1,647.2	12,328	+21	+0.17

^aGram atomic wt. = 26.98

^bAluminum contained in TiB₂ crucible. Others (without superscript) in EN crucible.

^cLast "drop" in EN crucible.

UNCLASSIFIED

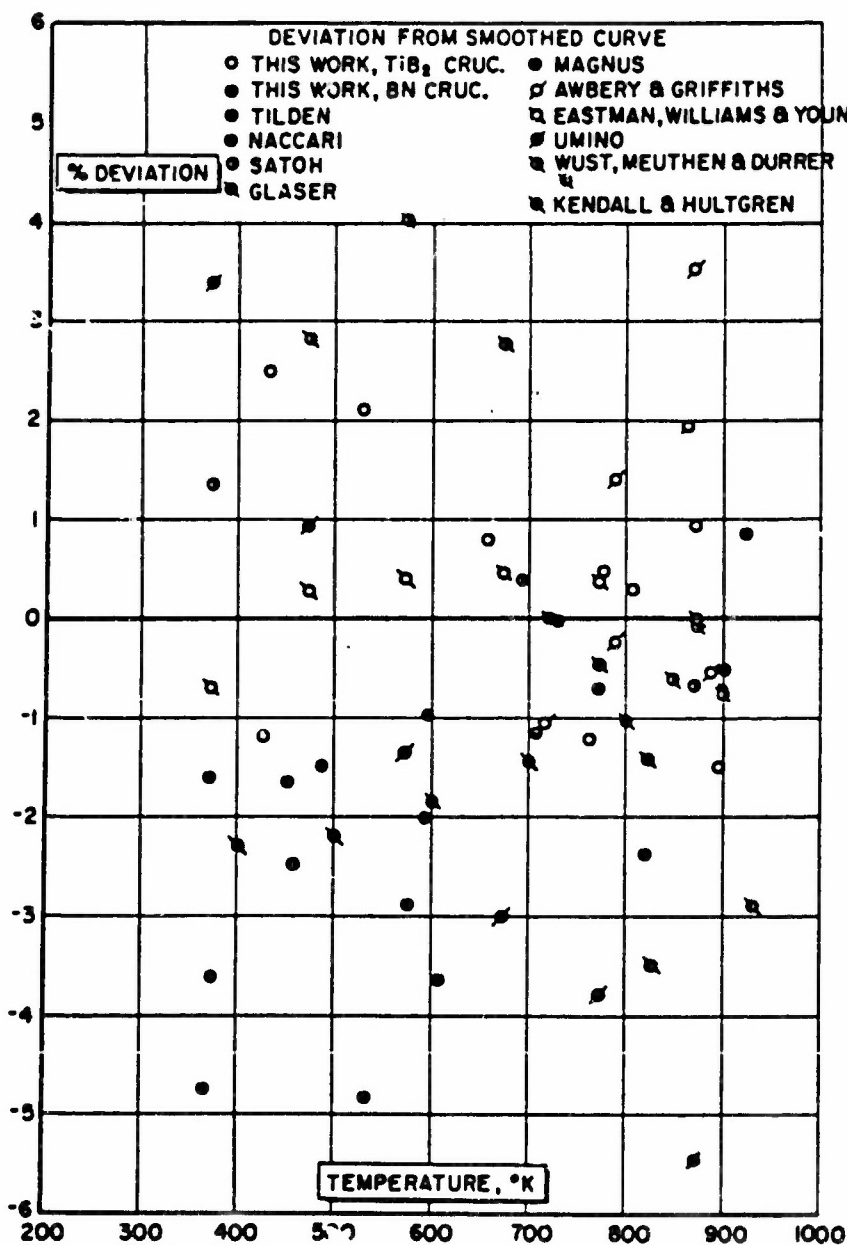
Table LII
(U) Smoothed Enthalpy and Heat Capacity of Aluminum^a

T, °K.	H _T -H _{298.15} cal./mole	C _p , cal./(mole°K.)	T, °K.	H _T -H _{298.15} cal./mole	cal./(mole°K.)
298.15	0	5.81	933(1)	6,888	7.59
300	11	5.81	1,000	7,396	7.59
400	611	6.16	1,100	8,155	7.59
500	1,242	6.45	1,200	8,914	7.59
600	1,900	6.72	1,300	9,673	7.59
700	2,586	7.00	1,400	10,431	7.59
800	3,303	7.37	1,500	11,190	7.59
900	4,065	7.90	1,600	11,949	7.59
933(c)	4,328	8.12	1,700	12,708	7.59

^aGram atomic wt. = 26.98

UNCLASSIFIED

UNCLASSIFIED



(U) Fig. 102 - Deviation of Enthalpy of Solid Aluminum from Smoothed Curve up to 1000°K.

UNCLASSIFIED

UNCLASSIFIED

There is a corresponding increase in the slope of the heat capacity vs. temperature curve as shown in Figure 103. This has also been reported by Awbery and Griffiths (40), Seekamp (53), Laemmel (54), and Pochapsky (55). Other heat capacity values have been given by Avramescu (56), Eastman et al. (41), Magnus (44), Maccari (45), Schubel (57), Tilden (47), and Umino (48) (see Figure 104).

The ogee-shaped heat capacity curve is similar to those of the solid alkali metals (58) and appears to be caused by more than just impurity-produced pre-melting.

The observed liquid aluminum enthalpies were smoothed using a least squares straight line fit:

$$H_T - H_{298.15}, \text{ cal./mole} = 7.588T - 191.2 \text{ (933}^\circ\text{-1650}^\circ\text{K.)}$$

from which:

$$C_p(l), \text{ cal./mole } ^\circ\text{K.} = 7.59 \text{ (933}^\circ\text{-1650}^\circ\text{K.)}$$

Deviations of experimental enthalpies from the straight line are given in Table LI and Figure 104. The data of Awbery and Griffiths (40) are in good agreement, those of Wust et al. (49) are lower, and the values reported by Umino (48) are about 11% to 12% lower.

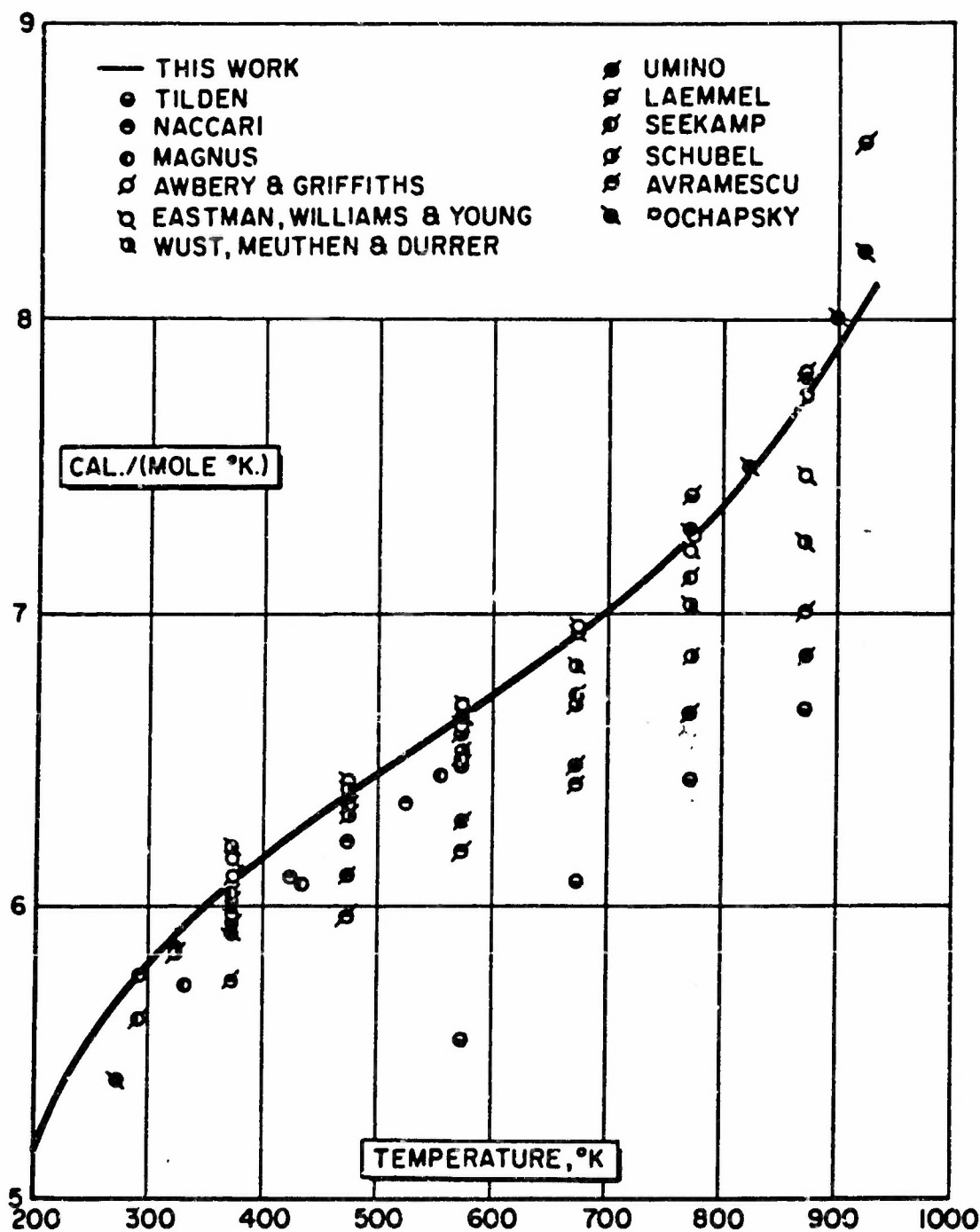
The paper by Awbery and Griffiths (40) gives 0.66 cal./ (g.°C.) for the mean specific heat of liquid aluminum between 657°C. and 760°C. which must be an error; it could have been 0.33 cal./ (g.°C.), which corresponds to about 8.9 cal./mole°K.). Umino (48) found 6.23 cal./mole°K.). Wust et al. (49) report 6.8-7.2 cal./ (mole°K.) from the melting point to 1273°K.

Extrapolation of the solid and liquid aluminum enthalpy curves to 933°K. yields 2560 cal./mole for the heat of fusion. [A melting point of 933°K. was chosen, at the limit of the popular "well established" $932 \pm 1^\circ\text{K.}$, as more likely representing pure aluminum. This choice was based mainly on the paper by Roeser and Wensel (59).] If one were to consider the "extra" increase in enthalpy below the melting point as pre-melting and ignored it in smoothing the data, then the heat of fusion would be about 2590 cal./mole. Because of the scatter of the observed enthalpy data, an error of ± 50 cal./mole in the heat of fusion is quite possible. Values found in the literature are listed in Table LIII.

The probable error in the enthalpy measurement caused by the reaction of the aluminum sample with the boron nitride crucible has been considered. If Kopp's additivity rule held true, the sum of the enthalpies of Al and BN would equal the sum of the enthalpies of AlN and B, and so on. For the two main reaction products, AlN and $9 \text{ Al}_2\text{O}_3 \cdot 2 \text{ B}_2\text{O}_3$, comparative summations indicate a maximum error of -10% in the experimental temperature range, and it is usually much less than this. Since only 2.5% or less of the aluminum

UNCLASSIFIED

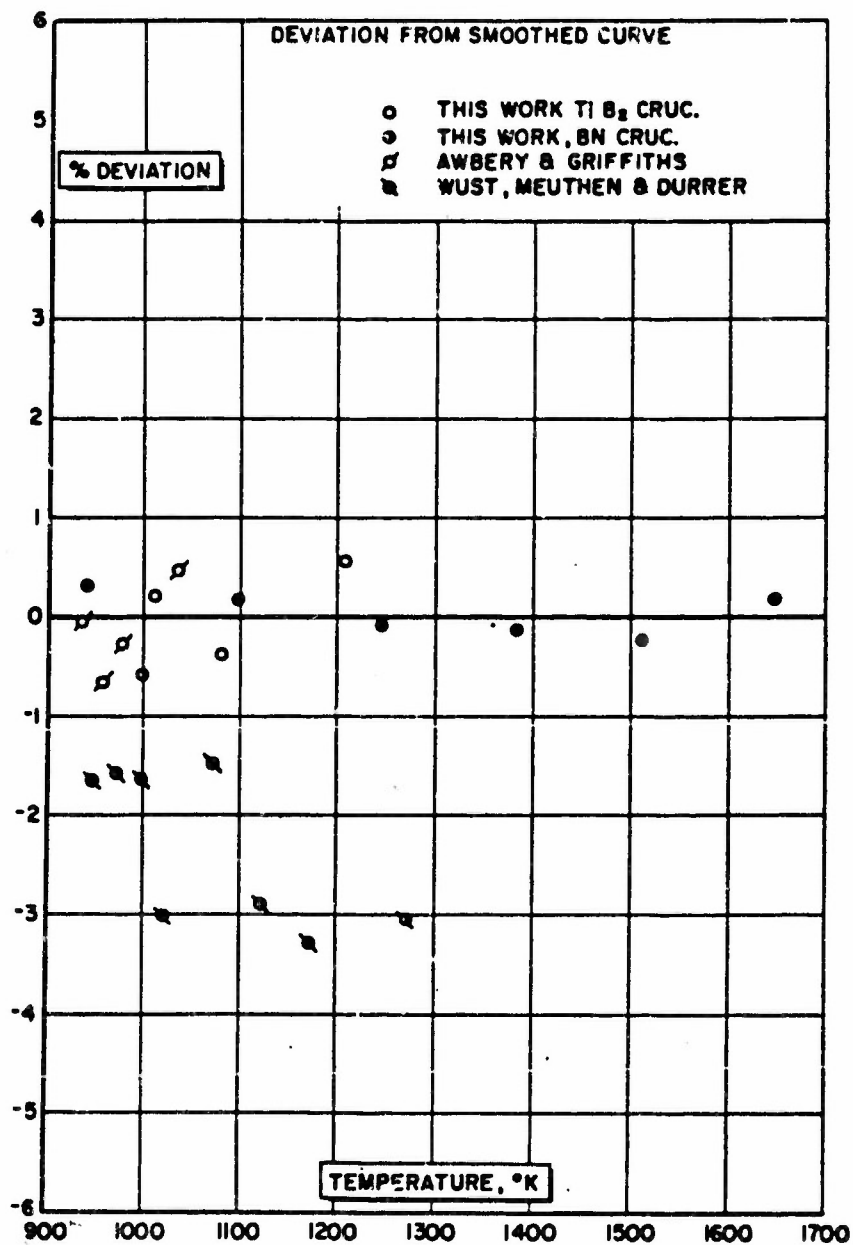
UNCLASSIFIED



(U) Fig. 103 - Heat Capacity of Aluminum

UNCLASSIFIED

UNCLASSIFIED



(U) Fig. 104 - Deviation of Enthalpy of Liquid Aluminum from Smoothed Curve up to 1700°C.

UNCLASSIFIED

CONFIDENTIAL

(This Page is Unclassified)

reacted, the error thus introduced should not exceed 0.25%. However, all of the error ends up in the aluminum enthalpy. With the quantities of materials used, the heat from the aluminum sample nearly equaled the heat from the boron nitride crucible, so one might expect the enthalpy of aluminum to be low by about 0.5%.

(U) The fact that the last measurement, at 727.5°K., falls well in line with earlier measurements, made before any reaction is presumed to have occurred, also indicates that no large error has been introduced.

Table LIII

(U) Heat of Fusion of Aluminum

ΔH_m , cal./mole	Observer or Evaluator
2149	Umino (48)
2493	Awbery and Griffiths (40)
2455	Awbery (60)
2500 \pm 30	Kubaschewski et al. (61)
2470 \pm 40	Wittig (62)
2660 \pm 50	Oelsen, Kieskamp, and Oelsen (63)
2630 \pm 50	Oelsen, Oelsen, and Thiel (64)
2550	Stull and Sinke (51)
2570	Kelley (50)
2570	Hultgren et al. (52)
2577	Seros and Woodhouse (65)
2560 \pm 50	This work

B. THERMODYNAMIC TABULATION (U)

1. JANAF Heat of Formation Propellant Ingredients (U)

(U) Series C of the classified tables was issued in April, 1965. This consisted of 50 tables which are listed in Table LIV and contained 36 Confidential compounds and 14 Unclassified compounds.

(U) Work on Series D continued and at the year's end 51 tables were completed, of which 26 were Confidential and 25 were Unclassified. These compounds are listed in Table LV. Series D will be issued for comment early in 1966.

CONFIDENTIAL

(This Page is Unclassified)

CONFIDENTIAL

Table LIV
(U) Series C of Propellant Ingredients

(II) Propellant Filing Index by Formula

Formula and Filing Order	State	Compound Name	Series	Page
AlH_6Li_3	c	Lithium aluminum hexahydride (LAHH), Trilithium hexahydroaluminate	C	14
CF_4O_2	1	bis(Fluoroxy)difluoromethane	C	15
CF_4O_2	g	bis(Fluoroxy)difluoromethane	C*	16
CF_6N_2	g	bis(Difluoroamino)difluoromethane (Compound H)	C	17
CF_6N_4	1	tetrakis(Difluoroamino)methane (Delta)	C	18
CF_6N_4	g	tetrakis(Difluoroamino)methane (Delta)	C*	19
$\text{C}_2\text{H}_4\text{N}_6\text{O}_6$	c	N,N,N',N'-Tetranitroethylenediamine (TNEDA)	C	20
$\text{C}_2\text{H}_6\text{N}_4\text{O}_4$	c	Ethylene dinitramine (EDNA)	C*	21
$\text{C}_2\text{H}_{18}\text{AlB}_3\text{N}$	1	Aluminum borohydride dimethylamine (Hybaline A-4)	C	22
$\text{C}_4\text{H}_4\text{F}_6\text{N}_4\text{O}$	1	tetrakis(Difluoroamino)tetrahydrofuran (THF)	C*	23
$\text{C}_4\text{H}_8\text{F}_4\text{N}_2$	1	2,2-bis(Difluoroamino)butane	C	24
$\text{C}_4\text{H}_8\text{F}_4\text{N}_2$	1	2,3-bis(Difluoroamino)butane (Stereo-isomer I)	C	25
$\text{C}_4\text{H}_8\text{F}_4\text{N}_2$	1	2,3-bis(Difluoroamino)butane (Stereo-isomer II)	C	26
$\text{C}_4\text{H}_8\text{N}_2\text{O}_7$	1	Diethylene glycol dinitrate (DEGDN)	C	27
$\text{C}_4\text{H}_9\text{N}_3\text{O}_4$	1	N,N-Dinitro-n-butylamine (DNBA)	C	28
$\text{C}_4\text{H}_{10}\text{N}_2\text{O}_2$	1	n-Butylnitramine	C	29
$\text{C}_5\text{H}_6\text{F}_2\text{N}_4\text{O}_{10}$	1	bis(2,2-Dinitro-2-fluoroethyl)formal (DENFEP)	C	30
$\text{C}_5\text{H}_9\text{N}_3\text{O}_9$	1	2-Hydroxymethyl-2-methyl-1,3-propanediol tri-nitrate (TNETN)	C	31
$(\text{C}_5\text{H}_{16}\text{N}_{14})_n$	s	Ethylenebis(aminoguanidine azide) - Formaldehyde copolymer (DB-27)	C	32
$\text{C}_6\text{H}_8\text{F}_{12}\text{N}_6\text{O}$	1	hexakis(Difluoroamino)dipropylether (HPE)	C	33
$\text{C}_6\text{H}_{12}\text{F}_4\text{N}_2$	1	1,2-bis(Difluoroamino)4-methylpentane	C*	34
$\text{C}_6\text{H}_{12}\text{F}_4\text{N}_2$	g	1,2-bis(Difluoroamino)4-methylpentane	C*	35
$\text{C}_6\text{H}_{12}\text{F}_4\text{N}_2$	1	2,2-bis(Difluoroamino)4-methylpentane	C*	36
$\text{C}_6\text{H}_{12}\text{F}_4\text{N}_2$	g	2,2-bis(Difluoroamino)4-methylpentane	C*	37
$\text{C}_6\text{H}_{12}\text{F}_4\text{N}_2$	1	2,3-bis(Difluoroamino)2-methylpentane	C	38
$\text{C}_6\text{H}_{12}\text{F}_4\text{N}_2$	g	2,3-bis(Difluoroamino)2-methylpentane	C	39
$\text{C}_6\text{H}_{12}\text{F}_4\text{N}_2$	1	2,3-bis(Difluoroamino)4-methylpentane (Stereo-isomer I)	C	40
$\text{C}_6\text{H}_{12}\text{F}_4\text{N}_2$	g	2,3-bis(Difluoroamino)4-methylpentane (Stereo-isomer I)	C	41

* Revised

CONFIDENTIAL

Table LIV (Contd.)

Formula and Filing Order	State	Compound Name	Series	Page
$C_6H_{12}F_4N_2$	l	2,3-bis(Difluoroamino)4-methylpentane (Stereo-isomer II)	C	42
$C_6H_{12}F_4N_2$	g	2,3-bis(Difluoroamino)4-methylpentane (Stereo-isomer II)	C	43
$C_7H_{12}N_4O_{10}$	c	bis(2,2-Dinitropropyl)formal (BDNPF)	C	44
$C_7H_{12}N_4O_{10}$	l	bis(2,2-Dinitropropyl)formal (BDNPF)	C	45
$C_8H_{14}N_4O_{10}$	c	bis(2,2-Dinitropropyl)acetal (BDNPA)	C	46
$C_8H_{14}N_4O_{10}$	l	bis(2,2-Dinitropropyl)acetal (BDNPA)	C	47
ClF_5	l	Chlorine pentafluoride	C	48
ClF_5	g	Chlorine pentafluoride	C	49
F_3NO	g	Trifluoroamine oxide	C	50
<u>Unclassified</u>				
CF_4O	g	Fluoroxytrifluoromethane	C*	1
$(C_6H_7N_3O_{11})_n$	s	Cellulose trinitrate	C	2
$(C_6H_8N_2O_9)_n$	s	Cellulose dinitrate (Pyroxylin)	C	3
$(C_6H_{10}O_5)_n$	s	Cellulose	C	4
$ClKO_4$	c	Potassium perchlorate	C	5
F_2O	g	Oxygen difluoride	C*	6
F_3N	g	Nitrogen trifluoride	C*	7
HNO_3	l	Nitric acid	C	8
HNO_3	g	Nitric acid	C	9
H_2O_2	l	Hydrogen peroxide	C	10
H_2O_2	g	Hydrogen peroxide	C	11
N_2O_4	l	Dinitrogen tetroxide	C	12
N_2O_4	g	Dinitrogen tetroxide	C	13

*Revised

CONFIDENTIAL

Table LV

(U) Series D of Propellant Ingredients

(U) Propellant Filing Index by Formula
(Confidential)

Formula and Filing Order	State	Compound Name	Series	Page
B ₁₀ H ₁₀ N ₂	c	Dodecahydrodecaborate diamina (Dekazene)	D*	26
C ₃ H ₈ F ₁₂ N ₂ O	c	N,N'-Di[tris(difluoroamino)methyl]urea (BTU)	D	27
C ₃ H ₇ ClF ₆ N ₄ O	c	2-[tris(Difluoroamino)methoxy]ethylamine hydrochloride (INFO 631C)	D	28
C ₃ H ₇ ClF ₆ N ₄ O ₃	c	2-[tris(Difluoroamino)methoxy]ethylamine perchlorate (INFO 635P)	D	29
C ₃ H ₈ N ₆	c	Trisaminoguanidine dicyanamide	D	30
C ₄ H ₈ N ₅	c	Hydrazine cyanoformate	D	31
C ₄ H ₇ F ₆ N ₃	1	1,1,3-tris(Difluoroamino)butane	D	32
C ₄ H ₈ F ₄ N ₂	1	2,3-bis(Difluoroamino)butane (Stereo-isomer I)	D*	33
C ₄ H ₈ F ₄ N ₂	1	2,3-bis(Difluoroamino)butane (Stereo-isomer II)	D*	34
C ₃ H ₃ N ₃	c	1,1,1-Tricyanoethane	D	35
C ₅ H ₈ N ₄ O ₁₂	c	Pentaerythritol tetranitrate (PETN)	D	36
C ₃ H ₈ N ₆	c	Triaminoguanidine cyanoformate	D	37
C ₆ H ₄ N ₂	c	1,4-Dicyano-2-butene	D	38
C ₆ N ₄	c	Tetracyanoethylene	D	39
C ₆ N ₆	c	s-Tricyanotriazine	D	40
C ₇ H ₈ N ₄	c	1,1,2,2-Tetracyanocyclopropane	D	41
C ₇ H ₃ N ₃	c	1,1,1-Tricyano-3-butyne	D	42
C ₇ H ₃ N ₃	1	1,1,1-Tricyano-3-butyne	D	43
C ₈ H ₁₀ F ₈ N ₄ O ₂	1	1,2,4,5-tetrakis(Difluoroamino)amyl acrylate (TAA)	D	44
C ₈ H ₁₈ F ₄ N ₂	1	2,2-bis(Difluoroamino)octane	D	45
C ₁₂ H ₄ N ₆	c	1,1,1,6,6,6-Hexacyano-3-hexyne	D	46
C ₁₂ H ₆ N ₆	c	1,1,1,6,6,6-Hexacyano-3-hexene	D	47
C ₁₄ H ₄ N ₆	c	1,1,1,8,8,8-Hexacyano-3,5-octadiyne	D	48
ClF ₃	1	Chlorine trifluoride	D	49
Cl ₂ H ₆ N ₂ O ₆	c	Hydrazinium diperchlorate	D	50
H ₄ N ₄	c	Ammonium azide	D	51

*Revised

UNCLASSIFIED

Table LV (Contd.)

Formula and Filing Order	State	Compound Name	Series	Page
<u>Unclassified</u>				
AlB ₃ H ₁₂	l	Aluminum borohydride (ABH)	D	1
AlB ₃ H ₁₂	g	Aluminum borohydride (APH)	D	2
C ₂ H ₅ N ₃ O	l	2-Triazoethanol	D	3
C ₃ H ₁₂ BN	c,III	Trimethylamineborane	D	4
C ₅ F ₁₁ N	l	Perfluoropiperidine	D	5
C ₅ F ₁₁ N	g	Perfluoropiperidine	D	6
C ₅ HN ₃	c	Tricyanoethylene	D	7
C ₅ H ₉ N ₃	l	Cyclopentyl azide	D	8
C ₆ H ₅ N ₃	l	Phenyl azide	D	9
C ₆ H ₁₁ N ₃	l	Cyclohexyl azide	D	10
ClF ₃	g	Chlorine trifluoride	D*	11
ClNO ₃	c	Nitrosyl perchlorate	D	12
CsN ₃	c	Cesium azide	D	13
F ₂	l	Fluorine	D	14
Fe ₂ O ₃	c	Ferric oxide (Hematite)	D	15
HN ₃	l	Hydrogen azide	D	16
HN ₃	g	Hydrogen azide	D	17
H ₂	l	Hydrogen	D	18
Hg ₂ Ne	c	Mercurous azide	D	19
KN ₃	c	Potassium azide	D	20
LiN ₃	c	Lithium azide	D	21
N ₂	l	Nitrogen	D	22
N ₃ Na	c	Sodium azide	D	23
N ₃ Pb	c	Lead azide	D	24
O ₂	l	Oxygen	D	25

*Revised

UNCLASSIFIED

UNCLASSIFIED

2. JANAF Thermochemical Tables (U)

During calendar 1965, four supplements to the JANAF Thermochemical Tables (No. 16, 17, 18, and 19) were mailed to the users and one additional supplement (No. 20) was prepared for comment. The composition of each supplement is listed in Tables LVI, LVII, LVIII, LIX, and LX, while the numerical statistics are given in Table LXI.

Tables for B, Al and S elements were revised. A new element, Fe, and its oxides, chlorides and fluorides and another new element, Cu, were added. All Al and B compounds were issued as white tables. In these supplements the following ionic gaseous species: e^- , Li^+ , Na^+ , K^+ , Cl^- , Al^+ , Be^+ , Cl^+ , F^- , O^- , C^- , H^- , Cu^+ , and NO_2^- were added for the first time.

UNCLASSIFIED

Table LVI

(U) JANAF Thermochemical Data

Supplement No. 16, issued December 31, 1964

Title Page	BF ₂ (g)	*B ₂ F ₄ (g)
B(ref)	BF ₃ (g)	B ₂ H ₆ (g)
B(c)	BH(g)	B ₂ O ₂ (g)
B(l)	BHO(g)	B ₂ O ₃ (c)
B(g)	BHO ₂ (c)	B ₂ O ₃ (l)
BBr(g)	BHO ₂ (g)	B ₂ O ₃ (g)
BBrCl(g)	BH ₂ (g)	B ₃ H ₃ O ₆ (g)
BBrCl ₂ (g)	BH ₂ O ₂ (g)	B ₁₀ H ₁₄ (c)
BBrF(g)	BH ₃ (g)	B ₁₀ H ₁₄ (l)
BBrF ₂ (g)	BH ₃ O ₃ (c)	B ₁₀ H ₁₄ (g)
BBr ₂ (g)	BH ₃ O ₃ (g)	CTi(c)
BBr ₂ Cl(g)	BH ₄ K(c)	CTi(l)
BBr ₂ F(g)	BH ₄ Li(c)	CZr(c)
BBr ₃ (l)	BH ₄ Na(c)	CZr(l)
BBr ₃ (g)	B ⁻ (g)	ClNa(g)
BCl(g)	BI ₂ (g)	*Cl ₂ Na ₂ (g)
BClF(g)	BI ₃ (g)	*NO ₃ (g)
BClF ₂ (g)	BLiO ₂ (c)	N ₂ O(g)
BCl ₂ (g)	BLiO ₂ (l)	N ₂ O ₃ (g)
BCl ₂ F(g)	BLiO ₂ (g)	N ₂ O ₄ (l)
BCl ₃ (g)	B ₂ (g)	N ₂ O ₅ (g)
BF(g)	B ₂ Cl ₄ (g)	

*New Table.

UNCLASSIFIED

Table LVII

(U) JANAF Thermochemical Data

Supplement No. 17, issued March 31, 1965

Title Page	$B_3FH_2O_3(g)$	$BeK_2O_{13}(c)$
$BBrO(g)$	$B_3F_2HO_3(g)$	$BeK_2O_{13}(l)$
$BClO(g)$	$B_3F_3O_3(c)$	$BeLi_2O_{13}(c)$
$BFO(g)$	$B_3F_3O_3(g)$	$BiO_{1.7}Pb_2(c)$
$BF_2HC(g)$	$*B_3H_3O_3(c)$	$*CCl_2(g)$
$PF_4K(c)$	$B_3H_3O_3(g)$	$*CCl_3(g)$
$BF_4K(g)$	$B_3H_6N_3(g)$	$CF_2O(g)$
$BLiO_2(g)$	$B_4Mg(c)$	$*CF_4O(g)$
$BNaO_2(c)$	$B_4Na_2O_7(c)$	$*Fe(ref)$
$BNaO_2(l)$	$B_4Na_2O_7(l)$	$*Fe(c)$
$*BNaO_2(g)$	$B_4O_7Pb(c)$	$*Fe(l)$
$BO(g)$	$B_5H_9(l)$	$*Fe(g)$
$BO_2(g)$	$B_5H_9(g)$	$*K^+(g)$
$BS(g)$	$BeK_2O_{10}(c)$	$*Li^+(g)$
$B_2Mg(c)$	$BeLi_2O_{10}(c)$	$*Na^+(g)$
$B_2O_4Pb(c)$	$BeNa_2O_{10}(c)$	$*e^-(g)$
$B_3Cl_3O_3(g)$	$BeO_{10}Pb(c)$	

*New Table.

UNCLASSIFIED

Table LVIII

(U) JANAF Thermochemical Data

Supplement No. 18, issued June 30, 1965

Title Page	BeCl ₂ (l)	*F ⁻ (g)
*Al ⁺ (g)	BeCl ₂ (g)	FN(g)
BT1(c)	BeI ₂ (c)	FO(g)
B ₂ BeO ₄ (g)	BeI ₂ (l)	*Fe _{0.947} O(c)
B ₂ Tl(c)	BeI ₂ (g)	*FeO(c)
B ₂ Tl(l)	Be ₂ Cl ₄ (g)	*FeO(l)
B ₂ Zr(c)	Be ₂ O ₄ Si(c)	*FeO(g)
B ₂ Zr(l)	*Cl ⁺ (g)	*Fe ₂ O ₃ (c)
B ₄ Li ₂ O ₇ (c)	*Cl ⁻ (g)	*Fe ₃ O ₄ (c)
B ₄ Li ₂ O ₇ (l)	*ClFe(g)	Na ₂ O ₃ Si(c)
*Be ⁺ (g)	*Cl ₂ Fe(c)	Na ₂ O ₃ Si(l)
BeBr ₂ (c)	*Cl ₂ Fe(l)	Na ₂ O ₅ Si ₂ (c)
BeBr ₂ (l)	*Cl ₂ Fe(g)	Na ₂ O ₅ Si ₂ (l)
BeBr ₂ (g)	*Cl ₃ Fe(c)	*O ⁻ (g)
BeClF(g)	*Cl ₃ Fe(l)	*O ₃ PbSi(c)
*BeCl ₂ (c,α)	*Cl ₃ Fe(g)	*O ₄ Pb ₂ Si(c)
*BeCl ₂ (c,β)	*Cl ₃ Fe ₂ (g)	O ₄ SiZr(c)

*New Table.

UNCLASSIFIED

Table LIX

(U) JANAF Thermochemical Data

Supplement No. 19, issued September 30, 1965

Title Page	CO ₂ (g)	FL10(g)
AlF ₃ (g)	*C ₂ F ₆ (g)	*F ₂ Fe(c)
AlF ₃ (g)	C ₂ H ₄ (g)	*F ₂ Fe(l)
AlO(g)	C ₂ H ₄ O(g)	*F ₂ Fe(g)
Al ₂ O(g)	C ₃ Al ₄ (c)	F ₂ OS(g)
Al ₂ O ₂ (g)	C ₃ O ₂ (g)	*F ₃ Fe(c)
BF ₃ (g)	ClF(g)	*F ₃ Fe(g)
BrCl(g)	ClF ₃ (g)	*F ₄ S(g)
BrF(g)	ClH ₄ N(c)	F ₆ S(g)
BrF ₃ (g)	ClI(c)	H(g)
BrF ₅ (g)	ClI(l)	*H ⁻ (g)
BrH(g)	ClI(g)	H ₃ N(g)
BrH ₄ N(c)	Cl ₂ (g)	N ₂ (g)
*C ⁻ (g)	F(g)	*OS ₂ (g)
CB ₄ (c)	*FFe(g)	O ₂ (g)
CO(g)	FHO(g)	O ₃ S(g)

New Table.

UNCLASSIFIED

Table LX

(U) JANAF Thermochemical Data

Supplement No. 20, issued December 31, 1965

Title Page	Cl ₂ Mg(l)	H ₂ S(g)
Al(ref)	Cl ₂ Mg(g)	*H ₄ N ₂ (l)
Al(c)	Cl ₂ O(g)	H ₄ N ₂ (g)
Al(l)	*Cu(ref)	MgO(c)
Al(g)	*Cu(c)	MgO(g)
AlF ₃ Na ₃ (c)	*Cu(l)	*NO ₂ ⁻ (g)
*Al ₂ O ₃ (γ, c)	*Cu(g)	OS(g)
*BF ₂ H(g)	*Cu ⁺ (g)	OZr(g)
*BF ₂ O(g)	FI(g)	O ₂ Zr(c)
B ₃ FH ₂ O ₃ (g)	FNO ₂ (g)	O ₂ Zr(l)
B ₃ F ₂ HO ₃ (g)	*F ₂ N ₂ (trans, g)	O ₂ Zr(g)
CB ₄ (c)	*F ₂ N ₂ (cis, g)	O ₁₀ P ₄ (c)
CB ₄ (l)	F ₂ Pb(c)	O ₁₀ P ₄ (g)
*CClO(g)	F ₂ Pb(l)	S(ref)
*CFO(g)	F ₂ Pb(g)	S(c)
ClNO(g)	HN(g)	S(l)
ClNO ₂ (g)	*H ₂ N(g)	S(g)
Cl ₂ Mg(c)	H ₂ N ₂ (g)	S ₂ (g)

UNCLASSIFIED

UNCLASSIFIED

Table LXI

(U) Summary of JANAF Tables

<u>Supplement No.</u>	<u>Date Issued</u>	<u>No. of Tables Issued</u>	<u>New Tables Issued</u>	<u>Revised Tables Issued</u>	<u>Total No. of Tables Issued</u>	<u>Tables Issued for</u>
16	12/31/64	64	3	61	808	Users
17	03/31/65	49	13	36	821	Users
18	06/30/65	50	23	27	844	Users
19	09/30/65	47	11	36	855	Users
20	12/31/65	53	15	38	---	Comments

(U) On July 2, 1965, eight hundred and eleven (811) tables together with the text on "method of calculation" were prepared and sent to Mr. Paul W. Larsen, U. S. Department of Commerce, National Bureau of Standards Institute for Applied Technology, Clearinghouse for Federal Scientific and Technical Information, Springfield, Virginia, for publication. The tables are now available for public sale by ordering: PB 168 370 - JANAF THERMOCHEMICAL TABLES (complete through Supplement No. 17, dated March 31, 1965) 945 pages \$10.00, from:

Clearinghouse for Federal
Scientific and Technical Information
U. S. Department of Commerce
Springfield, Virginia, 22151

The tables will be updated and revised periodically for public sale by the Clearinghouse.

(U) The JANAF Thermochemical Tables' mailing list was revised in November and made consistent with CPIA Publication No. 74 "Chemical Propulsion Mailing List." Our sponsoring agency instructed us to terminate distribution to all other recipients. Future copies of the tables must be obtained from the Clearinghouse.

UNCLASSIFIED

SECTION VI

(U) BIOCHEMICAL RESEARCH

An important branch of the integrated propellant program at The Dow Chemical Company is the environmental and toxicological research performed by the Biochemical Research Laboratory. This work falls into two categories:

- (1) Support functions to the synthesis laboratories.
- (11) Toxicological research on beryllium-containing materials.

A. SUPPORT FUNCTION TO THE SYNTHESIS LABORATORIES (U)

1. Environmental Research Support Function

The personnel of the Environmental Research Section of the Biochemical Research Laboratory serve as consultants in Industrial Hygiene to the Scientific Projects Laboratory.

2. Toxicological Research Support Function

The compounds TAZ and THA both possess the potential of being absorbed through the skin in acutely toxic amounts. A study of the effectiveness of rubber gloves as a barrier to skin contact by TAZ and THA has been completed.

The gloves submitted for study were as follows:

- (1) Playtex (green, light weight).
- (11) Snyder and Son (No. 1119, medium weight).
- (111) Edmot (Neox 924, heavy weight).

Results of the study indicate that the Snyder gloves are the most impervious. These gloves could be used safely for several days when handling TAZ and THA in solution and somewhat longer if the material were in a solid state.

The heavy weight Edmot glove is not recommended for use in handling either TAZ and THA. The light weight Playtex glove could be used with safety for handling either material when minimum contact is likely.

No other projects were initiated in 1965. The facilities and personnel in the Toxicological and Pharmacological Research Sections of the Biochemical Research Laboratory continue to be available as consultants, and to carry out laboratory studies, when needed by the Scientific Projects Laboratory.

UNCLASSIFIED

B. TOXICOLOGICAL RESEARCH ON BERYLLIUM-CONTAINING MATERIALS (U)

Toxicological studies on beryllium-containing materials were conducted first at Dow as part of a supporting role to Contract Nr. AF 33(616)-6149 on high energy chemical rocket propellants. With the emergence of beryllium and its compounds as strong contenders for use as high energy fuels, it was necessary to expand the study under Contract Nr. AF 04(611)-7554.

The chronic lung disease, reported to have been produced in man by the inhalation of very small amounts of certain beryllium-containing materials, has given cause for great concern over the potential hazards to health associated with the handling and use of beryllium and its compounds. This apprehension seriously hampers both military and commercial developments of beryllium.

Consequently, the research work carried out in the Biochemical Research Laboratory, under the above named contracts, has been directed toward obtaining an understanding of the fundamental biological, chemical and physical mechanisms involved in the toxic action of beryllium and its compounds in order to adequately evaluate the relative health hazards presented by beryllium-containing materials, including exhaust products from motor firings.

This work was centered on the study of animals, treated intratracheally with well-characterized samples of beryllium oxide, in order to determine the nature of the chronic lung disease in animals, including the cellular and biochemical changes that take place during the course of the disease. In this study, special attention has been given to the chemical and physical characterization of samples of beryllium oxide in an attempt to correlate biological activity with chemical and physical properties. Furthermore, attention has been given to determining the gradation in biological activity depending upon the characteristics of the beryllium oxide studied.

1. Materials (U)

a. Samples of Beryllium Oxide

(1) Physical and Chemical Properties

Extensive investigations of the influence of calcining conditions of beryllium oxides on their biological, chemical and physical properties are continuing. This intensive study of the properties of beryllium oxides has shown that the properties vary with the calcining temperature.

Many properties of key samples of beryllium oxides have been determined. These include surface area by nitrogen absorption; crystallinity by polarized light microscopy; crystallite dimensions by X-ray diffraction; density by a sink-float method;

UNCLASSIFIED

UNCLASSIFIED

refractive index by dispersion staining; and solubility in various media with detection by emission spectroscopy. The properties of three key samples that have been selected for extensive study are presented in Table LXII.

Table LXII

(U) Properties of Key Samples of Beryllium Oxide
Prepared by Calcining Beryllium
Hydroxide under Laboratory Conditions

Property	Calcined for 10 Hours at		
	500°C.	1100°C.	1600°C. ^a
Specific surface area, m. ² /g. (by nitrogen adsorption)	50.8	2.2	1.3
Average crystallite size, Å (by X-ray diffraction)	150	1500	1600
Crystallinity, % (by polarized light microscopy)	<10	100	85
Refractive index (by dispersion staining)			
10% of sample below	1.680	1.703	1.706
50% of sample below	1.682-1.684	1.704	1.711
90% of sample below	1.686	1.706	1.720
Density, g./ml. (by sink-float method)	2.80-2.94	2.97-3.00	2.97-3.03
Solubility in water (at room temperature)	Very, very slight	Very, very slight	Very, very slight

^aA different method of heating was used.

New techniques for studying beryllium oxide samples have been employed in an effort to obtain additional data that may be useful in correlating the chemical and physical properties of key samples with their biological activity.

The chemical reactivity of basic oxides has been studied at Dow using the reaction of an amine hydrochloride or ammonium chloride with the oxide. Using this procedure, beryllium oxides, prepared from beryllium hydroxide calcined for 10 hours at temperatures ranging from 400°-1600°C., have been investigated. A review of the results is under way.

UNCLASSIFIED

A technique using thermal analysis coupled with the mass spectrometer has been developed in the Dow laboratories in order to measure and identify very small quantities of volatile components released from materials. This technique is being used in the study of the series of beryllium oxides described in the preceding paragraph.

Solubility studies have been carried out on the three key samples described above using Ringer-phosphate-bicarbonate buffer, pooled rabbit sera, and water (Table LXIII). All three oxides are only very, very slightly soluble in both water and Ringer-phosphate-bicarbonate buffer. However, in rabbit serum there appears to be a greatly increased solubility of all three beryllium oxides. Further studies are being conducted in order to determine the mechanism of the uptake of these oxides by rabbit sera.

Table LXIII

(U) Solubility of Three Key Samples of Beryllium Oxide in Various Media at Room Temperature

Starting Material	Ten Hours at Calcination Temperature, °C.	Be Concentration in ppm. gamma/ml.		
		Water	Ringer-Phosphate-Bicarbonate Buffer	Pooled Rabbit Sera
Be (OH) ₂	500	0.0007	0.005	3.5
		0.0007	0.007	8.6
Be (OH) ₂	1100	0.004	<0.001	0.22
		0.004	0.006	0.30
Be (OH) ₂	1600 ^a	0.007	<0.001	1.05
		0.007	0.003	1.0

^aA different method of heating was used.

A method of dispersion staining for the determination of refractive index, developed by G. C. Crossmon (66), has been adapted and applied to several samples of beryllium compounds, including a series of beryllium oxides prepared under laboratory conditions by calcining beryllium hydroxide for ten hours at temperatures varying from 400°-1600°C. The results obtained from this series, presented in Table LXIV, show that, as the calcining temperature increases, the refractive index increases.

UNCLASSIFIED

Table LXIV

(U) Refractive Index Values for Laboratory Preparations of Beryllium Oxide using a Dispersion Staining Technique

Be(OH) ₂ for 10 Hours at Calcination Temp. °C.	Refractive Index		
	10% of Sample Below	50% of Sample Below	90% of Sample Below
400	1.650	1.654	1.658
500	1.680	1.682-1.684	1.686
600	1.684	1.688-1.694	1.698
700	1.690	1.693	1.696
800	1.696	1.700	1.712
900	1.700	1.702	1.704
1000	1.700	1.702	1.704
1100	1.703	1.704	1.706
1200 ^a	1.704	1.706	1.710
1400 ^a	1.706	1.706-1.708	1.710
1600 ^a	1.706	1.711	1.720

^aA different method of heating was used.

Evidence based on the study of infrared absorption spectra (67) and mass spectrometric thermal analysis patterns (68) suggests that the beryllium oxide which results from heating beryllium hydroxide retains a small amount of occluded water, even though the general structure of such beryllium oxide is of the expected bromellite type. The quantity of this residue decreases as the calcining temperature increases. It has been reported that there is a change in unit cell parameters with increasing temperature (69); for beryllium oxide samples prepared from various starting materials, including the hydroxide, sulfate and oxalate, and calcined to substantially the same high temperature; however, the cell parameters are the same (70). The best values for the hexagonal cell of beryllium oxide are:

$$a = 2.6979 \pm 0.0001 \text{ \AA}$$

$$c = 4.3772 \pm 0.0002 \text{ \AA at } 21^\circ\text{C.}$$

The variation in certain physical properties of beryllium oxide with its calcination temperature is marked, especially in the case of refractive index. This can be seen in Table LXIV, where a change from 1.65 to 1.72 is indicated for calcination temperatures in the range of 400°-1600°C. Similar reports are given by Quirk (69) and by Belyaev (71).

UNCLASSIFIED

In an attempt to verify the change in lattice parameters with calcination temperature, Debye-Scherrer powder patterns using CuK α X-radiation were obtained for the beryllium oxide samples listed in Table LXIV. The diffraction maxima for the materials calcined at the lower temperatures were so broad that precise measurements could not be made. This suggested the use of a shorter wavelength.

Electron diffraction provides a convenient way to increase the sharpness of the lines in a diffraction pattern by using a high-energy electron beam rather than an X-ray beam. Thus, electrons accelerated across 50 KV potential have an effective wavelength of 0.05 Å in contrast to 1.54 Å for CuK α X-ray. An Hitachi HU-11A electron microscope was modified to provide lattice measurements. This involved changes in the sample holder and in the internal photographic system of the microscope, since a reproducible specimen-to-photo distance is necessary to observe the expected pattern displacements, thought to be on the order of 0.1%. The samples listed in Table LXIV were again examined using this arrangement.

The diffraction patterns of the various samples were sharpened as predicted. No significant changes in measured d-spacings of equivalent lines were found from sample to sample. The measured d-spacings match quite well those listed in the ASTM X-ray Powder File (4-0843) and those from the cell parameters of Bellamy, Baker and Livey (70), as shown in Table LXV.

(2) Preparation of Samples of "Respirable Particle Size"

Several techniques for reducing particle size have been investigated. The most promising method for reducing the particle size of samples of beryllium oxide to "respirable particle size" is one using a lucite vial with two lucite balls on the Spex No. 8000 Mixer/Mill. A procedure which is both safe and effective has been developed using aluminum oxide, because it has certain properties similar to those of beryllium oxide and because it is considered to be non-hazardous. In the original sample of aluminum oxide (prior to grinding) most of the particles appeared to be agglomerates of the order of 100 μ comprised of 10-20 μ particles. The sample was ground for one hour in a lucite vial. A particle size distribution curve was determined using the Coulter Counter. About 99% of the particles were less than 3 μ and about 95% of the particles were less than 0.5 μ . Clearly, this is an effective way to reduce particle size. The contamination of the sample by the lucite was negligible, of the order of 0.002% by weight as determined by infrared analysis.

The partitioning of the ground aluminum oxide into particles in the size range 1-5 μ has been accomplished using a sedimentation technique. Large particles were removed by allowing sedimentation to take place for a relatively short period of time, which was calculated using Stokes' Law. The fines (less than 1 μ)

UNCLASSIFIED

were removed by allowing the sample to settle for a relatively long time, which was calculated using Stokes' Law, and discarding the suspended sub-micron particles. This procedure will be applied to beryllium oxide samples.

Table LXV

(U) d-Spacings from Powder Diffraction
Data for Beryllium Oxide

hkl	Calculated ^a Å	Observed ASTM 4-0843 from NBS (1951) Å	Observed, Electron Diffraction Pattern Å
100	2.3364	2.337	2.34
002	2.1186	2.189	2.19
101	2.0612	2.061	2.08
102	1.5973	1.598	1.59
110	1.3489	1.349	1.36
103	1.2376	1.238	1.25
200	1.16822	1.1682	1.17
112	1.14834	1.1482	---
201	1.12871	1.1287	---
004	1.09429	1.0958	---
202	1.03059	1.0308	---
104	0.99099	0.9920	---
203	0.91193	0.9118	---
210	0.88309	0.8832	---
211	0.86565	0.8657	---
114	0.84983	0.8498	---
105	0.81978	0.8199	---
212	0.81894	0.8179	---

^aOn basis of $a = 2.679 \text{ Å}$ and $c = 4.3772 \text{ Å}$.

b. Exhaust Products from Motor Firings

Four samples of exhaust products from motor firings were received from the 6570th Aerospace Medical Research Laboratories, Wright-Patterson Air Force Base, Ohio, early in October, 1965. Selected physical and chemical properties of these samples are being studied using the techniques listed below:

- (1) Surface area . B.E.T. method using nitrogen.
- (11) Average crystallite size - X-ray diffraction technique.

UNCLASSIFIED

- (iii) Solubility in water - soluble beryllium components determined using emission spectroscopy.
- (iv) Density - sink-float method.
- (v) Refractive index - dispersion staining technique.
- (vi) Trace element analysis - emission spectroscopy.
- (vii) Carbon-hydrogen analysis - micro-combustion technique.
- (viii) Chloride analysis - micro-volumetric technique.
- (ix) Beryllium analysis - gravimetric method.
- (x) Oxygen analysis - neutron activation technique.
- (xi) Organic components - infrared analysis of CS₂ extract.
- (xii) Crystallinity - polarized light microscopy.
- (xiii) Particle size - electron micrographs, photomicrographs, and Coulter counter technique.
- (xiv) Components - X-ray powder diffraction.

Three of these samples are exhaust products from motor firings conducted by Atlantic Research Corporation (72). They are Sample Nos. 1, 22, and 24. The fourth sample is an exhaust product from a motor firing conducted by Aerospace Corporation and is Sample No. 2. The physical properties studied are shown in Table LXVI.

In an effort to characterize these samples completely, analysis for trace elements and analyses for carbon, hydrogen, chlorine, oxygen and beryllium were run. Furthermore, X-ray powder diffraction patterns were run to identify components. The results from these analyses are presented in Tables LXVII, LXVIII, and LXIX.

The infrared analyses of the exhaust products from motor firings indicated that less than 1% of the total sample was benzene, toluene, aromatics or light alkanes in the four samples analyzed.

More information concerning the components in these samples was obtained by studying the water-soluble fraction using X-ray powder diffraction and emission spectroscopy.

UNCLASSIFIED

UNCLASSIFIED

Table LXVI

(U) Properties of Exhaust Products from Motor Firings

Property	Sample 1	Sample 22	Sample 24	Sample 2
Specific surface area, m. ² /g. (by nitrogen adsorption)	<2.5	0.8	0.7	Q.N.S. ^a
Average crystallite size, Å (by X-ray diffraction)	>5000	>5000	>5000	~5000
Crystallinity, % (by polarized light microscopy)	100	100	100	75
Refractive index (by dispersion staining)				
10% of sample below	1.700	1.706	1.706	1.706
50% of sample below	1.704	1.709	1.709	1.709
90% of sample below	1.708	1.712	1.712	1.712
Density, g./ml. (by sink-float method)	2.75-2.86	2.98-3.00	2.86-3.00	2.86-3.00
Solubility in water (gamma Be/g. sample at room temperature)	1.4	0.28	0.17	0.16

^aQuantity not sufficient.

UNCLASSIFIED

UNCLASSIFIED

Table LXVII

(U) Emission Spectrographic Analyses of Exhaust Products from Motor Firings

<u>Element</u>	<u>Percent of Element</u>			
	<u>Sample 1</u>	<u>Sample 22</u>	<u>Sample 24</u>	<u>Sample 2</u>
Al	0.04	0.08	0.1	0.3
Cu	0.04	0.005	0.02	0.6
Fe	3.0	0.7	0.3	0.4
Mg	0.05	0.02	0.02	0.09
Mn	0.04	0.01	0.009	0.009
Ni	0.04	0.02	0.02	0.02
Si	0.1	0.1	0.1	0.6

Table LXVIII

(U) Elemental Analysis of Exhaust Products from Motor Firings^a

<u>Element</u>	<u>Percent of Element</u>		
	<u>Sample 1</u>	<u>Sample 22</u>	<u>Sample 24</u>
Be ^b	32.0	35.3	35.3
C	0.43	~0.1	~0.5
H	0.23	0.052	0.06
Cl	3.95	0.69	1.21
O	61.2 ± 1.2	66.8 ± 1.4	65.7 ± 1.5

^aQuantity not sufficient for analysis on Sample No. 2.

^bExcept Be as BeCl₂.

UNCLASSIFIED

Table LXIX

(U) X-Ray Powder Diffraction Analysis of Exhaust Products from Motor Firings

<u>Sample No.</u>	<u>Components</u>
1	BeO - Chief Component Also contains some nearly amorphous β -FeOOH
22	BeO - Chief component Fe_2O_3 - ~5% NaCl - 1% Also a very weak line at 2.89 Å which was not identified
24	BeO - Chief component Fe_2O_3 - ~5% NaCl - <1% Also a very weak line at 2.89 Å which was not identified
2	BeO - Chief component Quartz - 5-10% Feldspar - 5-10% Unidentified material - 10-15%

A weighed quantity of each sample was mixed with an appropriate amount of water and held at room temperature for 3-4 hours. The suspensions were then filtered through sintered glass filters. Water was driven off the filtrates by placing them on watch glasses over a steam bath, and the residues were dried completely in an oven held at 108°C. The results of X-ray powder diffraction analysis of these residues are presented in Table LXX, and the results of trace element analysis of the same are presented in Table LXXI.

These data, presented in Tables LXVI through LXXI, as well as electron micrographs, and photomicrographs using polarized light, were sent promptly to the 6570th Aerospace Medical Research Laboratory, Wright-Patterson Air Force Base, Ohio.

The determinations that are in progress include particle size distribution using the Coulter Counter and mass spectrometric thermal analysis.

UNCLASSIFIED

UNCLASSIFIED

Table LXX

(U) X-Ray Powder Diffraction Analysis of Components
in the Water-Soluble Fraction of Exhaust
Products from Motor Firings

<u>Sample No.</u>	<u>Wt. % Sample Soluble in Water</u>	<u>Components in Soluble Fraction</u>
1	5	FeCl ₃ (seen in X-ray diffraction pattern as β -FeOOH which results from the hydrolysis of FeCl ₃)
22	0.5	NaCl - ~75% CaSO ₄ · 1/2 H ₂ O - ~25%
24	0.37	Na ₂ ZnCl ₄ - Chief component NaCl - 10-20%
2	---	Quantity not sufficient

Another sample of an exhaust product from a motor firing was received from Atlantic Research Corporation in December, 1965. It is a sample from firing No. 3 (72) containing beryllium oxide and a "crystalline phase" which has not been identified. Selected physical properties of this sample will be studied early in 1966.

This intensive study of the properties of beryllium oxide has shown that the properties vary with the calcining temperature. As the temperature of calcination increases the surface area decreases, and the average crystallite size, crystallinity, refractive index, and density increase. The solubility of a series of beryllium oxides in water and in Ringer-phosphate-bicarbonate buffer at room temperature is very, very slight, with no detectable differences using an emission spectrographic method. On the other hand, preliminary studies indicate a greatly increased solubility in rabbit serum. There are indications from mass spectrometric thermal analysis and the reaction of beryllium oxides with ammonium chloride that the chemical reactivity of beryllium oxide decreases as calcining temperature increases. Studies of this nature are being pursued.

2. Long-Term Experiments on Rats and Rabbits using Laboratory Prepared Samples of Beryllium Oxide

a. Rats

About three years ago, a toxicological study was started on two key samples of beryllium oxide prepared by calcining

UNCLASSIFIED

beryllium hydroxide for 10 hours at 500°C. and 1100°C., respectively. Each oxide was administered intratracheally to 50 rats of each sex. In this experiment, and in subsequent work, the test material was introduced intratracheally into the lungs of rats using a modification of the self-retaining illuminated laryngoscopic speculum developed by Dr. Paul Gross of the Industrial Hygiene Foundation, Mellon Institute (73). The usual dose for a rat was 25 mg. suspended in 0.5 ml. of physiological saline. Additional groups of rats were carried as controls. At intervals of time, ranging from one week to 68 weeks following the intratracheal injection, four to six rats from each group were killed and tissues saved for histopathological examination and beryllium analysis.

Table LXXI

(U) Emission Spectrographic Analysis of the
Water-Soluble Fraction of Exhaust
Products from Motor Firings

<u>Element</u>	<u>Percent of Element Present</u> <u>in Water-Soluble Fraction</u>		
	<u>Sample 1</u>	<u>Sample 22</u>	<u>Sample 24</u>
Al	0.3	0.5	0.2
B	0.01	0.07	0.06
Be	0.04	0.05	0.05
Ca	---	4.0	2.0
Cu	1.0	0.7	1.0
Cr	0.3	0.3	0.05
Fe	20-30	2.0	0.4
Mg	0.2	0.7	0.7
Mn	0.2	0.8	0.5
Ni	0.5	2.0	2.0
Pb	0.03	0.06	0.04
Si	0.2	1.0	1.0
Sn	0.02	0.02	---
Na	0.6	3.0	4.0
Ti	0.02	0.01	0.02
Zn	---	---	5.0
Ag	<0.005	~0.01	<0.005

UNCLASSIFIED

UNCLASSIFIED

Histopathological examination of the lungs from these animals showed very clearly a distinct difference in the biological response in the lungs of rats treated with the two oxides.

The lung response to the beryllium oxide calcined for 10 hours at 500°C. can be described as a widely dispersed focal pneumonitis of granulomatous nature. The lesion has a dense central core of proliferated histiocytes clustered around aggregates of beryllium oxide particles. Endothelioid type cells, one or two layers thick, and fibroblasts may be present, immediately investing the aggregates surrounded by histiocytes which frequently contain small particles of beryllium oxide. A few lymphocytes and plasma cells are present, usually enmeshed in a fine reticulum. Occasionally, multinucleated giant cells or attempts at their formation are evident. In the course of time the lesion becomes less cellular, more collagen appears, and, finally, there is hyalinization with or without fibrosis. Sometimes several lung lesions become confluent; in general, lesions occur more frequently in areas adjacent to blood vessels or bronchiolar elements. The lung parenchyma between the lesions discloses an inflammatory reaction in the alveolar walls and the latter appear irregularly thickened. Frequently, compensatory emphysema is seen. Bronchiolar hyperplasia and epithelialization of alveolar septal walls are commonly observed. Interstitial fibrosis occurs but does not seem to be an important aspect of the lung lesion in the rat. Hyperplasia, metaplasia and anaplasia are noted after several weeks, with the ultimate development of tumors seven months or longer following the intratracheal injection. These tumors include adenocarcinomas, bronchiogenic carcinomas, and mucinogenous adenocarcinomas.

Tissues (liver, kidney and bone) from many of these rats have been analyzed for beryllium content using emission spectrographic techniques. Results (shown in Table LXXII) indicate that these tissues contain considerable beryllium and that the beryllium concentration tends to increase with the length of time on the experiment.

In contrast, the lungs, from the rats that received the beryllium oxide calcined for 10 hours at 1100°C., were strikingly different in appearance. The particles tended to be present in the septal walls, although in some cases they were present within the alveoli. The affected septal walls were thickened due to cell proliferation and fibroblastic reaction. In a few animals granulomas were present, but not nearly to the extent observed in the case of the oxide calcined at 500°C. Nevertheless, the incidence of tumors was essentially the same in both groups. Beryllium analysis on tissues (shown in Table LXXIII) from these rats showed only a slight increase in beryllium content over control values, with a slight trend toward an increase in beryllium concentration with length of time on the experiment. Thus, there is evidence that this oxide (calcined at 1100°C.) is still

UNCLASSIFIED

UNCLASSIFIED

Table LXXII

(u) Beryllium Concentration in Tissues of Rats Treated Intratracheally with Beryllium Oxide Prepared by Calcining Beryllium Hydroxide for 10 Hrs. at 500°C.

Rat No.	Sex	No. of Weeks on Experiment	Beryllium Concentration in PPM (Gamma/Gram Wet Weight)			
			Liver	Kidney	Spleen	Bone
S-203	F	1	---	0.18	---	---
S-204	F	1	---	0.098	---	---
S-205	M	1	---	0.080	---	---
S-206	M	1	---	0.11	---	---
S-227	F	3	---	0.22	---	---
S-229	F	3	---	0.12	---	---
S-230	M	3	---	0.11	---	---
S-231	M	3	---	0.14	---	---
S-232	M	3	---	0.078	---	---
S-310	M	13	0.50	0.18	---	3.7
S-311	M	13	0.66	0.66	---	5.0
S-318	F	13	3.5	0.22	---	5.6
S-857	F	13	0.86	0.070	---	4.6
S-859	M	13	0.58	0.11	---	4.8
S-432	M	25	3.9	0.42	---	10.5
S-917	F	25	0.090	0.11	---	6.0
S-918	F	25	0.94	0.062	---	0.07
S-919	M	25	0.10	0.16	0.52	7.0
S-492	F	44	1.8	0.60	---	24
S-494	F	44	6.2	1.25	---	20
S-501	M	44	1.4	0.32	---	17
S-533	M	68	2.3	0.50	10.5	---
S-534	M	68	6.6	0.86	>50	24
S-541	F	68	8.0	0.64	>50	19
S-549	M	68	2.2	0.54	2.0	18
S-551	F	68	2.1	0.30	5.2	25
S-557	F	68	2.6	0.62	8.0	25
S-558	F	68	1.6	0.28	5.4	33
Control			<0.003	<0.003	<0.003	<0.2

UNCLASSIFIED

UNCLASSIFIED

Table LXXIII

(U) Beryllium Concentration in Tissues of Rats Treated Intratracheally with Beryllium Oxide Prepared by Calcining Beryllium Hydroxide for 10 Hrs. at 1100°C.

Rat No.	Sex	No. of Weeks on Experiment	Be Concentration in PPM (Gamma/Gram Wet Weight)			
			Liver	Kidney	Spleen	Bone
S-210	F	1	---	0.007	---	---
S-211	F	1	---	0.005	---	---
S-212	F	1	---	0.006	---	---
S-213	M	1	---	0.005	---	---
S-215	M	1	---	0.011	---	---
S-251	F	3	---	<0.003	---	---
S-252	F	3	---	<0.003	---	---
S-253	F	3	---	0.006	---	---
S-254	M	3	---	0.007	---	---
S-255	M	3	---	0.051	---	---
S-314	M	13	0.010	0.023	---	<0.2
S-315	M	13	0.16	0.04	---	0.2
S-321	F	13	0.018	<0.003	---	0.3
S-322	F	13	0.011	0.023	---	0.3
S-498	F	44	0.008	0.030	---	<0.2
S-504	M	44	<0.003	<0.003	---	<0.2
S-505	M	44	0.004	0.081	---	0.23
S-537	M	68	6.5	0.26	8.5	0.50
S-538	M	68	1.2	0.016	2.4	0.80
S-544	F	68	0.084	0.019	0.25	0.90
S-554	F	68	0.018	0.012	0.090	0.90
S-555	F	68	0.074	0.012	---	0.70
S-563	F	68	0.016	0.010	0.072	0.31
Control			<0.003	<0.003	<0.003	<0.2

UNCLASSIFIED

UNCLASSIFIED

biologically active; however, there is a marked quantitative difference between the two oxides in the magnitude of the tissue response, and in the translocation of beryllium to liver, kidney, and bone.

b. Rabbits

A similar serial study on rabbits was started about 28 months ago. The usual intratracheal dose for the rabbit was 100 mg. in 2 ml. of physiological saline. The material was administered by a modification of the self-retaining illuminated laryngoscopic speculum described by Gross (73). At intervals of 14, 30, 53, and 106 weeks, one or two animals from each group were killed and examined. In general, histopathological examinations and analytical work (Table LXXIV) on the tissues completed to date support the findings reported on the rats treated with these same oxides so far as the granulomatous response is concerned. However, no tumors have been observed in any of the rabbits examined.

Six animals are still on this experiment. These will be killed at appropriate time intervals and tissues saved for histopathological examination and beryllium analysis.

3. Twenty-four Week Experiments on Rats using a Laboratory Prepared Sample of Beryllium Oxide Calcined at 1600°C. (U)

The results (reported above) provided valid reasons to pursue the preparation of an oxide calcined at higher temperatures with the hope that a more nearly "inert" material could be prepared. Consequently, a sample of beryllium oxide was prepared from beryllium hydroxide by calcining at 1600°C. for 10 hours.

The physical and chemical properties of this oxide are listed in Table LXII. It is evident that this sample calcined at 1600°C. has the lowest surface area, the greatest average crystallite size, the highest refractive index, and the highest density. It is highly crystalline. Its solubility in water at room temperature is very, very slight, and of the same order as that of the other two key samples studied.

About a year ago, a toxicological study on rats (10 of each sex) was started on this oxide. Ignited aluminum oxide, and beryllium oxide calcined for 10 hours at 500°C. were included in this study for comparative purposes. At intervals of 3, 6, 12, and 24 weeks following the intratracheal injection, small groups of rats (four or five) were killed and examined. Tissues were saved for histopathological examination and beryllium analysis.

Histopathological examination of the lungs from these animals that received this oxide calcined for 10 hours at 1600°C. showed minimal pathological changes similar to those induced by relatively non-harmful "inert" dusts. The highly crystalline

UNCLASSIFIED

Table LXXIV

(U) Beryllium Concentration in Tissues of Rabbits Treated Intratracheally with Beryllium Oxide Prepared by Calcining Beryllium Hydroxide

Sample	Rabbit Number	Expt. Weeks	Be Concentration in PPM (Gamma/Gram Wet Weight)				
			Liver	Kidney	Spleen	Bone	Serum
BeO calcined for 10 hours at 500°C.	40	14	0.78	0.24	---	1.0	<0.003
	41	14	0.40	0.40	---	1.0	<0.003
	95	30	0.61	0.36	---	1.1	<0.003 ^a
	96	30	0.49	0.22	---	1.5	<0.003 ^a
	110	30	0.10	0.10	0.10	1.2	<0.003
	103	53	1.8	0.32	1.2	3.7	---
BeO calcined for 10 hours at 1100°C.	144	106	1.85	0.16	1.45	4.1	---
	145	106	1.20	0.25	0.82	3.7	---
	38	14	0.003	0.004	---	<0.2	---
	39	14	0.004	0.003	---	<0.2	---
	94	30	0.003	<0.003	---	<0.2	<0.003 ^a
	102	53	0.005	0.003	0.038	<0.2	---
Untreated controls	138	106	0.019	0.014	0.057	<0.2	---
	146	117	0.020	0.073	1.65	<0.2	---
	42	---	0.007	<0.003	---	<0.2	<0.003
aplasma	97	---	<0.003	<0.003	---	<0.2	---
	104	---	<0.003	<0.003	<0.003	<0.2	<0.003
	113	---	<0.003	<0.003	<0.003	<0.05	<0.003
	147	---	0.003	0.003	<0.003	<0.05	---

UNCLASSIFIED

UNCLASSIFIED

beryllium oxide particles were seen, either lying free in the alveoli or within the septal walls; the latter were irregularly thickened with minimal infiltration of lymphocytes and plasma cells. There was no effective encapsulation of this material and no evidence of collagen deposition. Certainly the cellular reaction produced by this oxide calcined at 1600°C. is of an entirely different order of magnitude than that produced by the oxide calcined at 500°C.

The analytical results obtained on tissues from rats treated with the oxide calcined at 1600°C. are given in Table LXXV. It is evident that there is only a slight increase in beryllium content of the liver even after 24 weeks on the experiment with barely detectable amounts of the kidney and bone.

4. Long-Term Serial Study on Rats and Rabbits using Key Samples of Beryllium Oxide (U)

Three of the most significant findings to date are: (i) that a characteristic biological response is produced in animals treated intratracheally with samples of beryllium calcined for 10 hours at 500°C.; (ii) that there is a gradation of biological response, from very "active" to very nearly "inactive," depending on the oxide administered; and (iii) that tumors develop in the lungs of rats treated with certain beryllium oxides several months following the intratracheal injection. It is essential to confirm these results by treating additional animals and observing them for a longer period of time. Specifically, it is imperative that a sufficient number of animals be carried throughout their lifetime following the intratracheal administration of beryllium oxide calcined for 10 hours at 1600°C., which has been shown to produce very little biological response in the lung during the time period studied to date. Since tumors were found after seven to eight months in the lungs of rats treated with the beryllium oxide calcined for 10 hours at 500°C. and 1100°C., it is very important to establish whether or not the beryllium oxide calcined 10 hours at 1600°C. will, in fact, produce tumors after a prolonged period of time (18 months to two years). A new study was started in November, 1964, to achieve this goal. The beryllium oxides used in this study were the oxides calcined at 500°C. and 1600°C., respectively (described in Table LXII).

One hundred and twenty rats and forty rabbits were selected carefully for this study. Pretreatment X-rays and serum protein fractionation were carried out on representative animals. Further, 16 rats on each sample, 16 control rats, and all of the rabbits (40) were selected for an extensive serial study of serum protein fractions using agar-gel electrophoresis. Serum samples have been analyzed at appropriate intervals following treatment.

A failure of the air-conditioning system for several hours on June 20, 1965, placed additional stress on these animals,

UNCLASSIFIED

UNCLASSIFIED

Table LXXV

(U) Beryllium Concentration in Tissues of Rats Treated
Intratracheally with Beryllium Oxide
Prepared by Calcining Beryllium Hydroxide
for 10 Hours at 1600°C.

<u>Rat No.</u>	<u>Sex</u>	<u>Experiment Weeks</u>	<u>Be Concentration in PPM</u> <u>(Gamma/Gram Wet Weight)</u>			
			<u>Liver</u>	<u>Kidney</u>	<u>Spleen</u>	<u>Bone</u>
S-849	F	3	0.004	0.003	---	0.11
S-851	M	3	0.012	0.008	---	0.11
S-852	M	3	0.010	0.005	---	<0.05
S-871	F	6	0.004	<0.003	---	<0.05
S-872	F	6	0.039	0.018	---	0.38
S-879A	M	6	0.004	0.003	---	0.06
S-880A	M	6	0.004	<0.003	---	<0.05
S-883	M	12	0.008	0.003	---	0.06
S-884	F	12	0.50	0.36	--	0.09
S-892	M	12	0.035	<0.003	---	<0.05
S-929	F	24	0.022	<0.003	0.10	0.10
S-936	M	24	0.053	<0.003	0.11	0.06
S-937	M	24	0.070	0.003	0.26	0.11
S-938	M	24	0.028	0.003	0.16	0.11
S-944	F	24	0.01	0.003	0.040	0.14
S-945	M	24	0.007	0.004	0.038	0.09
Control			<0.003	<0.003	<0.003	<0.05

UNCLASSIFIED

UNCLASSIFIED

resulting in an increased mortality in all groups, especially animals treated with beryllium oxide calcined for 10 hours at 500°C. Moribund animals were killed so that tissues could be obtained for histopathological examination and beryllium analysis. Small groups of the surviving rats were killed nine and twelve months following treatment. The tissues are being prepared for histopathological examination and for analysis of beryllium content. The remaining animals will be followed closely and sacrificed at appropriate intervals.

5. One-Year Experiments on Rats using Control Materials (U)

Several experiments using control materials have been completed. Rats were treated intratracheally and then small groups killed and examined 6, 12, 18, and 52 weeks following treatment. Some of the compounds studied were aluminum oxide, titanium dioxide, zirconium dioxide, yttrium oxide, carbon, and talc. These experiments have been very helpful in providing material for comparative study in the gross and microscopic examination of lungs from rats treated with beryllium oxide. Also, tissues are being analyzed for metal content in liver, kidney, spleen and bone. These studies should help in evaluating translocation of materials from the lung to other organs.

6. Studies on Exhaust Products from Motor Firings using Rats (U)

a. Sample of "Exhaust Products" from Edwards Air Force Base

A small sample of "exhaust products" from Edwards Air Force Base, California, was received in June, 1964. This sample consisted of particles ranging from 200 μ to about 1 μ . It was a heterogeneous mixture of Al_2O_3 , $BeAl_2O_4$, and Fe_3O_4 , as determined by X-ray diffraction. This sample was found to contain 4.7% beryllium, 17.7% iron and 29.5% aluminum. Beryllium metal and beryllium oxide were not found in this sample. The beryllium present was in the form of $BeAl_2O_4$. A more detailed report of the studies of physical properties is given in the 1964 Annual Technical Summary Report (1).

In August, 1964, eight rats were treated intratracheally with this material. Because of the large particles and heterogeneous nature, it was difficult to administer an accurate dose. Two animals were killed at 2, 10, 30, and 48 weeks following the intratracheal injection, and tissues were saved for histopathological examination and for analysis of beryllium concentration.

Histopathological examination of the lungs from these animals showed minimal non-specific pathological changes, ranging from no effect to slight thickening of the alveolar walls and the presence of a few macrophages and mononuclear cells surrounding the particulate matter. Many particles were seen either lying free in the alveoli or adjacent to the alveolar lining. Occasionally, the smaller particles were observed within the

UNCLASSIFIED

alveolar walls or engulfed by macrophages. In some areas the endothelial lining was elevated and the nucleus was prominent. Only slight proliferation of the fibroblasts were evident.

These results must be considered as preliminary. Conclusions cannot be drawn regarding the probable health hazard of this material. The sample was a very poor preparation for intratracheal work in rats. Since only eight rats were treated and only two rats killed at each interval, these results are preliminary. It is not appropriate to compare these results with the results on beryllium oxide since the beryllium compound found in the sample is one that has not been studied, and the beryllium content in the sample is quite low.

Further work on representative samples of exhaust products is needed. However, only well-defined beryllium-containing exhaust products from carefully controlled motor firings are recommended for intensive biological study. The chemical nature and physical properties of these exhaust products should be determined so that a correlation can be made with the properties of the key samples of beryllium oxide which have been studied extensively.

b. Exhaust Products from Wright-Patterson Air Force Base

Four samples of exhaust products from motor firings were received in October from Wright-Patterson Air Force Base, Ohio. Three of these samples, Nos. 1, 22, and 24, are exhaust products from motor firings conducted at Atlantic Research Corporation, and the fourth sample, Aerospace No. 2, is an exhaust product from a motor firing conducted at Aerospace Corporation. Many physical properties of these materials have been studied and are reported in Section B.1.b. of this report.

A small pilot experiment using rats was started in October, 1965, to study the biological effects of these materials. Each material was administered intratracheally. A total of 50 rats was treated. An additional group of 20 rats is being carried as controls. These animals will be killed at appropriate intervals, and tissues will be saved for histopathological examination. The first kill was made early in December, four weeks following treatment. Currently, these tissues are being prepared for histopathological examination.

7. A Pilot Experiment on Selected Beryllium Oxides, Beryllium Hydroxides, and Beryllium Metal Using Rats (U)

A pilot study was started in September, 1965, on a series of carefully prepared, well-characterized samples of beryllium oxides which were calcined at temperatures intermediate to those which have been reported, i.e., the oxide calcined 10 hours at 500°C. and the oxide calcined 10 hours at 1600°C. Also, a few rats have been treated with a nominally "fused beryllium oxide" and two samples of beryllium metal supplied by the Brush Beryllium

UNCLASSIFIED

UNCLASSIFIED

Company. Three samples of beryllium hydroxide, which were the starting materials for the series of calcined beryllium oxides which have been studied extensively over the past three years, are included in this study.

Rats were treated intratracheally with 25 mg. of the sample in 0.5 ml. of 0.9% saline. The first kill was made in November, and tissues were saved for histopathological examination. The findings from this experiment should help to elucidate the mechanism of the toxic nature of beryllium-containing materials.

C. BIOCHEMICAL STUDIES (U)

Since changes in serum protein patterns have been reported in clinical cases of beryllium disease, a method of electrophoresis for fractionating serum protein using the Beckman paper electrophoresis system was set up. The results using paper electrophoresis were unsatisfactory. Consequently, a method of agar gel electrophoresis was developed using the equipment available. The resolution of serum proteins is very good in all species tested (rat, rabbit, guinea pig and sheep). Extensive studies have been made using sera from rats and rabbits. Values for serum protein fraction on 210 normal rats and 70 normal rabbits have been determined. These values will be used as a base line with which to compare separation of serum proteins in animals treated with beryllium-containing materials.

While agar gel electrophoresis gives excellent resolution of the major protein fractions, a further definition can be obtained from their antigenic properties. A great many components can be resolved and identified by combining electrophoretic characteristics with immunological response. An immunoelectrophoresis system has been developed by modifying the agar gel electrophoresis system. Excellent results have been obtained using rat serum reacting with rabbit anti-rat globulin serum as a test system. Now that a means has been devised for studying certain antigenic properties in serum, investigations will be carried out on treated animals.

D. PROJECTED WORK (U)

The ultimate objective of this beryllium toxicology program is to gain an understanding of the fundamental biological, chemical and physical mechanisms involved in the toxic action of beryllium-containing materials, including exhaust products from motor firings, in order to evaluate the relative health hazards presented by these materials.

The research program, which will be continued, consists of four major interrelated experiments:

- (1) The completion of a long-term serial study on rats and rabbits using key samples of beryllium oxide.

UNCLASSIFIED

- (ii) The study of dosage-response relationships using beryllium oxide particles of "respirable size" only.
- (iii) The study of the mechanism of action (using animals from the above studies).
- (iv) The study of beryllium-containing exhaust products from motor firings.

The successful completion of these studies should contribute greatly to an understanding of the relative toxicity of beryllium oxides. The correlation of the chemical and physical properties of these oxides with their biological activity should help to furnish useful data for evaluating the relative health hazards presented by other beryllium-containing materials. Furthermore, the study in animals of carefully-selected and well-characterized exhaust products from motor firings should contribute greatly to the final solution of the problem.

CONFIDENTIAL

SECTION VII

REFERENCES

1. (U) The Dow Chemical Company, Annual Technical Summary Report Nr. AR-4Q-64, February 1, 1965, Contract Nr. AF 04(611)-7554(2).
2. (U) E. G. Prout and F. C. Tompkins, Trans. Faraday Soc., 40, 488 (1944).
3. (U) J. W. Mitchell, "Fundamental Mechanisms of Photographic Sensitivity," Buttersworth, London, p. 242 (1951).
4. (U) W. C. Garner and E. W. Haycock, Proc. Roy. Soc. (London), A211, 335 (1952).
5. (U) F. C. Tompkins and D. A. Young, Trans. Faraday Soc., 61, 1470-80 (1965).
6. (C) J. R. C. Duke, "Crystal Structure of Aluminum Hydride," Twenty-first Meeting of the Working Group on Analytical Chemistry (February, 1965).
7. (U) W. E. Garner, editor, "Chemistry of the Solid State," Butterworth, Sci. Publ., London, Chapter 7 (1955).
8. (U) "Investigation of Light Metal Hydride-1 by Mass Spectroscopy and X-ray Diffraction," Tech. Doc. Rept. No. RPL-TDR 64-11, Rocket Propulsion Laboratory, Edwards Air Force Base, California (December, 1963).
9. (U) The Dow Chemical Company, Annual Technical Summary Report Nr. AR-4Q-62, January 31, 1963, Contract Nr. AF 04(611)-7554.
10. (U) O. Glemser, V. Hanschild, and O. Bimmermann, Angew. Chem., 64, 456 (1952).
11. (U) F. D. Miles, "Cellulose Nitrate," Interscience, New York, p. 215 (1955).
12. (U) T. Higuchi, Anal. Chem., 22, 955 (1950).
13. (C) N. E. Matzek, "Characterization and Testing of Aluminum Hydride," Twenty-first Meeting of the Working Group on Analytical Chemistry, Midland, Michigan (February 24-26, 1965).
14. (U) L. K. Frevel, Acta Cryst., 17, 907 (1964).
15. (U) L. S. Nelson and N. A. Kuebler, J. Chem. Phys., 39, 1055 (1963).

CONFIDENTIAL

REFERENCES (Contd.)

16. (U) J. G. Kay, N. A. Kuebler and L. S. Nelson, Nature, 194, 671 (1962).
17. (U) L. S. Nelson and N. A. Kuebler, J. Chem. Phys., 37, 47 (1962).
18. (U) L. S. Nelson and J. L. Lundberg, J. Phys Chem., 63, 433 (1959).
19. (U) W. W. Watson, Phys. Rev., 32, 600 (1928).
20. (U) W. W. Watson, and R. F. Humpheys, Phys. Rev., 52, 318 (1937).
21. (C) Minnesota Mining and Manufacturing Company, Report No. 15, Fourth Annual Report, 1 Jan - 31 Dec 1962, Contract No. NOrd 18688.
22. (U) G. C. Sinke, J. Chem. Eng. Data, 10, 295 (1965).
23. (U) J. D. Cox and D. Harrop, Trans. Faraday Soc., 61, 1328 (1965).
24. (U) D. D. Wagman, W. H. Evans, I. Halow, V. B. Parker, S. M. Bailey, and R. H. Schumm, Natl. Bur. Std. Tech. Note 270-1, October 1, 1965.
25. (U) JANAF THERMOCHEMICAL TABLES, The Dow Chemical Company, Midland, Michigan, Supplement No. 19, September 30, 1965.
26. (U) E. S. Domalski and G. T. Armstrong, J. Res. Natl. Bur. Std., 69A, 137 (1965).
27. (U) E. Tschuikow-Roux, J. Chem. Phys., 43, 2251 (1965).
28. (U) A. M. Tarr, J. W. Coomber, and E. Whittle, Trans. Faraday Soc., 61, 1182 (1965).
29. (C) American Cyanamid Company, Progress Report No. 2, Contract No. NOW 65-0277-C, 30 July 1965.
30. (U) J. C. Brosheer, F. A. Lenfesty, and K. L. Elmore, Ind. Eng. Chem., 39, 423 (1947).
31. (U) R. A. McDonald and D. R. Stull, J. Chem. Eng. Data, 6, 609 (1961).
32. (U) B. E. Walker, C. T. Ewing and R. R. Miller, J. Phys. Chem., 61, 1682 (1957).

UNCLASSIFIED

REFERENCES (Contd.)

33. R. Mezaki, E. W. Tilleux, D. W. Barnes, M.S. Thesis, University of Wisconsin (1961).
34. D. Osment, Southern Research Institute Technical Documentary Report No. ASD-TDR-62-675 (January 1963).
35. C. H. Shomate, J. Phys. Chem., 58, 368 (1954).
36. R. A. McDonald, D. R. Stull, J. Phys. Chem., 65, 1918 (1961).
37. W. F. Giauque, P. F. Meads, J. Am. Chem. Soc., 63, 1897 (1941).
38. C. G. Maier, C. T. Anderson, J. Chem. Phys., 2, 513 (1934).
39. E. H. Griffiths, E. Griffiths, Proc. Roy. Soc. (London), 90A, 557 (1914).
40. J. H. Awbery, E. Griffiths, Proc. Phys. Soc. (London), 38, 373 (1926).
41. E. D. Eastman, A. M. Williams, T. F. Young, J. Am. Chem. Soc., 46, 1178 (1924).
42. F. Glaser, Metallurgie, 1 (7), 121 (1904).
43. W. B. Kendall, R. Hultgren, unpublished data, private communication to D. R. Stull from R. L. Orr, March 29, 1960.
44. A. Magnus, Ann. Physik, Ser. 4, 31, 597 (1910).
45. A. Naccari, Atti Torino, 23, 107 (1888).
46. S. Satoh, Sci. Papers Inst. Phys. Chem. Res. (Tokyo), 29, 19 (1936).
47. W. A. Tilden, Phil. Trans. Roy. Soc. (London), 201, 37 (1903).
48. S. Umino, Sci. Repts., Tohoku Imp. Univ., Ser. 1, 15, 597 (1926).
49. F. Wust, A. Meuthen, R. Durrer, Forsch. Arb. Ver. Deut. Ing., No. 204 (1918).
50. K. K. Kelley, U. S. Bur. Mines Bull. 584 (1960).

UNCLASSIFIED

REFERENCES (Contd.)

51. D. R. Stull, G. C. Sinke, "Thermodynamic Properties of the Elements," A. C. S. Monograph No. 18, Washington, D. C. (1956).
52. R. Hultgren, R. L. Orr, P. D. Anderson, K. K. Kelley, "Selected Values of Thermodynamic Properties of Metals and Alloys," John Wiley and Sons, Inc., New York (1963).
53. H. Seekamp, Z. Anorg. Chem., 195, 345 (1931).
54. R. Laemmel, Ann. Physik, 16, 551 (1905).
55. T. E. Pochapsky, Acta Met., 1, 747 (1953).
56. A. Avramescu, Z. Tech. Physik, 20, 213 (1931).
57. P. Schubel, Z. Anorg. Chem., 87, 81 (1914).
58. W. H. Evans, R. Jacobson, T. R. Munson, D. D. Wagman, J. Res. Natl. Bur. Std., 55A, 83 (1955).
59. W. F. Roeser, H. T. Wensel, J. Res. Natl. Bur. Std., 14, 247 (1935).
60. J. H. Awbery, Phil. Mag., 26, 776 (1938).
61. O. Kubaschewski, P. Brizgys, O. Huchler, R. Jauch, K. Reinartz, Z. Electrochem., 54, 275 (1950).
62. F. E. Wittig, Z. Metallk., 43, 158 (1952).
63. W. Oelsen, K. H. Rieskamp, O. Oelsen, Arch. Eisenhuettenw., 26, 253 (1955).
64. W. Oelsen, O. Oelsen, D. Thiel, Z. Metallk., 46, 555 (1955).
65. D. M. Speros, R. L. Woodhouse, Nature, 197, 1261 (1963).
66. G. C. Crossmon and W. C. Vandemark, A. M. A. Arch. Ind. Hyg. and Occup. Med., 9, 481-487 (1954).
67. A. Werbin, General Chemistry Technical Note No. 20, University of California, June 30, 1960.
68. H. Langer and R. S. Gohlke, Anal. Chem., 35, 1301 (1963).
69. J. F. Quirk, N. B. Mosby, and W. H. Duckworth, J. Am. Ceram. Soc., 40, 416-419 (1957).

UNCLASSIFIED

REFERENCES (Contd.)

70. B. Bellamy, T. W. Baker, and D. T. Livey, AERE-R-3774, July, 1961.
71. R. A. Belyaev, AEC-TR-1675, p. 14, 1962, TID-4500, 34th edition.
72. Atlantic Research Corporation, Technical Report no. AFRPL-TR-65-12, March, 1965, Contract No. AF 04(611)-09710.
73. P. Gross, A. M. A. Arch Indust. Health, 18, 429-30 (1958).

UNCLASSIFIED

~~CONFIDENTIAL~~

CONFIDENTIAL

Security Classification

DOCUMENT CONTROL DATA - R&D		
(Security classification of title, body of abstract and indexing annotation must be entered when the overall report is classified)		
1. ORIGINATING ACTIVITY (Corporate author) The Dow Chemical Company Midland, Michigan		2a. REPORT SECURITY CLASSIFICATION Confidential 2b. GROUP 4
3. REPORT TITLE (U) Development and Evaluation of Advanced Solid Propellants		
4. DESCRIPTIVE NOTES (Type of report, date, inclusive dates) Final Report January 1965 - December 1965		
5. AUTHOR(S) (Last name, first name, initial) Brower, Frank M.; Rausch, Douglas A.; Stull, Daniel A.; and Spencer, Howard C.		
6. REPORT DATE February 1966	7a. TOTAL NO. OF PAGES 325	7b. NO. OF REFS 73
8a. CONTRACT OR GRANT NO. AF 04(611)-7554(4) 8. PROJECT NO. 3148 * Task No. 314804	9a. ORIGINATOR'S REPORT NUMBER(S) R-4Q-65 9b. OTHER REPORT NO(S) (Any other numbers that may be assigned this report) AFRPL-TR-66-44	
10. AVAILABILITY/LIMITATION NOTICES In addition to security requirements which must be met, this document is subject to special export controls and each transmittal to foreign governments or foreign nationals may be made only with prior approval of AFAPL (RPRR-STINFO), Edwards, California 93523		
11. SUPPLEMENTARY NOTES		12. SPONSORING MILITARY ACTIVITY AFRPL, R&D Edwards Air Force Base, California
13. ABSTRACT (C) Intensive investigations were conducted on improving the thermal stability and crystallization of aluminum hydride. Areas considered included the solubility in various solvents with and without addition agents, "thermal seeding," growth processes, decomposition processes, aging, surface oxidation and treatment, and surveillance of both neat and formulated propellants at 25°C. and 40°C. A study of the kinetics of aluminum and beryllium hydride using flash heating with ultraviolet spectroscopy showed the existence of AlH , BeH and BeH^+ at 2,500°K. The reaction of tris-I with nitroform gave a new liquid oxidizer or plasticizer. Reactions of tris-Br with typical nucleophiles were not successful. The effect of impurities on the sensitivity of NF_2 compounds was not detected for the compounds examined. The heat of formation of $Al(BH_4)_3$, Hybaline A-4, C_2F_5 radical, UNFO-635P, and BTU, high temperature enthalpies of allotropic forms of $BeCl_2$, and the enthalpies and heat capacities of Al are reported. In the JANAF Tables, area, a summary of Series C and D of the Propellant Ingredients and four supplements of the Thermochemical Tables are given. The toxicological research was concentrated on Be-containing materials using controlled samples of the oxide, some hydrides, metal and firing residues. The animal response of the low-fired oxide is entirely different than the high-fired oxide and evidence of carcinogenic tumors was detected in the lung tissue of animals exposed to low-fired materials.		

DD FORM 1 JAN 64 1473

CONFIDENTIAL

Security Classification

~~CONFIDENTIAL~~

14	KEY WORDS	CLASSIFICATION		LIMITATION	
		GROUP	TYPE	GROUP	TYPE
	Light Metal Hydride Crystallization Oxidizers Fluorine Compounds Thermal Measurements JANAF Tables Toxicological Research Propellants Beryllium Compounds				

INSTRUCTIONS

1. **ORIGINATING ACTIVITY:** Enter the name and address of the contractor, subcontractor, grantee, Department of Defense activity or other organization (corporate author) issuing the report.

2a. **REPORT SECURITY CLASSIFICATION:** Enter the overall security classification of the report. Indicate whether "Restricted Data" is included. Marking is to be in accordance with appropriate security regulations.

2b. **GROUP:** Automatic downgrading is specified in DoD Directive 5200.10 and Armed Forces Industrial Manual. Enter the group number. Also, when applicable, show that optional markings have been used for Group 3 and Group 4 as authorized.

3. **REPORT TITLE:** Enter the complete report title in all capital letters. Titles in all cases should be unclassified. If a meaningful title cannot be selected without classification, show title classification in all capitals in parentheses immediately following the title.

4. **DESCRIPTIVE NOTES:** If appropriate, enter the type of report, e.g., interim, progress, summary, annual, or final. Give the inclusive dates when a specific reporting period is covered.

5. **AUTHOR(S):** Enter the name(s) of author(s) as shown on or in the report. Enter last name, first name, middle initial. If military, show rank and branch of service. The name of the principal author is an absolute minimum requirement.

6. **REPORT DATE:** Enter the date of the report as day, month, year, or month, year. If more than one date appears on the report, use date of publication.

7a. **TOTAL NUMBER OF PAGES:** The total page count should follow normal pagination procedure, i.e., enter the number of pages containing information.

7b. **NUMBER OF REFERENCES:** Enter the total number of references cited in the report.

8a. **CONTRACT OR GRANT NUMBER:** If appropriate, enter the applicable number of the contract or grant under which the report was written.

8b, 8c, & 8d. **PROJECT NUMBER:** Enter the appropriate military department identification, such as project number, subproject number, system numbers, task number, etc.

9a. **ORIGINATOR'S REPORT NUMBER(S):** Enter the official report number by which the document will be identified and controlled by the originating activity. This number must be unique to this report.

9b. **OTHER REPORT NUMBER(S):** If the report has been assigned any other report numbers (either by the originator or by the sponsor), also enter this number(s).

10. **AVAILABILITY/LIMITATION NOTICES:** Enter any limitations on further dissemination of the report, other than those

imposed by security classification, using standard statements such as:

- (1) "Qualified requesters may obtain copies of this report from DDC."
- (2) "Foreign announcement and dissemination of this report by DDC is not authorized."
- (3) "U. S. Government agencies may obtain copies of this report directly from DDC. Other qualified DDC users shall request through _____."
- (4) "U. S. military agencies may obtain copies of this report directly from DDC. Other qualified users shall request through _____."
- (5) "All distribution of this report is controlled. Qualified DDC users shall request through _____."

If the report has been furnished to the Office of Technical Services, Department of Commerce, for sale to the public, indicate this fact and enter the price, if known.

11. **SUPPLEMENTARY NOTES:** Use for additional explanatory notes.

12. **SPONSORING MILITARY ACTIVITY:** Enter the name of the departmental project office or laboratory sponsoring (paying for) the research and development. Include address.

13. **ABSTRACT:** Enter an abstract giving a brief and factual summary of the document indicative of the report, even though it may also appear elsewhere in the body of the technical report. If additional space is required, a continuation sheet shall be attached.

It is highly desirable that the abstract of classified reports be unclassified. Each paragraph of the abstract shall end with an indication of the military security classification of the information in the paragraph, represented as (TS), (S), (C), or (U).

There is no limitation on the length of the abstract. However, the suggested length is from 150 to 225 words.

14. **KEY WORDS:** Key words are technically meaningful terms or short phrases that characterize a report and may be used as index entries for cataloging the report. Key words must be selected so that no security classification is required. Identifiers, such as equipment model designation, trade name, military project code name, geographic location, may be used as key words but will be followed by an indication of technical context. The assignment of links, rules, and weights is optional.